



Università
di Genova

DISTAV DIPARTIMENTO
DI SCIENZE DELLA TERRA,
DELL'AMBIENTE E DELLA VITA



Università degli Studi di Genova and Sorbonne Université

**PhD in Marine Science and Technologies (curriculum: Marine Ecosystem
Science) and PhD in Complexité du Vivant**

**The monoaminergic system of *Mytilus
galloprovincialis*: possible developmental functions
and sensitivity to emerging contaminants**

Supervisors

Prof. Laura Canesi

Dr. Rémi Dumollard

PhD Candidate: Beatrice Risso

The thesis defence will be presented and defended on Thursday the 12th of December 2024.

Jury composition

Supervisors

Prof. Laura Canesi – Università degli Studi di Genova, IT

Dr. Rémi Dumollard – Sorbonne Université, IT

Reviewers

Prof. Roberto Feuda – University of Leicester, UK

Prof. Andreas Thomas Knigge – Université Le Havre Normandie, FR

Jury members

Prof. Laure Bonnaud-Ponticelli – Sorbonne Université, FR

Prof. Sara Ferrando – Università degli Studi di Genova, IT

Table of Contents

Abstract	I
Résumé	III
Introduction	1
Chapter 1	2
1 The Invertebrate Nervous and Neuroendocrine Systems	2
1.1 Nervous system: neurons and glial cells	2
1.2 Neurons organise to form ganglia	5
1.3 Central and Peripheral nervous system and controversies	6
1.4 Development of the larval nervous system in molluscs: an overview	6
1.4.1 The nervous system of bivalve larvae	8
2.1 The neuroendocrine system	13
2.1.1 Endocrine signalling: definition and controversies	13
2.1.2 Secretory neurons	13
Chapter 2	16
2 The monoaminergic system	16
2.1 Monoamines: definition	16
2.2 Monoaminergic system: enzymes, transporters and receptors and their presence/absence across different species.....	16
2.2.1 Synthesis enzymes	17
2.2.1.1 Aromatic amino acids hydroxylase (AAAHs)	17
2.2.1.2 Aromatic amino acid decarboxylases (AADCs)	17
2.2.1.3 Copper-dependent hydroxylases	18
2.2.2 Degradation enzymes	19
2.2.3 Vesicular and membrane transporters	19
2.2.4 Monoamines Receptors	19
2.3 Presence/absence of monoaminergic system across evolution	23
2.4 Roles of Monoamines in bivalve molluscs	26
2.4.1 Physiological roles.....	26

2.4.1.1	Serotonin (5-HT).....	26
2.4.1.2	Dopamine (DA)	27
2.4.1.3	Noradrenaline (NA)	28
2.4.1.4	Tyramine (TA) and Octopamine (OA).....	28
2.4.2	Monoamines roles in response to environmental stressors: focus on marine bivalves....	28
2.4.2.1	Adults.....	28
2.4.2.2	Larvae	30
Chapter 3.....		32
3	Contaminants of Emerging Concern	32
3.1	Endocrine Disrupting Chemicals (EDCs) and Neuro-Endocrine Disrupting Chemicals (NEDs)	32
3.2	Pharmaceuticals and personal care products (PPCPs)	34
3.2.1	The concepts of Mode-of-Action (MOA) and the Adverse Outcome Pathway (AOP)...	36
3.3	Selective Serotonin Reuptake Inhibitors (SSRIs)	38
3.3.1	Concentration of SSRIs in aquatic matrices	39
3.3.2	Effects of SSRIs on bivalves	39
3.3.2.1	Adults.....	39
3.3.2.2	Embryos and Larvae	41
3.4	Supplementary Table	43
Chapter 4.....		46
4	<i>Mytilus galloprovincialis</i>	46
4.1	General characteristics	46
4.2	The life cycle.....	46
4.3	The embryo-larval development	47
4.3.1	Shell biogenesis	49
4.3.2	Evolution of the ciliated epithelium	51
4.3.3	The nervous system	51
4.4	<i>Mytilus galloprovincialis</i> larvae as a model organism for evaluating the impact of CEC...	53
5	Aim of the Thesis.....	62
6	Aim 1: Ontogeny of the monoaminergic system during the embryo-larval development of the Mediterranean mussel <i>Mytilus galloprovincialis</i>	64

6.1	Material and Methods	65
6.1.1	Orthology assessment of monoaminergic system elements in <i>M. galloprovincialis</i> genome	65
6.1.2	Transcriptome analysis for characterizing the ontogeny of the monoaminergic system during <i>M. galloprovincialis</i> embryo-larval development.....	65
6.1.3	Mussel handling, spawning, fertilisation and conservation of larval samples.....	66
6.1.4	Morphological analysis of larvae.....	67
6.1.5	<i>In situ</i> Hybridization Chain Reaction (HCR)	67
6.1.6	Image acquisition and analysis	68
6.2	Results.....	70
6.2.1	Characterization of components of the monoaminergic system in <i>M. galloprovincialis</i>	70
6.2.1.1	Synthesis enzymes	70
6.2.1.2	Degradation enzymes.....	71
6.2.1.3	Transporters	72
6.2.1.4	Receptors	73
6.2.2	Developmental expression of monoaminergic genes in <i>M. galloprovincialis</i>	75
6.2.3	Spatiotemporal expression of serotonin and dopamine genes during <i>M. galloprovincialis</i> embryo-larval development evaluated by HCR: relationship with the neuroendocrine system....	79
6.2.3.1	Spatiotemporal analysis of the pan-neuronal marker 7B2	79
6.2.3.2	Spatiotemporal analysis of serotonin and dopamine producing cells	81
6.2.3.3	Spatiotemporal localisation of serotonin and dopamine transporters	84
6.2.3.4	Colocalisation of serotonin and dopamine receptors (5-HTRs and DRs) within neural tissue at D-Veliger stage	85
6.2.3.5	Colocalisation of 5-HTR1A2_inv and 5-HTR7 with TPH	87
6.2.3.6	Colocalisation of DR1 and DR3-like with TH.....	90
6.2.3.7	Localisation of 5-HTRs within neuronal and ciliated tissues	91
6.2.3.8	Localisation of DR1 within ciliated tissue.....	95
6.2.3.9	Localisation of DBHs-like	96
6.2.4	Effects of treatment with exogenous monoamines and pharmacological inhibitors of 5-HTRs and DRs on D-Veliger phenotypes (48 hpf)	97
6.3	Discussion.....	99
6.3.1	Six monoaminergic systems are present in the <i>M. galloprovincialis</i> genome.....	99
6.3.1.1	Synthesis enzymes	99

6.3.1.2	Degradation enzymes.....	101
6.3.1.3	Transporters	101
6.3.1.4	Receptors	101
6.3.2	Expression profiles of serotonin and dopamine gene suggest that they might have several key roles during <i>M. galloprovincialis</i> embryo-larval development	102
6.3.3	Expansion of neuronal clusters highlights growing complexity in <i>M. galloprovincialis</i> embryo-larval development.....	107
6.3.4	Serotonin and dopamine producing cells occur in different neuronal clusters that could correspond to the AO/CG and PG	108
6.3.5	Localisation of 5-HTRs and DRs: potential implications in synaptic and neuroendocrine functions	111
6.4	Supplementary Tables.....	113
6.5	Supplementary Figures	129
7	Aim 2: Sensitivity of <i>M. galloprovincialis</i> early development to fluoxetine and citalopram as model SSRIs.....	149
7.1	Materials and Methods.....	150
7.1.1	Analysis of human and mussel SERT sequences	150
7.1.2	Mussel handling, spawning, fertilisation and conservation	150
7.1.3	Exposure conditions	150
7.1.4	Morphological analysis of larvae.....	150
7.1.5	Statistical analysis.....	150
7.1.6	Retrieval of Nose Resistant to Fluoxetine (nrf) proteins in <i>Mytilus galloprovincialis</i> genome	150
7.1.7	Retrieval of Nose Resistant to Fluoxetine (nrf) proteins in other bilaterian organism models	151
7.1.8	Analysis of expression profile of nrf transcripts in <i>M. galloprovincialis</i> transcriptome	151
7.1.9	HCR.....	151
7.1.10	Image acquisition and analysis.....	151
7.2	Results.....	152
7.2.1	Analysis of presence/absence of conserved amino acids involved in SSRIs binding ...	152
7.2.2	Effects of fluoxetine (FLX) and citalopram (CIT) on larval development.....	155

7.2.3	Effects on serotonin synthesis enzyme Tryptophan Hydroxylase (TPH).....	155
7.2.4	Presence of Nore Resistant to Fluoxetine (nrf) proteins in <i>M. galloprovincialis</i> and other bilaterian species	157
7.2.5	Expression of nrf proteins during <i>M. galloprovincialis</i> embryo-larval development....	158
7.2.6	Localisation of four nrf genes at D-Veliger stage (48 hpf).....	159
7.3	Discussion	161
7.3.1	SSRIs may bind to SERT-like transporters of <i>M. galloprovincialis</i>	161
7.3.2	Effect of Fluoxetine (FLX) and Citalopram (CIT) on D-Larvae phenotypes.....	162
7.3.3	Serotonin Reuptake Transporters do not represent unique targets of SSRI.....	163
7.3.4	Expression of nfr proteins suggests a role in larval development and transport of SSRIs 166	
7.3.5	Possible Molecular Initiating Events (MIEs) and Adverse Outcome Pathway (AOP) caused by SSRIs in <i>M. galloprovincialis</i>	168
7.4	Supplementary Table	171
7.5	Supplementary Figures	173
8	Conclusions and future perspectives	179
	Annex.....	183
	References	224

Abstract

Calcifying larvae of marine invertebrates are highly sensitive to environmental stressors and contaminants of emerging concern (CEC), including endocrine disrupting chemicals (EDCs) and pharmaceutical and personal care products (PPCPs). Marine bivalves living in dynamic coastal environments have evolved sophisticated stress response mechanisms, with neuroendocrine regulation playing a critical role. Key components of this regulation include the monoamines (MAs) dopamine (DA) and serotonin (5-HT), which are pivotal neuromodulators in shell formation and larval development of bivalves and are targets of environmental stressors such as ocean acidification and CEC, notably EDCs and PPCPs. Despite the importance of monoamines in larval development, information on the ontogeny of the monoaminergic system during the early development of bivalve larvae is limited. Among PPCPs, serotonin selective reuptake inhibitors (SSRIs) are designed to bind to the serotonin reuptake transporter (SERT), yet there is currently no information regarding its presence in bivalves.

To fill this knowledge gap, *Mytilus galloprovincialis* was used as model organism. This study aimed to characterise the presence of MA systems in *M. galloprovincialis* genome, alongside their expression and localisation during embryo-larval development within the neuroendocrine tissue. The involvement of MAs in development was investigated through pharmacological experiments. The effects of SSRIs were evaluated using Fluoxetine (FLX) and Citalopram (CIT), alongside an examination of their targets in the genome and transcriptome.

Six MA systems were identified in *M. galloprovincialis* genome, with 5-HT and DA being the most expressed during development. Cells producing 5-HT and DA were localised in neuroendocrine areas, specifically in the Apical Organ/Cerebral Ganglion and Pedal Ganglia, respectively. The expression of L-Amino Acid Decarboxylase and serotonin and dopamine receptors (5-HTRs and DRs) prior to the synthesis of 5-HT and DA suggests that these components may be involved morphogenetic roles and environmental interactions. Both transcriptomic and pharmacological results indicate that 5-HT and DA play key roles in larval development and shell biogenesis. The localisation of 5-HTRs and DRs throughout development, along with their spatial relationship to the synthesis enzymes, suggests their potential involvement in synaptic and neuroendocrine functions. Moreover, the colocalisation of 5-HTR1A_{inv} and DR3-like implies a possible reciprocal regulation between the serotonin and dopamine systems. *M. galloprovincialis* possesses two types of SSRIs targets: selective (SERT) and non-selective (Nose Resistant to Fluoxetine – nrf, and 5-HTRs). Both targets were

found to be differentially expressed during embryo-larval development. Exposure to high concentrations of FLX and CIT did not strongly affect larval phenotypes, suggesting some mechanisms of resistance where nrf may play a role.

This work shows for the first time a comprehensive characterisation of the MA system in *M. galloprovincialis*; moreover, the identification of different targets of SSRIs lays the groundwork for future studies on the role of the MA system during development, and in response to different environmental stressors, including SSRIs and, potentially, other antidepressants released in coastal marine environments.

Keywords: *Mytilus galloprovincialis*, monoaminergic system, development, contaminants, toxicology

Résumé

Les larves calcifiantes des invertébrés marins sont particulièrement sensibles aux facteurs de stress environnementaux et aux contaminants émergents (CEC), y compris les perturbateurs endocriniens (EDC) et les produits pharmaceutiques et de soins personnels (PPCP). Les bivalves marins vivant dans des environnements côtiers dynamiques ont développé des mécanismes sophistiqués de réponse au stress, où la régulation neuroendocrine joue un rôle crucial. Parmi les éléments clés de cette régulation, on trouve les monoamines (MA), comme la dopamine (DA) et la sérotonine (5-HT), qui sont des neuromodulateurs essentiels pour la formation de la coquille et le développement larvaire des bivalves. Ces monoamines sont ciblées par des facteurs de stress environnementaux tels que l'acidification des océans et les CEC, notamment les EDC et les PPCP. Malgré leur importance dans le développement larvaire, les connaissances sur l'ontogenèse du système monoaminergique lors du développement précoce des larves de bivalves restent limitées. Parmi les PPCP, les inhibiteurs sélectifs de la recapture de la sérotonine (ISRS) sont conçus pour se lier au transporteur de recapture de la sérotonine (SERT), mais il n'existe actuellement aucune information sur sa présence chez les bivalves.

Pour combler cette lacune, *Mytilus galloprovincialis* a été utilisé comme organisme modèle. Cette étude vise à caractériser la présence des systèmes MA dans le génome de *M. galloprovincialis*, ainsi que leur expression et localisation pendant le développement embryonnaire-larvaire au sein des tissus neuroendocriniens. L'implication des MA dans le développement a été examinée par des expériences pharmacologiques. Les effets des ISRS ont été évalués en utilisant la fluoxétine (FLX) et le citalopram (CIT), avec une analyse de leurs cibles dans le génome et le transcriptome.

Six systèmes MA ont été identifiés dans le génome de *M. galloprovincialis*, avec la 5-HT et la DA étant les plus exprimés pendant le développement. Les cellules produisant de la 5-HT et de la DA se localisent dans les zones neuroendocrines, notamment l'organe apical/ganglion cérébral et les ganglions pédieux, respectivement. L'expression de la L-aminoacide décarboxylase et des récepteurs de la sérotonine et de la dopamine (5-HTRs et DRs) avant la synthèse de la 5-HT et de la DA suggère que ces éléments pourraient jouer des rôles morphogénétiques et être impliqués dans les interactions environnementales. Les résultats transcriptomiques et pharmacologiques indiquent que la 5-HT et la DA jouent des rôles clés dans le développement larvaire et la biogenèse de la coquille. La localisation des 5-HTRs et des

DRs au cours du développement, ainsi que leur relation spatiale avec les enzymes de synthèse, suggèrent leur implication potentielle dans les fonctions synaptiques et neuroendocriniennes. En outre, la colocalisation de 5-HTR1A_{inv} et de DR3-like implique une régulation réciproque possible entre les systèmes sérotoninergique et dopaminergique. *M. galloprovincialis* possède deux types de cibles pour les ISRS : sélectives (SERT) et non sélectives (Nose Resistant to Fluoxetine – nrf, et 5-HTRs). Ces cibles ont montré une expression différentielle pendant le développement embryonnaire-larvaire. L'exposition à des concentrations élevées de FLX et de CIT n'a pas fortement affecté les phénotypes larvaires, suggérant certains mécanismes de résistance où le nrf pourrait jouer un rôle.

Ce travail présente pour la première fois une caractérisation complète du système MA chez *M. galloprovincialis* ; en outre, l'identification de différentes cibles des ISRS ouvre la voie à des études futures sur le rôle du système MA au cours du développement et en réponse à divers facteurs de stress environnementaux, incluant les ISRS et, potentiellement, d'autres antidépresseurs libérés dans les milieux côtiers marins.

Mots-clés : *Mytilus galloprovincialis*, système monoaminergique, développement, contaminants, toxicologie

Introduction

Chapter 1

1 The Invertebrate Nervous and Neuroendocrine Systems

1.1 Nervous system: neurons and glial cells

The nervous system consists of specialised cells, neurons and glial cells, involved in perceiving and processing responses to internal and external stimuli, and it is present in all animals except Porifera and Placozoa (Figure 1.1) (Hartenstein, 2016; Miguel-Tomé and Llinás, 2021).

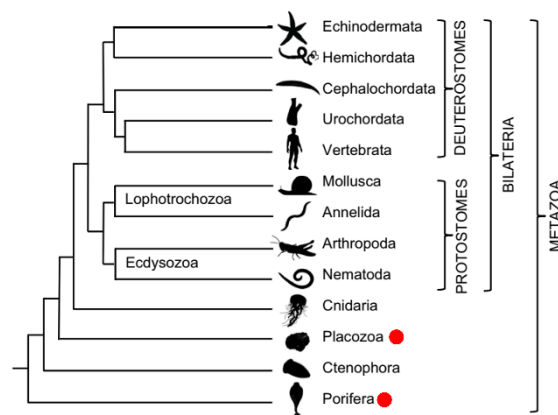


Figure 1.1. A phylogenetic tree showing the relationships between animal phyla. The red dots indicate the absence of the nervous system. Image taken from Elphick et al. (2018).

A neuron is a specialised cell, and it is identified by the presence of three key features that must be present simultaneously. Two cardinal features are excitability and the secretion of active substances. These two features are essential but not sufficient to identify a neuron. Indeed cells that are not neuronal can be electrically excitable, for example, muscle cells; moreover, cells capable of propagating action potentials were identified in sponges, animals that do not possess a nervous system (Meinertzhagen, 2019). The third and last universal characteristic that distinguishes neurons from other cells is the presence of a long cell process: the neurite. It is the triad of these features that defines a neuron (Meinertzhagen, 2019; Richter et al., 2010). Neurons consist of a cell body called *soma* (or *perikaryon*) and of cellular elongations, called neurites. Invertebrate soma can range from 1 μm in small insects to 1 mm in largest cells, such as the one of the gastropod *Aplysia*. It has been reported that in species where miniaturisation occurs, most of the soma is occupied by the nucleus (Meinertzhagen, 2019). Most invertebrates bear neurons that are called monopolar (or unipolar), meaning that the soma has a single neurite that can show several arborisations; moreover, the soma lacks neurites and cell contacts and

this is the main difference between invertebrates and vertebrates neurons (Figure 1.2A) (Meinertzhagen, 2019; Richter et al., 2010). The primary neurites of unipolar neurons present arborisations and connect the soma to dendrites and axons (Richter et al., 2010). Dendrites are generally considered as the region where the input arrives and the axon is the prolongation that transmits the signal to other cells (Nieuwenhuys et al., 2014). Unipolar neurons are particularly specific to arthropods, molluscs and several groups of annelids; in contrast, other invertebrates possess other types of neurons, including bipolar neurons, pseudounipolar neurons and multipolar neurons (Figure 1.2 B-D) (Meinertzhagen, 2019; Poli and Fabbri, 2018; Richter et al., 2010). Bipolar neurons have a soma that gives separately rise to an axon and one primary dendrite; pseudo-unipolar neurons are characterised by the primary neurite that splits into an axon and a dendrite, and multipolar neurons are characterised by one axon and/or many dendrites (Richter et al., 2010).

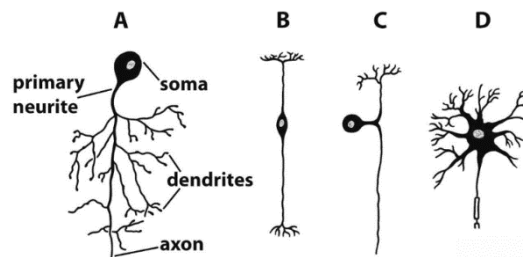


Figure 1.2 Schematic representation of different types of neurons. A. Unipolar neuron. B. Bipolar neuron. C. Pseudo-unipolar neuron. D. Multipolar neuron. Picture taken from Richter et al. (2010).

In most invertebrates, neurons bear cilia. Cilia are structures that extend from the soma and are characterised by the presence of microtubules arranged in the form 9+2 (when there is dynein), identifying thus motile cilia, or in the form 9+0, identifying primary cilia.

Neurons interact with each other or other cells through synapses. A synapse is a cell-to-cell junction and it can be a chemical or an electrical synapse (Richter et al., 2010). Electrical synapses are characterised by membrane apposition between two neurons and the current from the presynaptic neuron is sufficient to excite the postsynaptic one (Richter et al., 2010; Meinertzhagen, 2019). The current passes from the first to the second neuron *via* gap junctions, which are channel proteins. Channel proteins in protostomes are called innexins, and in deuterostomes connexins; moreover, a third family of protein, the pannexins, is present in all Metazoa except echinoderms (Meinertzhagen, 2019). Chemical synapses are characterised by the release of an active substance into the synaptic cleft and the activation of a receptor in the postsynaptic membrane (Nieuwenhuys et al., 2014; Richter et al., 2010). Although it has been reported that most invertebrate synapses lack a clear presynaptic organisation, they can be

identified by the presence of organelles called synaptic vesicles in the presynaptic neuron (Meinertzhagen, 2019). Two types of vesicles exist and differ in size and in the transmitters they contain. Small clear-core vesicles range from 30 to 80 nm in diameter and are packed with classical neurotransmitters such as acetylcholine or glutamate; large dense core vesicles have a diameter of up to 180 nm and are filled with bigger molecules, generally neuropeptides (Kirchner et al., 2023; Meinertzhagen, 2019; Purves et al., 2001). Differently from vertebrates, synapses called polyads (dyad and triad) are present in the invertebrate nervous system and even higher polyads were recorded (Meinertzhagen, 2019). Even though most of the synapses are monads, meaning that there is a single presynaptic element opposite to the postsynaptic site (Meinertzhagen, 2019).

As previously mentioned, most invertebrate neurons are unipolar, meaning that they lack somatic dendrites and reception of information and their integration occurs at the level of the neurite, where both pre- and postsynaptic contacts are mixed promiscuously (Meinertzhagen, 2019). Another important feature of invertebrate neurons is that they lack the myelin sheath (Meinertzhagen, 2019).

In the nervous system cells that are not neurons are found which are called the glial cells. These cells interact with neurons and are involved in different functions such as providing nutrients to neurons, removing the waste produced, supplying neurons with fuel, maintenance of neurite transmission and supporting and protecting neurons (Ortega and Olivares-Bañuelos, 2020; Richter et al., 2010). Even though glial cells were reported to be absent in marine invertebrates, several recent studies proved that these cells are present in different marine invertebrates (Ortega and Olivares-Bañuelos, 2020). A common feature of glial cells is their shape, which can be ovoid, symmetrical or asymmetrical; they have a soma ranging from 4 to 20 μm and process that can reach up to 600 μm in length (Ortega and Olivares-Bañuelos, 2020). There are three different types of glial cells: surface glia, involved in forming a “blood-brain” barrier regulating thus the flow of substance in and out the nervous system; the cortex glia, which is involved in wrapping fascicles of neurites and also neuronal cell body to isolate them from other brain regions or other neuronal structures; and the neuropile glia, which appear at the adult stage and can form a subtype, called ensheathing glia, responsible for clearing neurotransmitters from the extracellular space (Meinertzhagen, 2019).

1.2 Neurons organise to form ganglia

Neurons, especially in the adult form, aggregate to form a structure called ganglion (or ganglia, if multiple), where also glial cells can be present. In a ganglion, neurons display the soma at the surface, forming thus the cell cortex, the neurites are concentrated in the middle and form the so-called neuropil. In Protostomes the cell cortex is made up of unipolar neurons (Figure 1.2 A) and generally no synapses occur at the level of the cell cortex (Richter et al., 2010). In the neuropil of the ganglion, neurites of the neurons, whose soma is located in the cell cortex, interact with dendrites and axons of local interneurons (Richter et al., 2010). A ganglion can give rise to nerves (or neurite bundles), which are clusters of neurites arranged in parallel. Nerves connect the ganglion to the peripheral target, for example with sensory cells and/or effector cells (Richter et al., 2010). A ganglion can be composed of fused paired ganglia, thus a single ganglion, in this case, is called a hemiganglion (Richter et al., 2010). A ganglion can present connections within it, in the case of fused paired ganglion, or with other ganglion/ganglia. Commissures are neurite bundles constituted mainly of neurites and axons of interneurons and they extend typically from left to right and they medially link the ganglia; whereas a connective is again a neurite bundle with neurites and axons of interneurons but this term is used to indicate longitudinal interconnections between ganglia (Richter et al., 2010). To better understand the difference between commissure and connective, see Figure 1.3.

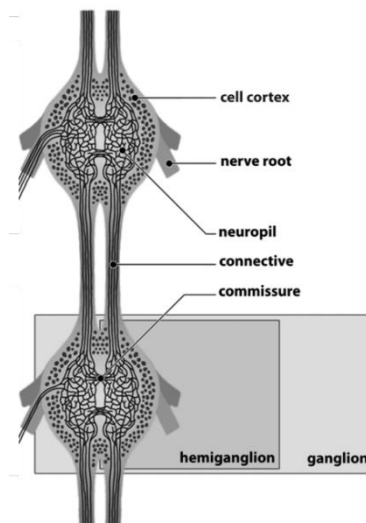


Figure 1.3. Schematic representation of two ganglia connected. Image taken from Richter et al. (2010).

1.3 Central and Peripheral nervous system and controversies

The nervous system is present in all animal taxa except Porifera and Placozoa (Hartenstein, 2016). The central nervous system can be divided into two major components: the central nervous system (CNS) and the peripheral nervous system (PNS) (Hartenstein, 2016) and this distinction is characteristic of bilaterian animals (Hartenstein, 2019; Richter et al., 2010). The CNS is characterised by regions with a high density of neurons that can be detected in some parts of the body that are involved in specialised roles, allowing the control of body functions and information integration (Hartenstein, 2016). The PNS consists of sensory neurons that can perceive stimuli such as touch, motion, sound, position, smell, taste and light (Hartenstein, 2016). Based on the type of stimulus received by the neurons of the PNS, we can divide them into mechanoreceptors, proprioceptors, chemoreceptors and photoreceptors (Hartenstein, 2016; Poli and Fabbri, 2018). Typically, the sensory neurons of the PNS form peripherally localised sensory organs (or ganglia) (Hartenstein, 2016). Moreover, part of the PNS is associated with the digestive system and muscles and, for this reason, it is called the “visceral”, autonomic or “stomatogastric” nervous system (Hartenstein, 2019, 2016). According to what was said before, the main characteristic of the CNS is the high density of neurons, but when this is the only parameter taken into account, it is difficult to identify a CNS, especially in bilaterian animals that are positioned very low in evolution, such as cnidarians; for this reason Richter et al. (2010) proposed to avoid using the terms CNS and PNS but to characterise and name thereafter cluster of neurons by their position in the body and their size (Richter et al., 2010).

1.4 Development of the larval nervous system in molluscs: an overview

Molluscs are bilaterian animals which fall into the spiralian group, due to the spiral cleavage pattern of the embryo (Escoubas et al., 2016; Hartenstein, 2019; Martín-Durán and Hejnol, 2021). Molluscs are the second largest phylum, after arthropods, regrouping several clades: the basal ones represented by Aplacophorans, Monoplachophora and Polyplachophora and the more derived clades with Gastropoda, Bivalvia, Scaphoda and Cephalopoda (Escoubas et al., 2016; Hartenstein, 2019; Wanninger and Wollesen, 2015).

The ganglia that will form the adult nervous system of molluscs originate in the proliferative region of the ectoderm. The cerebral ganglia originate from a paired cephalic plate in the

anterior pole of the developing animal; the pedal ganglia develop similarly but in the ventral region (Croll and Dickinson, 2004). It is important to note that the structure of the adult nervous system varies from species to species; for example, gastropod molluscs are endowed with other ganglia such as the buccal ganglia, the pleural ganglia and the abdominal ganglion (Kriegstein, 1977; Lin and Leise, 1996), whereas three pairs of ganglia are present in bivalve molluscs, the paired cerebropleural ganglion (CPG), the pedal and the visceral ganglia (PG and VG); reduced PG are observed in oysters due to the loss of the foot after metamorphosis (Kniazkina and Dyachuk, 2022; Nikishchenko et al., 2023; Yurchenko et al., 2018; Yurchenko and Dyachuk, 2022). A different situation is found in cephalopods where the ganglia of the head and trunk fuse to form a structure called *brain* (Hartenstein, 2019).

Among Molluscan larvae, the nervous system shows similarities and discrepancies due to differences in development (free-living planktonic larvae vs larvae subject to hatching at different points during larval development). However, some similarities are found such as the presence of an apical sensory organ and cells containing FMRFamide and catecholamines (Croll and Dickinson, 2004). The apical sensory organ or apical organ (AO) is a structure located anteriorly in the larval body. Commonly, the AO is one of the first structures to appear and is considered to have a sensory function but its function is still debated and is mostly unknown (Croll and Dickinson, 2004; Yurchenko et al., 2019). The AO in gastropods and bivalves is mainly composed of vase-shaped cells; generally, the basal portion is subepithelial and the apical portion is extended through the epidermis, and these features give them the morphology of typical sensory cells (Croll and Dickinson, 2004). There are three different types of vase-shaped cells: the ciliated-tuft cells, which bear twenty or more cilia protruding from the epidermal layer and contributing to the formation of an apical tuft; the ampullary cells, which are characterised by ciliated and deep lumens but without cilia extending above the epidermis; and the parampullary cells, which bear few cilia extending above the epidermis (Croll and Dickinson, 2004). Moreover, in the AO some round cells can be found, lacking dendritic processes (Croll and Dickinson, 2004). The number of cells in the AO varies from species to species, reflecting, probably, differences in their life history (Croll and Dickinson, 2004). Interestingly, the predominant neurotransmitter found in the AO is serotonin (5-HT), thus reflecting its probable conserved role in neuronal control of larval behaviour (Croll and Dickinson, 2004). The AO appears to project neurites towards the forming velum, an organ involved in locomotion and feeding; these neurites are positive for 5-HT, FMRFamide and catecholamines (Croll et al., 1997, 1997; Croll and Dickinson, 2004; Dickinson et al., 1999).

The presence of these neurotransmitters in neurites suggests that there could be a neuronal control of the velum ciliary activity and retraction (Croll and Dickinson, 2004; Kempf et al., 1997). The AO has been suggested to have a sensory function because of the presence of sensory cells, characterised by a vase shape and the presence of cilia, but it has also been suggested that it could be involved in responding to metamorphic cues (Croll and Dickinson, 2004; Hadfield et al., 2000). In some cases, before the emergence of the AO, other neurons, positive for the neuropeptide FMRFamide, were described to appear dorsally and ventrally (Croll and Dickinson, 2004; Yurchenko et al., 2019, 2018). In some molluscan species, these peptidergic cells were observed near the anal ciliary tuft (telotroch) suggesting a possible involvement in locomotion (Croll and Dickinson, 2004). Peripheral FMRFamide neurons are supposed also to have a role in the scaffolding of the adult nervous system (Croll and Dickinson, 2004; Yurchenko et al., 2018). Catecholaminergic cells are reported to be near the mouth but also in the velum, foot and nervous system, suggesting a possible involvement in feeding and locomotion (Croll et al., 1997; Croll and Dickinson, 2004). The fate of the AO in the adult nervous system is still debated as well as the fate of other cells here analysed (Croll and Dickinson, 2004).

1.4.1 The nervous system of bivalve larvae

Data on the neurodevelopment of bivalve molluscs are sparse and they are generally focused on the localisation of specific neurotransmitters or neuropeptides (e.g.: 5-HT and FMRFamide) and the description of the nervous system relies mostly on immunocytochemistry and histochemistry techniques because, to date, no analysis was carried out using a pan-neuronal marker (Croll and Dickinson, 2004). The data available on different species at different stages of development is reported in Figure 1.4 (Kniazkina and Dyachuk, 2022; Miglioli et al., 2021b; Nikishchenko et al., 2023; Nikishchenko and Dyachuk, 2024; Pavlicek et al., 2018; Voronezhskaya et al., 2008; Yurchenko et al., 2018). First neurons are reported to appear at the Trochophore stage in the non-paired apical sensory structure Apical Organ (AO), a structure formed of neurons bearing cilia (Kniazkina and Dyachuk, 2022; Yurchenko et al., 2019). Neurons of the apical organ were found to be positive for 5-HT- and FMRFamide-like immunoreactive (*lir*). Moreover, at the Trochophore stage, different accessory neurons were found, and they are generally FMRFamide-*lir* (Figure 1.4 A-B). No catecholamine positive cells could be found before the Veliger stage in any of the species analysed except in *Mytilus galloprovincialis*, where dopaminergic cells were observed from the late Trochophore stage by *in situ* hybridisation imaging Tyrosine Hydroxylase (TH) gene expression (Miglioli et al.,

2021b). Interestingly, in *Crassostrea gigas* the neurons forming the AO were exclusively 5-HT-*lir*, and FMRFamide-*lir* neurons in the AO appeared starting from the early Veliger stage. *Azumapecten farreri* was the only species where no FMRFamide-*lir* and 5-HT-*lir* could be detected during Trochophore stage.

At the Veliger stage more structures appeared and the AO seemed to subside in the larval body giving rise to the Apical Organ/ Cerebral Ganglion (AO/CG; to date, it is not sure if cells of the AO persist or disappear; Nikishchenko et al., 2023; Yurchenko et al., 2019). The ventral neurons (vn), which were FMRFamide-*lir* and seem to give rise to the Pedal Ganglia (PG) in *A. farreri*, *C. gigas* and *M. trossulus*; whereas only in *Spisula sybillae* it seemed that vn were not involved in forming the PG. However, the position of vn described for *S. sybillae* seemed to be more similar to the localisation of posterior neurons (pn) found in *C. gigas* and *D. polymorpha*. The pn, whose presence is detected already during Trochophore stage, in *C. gigas* and *D. polymorpha*, remained present at the Veliger stage but did not give rise to any ganglia. The Visceral Ganglia (VG) is the latest ganglionic structure to appear, and it was reported to arise at the late-Veliger stage for *C. gigas*, *M. trossulus*, and *S. sybillae* and at the pediveliger stage for *A. farreri*. Other accessory neurons were detected in different regions of the larval body with differences from species to species. *Acila insignis*, contrary to other bivalves, is characterised by the presence of a short pelagic larval stage, called pericalymma, which has been defined as a modified Veliger by Nikishchenko and Dyachuk (2024). 5-HT-*lir* neurons were detected during pericalymma stages apically, in what was named the AO. Finally, at the Pediveliger stage, all the ganglia typical of the adult nervous system appeared to be present in all the species analysed. Indeed, the structure of the AO/CG and the Pleural Ganglia (PIG), which will then fuse to give rise to the cerebro-pleuralganglia (CPG), were detected along with PG and VG. All the ganglia were interconnected to each other, and it appeared that at this stage there was already the structure of the nervous system that will remain in the adult body. Also at this stage, different accessory neurons were detected. In *C. gigas* acetylcholine was studied by using immunocytochemistry techniques (antibody against the mammalian vesicular acetylcholine transporter, VAChT). Positivity to VAChT was found starting from the Veliger stage with neurons localising within the AO/CG and pn at the early Veliger stage and in the PG at the late Veliger stage (not shown in Figure 1.4).

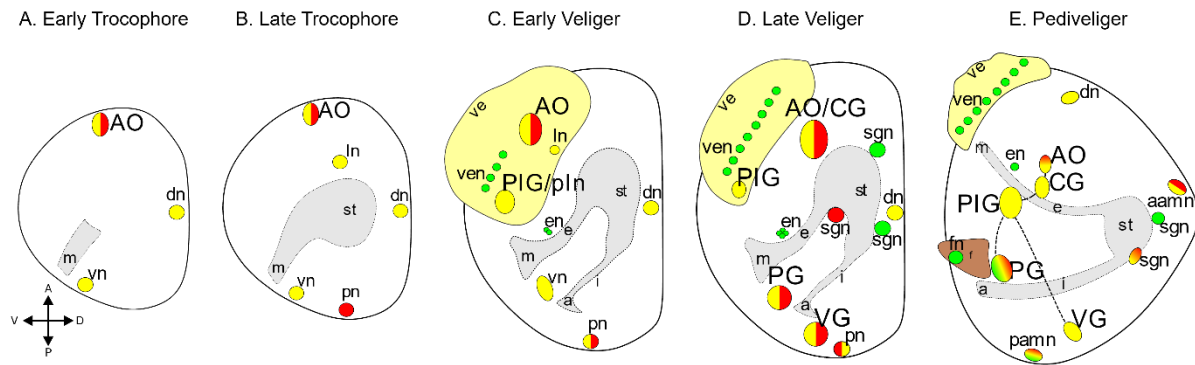


Figure 1.4. Schematic representation of neurodevelopment of different bivalve molluscs at several larval stages in lateral view. Red and yellow indicate neurons positive to 5-HT and FMRFamide antibodies, and green indicates cells positive to the catecholamine histochemistry technique. Data from early Trochophore to late Veliger are from *A. farreri*, *C. gigas*, *D. polymorpha*, *M. galloprovincialis*, *M. trossulus* and *Spisula sybilla* (for this latter data are collected starting from late Trochophore); data on *Acila insignis*, which has a pericalymma larva, are reported in the Veliger stages, data of pediveliger stage are from *A. farreri*, *Callista brevisiphonata*, *C. gigas*, *Crenomytilus grayanus*, *Kellia japonica*, *Mactomeris polynyma*, *M. trossulus* and *Mizuhopecten yessoensis*. For *M. galloprovincialis* and *A. farreri* 5-HT-*lir*, FMRFamide-*lir* and catecholamines were studied; for *C. gigas* and all the species studied at the Pediveliger stage just 5-HT-*lir* and FMRFamide-*lir* were investigated; finally, in *D. polymorpha* only 5-HT-*lir* were analysed.

- Scheme of the early Trochophore stage bearing anteriorly and apically the Apical Organ (AO) and two accessory neurons: the dorsal neurons (dn) and the ventral neurons (vn) which were FMRFamide-*lir*. At this stage, the digestive system seemed to start forming with the appearance of the mouth.
- Scheme of the late Trochophore stage. AO is still present anteriorly and other accessory neurons appeared: the lateral neurons (ln) and the posterior neurons (pn); moreover, the pn appeared to be 5-HT-*lir* in *D. polymorpha*.
- Scheme of the early Veliger stage. At this stage of development, the AO was still located anteriorly but seemed to start subsiding in the larval body within the velum. Only in *S. sybilla* the Pleural Ganglia (PIG) appeared at early Veliger. Other accessory neurons appeared: the oesophageal neurons (en), the pleural neurons (pln) the velum neurons (ven, located in the velum) and the ventral neurons (vn) located in the region between the mouth and the anus (a). At this point, the digestive system seemed to completely differentiate.
- Scheme of the late Veliger stage. At this point, the AO seemed to be completely subsided and formed the AO/CG, the ventral neurons seemed to give rise to the Pedal Ganglia (PG) and the pn seemed to give rise to the Visceral Ganglia (VG). At this stage, the number of accessory neurons increased: the en and ven increased in number, moreover different neurons called stomatogastric neurons (sgn) appeared around the stomach (st) and were positive to 5-HT and catecholamines.
- Scheme of the Pediveliger stage. At this stage of development, all ganglia were present: AO/CG, Pleural Ganglia (PIG), PG and VG. Three new types of accessory neurons appeared: the anterior adductor muscle neurons (aamn), the posterior adductor muscle neurons (pamn) and the foot neurons (fn).

Anatomical abbreviations: a: anus, e: oesophagus, i: intestine, m: mouth, st: stomach and ve: velum. Axis orientation abbreviations: A: anterior, D: dorsal, P: posterior and V: ventral. Figures were adapted from Nikishchenko et al. (2023) and Voronezhskaya et al. (2008).

As reported in Table 1.1, differences in neurotransmitters (NT) localisation occur from species to species. Of course, it must be kept in mind that not all species presented in the table were subjected to the same type of analysis, meaning that not all NTs were studied in all the species

here listed; for example, catecholamines were analysed only in *A. farreri* and *M. trossulus* by using the induced fluorescence technique (Kniazkina and Dyachuk, 2022; Voronezhskaya et al., 2008). On the contrary, 5-HT was analysed in all the species listed as shown in Table 1.1, and differences occurred across species of different infraclasses in terms of positive cells found. 5-HT-*lir* were found in all species in the AO-AO/CG from Trochophore to D-Veliger stage, with the only exception of *A. farreri*, which showed no positive cells during all the Trochophore stage, representing an unicum (Kniazkina and Dyachuk, 2022; Miglioli et al., 2024, 2021a; Pavlicek et al., 2018; Voronezhskaya et al., 2008; Yurchenko et al., 2018). Concerning *A. insignis*, as previously described, its larval stage is very short and comparable to a Veliger, where 5-HT-*lir* cells were found in the AO/CG (Nikishchenko and Dyachuk, 2024; Yurchenko and Dyachuk, 2022). Numbers of 5-HT-*lir* display a variability across larval development of all species, with the highest number of 5-HT-*lir* found in Heteroconchia (8 cells). Differences could be attributed to species-specific factors. 5-HT-*lir* were found exclusively in the PG and VG of *A. farreri* (Kniazkina and Dyachuk, 2022). Surprisingly, 5-HT-*lir* were found in accessory neurons in Pteriomorphia only in *C. gigas*, perhaps representing a peculiarity of this species; the two species of Heteroconchia, *D. polymorpha* and *A. farreri* presented both accessory neurons positive to 5-HT (Kniazkina and Dyachuk, 2022; Pavlicek et al., 2018; Yurchenko et al., 2018). FMRFamide-*lir* were found to be present in the four main ganglia: in all species analysed, FMRFamide-*lir* were present in the AO-AO/CG, PG and accessory neurons. In *A. farreri*, *M. trossulus* and *S. sybillae* FMRFamide-*lir* were also found in PIG and VG, but PIG was not found in *M. trossulus* until Pediveliger stage. *M. trossulus* displayed the highest number of FMRFamide-*lir* in the PG and VG. (Kniazkina and Dyachuk, 2022; Nikishchenko and Dyachuk, 2024; Voronezhskaya et al., 2008; Yurchenko et al., 2018). Catecholamines were found only in accessory neurons and never in any ganglia until the Pediveliger stage (Kniazkina and Dyachuk, 2022; Nikishchenko et al., 2023; Voronezhskaya et al., 2008).

	Infraclass	Pteriormorphia				Heteroconchia		Protobranchia
		Order	Mytiloidea	Mytiloidea	Ostreida	Pectinida	Venerida	Myida
	Species	<i>M. galloprovincialis</i>	<i>M. trossulus</i>	<i>C. gigas</i>	<i>A. farreri</i>	<i>S. sybillae</i>	<i>D. polymorpha</i>	<i>A. insignis</i>
	NT analysed	■	■ ■ ■	■ ■	■ ■ ■	■ ■	■	■
Early Trochophore	AO	2	1	2	0	N.A.	1	N.A.
	AO	/	1	0	0	N.A.	/	N.A.
	AO	/	0	/	0	0	/	N.A.
Late Trochophore	AO	3	3	2	0	1	4	N.A.
	AO	/	3-4	2	0	6	/	N.A.
	AO	/	0	/	0	/	/	N.A.
Early Veliger	AO/CG	4	3	3	5	2	7	2
	AO/CG	/	5	2-4	2	2	/	/
	AO/CG	/	0	/	0	/	/	/
	PIG	N.D.	N.D.	N.D.	N.D.	0	N.D.	N.D.
	PIG					2		
PIG					0			
Late Veliger	AO/CG	7	5	>5	>5	8	8	3
	AO/CG	/	8	6	8	6	/	-
	AO/CG	/	0	/	0	-	/	-
	PIG	N.D.	N.D.	N.D.	0	0	N.D.	N.D.
	PIG				N.C.	4		
	PIG				0	0		
	PG	N.D.	0	N.C.	N.C.	0	N.D.	N.D.
	PG		2×(3-5)	2	N.C.	4		
	PG		0	0	0	0		
	VG	N.D.	0	N.D.	N.C.	0	N.D.	N.D.
VG	2×(2-3)		N.C.		2			
VG	0		/		0			
All stages	Accessory neurons	/	■ ■	■ ■	■ ■	■ ■	■	/

Table 1.1. Table showing the localisation of neurotransmitters (NTs) and the number of positive cells in different species of bivalve molluscs during embryo-larval development until the late Veliger stage. The colour coding is as follows: red for 5-HT-*lir*, yellow for FMRFamide-*lir* and green for catecholamines. Abbreviation coding is as follows: N.A. = not analysed, N.C. = not counted, N.D. = not detected. Infraclasses and orders were retrieved from WoRMS Editorial Board (2024).

As previously described and as shown in Figure 1.4, information regarding the nervous system in bivalve molluscs is sparse and focuses on 5-HT, FMRFamide and catecholamines only. Moreover, it is necessary to point out that the technique to detect catecholamines (the Formaldehyde-Glutaraldehyde-induced fluorescence) does not make any distinction between DA, NA and A ; moreover, it can target also 5-HT and its precursor, 5-hydroxytryptophan (Kniazkina and Dyachuk, 2022). The techniques used to date allowed to identify different populations of neurons, but it remains unknown if with antibodies and induced fluorescence the targeted structures represent the site of synthesis of the neurotransmitter or a centre where the neurotransmitter may be concentrated because it exerts in a specific tissue its action. Moreover, the nervous system structure has been so far described only by the presence/absence of neurotransmitters with no information about the neurotransmitters' metabolic pathways (synthesis enzymes, degradation enzymes) and receptors.

2.1 The neuroendocrine system

2.1.1 Endocrine signalling: definition and controversies

As mentioned above, the nervous system is involved in perceiving external and internal stimuli and it is involved in communicating information to elaborate physiological responses (Carrillo-Baltodano et al., 2024; Hartenstein, 2016; Miguel-Tomé and Llinás, 2021). To do so, a signalling method is required and it involves two main types of communication: paracrine, where the cells involved are in direct contact such as in chemical synapses (Hartenstein, 2006; Nickel, 2010; Wang et al., 2013), and endocrine, where the cells are not in direct contact and involves the secretion of messengers (i.e. hormones or other signalling molecules) (Hartenstein, 2006). In bilaterians, the endocrine system consists of different specialised cell populations releasing chemicals in circulating body fluids which act on distant targets (Fabbri et al., 2024; Nussey and Whitehead, 2001). The chemicals released by the endocrine systems are called hormones, whose original definition by Starling (1905) was: “a substance produced by glands with internal secretion, which serve to carry signals through the blood to target organs” (Stárka and Dušková, 2020). This definition was improved to try to encompass the definition of hormone to other chemicals that are not necessarily produced by specialised glands but in other tissues (Stárka and Dušková, 2020). A newer definition is the one proposed in the Encyclopaedia Britannica: “Hormone, an organic substance secreted by plants and animals that functions in the regulation of physiological activities and in maintaining homeostasis.” (Barrington, 2024; Stárka and Dušková, 2020). This definition, in this context, is more correct because it does not impose the presence of a canonical endocrine system; indeed the majority of invertebrates (except Arthropoda) lack well defined glands typical of canonical endocrine system (Fabbri et al., 2024). By the way, this lack does not necessarily imply that there are no endocrine communications in invertebrates; indeed neuroendocrine cells, present in all animals endowed with a nervous system, possess neurosecretory neurons (Hartenstein, 2006; Schwartz and Norris, 2024; Tessmar-Raible, 2007). Thus, it is possible to talk of neuroendocrine system, defined as follows: “A neuroendocrine system consists of a neural cell or cells which secrete into the extracellular fluid a substance which upon reaching other cells modify their behaviour.” (Porter, 1973).

2.1.2 Secretory neurons

Neurosecretory neurons are characterised by the presence of large dense core vesicles (DCVs) distinct from the synaptic vesicles found at the synapse level, these DCVs are produced in the

soma and are distributed throughout the neuron cell body (Hartenstein, 2006; Tessmar-Raible, 2007). Such neurons can synthesise hormones of different chemical nature:

- Peptides: produced first in the rough endoplasmic reticulum and then processed in the Golgi apparatus, stored in vesicles and exerting their action through G-protein-coupled receptors (GPCRs).
- Lipid derivatives: synthesised in the smooth reticulum but not stored in vesicles which exert their action through transcription factors localised in the cytoplasm.
- Amino acids derivatives (e.g.: monoamines) (Hartenstein, 2006; Joyce and Vogeler, 2018; Kleine and Rossmann, 2016; Tessmar-Raible, 2007; Wuttke et al., 2010).

Neurosecretory neurons are endowed with a specific molecular repertoire: peptidases, involved in processing the precursor of neuropeptide and hormones, enzymes for specification and activation of neuropeptides (e.g.: N-terminal acylation and pyrolylation, C-terminal amidation) and hormones, and molecules required for the release of peptide and non-peptidic modulators through a Ca^{2+} -dependent release.

The presence of secretory neurons is reported in animals possessing a nervous system, even in low phylogenetically animals such as cnidarians (Hartenstein, 2006; Jékely, 2021; Tessmar-Raible, 2007). In molluscs a neuroendocrine system has been reported; in particular, the presence of neurosecretory cells and neurohemal structures were shown where the neurites terminations release their content into the haemolymph. Moreover, in many cases, non-neuronal secretory cells are found at the level of neurohemal regions and they are under the control of the nervous system (Figure 1.5) (Hartenstein, 2006; Tessmar-Raible, 2007). Bodies of neurosecretory cells are often localised in specific areas of the nervous system; but finding homologies between neurosecretory systems between adults is difficult, as neurons can undergo long migration during development (Hartenstein, 2006).

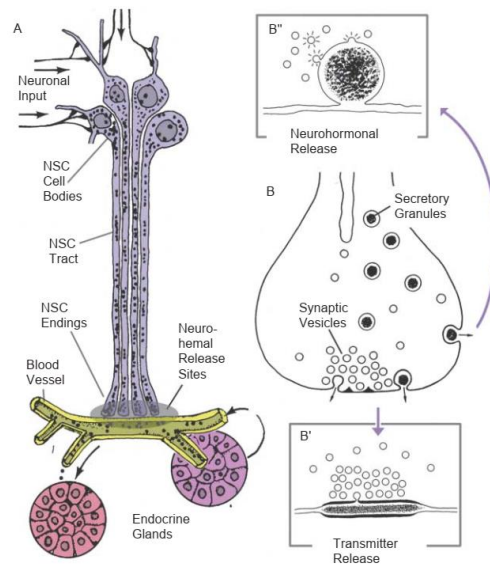


Figure 1.5. Schematic representation of the neuroendocrine system. A. Neurosecretory cells (NSC) are represented in violet, and their soma is localised in the nervous system, the neurite projects from the soma to reach the sites of neurohemal release, where blood vessels are located (yellow); in pink/purple glands are represented even though they are not always present. B. Magnification of neurite terminal containing synaptic. B' and B'' show a greater magnification of neurotransmitter release and hormone release, respectively. Image taken from Hartenstein (2006).

Chapter 2

2 The monoaminergic system

2.1 Monoamines: definition

Monoamines are biogenic amines typical of bilaterian animals and they function as neurotransmitters, neuromodulators and/or neurohormones (Donly and Caveney, 2005; Gallo et al., 2016; Goulty et al., 2023; Libersat and Pflueger, 2004; Liu et al., 2018; Sloley and Juorio, 1995; Tierney, 2020). This means that they exert their action in the nervous system at the synaptic level, modulating the activity of neurons, but also in broader areas far away from the synthesis site, exerting their action within the organism by circulating in the blood or haemolymph (Libersat and Pflueger, 2004). Monoamines are involved in the regulation of a variety of functions such as motor control, feeding, social and sexual behaviours, reproduction, growth, circadian rhythms, emotional state, cardiovascular homeostasis, thermoregulation, endocrine secretion, learning, memory and stress response (Blenau and Baumann, 2001; Brown et al., 2018; Canesi et al., 2022; Donly and Caveney, 2005; Maugars et al., 2020; Swallow et al., 2016; Tierney, 2020).

Monoamines include the indoleamines serotonin (5-HT) and melatonin (MT), the catecholamines dopamine (DA), noradrenaline (NA) and adrenaline (A), the phenolamines tyramine (TA) and octopamine (OA) and the imidazolamine histamine (HS) (Donly and Caveney, 2005; Maugars et al., 2020).

2.2 Monoaminergic system: enzymes, transporters and receptors and their presence/absence across different species

Monoamines are synthesised from amino acids in single and/or multistep reactions: L-Tryptophan is the precursor of indolamines, L-Tyrosine of catecholamines and phenolamines and L-Histidine is the precursor of histamine (Blenau and Baumann, 2001; Verlinden, 2018). Animals are, thus, dependent on the intake of essential amino acids from food but the supply of L-Tyrosine is scarce; for this reason, monoamines that require L-Tyrosine as a precursor are mostly derived from L-Phenylalanine (Yamamoto and Vernier, 2011). Monoamine synthesis is necessary but not sufficient to exert their actions; indeed, the need to be stored, release and

eventually cleared from the extracellular medium to act properly (Gallo et al., 2016; Goulty et al., 2023). Moreover, their concentration can be regulated by degradation by catabolic enzymes. Finally, monoamines exert their action by binding to receptors, which are represented by G-protein coupled receptors (GPCRs) and (Goulty et al., 2023; Yamamoto and Vernier, 2011). All monoamines exert their action by binding to GPCRs; serotonin only can exert its action also by binding to a specific family of receptors that are ligand-gated ion channel receptors (Bauknecht and Jékely, 2017; Hoyer, 2019a; Schwartz et al., 2021; Yamamoto and Vernier, 2011). A schematic representation of the monoaminergic system is provided herein at the end of this section, along with all the necessary abbreviations (see Figure 2.2).

2.2.1 Synthesis enzymes

Reactions catalysed by the enzymes mentioned below and their products are summarised in Figure 2.1.

2.2.1.1 Aromatic amino acids hydroxylase (AAAHs)

L-Phenylalanine is converted into L-Tyrosine by the enzyme phenylalanine hydroxylase (PAH) (Yamamoto and Vernier, 2011). Indolamines and catecholamines synthesis begins with the addition of a hydroxyl group to the amino acid by enzymes of the family of aromatic amino acids hydroxylases (AAAHs). This family of enzymes encompass PAH, mentioned before, tryptophan hydroxylase (TPH) and tyrosine hydroxylase (TH); the last two enzymes are the rate-limiting enzymes of indolamines and catecholamines biosynthesis (Goulty et al., 2023; Verlinden, 2018).

2.2.1.2 Aromatic amino acid decarboxylases (AADCs)

The aromatic amino acid decarboxylase family includes the enzymes: aromatic L-amino acid decarboxylase (AADC, also known as dopa decarboxylase DDC) which removes a carboxyl group from 5-hydroxy-tryptophan and L-3,4-dihydroxyphenylalanine producing 5-HT and DA, tyrosine decarboxylase (TDC) which adds a carboxyl group to L-Tyrosine to produce tyramine, and histidine decarboxylase (HDC) which converts L-Histidine into histamine. AADC bears this name because it shows affinity towards a broad range of substrates (aromatic L-amino acids and α -methylated amino acids) (Zhu and Juorio, 1995); moreover it was reported that it is able to decarboxylate L-tyrosine to produce tyramine (Pryor et al., 2016).

Serotonin and dopamine can undergo further modification to give rise to melatonin (MT), noradrenaline, and adrenaline, respectively. Concerning melatonin genes were found so far only

in tetrapods. For this reason, MT will not be further analysed in this thesis because of scarce data available in invertebrates.

2.2.1.3 Copper-dependent hydroxylases

Dopamine and tyramine can be further metabolised by the addition of a second hydroxyl group by, respectively, dopamine- β -hydroxylase (DBH) and tyramine- β -hydroxylase (TBH) which belong to the family of copper-dependent hydroxylases (Vendelboe et al., 2016; Verlinden, 2018, 2018; Xu et al., 2016). This family also contains the enzyme monooxygenase DBH-like (MOXD), whose function is still unknown (Goultly et al., 2023; Xin et al., 2004). Furthermore, noradrenaline can be further metabolised by phenylethanolamine-N-methyltransferase (PNMT) to produce adrenaline. Of note, adrenaline synthesis enzyme is found within vertebrates (Goultly et al., 2023).

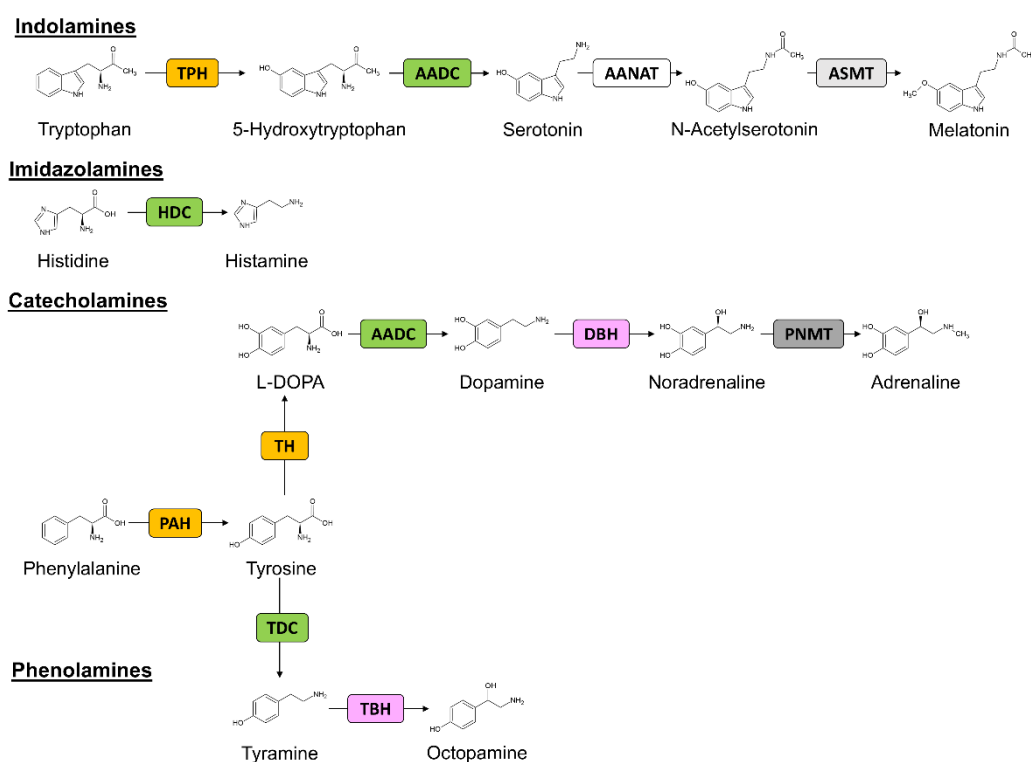


Figure 2.1. Overview of monoamines and their synthetic pathway. Monoamines are classified in each line depending on their chemical structure. Each synthesis pathway includes the substrates and products, arrows indicate the reaction with the abbreviations of the enzyme's name. Enzymes belonging to the same family are highlighted with the same colour: yellow for aromatic amino acid hydroxylase (AAAH), green for aromatic amino acids decarboxylase (AADC) and rose for copper-dependent hydroxylases. In white, light grey and dark grey, there are the enzymes responsible for melatonin (black and light grey) and adrenaline (dark grey) synthesis, which belong to different enzyme families. PAH phenylalanine hydroxylase, TPH tryptophan hydroxylase, TH tyrosine hydroxylase, AADC aromatic L-amino acid decarboxylase, HDC histidine decarboxylase, TDC tyrosine decarboxylase, DBH dopamine- β -hydroxylase, TBH tyramine- β -hydroxylase, AANAT aralkylamine N-acetyltransferase, ASMT acetylserotonin N-methyltransferase, PNMT phenylethanolamine N-methyltransferase.

2.2.2 Degradation enzymes

Endogenous and exogenous monoamines are known to be metabolised by monoamine oxidases (MAOs) in vertebrates and invertebrates. There are two isoenzymes of MAOs: MAO-A and MAO-B, characterised by different affinities towards their substrate and inhibitors (Finberg and Rabey, 2016; Wilson et al., 2020). MAO-A acts mostly on hydroxylated amines, such as serotonin and noradrenaline, whereas MAO-B shows a higher affinity towards non-hydroxylated amines (e.g.: benzylamine and beta-phenylethylamine). Dopamine and tyramine are substrates of both isoforms (Finberg and Rabey, 2016).

Invertebrates were reported to inactivate monoamines by N-acetylation, γ -glutamyl-conjugation, sulfation, β -alanyl-conjugation and sugar-conjugation but the specific enzymes involved in these pathways were not reported (Sloley, 2004).

2.2.3 Vesicular and membrane transporters

Once synthesised, monoamines are actively stored in vesicles by the vesicular monoamine transporters (VMATs), which are fuelled by a V-type H⁺-ATPase, which exchanges one cytosolic monoamine with luminal protons (Anne and Gasnier, 2014). VMATs belong to the Solute Ligand Carrier 18 (SLC18) group of the Major Facilitator Superfamily (MFS) Transporters. Once released in the synaptic cleft, the control of duration of signal transmission is regulated by the re-uptake of the monoamine. Monoamines are subject to re-uptake by specific re-uptake transporters that belong to the group SLC6A (or sodium: neurotransmitter symporter family – SNF) (Caveney et al., 2006; Lai, 2013). Differently from VMAT, which is typical to all monoamines, different subtypes of SLC6A are specific for one (or two) monoamines. Indeed, there are the serotonin re-uptake transporter (SERT, SLC6A4), the dopamine transporter (DAT, SLC6A3), the noradrenaline/adrenaline transporter (NET, SLC6A2) and the octopamine/tyramine transporter (OAT) (Caveney et al., 2006; Lai, 2013; Ribeiro and Patocka, 2013). To date, no histamine transporter was found and none of the previous ones appear to recognise histamine (Ribeiro and Patocka, 2013).

2.2.4 Monoamines Receptors

Serotonin receptors (5-HTRs)

Serotonin receptors are divided into seven families and fourteen different receptors were identified in vertebrates (Hasan et al., 2019; Nichols and Nichols, 2008; Tierney, 2018). In Table 1.1 the different subtypes identified are listed. Except for 5-HTR3, which is a ligand-

gated ion channel, the other families are GPCRs (Hasan et al., 2019; Hoyer, 2019b; Nichols and Nichols, 2008; Tierney, 2018).

5-HTR1	5-HTR2	5-HTR3	5-HTR4	5-HTR5	5-HTR6	5-HTR7
5-HTR1A	5-HTR2A	5-HTR3A	5-HTR4	5-HTR5A	5-HTR6	5-HTR7
5-HTR1B	5-HTR2B	5-HTR3B		5-HTR5B		
5-HTR1D	5-HTR2C	5-HTR3C				
5-HTR1E		5-HTR3D				
5-HTR1F		5-HTR3E				

Table 2.1. Classification of 5-HTRs in the seven families identified to date and their respective subtypes in vertebrates.

Each of the family identified trigger a specific intracellular response by binding a G-protein. 5-HTR1 and 5-HTR5 couple preferentially with $G_{i/o}$ proteins, leading to a decrease of intracellular cyclic-AMP (cAMP); however the role of 5-HTR5 and the response it triggers is still debated (Frazer and Hensler, 1999; Hoyer, 2019a; Tierney, 2020). Indeed only 5-HTR5A product was reported in human where it was reported to a decrease of intracellular cAMP levels; on the contrary 5-HTR5B transduction properties are still unknown (Carson et al., 1996; Frazer and Hensler, 1999). 5-HTR2 couples with $G_{q/11}$ and triggers the activation of phospholipase C (PLC) leading to the production of inositol-triphosphate that induces elevated Ca^{2+} levels (Frazer and Hensler, 1999; Hoyer, 2019a; Tierney, 2018). 5-HTR3 is the only receptor to be a ligand-gated ion channel, 5-HTR3 is a non-selective cation channel, thus it allows the influx of Na^+ and K^+ , leading to a transient depolarisation (Hoyer, 2019a). 5-HTR4, 5-HTR6 and 5-HTR7 lead to an increase in cAMP by coupling to G_s proteins (Frazer and Hensler, 1999; Hoyer, 2019a; Tierney, 2018).

Melatonin receptors (MTRs)

Melatonin receptors are phylogenetically classified in tetrapods in three distinct subtypes: MTR1, MTR2 and MTR3. MTR3 was identified in mammals but cannot bind MT. Another receptor, Mel1d, was recently discovered to be present in bony fish and tetrapods but lost in birds and mammals (Denker et al., 2019; Maugars et al., 2020; Wang et al., 2022). Mel1d was also called MTR1-like due to its similarity with MTR1 (Denker et al., 2019; Maugars et al., 2020). MTR1 is coupled with different G-proteins creating, thus, a variety of responses, whereas MTR2 is preferentially coupled with G_i (Amini et al., 2021; Jockers et al., 2008; Witt-Enderby et al., 2003).

Dopamine receptors (DRs)

Dopamine receptors are all GPCRs, they are divided into two families, based on the G-protein recruited and up to five subtypes were identified in vertebrates. The families are called DR1-like and DR2-like and they recruit G_s , leading to an increase in cAMP levels, and G_i , leading to a decrease in intracellular cAMP respectively (Bhatia et al., 2024; Le Crom et al., 2003; Mustard et al., 2005; Schwartz et al., 2021; Suo et al., 2004). For subtypes classification, see Table 2.2. In protostomes, a specific invertebrate dopamine receptor (DR2/INDR) was identified and phylogenetically it resulted to be close to the vertebrate DR1-like family, indeed the activation of this subtype leads to an increase of cAMP intracellular levels and, in addition to this, it can also couple to G_q leading, thus, to an increase of Ca^{2+} (Schwartz et al., 2021). Moreover, in Arthropoda, a receptor that binds both DA and steroid hormone (e.g.: ecdysone) called DR/EcdR was identified (Schwartz et al., 2021).

DR1-like	DR2-like
DR1	DR2
DR5	DR3
	DR4

Table 2.2. Classification of DRs in the two families with the respective subtypes.

Adrenergic receptors (ARs)

Adrenergic receptors are GPCRs for NA and A (Gnegy, 2012). ARs are classified into three families: $\alpha 1$ -ARs, $\alpha 2$ -AR and β -ARs and NA and A can bind to the same AR (Bylund, 2003; Waxham, 2014). Each of the family possesses three receptor subtypes (Table 2.3) (Bylund, 2003; Waxham, 2014). Adrenergic receptors recruit different G-proteins based on their classification: $\alpha 1$ -ARs are coupled with G_q , $\alpha 2$ -ARs are coupled with G_i and β -ARs with G_s (Farzam et al., 2024; Gnegy, 2012).

$\alpha 1$ -AR	$\alpha 2$ -AR	β -AR
$\alpha 1A$ -AR	$\alpha 2A$ -AR	$\beta 1$ -AR
$\alpha 1B$ -AR	$\alpha 2B$ -AR	$\beta 2$ -AR
$\alpha 1D$ -AR	$\alpha 2C$ -AR	$\beta 3$ -AR

Table 2.3. Classification of ARs in three families with their respective subtypes.

Octopamine receptors (OARs)

Octopamine is generally thought to be the invertebrate counterpart of NA, even though trace amounts of OA were reported in the central and peripheral nervous system of vertebrates (Farooqui, 2012, 2007; Pryor et al., 2016). Octopamine receptors are nowadays classified into two or three classes depending on the author's way of classification, but the new classification

of OARs identifies two classes with their respective subtypes and studies were mainly conducted in insects (see Table 2.4) (Bauknecht and Jékely, 2017; Blenau et al., 2022; Farooqui, 2012, 2007). The two families are the following and they comprehend different subtypes: α -OAR and β -OAR (Bauknecht and Jékely, 2017; Farooqui, 2012, 2007). α -OAR σ are coupled with G_q and with G_s proteins, β -OARs are coupled solely with G_s (Farooqui, 2012).

α -OAR	β -OAR
α -OAR	β 1-OAR
	β 2-OAR
	β 3-OAR

Table 2.4. Classification of OARs in three families with their respective subtypes.

Tyramine receptors (TARs)

Tyramine, as well as OA, is typical of invertebrates and it is found in traces in vertebrates (Pryor et al., 2016). In insects, tyramine receptors have been well characterised and are classified into two families: tyramine type 1 (TAR1), tyramine type 2 (TAR2) and tyramine type 3 (TAR3) and, to date, just one gene of the fruit fly, *Drosophila melanogaster*, was found to represent the TAR3 type (Bauknecht and Jékely, 2017; Blenau et al., 2022; Farooqui, 2012; Finetti et al., 2021). Different from other receptors, TARs have no subtypes in their family (Farooqui, 2012). TAR1 is coupled with G_i and G_q proteins, TAR2 is coupled with G_q protein and TAR3 can couple with G_s and G_q (Blenau et al., 2022; Farooqui, 2012; Finetti et al., 2021).

Histamine receptors (HSRs)

In vertebrates, and more generally in deuterostomes, four different subtypes of histamine receptors were identified: HSR1, HSR2, HSR3 and HSR4, this latter not found in protostomes (Ravhe et al., 2021). HSR1 is linked with G_q , HSR2 with G_s and HSR3 and HSR4 with G_i (Hill, 1991; Parsons and Ganellin, 2006; Unen et al., 2016).

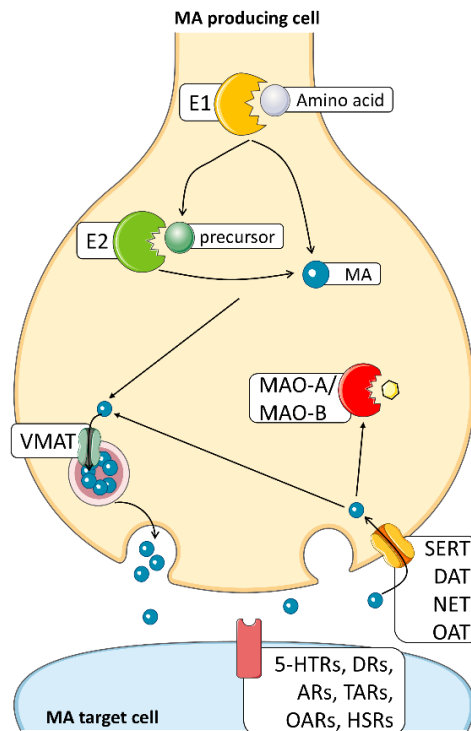


Figure 2.2. Schematic representation of a monoamine (MA) producing cell. E1 and E2 represent enzyme 1 and enzyme 2, respectively, depending on the synthetic pathway of the MA (see Figure 2.1). Degradation enzymes (2.2.2), vesicle and membrane transporters (2.2.3) and receptors (2.2.4) and are indicated with the abbreviations provided in the sections above. Figure adapted from Goulty et al. (2023). Images adapted from Servier Medical Art, licensed under CC BY 4.0 (<https://smart.servier.com>).

2.3 Presence/absence of monoaminergic system across evolution

A recent study based on phylogenomic analysis pointed out that the monoaminergic system is a bilaterian innovation (Goulty et al., 2023). In Table 2.5, a state-of-the-art of the presence/absence of genes across the following bilaterian species is reported for *Caenorhabditis elegans*, *Drosophila melanogaster*, *Crassostrea gigas*, *Strongylocentrotus purpuratus*, *Ciona intestinalis*, *Branchiostoma floridae*, *Danio rerio* and *Homo sapiens*.

The synthesis enzymes of 5-HT and DA (i.e.: TPH, TH and AADC) are found across all the species listed. HDC was found in all species listed here except for *C. elegans* and *C. intestinalis*. *C. elegans* does not produce histamine itself but obtains it from the environment, (Anctil, 2009; Burke et al., 2006; Candiani et al., 2012; Cao et al., 2010; Dag et al., 2023; Dehal et al., 2002; Francis et al., 2017; Goulty et al., 2023; Iyer et al., 2004; Kezmarsky et al., 2005; Kutchko and Siltberg-Liberles, 2013; Li et al., 2018; Lin et al., 2020; Marquina-Solis et al., 2022; Moroz et al., n.d.; Paganos et al., 2021; Pennati et al., 2024, 2007; Sáenz-de-Miera and Ayala, 2004;

Siltberg-Liberles et al., 2008, 2008; Watanabe et al., 2011; Xu et al., 2019; Yamamoto et al., 2010). TDC synthesizes tyramine, which signals through specific receptors present in Protostomia but not in Deuterostomia (Bauknecht and Jékely, 2017; Goulty et al., 2023). Consistently, TDC is reported to be present in Ecdysozoa and Mollusca and not in Deuterostomia except, surprisingly, in *S. purpuratus* where the presence of a TDC was recently reported. DBH and TBH are responsible for the synthesis of NA and OA, respectively. Ecdysozoa have TBH and not DBH; whereas other Protostomia and Deuterostomia possess DBH and not TBH, consistent with octopamine found in this species, in mammals as well as trace amine (Goulty et al., 2023; Pryor et al., 2016).

As mentioned earlier in section 2.2, invertebrates degrade MOA by forming conjugated substances (Sloley and Juorio, 1995) but MAOs are present across all Bilateria. Indeed, one MAO has been found in all the species here analysed except *D. melanogaster*, where MOAs are absent. No information is available for the presence or absence of MAOs in *Branchiostoma floridae* (Baronio et al., 2022; Boos et al., 2021; Boutet et al., 2004; Finberg and Rabey, 2016; Martin and Krantz, 2014; Roelofs and Van Haastert, 2001; Squires et al., 2010; Wilson et al., 2020).

Regarding transporters, VMAT is reported to be present in all the species analysed here (Byrne, 2019; Duerr et al., 1999; Goulty et al., 2023; Lawal and Krantz, 2013). As for membrane transporters, most information concerns SERT and DAT. SERT is present in all Bilateria, but no data are available for the bivalve mollusc *C. gigas* (Amador and McDonald, 2018; Burke et al., 2006; Camicia et al., 2022; Candiani et al., 2012; Caveney et al., 2006; Dag et al., 2023; Frese et al., 2024; Larsen et al., 2011; Matsuo et al., 2016; Pörzgen et al., 2001; Ribeiro and Patocka, 2013). Similarly, DAT is found across Bilateria, with no data available for *C. gigas*. Interestingly, it has been reported that DAT exists in invertebrates as the invertebrate dopamine transporter (iDAT), forming a separate clade in phylogenetic analysis, which acts as a sister group to vertebrate DAT and NET. NET is not reported to be present in protostome species but only in deuterostomes (Burke et al., 2006; Camicia et al., 2022; Caveney et al., 2006; Larsen et al., 2011; Pörzgen et al., 2001). Conversely, OAT has been found in various Arthropoda species (but not in *D. melanogaster*, which appears to be a specific case) and in other protostome species like the annelid *Lumbricus terrestris* and the Platyhelminthes *Schistosoma* and *Schmidtea*, suggesting that OAT might be present in other protostome species, but not in deuterostomes (Camicia et al., 2022; Caveney et al., 2006; Donly and Caveney, 2005). It should be noted that research on OAT is very limited.

Finally, the analysis of the presence/absence of receptors helps determining if the complete machinery of a MOA system is present. 5-HTRs and DRs have been extensively studied, and found in all species analysed; the only exception is *C. intestinalis*, for which no data regarding the presence of DRs were found (Albert and Lemonde, 2004; Blenau et al., 2022; Blenau and Baumann, 2001; Burke et al., 2006; Burman and Evans, 2010; Canesi et al., 2022; Dag et al., 2023; Opazo et al., 2018; Pennati et al., 2024; Rosikon et al., 2023; Schwartz et al., 2021; Sourbron et al., 2016; Souza et al., 2021; Yamamoto et al., 2010; You et al., 2023). Histamine receptors (HSRs) have been less studied, with data available for all species analysed here except for *C. gigas* and *C. intestinalis* (Burke et al., 2006; Burman et al., 2007; D’Aniello et al., 2020; Panula et al., 2022; Ravhe et al., 2021; Rosikon et al., 2023).

Regarding adrenergic receptors, α 1-ARs and α 2-ARs are present in both protostomes and deuterostomes, while β -ARs are exclusive to chordates as well as the synthesis enzyme for A, for this reason, it will not be further discussed in this thesis (Apaydin et al., 2023; Bauknecht and Jékely, 2017; Burke et al., 2006; Ruuskanen et al., 2005). Finally, OARs and TARs are reported to be exclusive of protostomes and hemichordates, and thus absent in all the rest of the deuterostomes (Bauknecht and Jékely, 2017; Evans and Maqueira, 2005; Rosikon et al., 2023; Schwartz et al., 2021).

The presence or absence of monoaminergic genes is summarised in Table 2.5.

		Protostomia				Deuterostomia			
		Ecdysozoa		Lophotocozoa	Ambulacria	Chordata			
		Nematoda	Arthropoda	Mollusca	Echinodermata	Cephalochordata	Urochordata	Vertebrata	
		<i>C. elegans</i>	<i>D. melanogaster</i>	<i>C. gigas</i>	<i>S. purpuratus</i>	<i>B. floridae</i>	<i>C. intestinalis</i>	<i>D. rerio</i>	<i>H. sapiens</i>
Synthesis	TPH	✓	✓	✓	✓	✓	✓	✓	✓
	TH	✓	✓	✓	✓	✓	✓	✓	✓
	AADC	✓	✓	✓	✓	✓	✓	✓	✓
	HDC		✓	✓	✓	✓		✓	✓
	TDC	✓	✓	✓	✓				
	DBH			✓	✓	✓	✓	✓	✓
	THB	✓	✓						
Transporters	VMAT	✓	✓	✓	✓	✓	✓	✓	✓
	SERT	✓	✓	N.A.	✓	✓	✓	✓	✓
	DAT	✓	✓	N.A.	✓	✓	✓	✓	✓
	NET			N.A.	✓	✓	✓	✓	✓
	OAT	N.A.		N.A.					
Receptors	5-HTRs	✓	✓	✓	✓	✓	✓	✓	✓
	DRs	✓	✓	✓	✓	✓	N.A.	✓	✓
	HSRs	✓	✓	✓	✓	✓	N.A.	✓	✓
	α -ARs	N.A.	N.A.	✓	✓	✓	✓	✓	✓
	β -ARs					✓	✓	✓	✓
	TARs	✓	✓	✓					
OARs	✓	✓	✓						
Degradation	MAO	✓		✓	✓	N.A.	✓	✓	✓

Table 2.5. Distribution of monoaminergic genes across different species of bilaterians. Green check boxes indicate the presence, blank cells absence and N.A. stands for not available data.

2.4 Roles of Monoamines in bivalve molluscs

2.4.1 Physiological roles

2.4.1.1 Serotonin (5-HT)

In bivalves, 5-HT was shown to have pleiotropic functions (Canesi et al., 2022). 5-HT induces spawning in several bivalve species and its concentration undergoes seasonal variations following spawning (Alavi et al., 2017). Injection of 2 mM 5-HT induced different species to spawn (*Artica islandica*, *Argopecten irradians*, *C. virginica*, *Geukensia demissa*, *Mercenaria mercenaria* and *Spisula solidissima*) with males appearing more sensitive to 5-HT than females (Gibbons and Castagna, 1984). Moreover, 5-HT-induced spawning in other species such as *Hippopus hippopus*, *H. porcellanus*, *Sphaerium transversum*, *S. striatum*, *Tridacnia gigas*, *T. dersasa*, *T. maxima*, *T. crocea* and *T. squamosa* (Braley, 1985; Fong et al., 1996; Hirai et al., 1988; Ram et al., 1993). 5-HT was shown to be involved also in meiosis re-initiation in *Hiattella flaccida* and *S. solidissima*. In *H. flaccida* addition of exogenous 5-HT at a concentration higher than or equal to 1 μ M induced the germinal vesicle breakdown (GVBD) through an increase in Ca^{2+} intracellular levels and in pH; moreover, 5-HT at concentrations equivalent to or higher than 100 nM triggered the polar body formation (Deguchi and Osanai, 1995). In *S. solidissima* 5-HT induced GVBD and extrusion of the first and second polar bodies (Hirai et al., 1988). 5-HT was shown to act also on sperm by increasing its motility (Boulais et al., 2019). In larvae of *C. gigas* 5-HT was shown to be pivotal for larval development: indeed inhibition of its synthesis led to malformed larvae (Liu et al., 2020). Liu et al. (2020) also showed that 5-HT and also DA are pivotal for a normal larval development because they control two enzymes involved in the process of shell biogenesis: tyrosinase and chitinase by triggering a TGF- β pathway. Tyrosinase was shown to play a key role in shell biogenesis also in *M. galloprovincialis* because, in concert with other enzymes/proteins, it regulated the deposition of the organic shell (mainly composed of chitin) that acts as a blueprint for the deposition of the inorganic one (Miglioli et al., 2019).

Bivalves are filter feeders and filter huge amounts of water each day (about 40 L for *Mytilus* spp.) with gills being involved in water current creation to allow both feeding and respiration (Canesi et al., 2022; Carroll and Catapane, 2007; Fabbri et al., 2023). *C. virginica* exposed to exogenous 5-HT showed a dose-dependent increase in gill ciliary beating; moreover, the application of 5-HT to visceral ganglia alone and the application of 5-HT to cerebral ganglia resulted in a dose-dependent increase of ciliary beating rates, showing that the serotonergic

system is involved in gill functioning (Carroll and Catapane, 2007). Isolated gills of *M. mercenaria* showed a dose-dependent increase in gills contraction in response to 5-HT (Gainey et al., 2003).

5-HT is also involved in controlling the siphon/mantle contraction-relaxation, the heart and the catch muscle (Canesi et al., 2022). In *D. polymorpha* exogenous 5-HT addition induced biphasic responses depending on the concentration. Low concentrations (10^{-6} , 10^{-5} M) induced relaxation, whereas high concentration (10^{-3} M) induced contraction resulting in the opening of both siphons; whereas 10^{-4} M induced a biphasic response, first a relaxation followed by a slow contraction (Ram et al., 1999). In the ventricle of *M. mercenaria* 5-HT induced positive inotropic responses in a dose-dependent way; moreover, a positive correlation between contraction after exposure and an increase in cAMP concentration was reported (Paciotti and Higgins, 1985). Moreover, 5-HT produced positive inotropic and chronotropic effects in the heart of *Meretrix lusoria* (Lee et al., 1993). Catch and adductor muscles were shown to be innervated by 5-HT positive fibres in *M. edulis* and *C. gigas*. 5-HT was shown to induce a rapid relaxation of the catch muscle by inducing an increase in intracellular levels of cAMP (Dyachuk et al., 2012).

2.4.1.2 Dopamine (DA)

In contrast to 5-HT, DA did not induce spawning nor oocyte maturation in *S. solidissima*, *S. transversum* and *S. striatum* (Fong et al., 1996; Hirai et al., 1988). However, in *C. angulata*, DA is involved in oocyte maturation: a receptor called Ca-DAR1 is particularly expressed in the gonad during the proliferation stage, whereas its expression profile declines in the following stages up to the release of oocytes (Yang et al., 2013). In *C. gigas* a dopamine invertebrate receptor (CgDOP2R) was found to be abundantly expressed during oocyte maturation, and in the early developmental stages suggesting a possible role in embryo development (Schwartz et al., 2021). As discussed above for 5-HT, DA is involved in the shell biogenesis process. Further involvement of DA in larval development was shown by specifically inhibiting dopamine receptor type one with SCH 23390 in *M. galloprovincialis*. Receptor inhibition impaired shell formation (Miglioli et al., 2021b). Larvae of the mussels *M. galloprovincialis* and *Perna canaliculus* showed an increase in settlement when exposed to L-DOPA and DA (Young et al., 2015; Sánchez-Lazo and Martínez-Pita, 2012)

Dopaminergic nerves were shown to be localised in cerebrovisceral connectives and in the branchial nerve, which innervates the gills and extends from the visceral ganglia. Contrary to

5-HT, DA application on gills or CG or VG resulted in a decrease in ciliary beating (Carroll and Catapane, 2007).

2.4.1.3 Noradrenaline (NA)

NA was found to induce metamorphosis in two oyster species, *C. gigas* and *C. virginica*, and metamorphosis seemed to be controlled by adrenergic receptors in *C. gigas* (Coon et al., 1986; Coon and Bonar, 1987). In addition to this, in the oyster *C. angulata*, an adrenergic receptor was identified and its RNA concentration was analysed during larval development and it peaked just before metamorphosis (Yang et al., 2012). NA is a key mediator of the neuroendocrine-immune (NEI) system, a complex system that plays indispensable roles in keeping immunity. NA is involved in regulating apoptosis, phagocytosis and immune response in *C. gigas* (Liu et al., 2018). Moreover, NA was found to be associated with apoptosis induction in the pearl oyster, *Pinctada imbricata*, and in the rocky oyster, *Saccostrea glomerata* (Aladaileh et al., 2008; Kuchel and Raftos, 2011). In *P. imbricata*, haemocytes exposed to NA displayed DNA fragmentation at each concentration tested (2.5, 5 and 10 ng NA/ μ g protein); moreover, marker of early apoptosis events (i.e.: Annexin V) was evident in haemocytes exposed to 5 and 10 ng NA/ μ g protein. Haemocytes displayed also morphological changes when exposed to NA such as cytoplasmic and chromatin condensation, vacuolisation, formation of apoptotic bodies and blebbing (Kuchel and Raftos, 2011). Similar results were found for *S. glomerata*. Haemocytes suspended in a solution containing 150 nM NA displayed typical apoptotic markers such as DNA fragmentation, DNA aggregation, mitochondrial degeneration and blebbing (Aladaileh et al., 2008).

2.4.1.4 Tyramine (TA) and Octopamine (OA)

AO is reported to mediate cardiac function in the clam *Tapes watlingi* and in the oyster *C. virginica*. However, TA and OA are poorly studied and documented as reported by Fabbri et al. (2024).

2.4.2 Monoamines roles in response to environmental stressors: focus on marine bivalves

2.4.2.1 Adults

The bivalve neuroendocrine system includes several neurotransmitters, neuropeptides, hormones and cytokines; among all the molecular components characterised to date, components of the monoaminergic system are involved in response to environmental stressors (Fabbri et al., 2024; Liu et al., 2018).

Several experiments suggest that 5-HT may be involved in *C. gigas* in immune response. Haemocytes exposed to lipopolysaccharide (LPS, component of the outer membrane of Gram-negative bacteria) showed an increased expression of a putative 5-HTR1, and addition of a non-selective inhibitor of 5-HTR (methiothepin) induced a decrease in mRNA levels of a pro-inflammatory cytokine: tumour necrosis factor (TNF) and an increase in activity of the superoxide dismutase (SOD) (Jia et al., 2018).

Components of the MA system were shown to be involved in hypoxia, which can impact the neuroendocrine system (Dong et al., 2017; Kotsyuba and Dyachuk, 2023; Liu et al., 2018). In the Pacific oyster, *C. gigas*, exposure to air for one day led to an increase of 5-HT concentration in the haemolymph, moreover, it was demonstrated that the addition of exogenous 5-HT could extend the survival rate after four and six days of exposure to air and it was also able to reduce the rate of apoptosis of haemocytes (Dong et al., 2017; Fabbri et al., 2024). DA was also found to be involved in hypoxia but, contrary to 5-HT, DA showed a decrease in concentration in the haemolymph of the scallop, *Chlamys farreri*, and in the muscle of the mussel *Perna perna* after 24 hours of exposure to air (Kotsyuba and Dyachuk, 2023). Exposure to air triggers also noradrenaline, indeed its concentration in *C. farreri* was found to increase, contrary to dopamine which showed a decrease in concentration (Chen et al., 2008).

Other stressors such as high temperature and low salinity were shown to affect DA and NA concentrations in the haemolymph of *C. farreri*. When the two stressors were applied, NA concentrations showed an increase, whereas DA showed an inverse trend in response to these stressors (Chen et al., 2008; Fabbri et al., 2024).

The application of mechanical stressors, such as agitation, on *C. gigas* showed that haemolymph concentrations of DA and NA were higher than those found in controls (Lacoste et al., 2001).

In the experiments of Chen et al. (2008) and Lacoste et al. (2001), adrenaline was analysed. Its presence/absence was debated by the authors because it was found to be present in some bivalve species and absent in others. Moreover, the recent phylogenomic analysis showed that the enzyme required for A synthesis is exclusive to chordates, raising thus more doubts about its real presence or absence in bivalves (Goultly et al., 2023). However, this subject will not be analysed in this thesis.

Effects on *M. edulis* serotonergic system were studied by exposing mussel to different concentration, in the environmental range, of manganese (Mn 10, 100, 1000 nM), lead (Pb, 0.01, 0.1 and 10 nM) and cadmium (Cd, 0.01, 0.1 and 10 nM) (Fraser et al., 2018). It was shown

that metals did not induce any change in the concentration of 5-HT and no differences were found among females and males specimens with the exception of Cd, which caused a significant decrease in serotonin levels in males compared to females at the lower concentration tested (0.01 nM) but not at higher concentrations (Fraser et al., 2018). Moreover, the serotonin reuptake transporter (SERT) was analysed in terms of protein expression, and it was found that all metals induced a decrease in its expression in the mantle (except for 10 nM Mn tested). In addition to this, the enzyme responsible for monoamines degradation (MAO) was analysed. The activity of MOA was found to be decreased in the mantle of mussels treated with Cd and with effects in both sexes (increased in males and decreased in females), whereas Pb has no effect on MAO activity (Fraser et al., 2018).

2.4.2.2 Larvae

Calcifying larvae of marine invertebrates, such as molluscs and echinoderms, are particularly sensitive to environmental stressors (Ross et al., 2016). Serotonin and dopamine were shown to be affected in response to acidification in the larvae of the Pacific oyster, *C. gigas* (Liu et al., 2020). Trochophore larvae of the oyster were treated with a severe acidification (pH 7.4, control pH 8.1) and it was shown that treated larvae presented abnormalities in the calcified shell, in particular the shell was full of wrinkles and the calcified shell was barely formed compared to larvae grown in control conditions. The content of 5-HT and DA was measured in D-veliger larvae and acidification treatment induced a reduction in the content of both 5-HT and DA levels (Liu et al., 2020).

Liu et al. (2020) showed that acidification decreased the level of mRNA expression of the rate limiting enzyme for 5-HT synthesis, TPH, and the enzymes involved in the second step of synthesis of both 5-HT and DA were significantly downregulated. Moreover, genes involved in the synthesis of the organic shell (composed of chitin, which is the main component, acid polysaccharides, proteins and glycoproteins) were affected: in particular there was an upregulation of chitinase and the expression of tyrosinase was hindered (Liu et al., 2020; Miglioli et al., 2019). Different genes were shown to be involved in shell biogenesis process in the Mediterranean mussel *M. galloprovincialis*, contributing to the formation of the organic shell: tyrosinase, chitin synthase, carbonic anhydrase and extrapallial proteins but, among them, tyrosinase was shown to be pivotal for the shell biogenesis process (Miglioli et al., 2019). Since TPH and other synthesis enzymes were downregulated after acidification treatment and expression profiles of shell biogenesis genes altered, Liu et al. (2020) imagined a possible connection between 5-HT and DA and the shell biogenesis process. They hypothesised a

regulation of shell biogenesis genes mediated by a TGF- β smad pathway mediated by a serotonin receptor, named 5-HTR1, and a dopamine receptor, named DR1. They showed that treatment with exogenous 5-HT and DA triggered the phosphorylation of TGF- β type I receptor (TIR) and the translocation of smad4 from cytoplasm to nucleus and upregulated both tyrosinase and chitinase. Ocean acidification hindered both TIR phosphorylation and smad4 translocation. Thus authors hypothesised that 5-HT and DA control shell biogenesis process by triggering the phosphorylation of TIR and the nuclear translocation of smad4 which, in normal conditions, should promote the transcription of tyrosinase and the inhibition of transcription of chitinase (Liu et al., 2020).

Effects of acidification were tested also *M. galloprovincialis* (Kapsenberg et al., 2022, 2018). It was shown that acidification (pH 7.4) induced malformations in development and in CaCO₃ deposition, resulting in a “keyhole shaped indentation” meaning that no deposition of inorganic shell was occurring in that spot (Kapsenberg et al., 2018). Moreover, acidification induced a reduction in size of organic and inorganic shell in treated samples compared to controls (pH 8.1) (Kapsenberg et al., 2018). Acidification treatment was also shown to alter tyrosinase and chitinase expression, as it happened in Pacific oyster (Kapsenberg et al., 2022). These results show that OA can affect embryo-larval development directly.

Recently, a class of contaminants, called Contaminants of Emerging Concern (CEC) were shown to alter the monoaminergic system of adult and larval stages of bivalves. For this reason, the next chapter will show the state of the art of CEC.

Chapter 3

3 Contaminants of Emerging Concern

Contaminants of emerging concern (CEC) are defined as follows: “naturally occurring, manufactured or manmade chemicals or materials which have now been discovered or are suspected to be present in various environmental compartments and whose toxicity or persistence are likely to significantly alter the metabolism of a living being.” (Sauvé and Desrosiers, 2014). Sauvé and Desrosiers (2014) discuss also the importance of the terminology, especially the difference between “emerging contaminants” and “contaminants of emerging concern”. Emerging contaminants can be defined as compounds or molecules which are new, meaning that previously they were not known, or they could be substances that only recently appeared in the scientific literature. On the contrary, contaminants of emerging concern are compounds already known to exist, but their potential environmental impacts and risks were not fully understood until new findings arose.

CEC include different types of chemicals that can be classified as endocrine disrupting chemicals (EDCs), Brominated and per- and polyfluorinated compounds (brominated flame retardants - BFRs and per- and polyfluorinated alkyl substance - PFAS), pharmaceuticals and personal care products (PPCPs), plasticizers, nanomaterials, marine biotoxins, siloxanes and microplastics (Álvarez-Muñoz et al., 2016; Canesi et al., 2022; Fabbri et al., 2014; Feng et al., 2023).

3.1 Endocrine Disrupting Chemicals (EDCs) and Neuro-Endocrine Disrupting Chemicals (NEDs)

Endocrine Disrupting Chemicals (EDCs) are a class of molecules highly heterogeneous. They are represented by synthetic chemicals originally designed for different specific functions (Diamanti-Kandarakis et al., 2009; Noguera-Oviedo and Aga, 2016; Schug et al., 2011). EDCs include solvent and lubricants and their byproducts (polychlorinated biphenyls – PCBs, polybrominated biphenyls – PBBs, dioxins), plastics (bisphenol A – BPA), plasticizers (phthalates), pesticides (dichlorodiphenyltrichloroethane - DDT), fungicides, antifouling agents (tributyltin - TBT), flame retardant agents, pharmaceutical, cosmetics, metals and also natural chemicals found in food (e.g.: phytoestrogens) (Álvarez-Muñoz et al., 2016; Bergman et al., 2012; Bertram et al., 2022; Diamanti-Kandarakis et al., 2009; Schug et al., 2011; Stiefel and

Stintzing, 2023). Moreover, it has been shown that most EDCs are persistent or pseudo-persistent in the environment (Bergman et al., 2012; Pironti et al., 2021).

EDCs enter the environment in several ways, and the most common is represented by human related activities, coming from municipal wastewater treatment plants (WWTPs) discharge, industrial waste but also from agriculture, aquaculture and rainwaters (Bertram et al., 2022; Noguera-Oviedo and Aga, 2016; Pironti et al., 2021). EDCs are known to contaminate surface and ground waters, rivers, lakes and the marine environment (Pironti et al., 2021). Concentrations of EDCs vary depending on the compound and the sampling area. Indeed, concentrations of the hormone 17- β -estradiol in the African country were shown to be 3000 to 20'000 times higher than in Europe (510 – 45'000 ng/L vs 3310 – 15'700 ng/L) (Pironti et al., 2021). Pironti et al. (2021) reported a list of different EDCs, showing that their concentration in freshwater and seawater ranges from a minimum of < 1 ng/L to a maximum of \approx 170'000 ng/L.

The term Endocrine Disruptor (ED) was first introduced at the at the Wingspread Conference in Wisconsin, USA in 1991. In 1996 an ED was defined by the Testing Advisory Committee (EDSTAC) as *“an exogenous chemical substance or mixture that alters the structure or function(s) of the endocrine system and causes adverse effects at the level of the organism, its progeny, populations, or subpopulations of organisms, based on scientific principles, data, weight-of-evidence, and the precautionary principle.”* (Zoeller et al., 2012). Also in 1996, the Environmental Protection Agency (EPA) defined an ED as *“exogenous agents that interfere with the synthesis, secretion, transport, binding, action or elimination of natural hormones in the body that are responsible for the maintenance of homeostasis, reproduction, development and/or behaviour”* (Yilmaz et al., 2020; Zoeller et al., 2012). Subsequently, the definition of ED has been updated and now the most common definition of ED is: *“an exogenous substance or mixture that alters function(s) of the endocrine system and consequently causes adverse health effects in an intact organism, or its progeny, or (sub) populations”* (Bertram et al., 2022; Pironti et al., 2021).

EDCs were thought to exert their action primarily through nuclear hormone receptor, including oestrogen and androgen receptors, progesterone receptors, thyroid receptors and retinoid receptors (Diamanti-Kandarakis et al., 2009). However, other mechanisms of action of EDCs were demonstrated; indeed, they can exert their action not only by binding to nuclear hormone receptors but also by interfering with the synthesis, metabolism and delivery of an hormone, by binding to non-steroid receptors (e.g.: neurotransmitter receptors such as serotonin, dopamine

and noradrenaline receptors) and orphan receptors (Bergman et al., 2012; Diamanti-Kandarakis et al., 2009; Gore, 2010; Schug et al., 2011).

Since hormones can be of different chemical nature and since the EDCs have a broad spectrum of targets, several EDCs were found to act also as Neuro-Endocrine Disruptors (NEDs) in vertebrates (Canesi et al., 2022; Gore, 2010; Rosenfeld et al., 2017; Seralini and Jungers, 2021).

As previously described in chapter one, invertebrates, with the exception of Arthropoda, lack a canonical endocrine system but they are endowed with a neuroendocrine system made up of secretory neurons (Fabbri et al., 2024; Hartenstein, 2016; Tessmar-Raible, 2007). Moreover, hormones display different chemical natures, they can be peptides, lipids and amino acids derivatives, such as monoamines (Hartenstein, 2006; Joyce and Vogeler, 2018; Kleine and Rossmannith, 2016; Tessmar-Raible, 2007; Wuttke et al., 2010). It could be thus possible to argue that effects of disruption of EDCs in invertebrates are mainly neuroendocrine, acting thus as NEDs (Canesi et al., 2022).

EDCs include pharmaceuticals, among others. The next chapter will focus on the description of Pharmaceuticals and Personal Care Products, with a focus on a class of pharmaceutical drugs that act specifically on the monoaminergic system.

3.2 Pharmaceuticals and personal care products (PPCPs)

PPCPs are a class of several organic chemicals used to treat human and animal diseases and for healthcare. When released into the environment, they can be found as neutral, cationic, anionic or zwitterionic. Pharmaceuticals are represented by drugs and agents designed to heal/treat diseases and they are classified based on their therapeutic purpose: analgesics, nonsteroidal anti-inflammatory drugs (diclofenac, ibuprofen), antibiotics (sulfamethoxazole, roxithromycin, erythromycin), diagnostic agents, diuretics, hormones (17- β -estradiol), nutritional supplements, psychiatric drugs (citalopram, fluoxetine, diazepam, carbamazepine) and β -blockers. Personal care products (PCPs) include different types of compounds such as cosmetics, disinfectants, fragrances, gels, preservatives, soaps and sunscreen creams (Álvarez-Muñoz et al., 2016; Chopra and Kumar, 2018).

When pharmaceuticals are administered, they are bio-transformed in more polar molecules. However, not all administered dose is subjected to metabolism, that can frequently be incomplete. Indeed PPCPs are excreted both as metabolites and pristine forms (Álvarez-Muñoz

et al., 2016; Chopra and Kumar, 2018). On the contrary, PCPs are designed for topical use/application, thus they are not subject to metabolism.

PPCPs enter the ecosystem through effluents from wastewater treatment plants (WWTPs), sewage treatment plants (STPs) and through domestic waste, large farms and aquaculture facilities and horticulture (Álvarez-Muñoz et al., 2016; Chopra and Kumar, 2018). PCP used for topical application can enter the environment directly (Chopra and Kumar, 2018). In WWTPs, two main processes are involved in eliminating PPCPs: adsorption to suspended solids (sewage sludge) and biodegradation. Adsorption depends on a compound's electrostatic and hydrophobic characteristics; in general, adsorption of acid pharmaceuticals to sludge is considered irrelevant. Thus, for dissolved compounds, biodegradation, in aerobic or anaerobic conditions, is the most common elimination process occurring (Fent et al., 2006). The removal rates of WWTPs and STPs can be affected by environmental factors such as pH, redox condition and temperature and by properties of the chemicals (solubility, half-life, tendency to volatilise) (Álvarez-Muñoz et al., 2016; Gaw et al., 2014). WWTPs were reported to be inadequate for completely removing PPCPs and removal rates were shown to vary from chemical to chemical (e.g.: ibuprofen and ketoprofen are subjected to an elimination rate between 94-100%, for diclofenac it is around 26%) (Fent et al., 2006). Moreover, PPCPs can react with each other, or other compounds present in WWTPs forming conjugated compounds. PPCPs are widely detected in aquatic environments (lakes, rivers, groundwater and sea). PPCPs are also found in waters used for irrigation because it is water generally recycled from WWTPs and STPs resulting, thus, in a possible contamination through the food chain. In addition to this, PPCPs were found in drinking water as well (Álvarez-Muñoz et al., 2016; Chopra and Kumar, 2018). The continuous input of PPCPs in the environment and the low capability of WWTPs to remove PPCPs (and more in general CEC) led them to become pseudo-persistent contaminants (Chopra and Kumar, 2018; Fabbri and Franzellitti, 2016; Mole and Brooks, 2019). Pharmaceuticals, once in the environment, also deposit on sediments, turning in sediments as a second pollution source of pharmaceuticals (Fabbri et al., 2023).

Domestic, hospital, aquaculture and industrial effluents are often associated with very high concentrations of PPCPs, that can reach the range of mg/L; on the contrary, the concentration in environmental matrices is lower, in the range of ng-µg/L (Duarte et al., 2023; Fabbri et al., 2023). A problem represented by PPCPs is that their prescription has increased worldwide in the past decade and this trend is expected to continue, associated with population growth resulting in higher demand for PPCPs. In addition to this, human activities, such as aquaculture,

and the increase of people inhabiting coastal areas pose relevant implications for the risk assessment of PPCPs (Duarte et al., 2023; Fabbri and Franzellitti, 2016). Another problem represented by pharmaceuticals is that they are designed to act on a specific target (enzyme, receptor or transporter) that can be evolutionary conserved in other animals, eliciting responses at very low dosages (Ankley et al., 2007; Duarte et al., 2023; Fabbri and Franzellitti, 2016; Franzellitti et al., 2015, 2013; Gunnarsson et al., 2008). For this reason, dilution in marine environments does not represent a safety factor (Fabbri and Franzellitti, 2016). Indeed, the European Legislation included pharmaceuticals as emerging contaminants of priority concern, given the potential toxicity of pharmaceutical compounds in the environment (Duarte et al., 2023; European Commission, 2022).

3.2.1 The concepts of Mode-of-Action (MOA) and the Adverse Outcome Pathway (AOP)

A conceptual model defined as “mode-of-action” was developed to assess the environmental risks of pharmaceuticals. This model assumes that the properties and toxicity of a pharmaceutical in mammals must be taken into account and integrated with the knowledge available regarding the species used as model organism (Ankley et al., 2007; Franzellitti et al., 2013). Thus, knowledge of pharmaceutical pathways can be used to identify tests, species and appropriate endpoints for assessing the ecological risk (Figure 3.1) (Ankley et al., 2007). Knowledge of MOAs can be pivotal to lead scientists to identify drugs that could be of less concern in non-target species (Ankley et al., 2007). However, side effects in non-target species can cause toxicity through other pathways than what they were designed for (Ankley et al., 2007; Fabbri and Franzellitti, 2016).

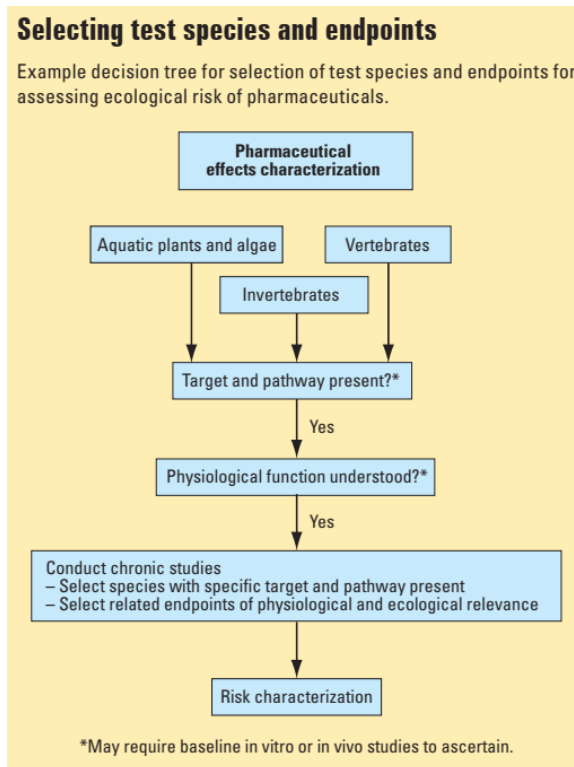


Figure 3.1. Schematic representation of characterisation of risk assessment.

In assessing the potential toxicological effect of PPCPs, the concept of “adverse outcome pathway” (AOP) represents a good tool for ecological risk assessment (Hutchinson et al., 2013). The AOP is defined as the sequence of events that from the exposure of an individual to a chemical, lead to its adverse effect at the individual or population level (OECD, 2020). The AOP is a sequence of events that connects the molecular initiating event (MIE) with the final AOP. The MIE is characterised by a chemical interacting with a biological target which leads to a first cellular response and a subsequent series of responses at higher levels (organ, organism and, finally, population) to produce the adverse outcome (see Figure 3.2 taken from Ankley et al. (2010).

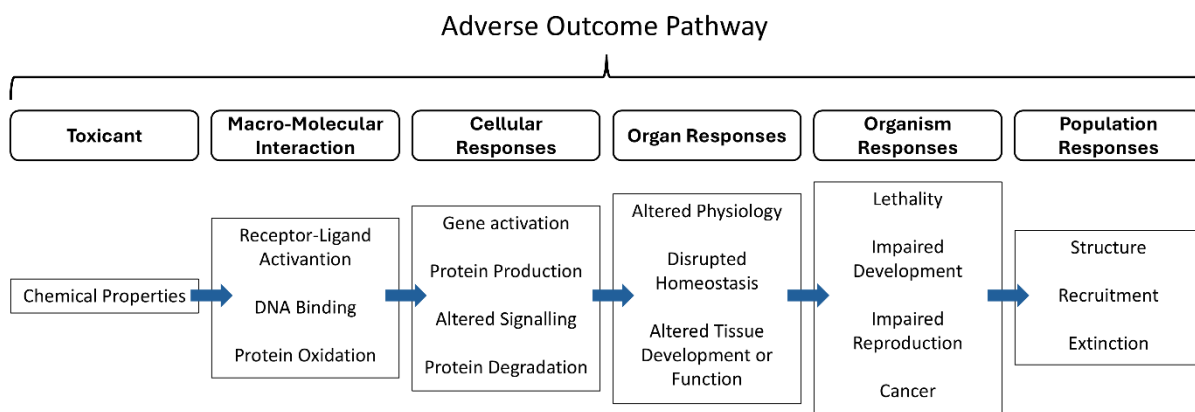


Figure 3.2. Conceptual diagram representation of the events that lead to an adverse outcome pathway (AOP). Image adapted from Ankley et al. (2010).

The following section will focus on the PPCPs object of study of this PhD thesis: the Selective Serotonin Reuptake Inhibitors, designed to act specifically towards the serotonergic system, in particular to bind the Serotonin Reuptake Transporter (SERT).

3.3 Selective Serotonin Reuptake Inhibitors (SSRIs)

Selective serotonin reuptake inhibitors are a class of pharmaceuticals commonly prescribed to treat several psychiatric disorders such as depression, anxiety, compulsive behaviour, eating and personality disorders (Andersen et al., 2009; Brooks et al., 2003; Chu and Wadhwa, 2024).

Fluoxetine (FLX) was the first SSRI to be approved in 1986. In the following years, many other SSRIs have been commercialised, including Citalopram (CIT), Escitalopram (ESC), Paroxetine (PAR), Sertraline (SER) and Fluvoxamine (Chu and Wadhwa, 2024; Robert et al., 2017). Generally, SSRIs are known by their brand names(s): FLX is commercialised under the name of Prozac (but also Sarafem and Symbax), CIT is known as Celexa, Escitalopram as Lexapro, PAR as Paxil (or Paxil CR, Paxeva), SER as Zoloft and Fluvoxamine as Luvox (FDA, 2018). SSRIs are among the most widely prescribed antidepressants and the most prescribed ones are FLX, SER and CIT (Canesi et al., 2022; Chen et al., 2022).

SSRIs are designed to bind the serotonin reuptake transporter (SERT) resulting in an inhibition of the recycling of 5-HT thereby increasing the 5-HT concentration at the synaptic level (Andersen et al., 2014, 2009; Zhou et al., 2009). However, the mechanisms of inhibition of SERT were reported to be poorly understood by Andersen et al. (2014, 2009). They tried to shed light on the mechanisms of recognition of SSRIs towards SERT using the X-ray crystal structure of a bacterial molecule, showing that several amino acids are involved in the binding.

3.3.1 Concentration of SSRIs in aquatic matrices

Generally, their concentration ranges from $\mu\text{g/L}$ in inland waters to ng/l in marine water and up to 500 ng/L in urban estuaries (Canesi et al., 2022). Their concentration varies from place to place. Supplementary Table 1 shows the values of different SSRIs found in different types of samples and areas. As it is possible to see from Supplementary Table 1, most data are reported for FLX, CIT PAR and SER. FLX and CIT, show the highest concentrations: $\geq 500 \text{ ng/L}$ and $\approx 92 \text{ ng/L}$ respectively. FLX active moiety range is $120/160\text{-}300 \text{ ng/mL}$, CIT range is $10\text{-}200 \text{ ng/L}$ (Eibak et al., 2010; Koelch et al., 2011).

3.3.2 Effects of SSRIs on bivalves

3.3.2.1 Adults

In *Sphaerium striatinum* fluvoxamine and PAR but not FLX were shown to induce parturition, as well as the addition of exogenous serotonin (Fong et al., 1996; Fong and Ford, 2014). In *Macoma balthica* it was found that combination with thermal stress and addition of 1 mg/L of FLX could extend the spawning seasons (Fong and Ford, 2014; Honkoop et al., 1999).

Juveniles of *C. gigas* (eight months old) were exposed to increasing concentrations of FLX (1 , 100 and $10'000 \text{ ng/L}$) and different endpoints and biomarker were analysed. FLX did not induce any differences in mortality during all the experiments sampling points (7 , 14 and 28 days) (Di Poi et al., 2016). Activity of CAT and GST were investigated in gills and digestive glands (analysed together) and these biomarkers displayed a bell-shaped response: GST at 1 ng/L was increased after 1 day of exposure and then inhibited at 7 days, for CAT 100 ng/L induced first an increase (7 days) and then an inhibition (14 and 28 days) (Di Poi et al., 2016). No differences in the maturation of gonads were observed at any of the concentrations tested (1 , 100 and $10'000 \text{ ng/L}$) (Di Poi et al., 2016). In juveniles shell length was shown to increase when exposed to 100 and $10'000 \text{ ng/L}$ (7 , 14 and 28 days) but not for the lowest concentration (1 ng/L) (Di Poi et al., 2016).

D. polymorpha exposed to FLX 500 ng/L was sampled at different time points after exposure (4 , 7 , 11 and 14 days). Antioxidants enzymes were affected by FLX exposure with differences depending on the time. CAT showed first a decrease in activity (4 and 7 days) followed by an increase at the end of exposure. CAT activity showed a significant increase in activity after 11 and 14 days of exposure. Glutathione peroxidase (GPx) activity was also affected by FLX exposure, resulting in an increase in activity at the end of the exposure, whereas glutathione S-transferase (GST) was not affected by FLX (Magni et al., 2017). In another study, *D.*

polymorpha individuals were exposed to FLX at 20 and 200 ng/L for six days. It was found that the number of oocytes per follicle and spermatozoa density in tubules decreased in treated specimens compared to controls, suggesting a possible induction of FLX in inducing spawning, given the differences found in gonads (Fong and Ford, 2014; Lazzara et al., 2012). FLX and Fluvoxamine were found to induce spawning in both males and females of *D. polymorpha*, with males being more responsive than females in concentrations ranging from 10^{-9} to 10^{-5} M and 5×10^{-7} to 5×10^{-4} M, respectively (Fong, 1998; Fong and Ford, 2014).

In *M. californianus*, long-term exposure to FLX for 107 days at concentrations ranging from 0.3 to 300 ng/L showed that algal clearance rates were inversely proportional to FLX concentrations. Shell growth was affected at 30 and 300 ng/L, and the gonadosomatic index (GSI) was reduced in mussels exposed to any concentration of fluoxetine (Canesi et al., 2022; Peters and Granek, 2016).

In *M. edulis*, FLX caused loss of haemocyte cell viability at 10 and 15 mg/L, decreased phagocytosis at 10 and 15 mg/mL, and induced genotoxicity at these concentrations. Fluoxetine also led to a significant production of reactive oxygen species (ROS) at 10 and 50 mg/mL (Lacaze et al., 2015).

In *M. galloprovincialis*, exposure to 75 ng/L FLX caused a decrease in superoxide dismutase (SOD) activity in the gills after two weeks, while CAT activity increased in the digestive gland and gills. Acetylcholinesterase (AChE) activity increased in the gills after 3 days, followed by a subsequent decrease (Gonzalez-Rey and Bebianno, 2013). Specimens exposed to FLX 0.3 ng/L for 7 days led to decreased levels of cyclic AMP (cAMP) in the digestive gland, and mantle gonads causing, therefore, a reduced activity of Protein kinase A (PKA), consistent with higher 5-HT levels caused by FLX and consequent binding to 5-HTR1 receptor. FLX increased the expression of 5-HTR1, while mRNA levels of ABCB were decreased, thus the expression of P-glycoprotein (Franzellitti et al., 2013). P-glycoprotein is a component of the multi-xenobiotic resistance (MXR) mechanism of defence against xenobiotics, which prevents the accumulation of cytotoxic drugs in the cells by extrusion. Thus, FLX may seriously affect defence strategies against chemical exposure (Bard, 2000; Canesi et al., 2022). Incubation with FLX 0.3 ng/L for 7 days affected different biomarkers in the digestive gland. FLX reduced the lysosomal membrane stability (LMS) in haemocytes and led to the accumulation of neutral lipids (NL). Among other biomarkers analysed (catalase CAT, glutathione-S-transferase GST, and DNA damage), only GST resulted to be slightly modified (Franzellitti et al., 2015). Moreover, FLX affected lysosomal membrane stability (LMS) at tested concentrations (0.5, 5, 10 ng/L), with

an increased lysosome/cytosol ratio (LYS/CYT) at 5 and 10 ng/L and neutral lipid (NL) accumulation up to 200% at all concentrations (Rafiq et al., 2023).

In *Perna perna*, after 48 hours of exposure to FLX 30 ng/L, DNA damage was found in the digestive gland, with decreased lysosomal membrane stability starting from the lowest concentration of FLX (3 ng/L) for both exposure periods (Canesi et al., 2022; Cortez et al., 2019).

In the clam *Venerupis philippinarum* FLX significantly affected immune parameters and increased AChE activities at $\mu\text{g/L}$ concentrations (Fabbri et al., 2023).

D. polymorpha specimens exposed to CIT 500 ng/L showed alterations in the enzymes involved in oxidative stress. SOD and CAT activities showed first a decrease (4 days) and then an increase of activity in the following days of exposure (7, 11 and 14 days), except for CAT that showed a decrease after 14 days of exposure. GPx and GST were also affected by CIT: GPx showed first a significant decrease after 4 days of exposure and a significant increase at the end of the exposure period; GST showed a significant inhibition at both 4 and 14 days of exposure (Magni et al., 2017). Exposure to a mix of FLX and CIT (500 ng/L for each) showed that enzymes involved in oxidative stress were affected, and a bell-shape trend could be observed. SOD was first inhibited (4 days) and then followed by an increase in activity, with a little decrease in activity at 14 days compared to 7 and 11 days of exposure. Same profile was shown by CAT, GPx and GST (Magni et al., 2017).

3.3.2.2 Embryos and Larvae

In *C. gigas*, SER induced a decrease in normal D-larvae in a dose dependent way starting from a concentration of 100 $\mu\text{g/L}$ and 0% of normal D-larvae were found at 250 $\mu\text{g/L}$; concentrations ranging from 0.1 to 10 $\mu\text{g/L}$ did not induce any differences in the percentage of normal D-larvae compared to controls (Di Poi et al., 2014). Larvae treated with SER showed an increase in malformations with protruding mantle, malformed hinge, previous phenotypes found together and arrested developmental stages being the most abundant phenotypes (Di Poi et al., 2014).

In *M. galloprovincialis*, SER induced a small but significant decrease in the percentage (15% of decrease) of normal D-larvae at 0.1, 1, 10 and 50 $\mu\text{g/L}$, followed by a drastic dose dependent decrease at 100, 200 and 300 $\mu\text{g/L}$, and a 300 $\mu\text{g/L}$ no developed D-larvae could be observed. Effect caused by SER in terms of phenotypes were mainly arrest in development, indeed arrested trochophore were the most abundant phenotype registered (Estévez-Calvar et al., 2017).

Larvae of *C. gigas* exposed to FLX exhibited a significant decrease in normal D-larvae from 150 µg/L to 400 µg/L, with observed abnormalities. The metamorphosis rate decreased starting from 100 to 400 µg/L. D-veliger larvae were shown to be more sensitive to FLX than pediveliger larvae (Di Poi et al., 2014). For *P. perna*, inhibition of cholinesterase was observed at 48 hours post-fertilization (hpf) for concentrations ranging from 3 to 30 ng/L, and at 96 hpf for concentrations of 30 and 300 ng/L (Canesi et al., 2022; Cortez et al., 2019). In a more recent study, FLX exposure resulted in a 4% decrease in egg fertilization at concentrations ranging from 100 to 500 ng/L in *M. galloprovincialis*. Normal D-larvae were affected at concentrations from 100 to 500 ng/L, showing delayed development (Rafiq et al., 2023).

In *M. galloprovincialis*, CIT (concentrations tested range: 0.5 – 500 ng/L) decreased egg fertilisation only at 500 ng/L by 10%. Larval development was affected at 25, 100 and 500 ng/L causing different abnormalities. LMS and lysosome/cytosol ratio (LYS/CYT) were affected at all the concentrations tested (0.5, 5, 10 ng/L) in haemocytes (Rafiq et al., 2023).

As it is possible to understand from this section, most of the studies focus on the effect of FLX, probably because it was the first SSRI to be released. Moreover, effects on the monoaminergic system and, therefore, on neuroendocrine signalling are mostly absent. In this context, understanding the MOA of SSRIs on the monoaminergic system of bivalves is needed in order to shed some light on the possible molecular initiating events after exposure to SSRIs helping, thus, to understand their MOA and establish better their AOP.

3.4 Supplementary Table

SSRI	Country	Environment	Concentration (ng/L)	Reference
Fluoxetine	Canada	Surface water	12- 46	Gust et al. (2009)
		Coastal environment	≤ 3 - 596	Franzellitti et al. (2015)
	Croatia	Surface water	66	Franzellitti et al. (2013)
	Canada	Surface water	46	
	USA	Surface water	2.6 - 111	
	Belgium	Harbor water	13	
	North Sea	Seawater	≤3	
		Surface water	10 - 500	
	Portugal - Duoro	Estuaries water	< LOQ	Duarte et al. (2023)
	Portugal - Tejo		< LOQ	
	Portugal - Sado		3.5 - 24	
	Portugal - Mira		8 - 133	
		WWTPs	12 - 3500	Brooks et al. (2003)
	Asia-Pacific, Europe, North America	WWTPs influent	ND - 3465	Mole and Brooks (2019)
	Asia-Pacific, Europe, North America	WWTPs effluent	ND - 2700	
	Asia-Pacific, Europe, North America	Freshwater	ND - 330	
	Asia-Pacific, Europe	Seawater	ND - 36	Madikizela et al. (2020)
	Tunisia	Coastal environment	ND - 41	
	Spain (South-West)	Coastal environment	ND - 0.6	
	Spain (North-West)	Coastal environment	ND - 10.6	
	USA	Ocean (Pacific)	90	Mezzelani et al. (2018)
	Greece	Seawater	ND	
	Norway	Seawater	1.4 - 4.8	
	Portugal	Estuaries water	1 - 2	
	Spain	Seawater	ND	
	Spain	Ocean (Atlantic)	ND - 1.6	
	USA	Seawater	3	
		WWTPs influent	540	
		WWTPs influent	0.4 - 2.4	Lacaze et al. (2015)
		WWTPs influent	1.1 - 18.7	
		WWTPs influent	3.1 - 3.5	
		WWTPs effluent	240	
		WWTPs effluent	< 0.12 - 1.3	
	WWTPs effluent	0.6 - 8.4		
	WWTPs effluent	2.0 - 3.7		
	Surface water	12		
	Surface water	56		
	Surface water	0.42 - 1.3		
Norway (Langnes)	WWTPs influent	0.4	Vasskog et al. (2006)	
Norway (Langnes)	WWTPs effluent	ND		
Norway (Breivika)	WWTPs influent	1.3		

	Norway (Breivika)	WWTPs effluent	1.2	
	Norway (Hamna)	WWTPs influent	2.4	
	Norway (Hamna)	WWTPs effluent	1.3	
Fluvoxamine	Norway (Langnes)	WWTPs influent	0.4	Vasskog et al. (2006)
	Norway (Langnes)	WWTPs effluent	ND	
	Norway (Breivika)	WWTPs influent	3.9	
	Norway (Breivika)	WWTPs effluent	ND	
	Norway (Hamna)	WWTPs influent	2.4	
	Norway (Hamna)	WWTPs effluent	0.8	
Citalopram	Portugal - Duoro	Estuaries water	0.7 - 2	Duarte et al. (2023)
	Portugal - Tejo	Estuaries water	0.8 - 4.6	
	Portugal - Sado	Estuaries water	0.7 - 54	
	Portugal - Mira	Estuaries water	1.1 - 77	
	Asia-Pacific, Europe, North America	WWTPs influent	ND - 17100	Mole and Brooks (2019)
	Asia-Pacific, Europe, North America	WWTPs effluent	ND - 9200	
	Asia-Pacific, Europe, North America	Freshwater	ND - 426.6	
	Europe	Seawater	0.9 - 5.4	Madikizela et al. (2020)
	Greece	Seawater	< 0.06 - 8	
	Spain (North-West)	Seawater	ND - 92.5	
	Israel	Seawater	43	
	USA	Seawater (Pacific Ocean)	27	Mezzelani et al. (2018)
	Greece	Seawater	< 0.06 - 8	
		Surface water	0.33 - 76	
		Seawater	0.9 - 27	Cunha et al. (2017)
	Brazil	Coastal environment	0.2 - 0.6	
				Roveri et al. (2020)
	Norway (Langnes)	WWTPs influent	13	
	Norway (Langnes)	WWTPs effluent	9.2	
Norway (Breivika)	WWTPs influent	145		
Norway (Breivika)	WWTPs effluent	62		
Norway (Hamna)	WWTPs influent	612		
Norway (Hamna)	WWTPs effluent	382		
Paroxetine	Portugal - Duoro	Estuaries water	< LOQ	Duarte et al. (2023)
	Portugal - Tejo	Estuaries water	> LOQ	
	Portugal - Sado	Estuaries water	9.3	
	Portugal - Mira	Estuaries water	1.1 - 6.2	
	Asia-Pacific, Europe, North America	WWTPs influent	ND - 39732	Mole and Brooks (2019)
	Asia-Pacific, Europe, North America	WWTPs effluent	ND - 740	
	Europe, North America	Freshwater	ND - 40	
	Europe	Seawater	ND	
	Greece	Seawater	ND	
	Norway	Seawater	0.6- 1.4	
	Spain	Seawater	ND	
		WWTPs influent	16	Lacaze et al. (2015)
		WWTPs influent	0.6 - 12.3	

		WWTPs influent	2.9 - 12.9		
		WWTPs influent	4.6 - 5.3		
		WWTPs effluent	7		
		WWTPs effluent	0.5 - 1.6		
		WWTPs effluent	1.0 - 11.7		
		WWTPs effluent	4.3 - 5.2		
		Surface water	0.6 - 1.4		
		Surface water	1.3 - 3.0		
	Norway (Langnes)	WWTPs influent	12.3		Vasskog et al. (2006)
	Norway (Langnes)	WWTPs effluent	0.7		
Norway (Breivika)	WWTPs influent	0.6			
Norway (Breivika)	WWTPs effluent	0.5			
Norway (Hamna)	WWTPs influent	2.8			
Norway (Hamna)	WWTPs effluent	1.6			
Sertraline	Portugal - Duoro	Estuaries water	1.1 - 1.5	Duarte et al. (2023)	
	Portugal - Tejo	Estuaries water	1.1 - 1.4		
	Portugal - Sado	Estuaries water	113		
	Portugal - Mira	Estuaries water	2.4 - 76		
	Asia-Pacific, Europe, North America	WWTPs influent	< 0.13 - 997		
	Asia-Pacific, Europe, North America	WWTPs effluent	ND - 1930		
	Asia-Pacific, Europe, North America	Freshwater	ND - 75		
	Europe	Seawater	ND	Mezzelani et al. (2018)	
	Greece	Seawater	ND		
	Norway	Seawater	< 0.16		
	Norway (Langnes)	WWTPs influent	1.8	Vasskog et al. (2006)	
	Norway (Langnes)	WWTPs effluent	1.6		
	Norway (Breivika)	WWTPs influent	2.5		
	Norway (Breivika)	WWTPs effluent	2		
Norway (Hamna)	WWTPs influent	2			
Norway (Hamna)	WWTPs effluent	0.9			
Escitalopram	Europe	WWTPs influent	ND - 32228	Duarte et al. (2023)	

Supplementary Table 1. Concentration in different areas and matrices of four different SSRIs. < LOQ: the compound was found with a concentration that is below the quantitation levels. ND: no detection.

Chapter 4

4 *Mytilus galloprovincialis*

4.1 General characteristics

Mytilus galloprovincialis (Lamarck, 1819) is a lamellibranch mollusc belonging to the class of Bivalvia and the family of Mytilidae and characteristic of the Mediterranean region and eastern Atlantic (Figure 4.1). It inhabits the rocky intertidal zone and, in some areas, also the shallow subtidal zone (Gosling, 2015; Oyarzún et al., 2024). Nowadays, *M. galloprovincialis* is considered an invasive species, among the 100 most invasive species (Oyarzún et al., 2024). Indeed it invaded coastal habitats in both hemispheres and it is found in Australia, Japan, New Zealand, North and South America and South Africa (Gosling, 2015; Oyarzún et al., 2024). It is also one of the major species in the yearly shellfish aquaculture production in the southern European region, assuming, thus, relevant importance in the socioeconomic context of the Mediterranean territory (FAO, 2022).

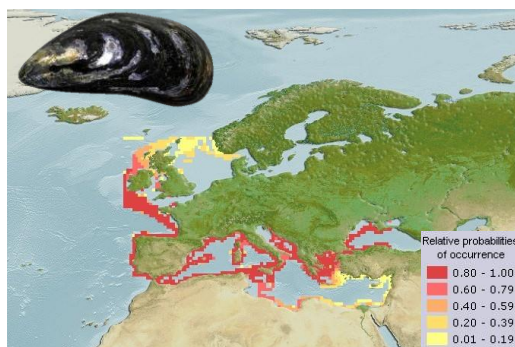


Figure 4.1. Distribution of *Mytilus galloprovincialis* in the Mediterranean region. In the box on the right, there are the relative probabilities of occurrence. Image taken from AquaMaps (2019).

4.2 The life cycle

M. galloprovincialis is a dioecious and seasonal broadcast spawner. Fertilisation happens externally, upon the release of gametes in the seawater column. Timing and duration of the reproductive cycle vary due to local environmental conditions, especially temperature and food availability but, generally, the spawning period occurs in winter (Azpeitia et al., 2017; Gosling, 2015; Rouabhi et al., 2019). Meiosis is completed in the egg once fertilisation has occurred (Gosling, 2015). The morula stage is reached at 4 hours post fertilisation (hpf), at 8 hpf *M. galloprovincialis* enters the blastula stage and at 12 hpf gastrulation begins. The transition from

embryo to the first larval stage, the trochophore, happens between 16 and 20 hpf. The stage of D-Veliger is reached at 44-48 hpf (Miglioli et al., 2024). The pediveliger stage is reached approximately after 17 days pf (dpf), when they become competent for settlement (Figure 4.2) (Janah et al., 2024). At the pediveliger stage larvae have specific characteristics such as foot, ciliated palps, a few pairs of gill filaments, a well-differentiated digestive system, the mantle involved in the secretion of the shell and the nervous system, organised in ganglia, whose organisation in a tetraneural structure will be kept in the adult form (Gosling, 2015; Nikishchenko et al., 2023). After metamorphosis, *M. galloprovincialis* larvae reach the final life stage that signs the start of the sessile benthic adult phase (Gosling, 2015).

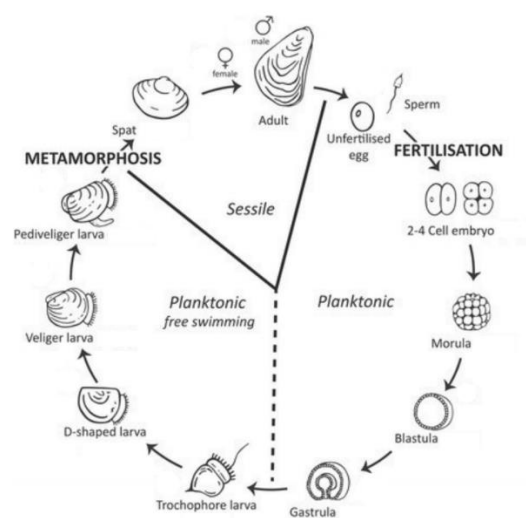


Figure 4.2. The life cycle of *M. galloprovincialis*. Image adapted from Vogeler et al. (2016).

4.3 The embryo-larval development

Once egg is fertilised, it starts to divide, undergoing a holoblastic and unequal cleavage pattern with the embryonic stages represented by morula, blastula and gastrula (Gosling, 2015; Miglioli et al., 2024; Wanninger and Wollesen, 2015). The first larval stage is reached at 20 hpf and it is represented by a trochophore. Trochophore larvae take the name from a ciliated structure: the prototroch. The prototroch is a ciliary ring, from one to three rows of cilia (Piovani et al., 2023; Wanninger and Wollesen, 2015). The prototroch divides the larval body in two parts: the pretrochal episphere and the posttrochal hyposphere. In the pretrochal episphere there is the apical organ (AO), characterised by the presence of a tuft of cilia, called the apical tuft (Piovani et al., 2023; Wanninger and Wollesen, 2015). The stomodeum, the future mouth, is localised immediately adjacent to the prototroch and it is localised in the hyposphere (Piovani et al., 2023; Wanninger and Wollesen, 2015). The hyposphere will give rise to the visceral part of the

body and bears cells involved in the shell biogenesis process, the shell gland, which is involved in secreting the first larval shell, the prodissoconch I (Gosling, 2015; Wanninger and Wollesen, 2015). The trochophore stage is followed by the veliger stage, which represents the second larval stage (Wanninger and Wollesen, 2015). The name veliger comes from the velum, a ciliated and lobed structure that evolves from the prototroch, and enables locomotion, feeding and gas exchange, enabling thus a long planktonic life (Wanninger and Wollesen, 2015). At this stage the veliger is called D-Veliger because of its D-shaped outline, where the shell covers the entire larval body and the larva starts to produce the second larval shell: the prodissoconch II (Wanninger and Wollesen, 2015).

The embryo-larval development of *M. galloprovincialis* has been recently analysed through RNA sequencing (RNA-Seq) analysis that allowed the identification of embryonic development and larval development and the presence of four transitions, allowing the identification of embryo and larval stages based on the analysis of differentially expressed genes (Figure 4.3) (Miglioli et al., 2024). Moreover, it was possible to describe embryo-larval development anatomically by using specific gene markers (Miglioli et al., 2024).

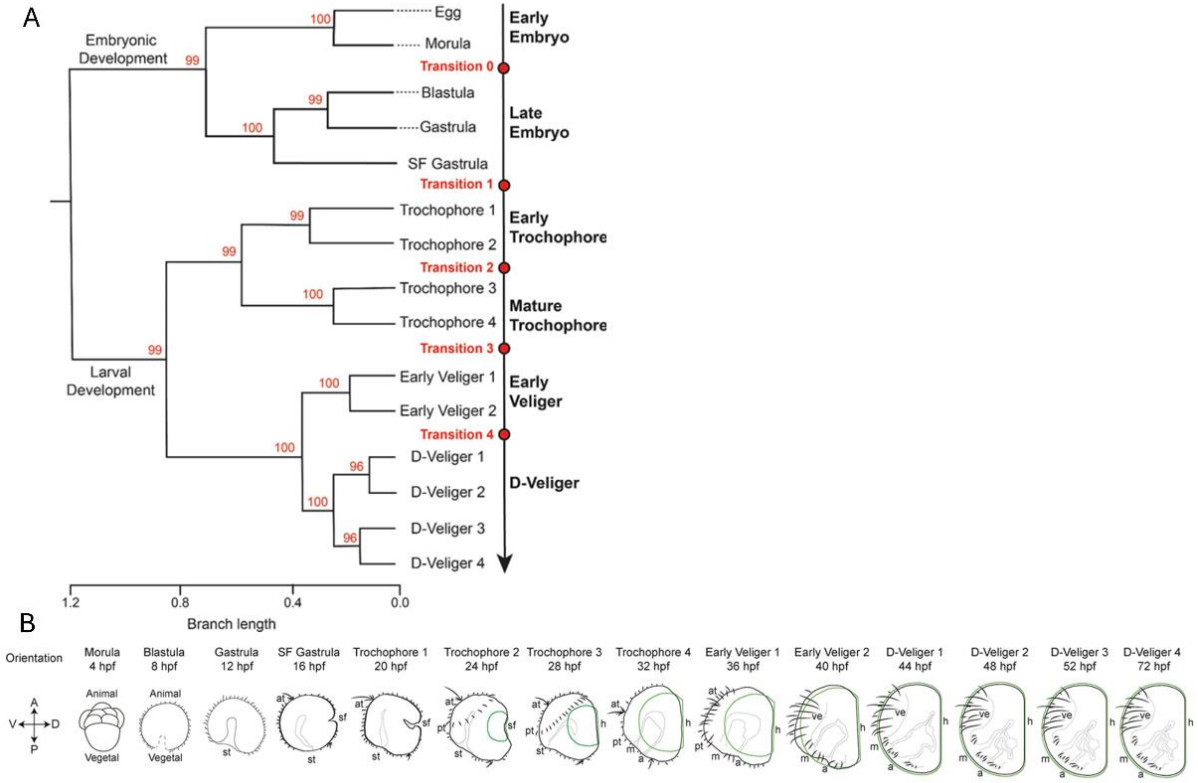


Figure 4.3. Transcriptomic and anatomical characterisation of *M. galloprovincialis* embryo-larval development. A. Hierarchical clustering identifying the phase of embryonic and larval development B. Schemes of morphotype of each stage of the developmental transcriptome. Image adapted from Miglioli et al. (2024).

From the trochophore to the D-Veliger stage key events take place such as shell biogenesis, prototroch evolution into the velum and neurogenesis. Despite the ecological and commercial importance of *M. galloprovincialis*, the mechanisms underlying key steps of early development and the transition between the trochophore and the first shelled veliger and their physiological regulation by neuro-endocrine factors are poorly understood. Available data obtained so far are reported below.

4.3.1 Shell biogenesis

Once gastrulation is ended, a group of ectodermic cells, called shell field, thicken and undergo invagination (Figure 4.4 A). The shell field is an area of pivotal importance since it leads to the formation of the shell gland which will later produce the first anlage of the organic shell, which is indispensable for the shell biogenesis process. The cells that get in touch with the endoderm will form the shell gland characterised by a glandular canal which is then occluded (Figure 4.4 B-D). Once invagination is ended and the glandular canal occluded, only a few cells are in contact with the external surface. After the occlusion, the process of shell biogenesis starts with the secretion of a pellicle which constitutes the organic shell (Kniprath, 1981, 1980; Miglioli et al., 2019). The process of shell formation begins with the secretion of the organic shell, composed of chitin (main component), acid polysaccharides, proteins and glycoproteins (Figure 4.4 D). The shell field becomes then straight due to cell evagination and then expands and differentiates into the mantle (Figure 4.4 E) (Kniprath, 1981, 1980; Kocot et al., 2016; Wanninger and Wollesen, 2015).

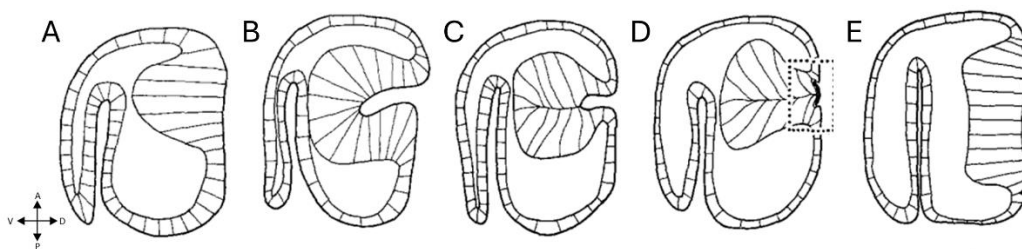


Figure 4.4. Schematic representation of shell field formation and organic shell formation. Axis abbreviations: A: anterior, D: dorsal, P: posterior, V: ventral. Image adapted from Kniprath (1980).

The role of the organic shell is pivotal, because it acts as a blueprint for the inorganic shell deposition, allowing the nucleation of CaCO_3 (Miglioli et al., 2019). The shell biogenesis process can be followed during larval development by staining the organic and inorganic shells. The first signal of organic matrix deposition is at the trochophore stage (24 hpf), and no CaCO_3 can be detected. CaCO_3 deposition starts after at 28 hpf. A full calcified shell is reached at the D-Veliger stage (48 hpf).

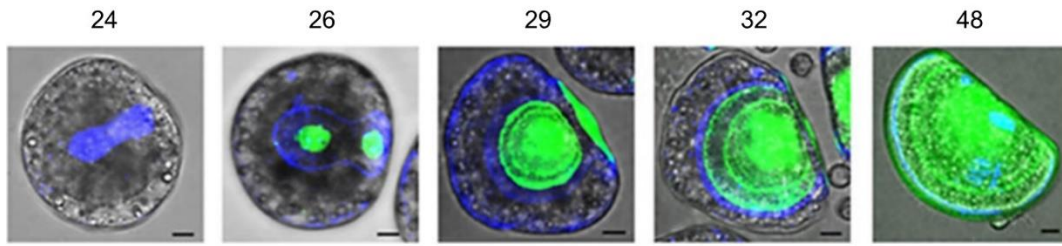


Figure 4.5. Shell biogenesis process followed by using calcofluor-calcein (blue and green, respectively) staining. Calcofluor stains chitin, thus the organic shell, and calcein stains calcium carbonate. Scale bars: 10 μm . Image adapted from Miglioli et al. (2019).

Several proteins are involved in the shell biogenesis process allowing the formation of the organic shell: tyrosinase, chitin synthase, extrapallial proteins and carbonic anhydrase. Among all of these, tyrosinase was shown to be pivotal for the process, indeed its inhibition led to a completely altered shell biogenesis. Imaging of Tyrosinase gene expression can be used to follow the shell biogenesis process through *in situ* hybridisation (Miglioli et al., 2024, 2019). Tyrosinase is detectable at 16 and 20 hpf, the stages called shell field (SF) gastrula and early trochophore stage, with two islets in the region of the shell field (Figure 4.6 A-B), which undergoes, then, evagination. The evagination process is completed at 28 hpf, and a straight hinge is thus formed dorsally (Figure 4.6 C). Tyrosinase is detected at the hinge margins and shell borders of the growing shell. At 36 hpf tyrosinase expression suggests that the larval shell is covering most of the larval body (Figure 4.6 D) and, at the D-Veliger stage (44 hpf, Figure 4.6 E), tyrosinase is found at the periphery of the larva, ventrally and at the hinge margins, enclosing completely the larval body (Figure 4.6) (Miglioli et al., 2024).

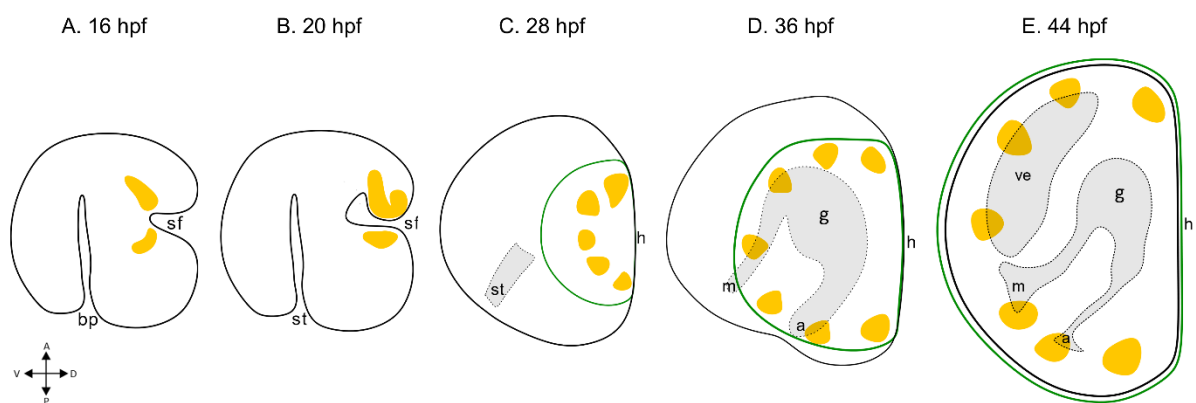


Figure 4.6. Schematic representation of tyrosinase expression during *M. galloprovincialis* embryo-larval development. Tyrosinase is indicated in yellow, shell in green. Abbreviations: a: anurs, g: gut, h: hinge, m: mouth, sf: shell field, st: stomodeum, ve: velum.

4.3.2 Evolution of the ciliated epithelium

The ciliated epithelium was studied using a specific marker: tektin. In SF gastrula and early trochophore, tektin was mainly expressed anteriorly and posteriorly forming, respectively, the apical and posterior tufts (Figure 4.7 A-B). At 28 hpf (trochophore stage) tektin signal expands, forming a ciliary band, called prototroch (Figure 4.7 C), that divides approximately the larval body into two hemispheres: the anterior episphere and the posterior hyposphere. In the episphere apical tuft persists, in the hyposphere two ciliated islets are localised in proximity to the stomodeum (the future mouth) and the area of the future anus (Miglioli et al., 2024; Piovani et al., 2023). In early-Veliger (36 hpf,) the prototroch localises ventrally (Figure 4.7 D) and at the D-Veliger stage (44 hpf) the prototroch is internalised and gives rise to the velum (Figure 4.7 E) (Miglioli et al., 2024).

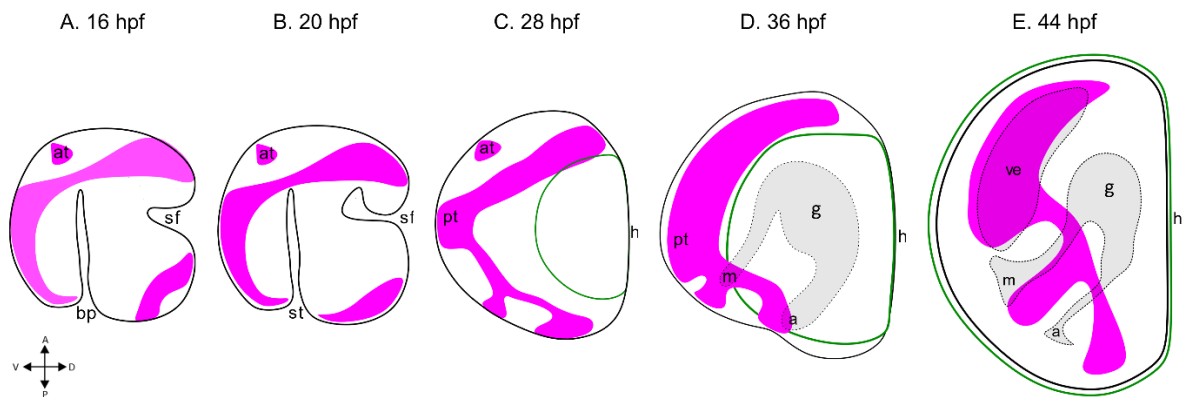


Figure 4.7. Schematic representation of tektin expression during *M. galloprovincialis* embryo-larval development. tektin is indicated in pink. Abbreviations: a: anus, at: apical tuft, g: gut, h: hinge, m: mouth, pt: prototroch sf: shell field, st: stomodeum, ve: velum.

4.3.3 The nervous system

In *M. galloprovincialis* scarce data is available concerning the nervous system. Serotonin-positive cells were investigated through immunocytochemistry (Figure 4.8). Two *5-HT-lir* appear at the trochophore stage (24 hpf) anteriorly; the number of *5-HT-lir* increases through development to reach the number of seven at the D-Veliger stage (48 hpf). Moreover, two neurites spread from the cluster of seven neurons at the D-Veliger stage (Miglioli et al., 2021b, 2021a).

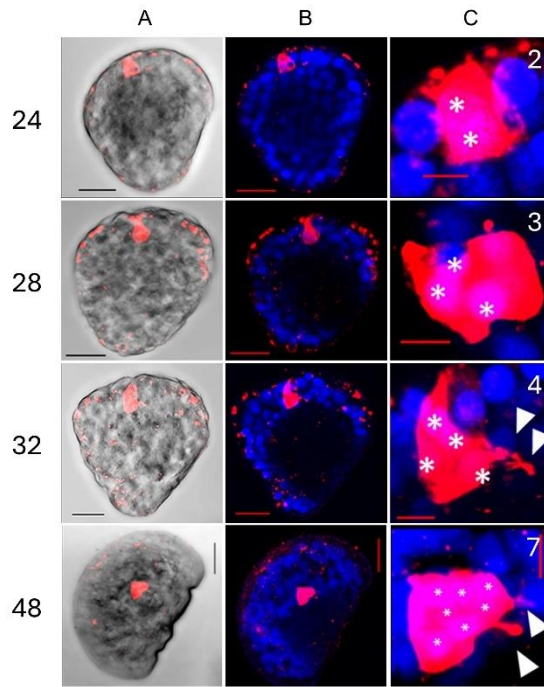


Figure 4.8. Confocal images of 5-HT-*lir* cells during *M. galloprovincialis* embryo-larval development. Rows from top to bottom: 24, 28, 32, 48 hpf. A. Position of the 5-HT-*lir* (red) in the larval body. B. 5-HT-*lir* with the nuclei (bleu). C. Number of nuclei positive to 5-HT anti-body, highlighted with the asterisks. Scale bars: columns A, B: 20 μm ; column C: 5 μm . Image adapted from Miglioli et al. (2021a).

Components of the dopaminergic system were identified through chromogenic *in situ* hybridisation. The rate-limiting enzyme for DA synthesis, tyrosine hydroxylase, showed an inconspicuous localisation at 24 hpf; from 28 hpf to 32 hpf two clusters are formed and at 48 hpf just one cluster is present (Figure 4.9 A). A dopamine receptor, called DR1, is detectable clearly from 28 hpf to 48 hpf at the shell margins (Figure 4.9 B). Dopamine- β -hydroxylase is detectable starting from 28 hpf in the centre of the larval body and localises more marginally, centrally and near the hinge, at 48 hpf (Figure 4.9 C) (Miglioli et al., 2021b).

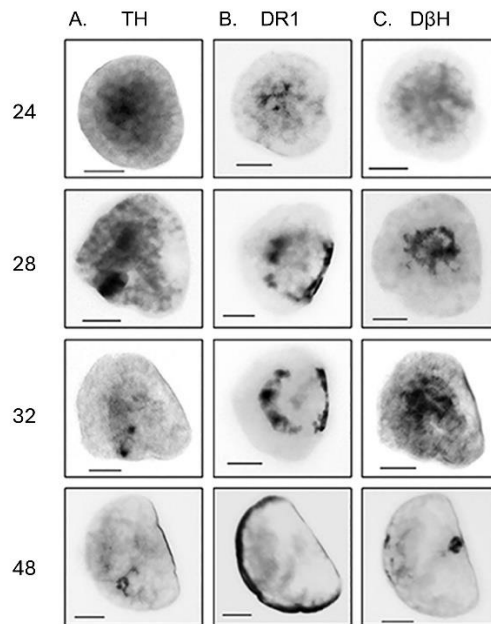


Figure 4.9. Chromogenic *in situ* hybridisation of dopaminergic components. A. Tyrosine hydroxylase (TH). B. Dopamine receptor 1 (DR1). C. Dopamine- β -hydroxylase (D β H). Rows from top to bottom: 24, 28, 32, 48 hpf. Scale bar: 20 μ m. Image adapted from Miglioli et al. (2021b).

GABA was also investigated through immunocytochemistry (Figure 4.11). GABA-*lir* cells are present along the shell field/hinge and in the centre of the body during early trochophore stages (24-28 hpf). At mature trochophore (32 hpf), GABA-*lir* is localised at the margins of the larval body and in the D-Veliger stage (48 hpf) it is localised at the ventral margins of the larval body (Miglioli et al., 2021b).

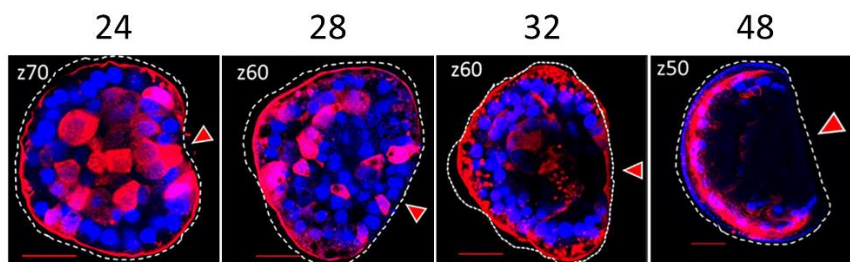


Figure 4.10. Confocal images of GABA-*lir* cells during *M. galloprovincialis* embryo-larval development. Columns from left to bottom: 24, 28, 32, 48 hpf. Scale bars: 20 μ m. Image adapted from Miglioli et al. (2021a).

4.4 *Mytilus galloprovincialis* larvae as a model organism for evaluating the impact of CEC

M. galloprovincialis is a suitable organism model, it is low-cost and easy to handle in the laboratory. It is used as an indicator of pollution in marine areas due to its benthic lifestyle, but it is also used in ecotoxicology, medicine and invertebrate immunology (Franzellitti et al., 2015;

Kristan et al., 2014; Salatiello et al., 2022). Larvae of *M. galloprovincialis* can be used in the 48 hpf acute embryotoxicity assay to evaluate the developmental effects of contaminants (Fabbri et al., 2014). At 24 hpf at 16 ± 1 °C in laboratory conditions, larvae reach the trochophore stage, at 48 hpf the D-Veliger stage (Gosling, 2015). At 48 hpf a larva is considered normal when it presents a straight hinge, the mantle does not protrude and there are no malformations (Figure 4.11 A) (Fabbri et al., 2014). The 48 hpf embryotoxicity assay is considered acceptable when there is more than 75% of normal D-larvae in the control condition (ASTM, 2004; Fabbri et al., 2014). In the presence of stressors or contaminants, malformations can occur, there could be the presence of a protruding mantle, malformations at the level of the hinge or the presence of early developmental stages (Figure 4.11 B-D).

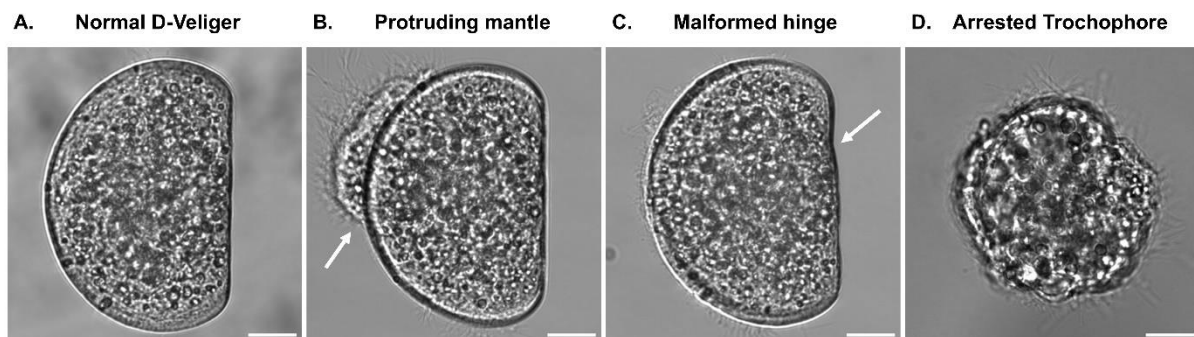


Figure 4.11. Representation of most common malformations occurring. In B. and C. malformations are indicated with a white arrow. Scale bar: 20 μ m.

M. galloprovincialis larvae been shown to be sensitive to different CEC, which will be described here. In addition to the 48 h embryotoxicity test, different genes were tested with qPCR to check alteration of specific functions and are listed in Table 4.1, genes are retrieved from different articles thus, for each chemical it will be specified which have been analysed and which not.

Function	Gene
Antioxidant defence	SOD
	CAT
Detoxification response	GST
	ABC transporter p-glycoprotein (ABCB)
	Metallothionein 10 (MT10)
	Metallothionein 20 (MT20)
Stress Response	Heat Shock Protein (HSP70)
Apoptosis	p53
Proliferation	Proliferating Cell Nuclear Antigen (PCNA)
Shell biogenesis	Tyrosinase (TYR)
	Chitin Synthase (CS)
	Extrapallial Protein (EP)
	Carbonic Anhydrase (CA)
	Runx
Immune response	Toll-Like Receptor (TLR-i)
	Lysozyme (LYS)
	Mytlin B (mytB)
	MyticinC (mytC)
Lysosomal response	Cathepsin L (CTSL)
	β -glucuronidase (GUSB)
	Hexoaminidase (HEX)
Autophagy	Serine/Threonine Protein Kinase (mTOR)
Neuroendocrine signalling	Estrogen Receptor 1 (ER1)
	Estrogen Receptor 2 (ER2)
	Serotonin Receptor (5-HTR)
	Dopamine Receptor 1 (DR1)

Table 4.1. Table showing the genes investigated with qPCR in different experiments where *M. galloprovincialis* larvae were exposed to different CEC. Genes are grouped based on their function.

Bisphenol-A (BPA) is used in plastics, it is weakly estrogenic and known to act as an EDC (Balbi et al., 2016; Canesi and Fabbri, 2015; Fabbri et al., 2014; Miglioli et al., 2021a). Concentrations ranging from 0.01 to 1000 $\mu\text{g/L}$ were tested (scale factor of ten between each concentration) and from 0.1 $\mu\text{g/L}$ a dose-dependent decrease in normal D-larvae was shown (Fabbri et al., 2014). BPA was shown to impair the transcription profile of different genes (see Figure 4.12) at both 1 and 10 $\mu\text{g/L}$. At 24 hpf genes were generally upregulated at both 1 and 10 $\mu\text{g/L}$ except for SOD and EP at 1 $\mu\text{g/L}$ and HSP at 10 $\mu\text{g/L}$ (Figure 4.12). at 48 hpf genes were mostly upregulated when treated with BPA 1 $\mu\text{g/L}$, except for SOD, p53 and CA which were downregulated) and downregulation was generally observed when treated with 10 $\mu\text{g/L}$, but SOD. HSP70 and CA showed upregulation (Figure 4.12) (Balbi et al., 2016). BPA was also shown to impair shell biogenesis process at 0.05, 0.5 and 5 μM (11.42, 114.2 and 1142 $\mu\text{g/L}$):

lower concentrations induced mainly malformed hinge and altered mainly the calcification pattern, the highest concentration affected both the organic and inorganic shell deposition. Measurements of area covered by organic and inorganic shell revealed that 0.5 μM BPA reduced their area at different time points, BPA 0.05 μM affects both organic and inorganic shell area only at D-Veliger stage and induced a reduction in calcified area only at 32 hpf (Miglioli et al., 2021a). In addition to this, larvae exposed to BPA 0.05 μM displayed a significant reduction in the number of 5-HT-*lir* especially at 48 hpf where the magnitude of decrease was dependent on the phenotype (e.g.: in presence of protruding mantle five 5-HT-*lir*, in presence of arrested trochophore three 5-HT-*lir*). The expression pattern of TYR was affected, especially at the highest concentration tested where big differences at different developmental stages could be detected (Miglioli et al., 2021a).

Function	Gene	24 hpf		48 hpf	
		1 $\mu\text{g/L}$	10 $\mu\text{g/L}$	1 $\mu\text{g/L}$	10 $\mu\text{g/L}$
Antioxidant defense	SOD	↓	↑	↓	↑
	CAT	↑	↑	↑	↓
Detoxification response	GST	↑	↑	↑	↓
	ABCB	●	↑	↑	●
Stress Response	HSP70	↑	↓	↑	↑
Apoptosis	p53	↑	↑	↓	↓
	EP	↓	↑	●	↓
	CA	●	↑	↓	↑
Immune response	TLR-i	↑	↑	↑	↓
Autophagy	mTOR	●	↑	●	↓
Neuroendocrine signalling	ER1	↑	↑	↑	↓
	ER2	↑	↑	↑	↓
	5-HTR	↑	↑	↑	↓

Figure 4.12. Genes analysed with qPCR to evaluate BPA effects on *M. galloprovincialis* larvae. Green arrows indicate upregulation, red arrows indicate downregulation of genes with respect to control conditions. Grey dots indicate that no differences were observed between control conditions and treatment conditions. Figure adapted from Balbi et al. (2016).

Tetrabromobisphenol A (TBBPA) is a derivate of BPA and is mostly used as a brominated flame retardant but it is also employed in the production of plastics, electronic devices and textiles (Fabbri et al., 2014; Miglioli et al., 2021b). Concentrations ranging from 0.01 to 1000 $\mu\text{g/L}$ were tested and it induced a significant dose dependent decrease of normal D-Veliger from 0.1 $\mu\text{g/L}$ and at the highest concentration tested larvae were arrested at the trochophore stage (Fabbri et al., 2014). Effects of 1 and 10 $\mu\text{g/L}$ were investigated more in details. Exposure to 1 $\mu\text{g/L}$ caused shell fractures and immature shells characterised by the presence of asymmetric valve and polygonal shapes; effects were more potent in larvae treated with 10 $\mu\text{g/L}$ where fractures, irregular surfaces, holes and convex hinges could be observed by scanning electron microscopy (SEM) (Miglioli et al., 2021b). Shell biogenesis process was shown to be altered after exposure to TBBPA 10 and 100 $\mu\text{g/L}$, especially from 28 hpf the deposition of calcium carbonated was reduced and absence of calcification was observed in the centre of the

valve from 28 to 48 hpf (Miglioli et al., 2021b). Thus, expression profile of enzymes involved in shell biogenesis (CA, CS, EP and TYR) were evaluated (TBBPA 10 µg/L). Generally, TBBPA induced upregulation of the genes tested, exception made for CA which was unaffected (Miglioli et al., 2021b). TYR expression pattern was also evaluated with *in situ* hybridisation and it was upregulated, in line with PCR experiments (Miglioli et al., 2021b). Effects of TBBPA 10 µg/L were also evaluated for 5-HT-*lir* and dopaminergic genes (Tyrosine Hydroxylase – TH, Dopamine-β-Hydroxylase – DBH, and DR1). 5-HT-*lir* cell number was reduced by TBBPA, The expression profile was delayed whereas DBH was upregulated, finally DR1 expression pattern was impaired after TBBPA exposure (Miglioli et al., 2021b).

Nonylphenol (NP), a known EDC, was also tested on *M. galloprovincialis* in concentrations ranging from 0.01 to 1000 µg/L. It induced a significant decrease in normal D-Veliger starting from 0.1 µg/L but it did not induce an evident dose-dependent decrease effects. The highest concentration tested turned out to be completely toxic, since no viable larvae could be observed (Fabbri et al., 2014).

The estrogen 17β-estradiol (E2) and its synthetic derivate, the contraceptive 17α-ethinylestradiol (EE2) are classified both as an EDC and a pharmaceutical (Pironti et al., 2021). It was shown that concentrations ranging from 0.1 to 1000 µg/L of E2 (scale factor of ten between each concentration) affected significantly normal D-Veliger in a dose dependent manner. E2 induced mainly delay in development, with presence of increasing of not fully developed D-Veliger and arrested trochophores (Balbi et al., 2016). At 10 µg/L, the most common alterations were represented by alterations at the shell level, with malformed hinges, asymmetric valves and a rough valve surface (Balbi et al., 2016). Moreover, E2 10 µg/L altered gene transcription profiles at trochophore (24 hpf) and D-Veliger (48 hpf) stages. EE2 has been tested as well on *M. galloprovincialis* larvae (5, 50 and 500 ng/L) and it was shown to cause significant reduction in the presence of normal D-larvae at all the concentrations tested (Capolupo et al., 2018).

The two thyroid hormones, Triiodothyronine (T3) and Tetraiodothyronine (T4), at 2 µM (1345.92 µg/L and 1553.74 µg/L, respectively) were tested on *M. galloprovincialis* larvae but they resulted to be ineffective on larval development (scale factor of ten between each concentration).

Among the perfluorinated compounds, perfluorooctanoic acid (PFOA) and perfluorooctane sulphonate (PFOAS) were tested in concentrations ranging from 0.01 to 1000 µg/L. Both were

shown to induce a dose-dependent effect, with a significant decrease of normal D-Veliger from 0.1 µg/L. Maximal effects were observed at 100 µg/L, with no further decrease at higher concentrations. Most abundant phenotypes were represented by immature D-Veliger (Fabbri et al., 2014).

In Balbi et al. (2023) the antimicrobial Triclosan (TCS), used in a variety of household and healthcare products was studied. Its effects were evaluated from 0.001 to 1000 µg/L (from 0.01 to 100 µg/L scale factor of ten, then 250, 500, 750 and 1000 µg/L were tested). Larvae were affected from 0.1 µg/L, with small decrease observed up to 100 µg/L with malformed hinge being the most abundant phenotype; at 250 µg/L mostly pre-Veliger were detected and from 750 µg/L the larval development was completely arrested. Genes involved in shell biogenesis, neuroendocrine signalling, stress and detoxification response, apoptosis and proliferation were evaluated for TCS 1 and 10 µg/L at 24 and 48 hpf. Shell biogenesis genes were affected by TCS at trochophore stage, neuroendocrine signalling was mainly not affected (except for oestrogen receptors), stress response was not affected, and detoxification genes were affected by both concentrations only at 48 hpf, on the contrary apoptotic genes were affected by both concentrations at both 24 and 48 hpf. Larvae exposed to TCS 10 µg/L displayed calcification and mineralisation alterations: calcification was decreased in the hinge region, moreover evaluations with polarised light showed that the typical birefringence represented by CaCO₃ mineralisation, was absent in treated larvae, indicating that CaCO₃ was absent in the mineralised form. SEM analysis of larvae treated with TCS (from 0.1 to 100 µg/L) showed the presence of impaired shells. Indeed, low concentrations showed no malformed hinge but asymmetric valve, malformed shells and broken shells; cracked and irregular surfaces, asymmetric or incomplete valve were typical features of higher concentrations (10 and 100 µg/L). Moreover, samples analysed showed presence of granules on the surface, resembling to amorphous calcium carbonate.

Function	Gene	24 hpf		48 hpf	
		1 µg/L	10 µg/L	1 µg/L	10 µg/L
Antioxidant defense	SOD	●	●	●	●
	CAT	●	●	●	●
Detoxification response	GST	●	●	↓	↓
	ABCB	●	●	↑	↑
Apoptosis	p53	↓	↑	↑	↑
Proliferation	PCNA	●	●	●	●
Shell biogenesis	TYR	●	●	●	●
	CS	●	↑	●	●
	EP	↑	↑	●	●
	CA	↓	↑	●	●
	Runx	●	●	↑	●
Neuroendocrine signalling	ER1	●	↓	●	↑
	ER2	●	↑	●	●
	5-HTR	●	●	●	●
	DR1	●	●	●	●

Figure 4.13. Genes analysed with qPCR to evaluate TCS effects on *M. galloprovincialis* larvae. Green arrows indicate upregulation, red arrows indicate downregulation of genes with respect to control conditions. Grey dots indicate that no differences were observed between control conditions and treatment conditions. Figure adapted from Balbi et al. (2023).

Concerning pharmaceuticals, the non-steroidal anti-inflammatory Ibuprofen (IBU) and the fibrate lipid-lowering Bezafibrate (BEZA) were tested in the same concentrations range of perfluorinated compounds (Fabbri et al., 2014). IBU induced a small dose-dependent decrease in development at 100 and 1000 µg/L with malformed hinge representing the most abundant phenotype (Fabbri et al., 2014). BEZA induced a small dose-dependent decrease from 10 µg/L (Fabbri et al., 2014).

The non-steroidal anti-inflammatory Diclofenac (DCF) was also analysed on *M. galloprovincialis* larvae (Balbi et al., 2018; Fabbri et al., 2014). Effects on larval development displayed a U-shaped dose response, with maximal effects in the range of 0.1 – 100 µg/L with malformations at the hinge level, no effects were shown at the highest concentration tested (1000 µg/L). At 1 and 10 µg/L effects to the larval shell were visible with electron microscopy (SEM), displaying dorsal deformations, asymmetric valve, rough surface or incomplete growth and undulated shell edges. Gene expression was thus evaluated for genes involved in shell biogenesis, biotransformation, antioxidant and stress response, neuroendocrine signalling and apoptosis (Figure 4.14). DCF 1 µg/L impaired the expression of six out of 12 genes at 24 hpf: SOD, ABCB, EP and CA were downregulated, on the contrary GST was upregulated. Only three genes were affected by DCF 10 µg/L at 24 hpf: GST resulted to be downregulated, whereas ABCB and CA resulted to be downregulated (Figure 4.14). At 48 hpf, less effects were observed at both concentrations: 1 µg/L induced upregulation of ABCB- p53, CA and 5-HTR; 10 µg/L downregulated ABCB, p53 and CS and upregulated GST (Figure 4.14). CAT, HSP70 and oestrogen receptors were never affected by exposure to DCF (Figure 4.14).

Function	Gene	24 hpf		48 hpf	
		1 µg/L	10 µg/L	1 µg/L	10 µg/L
Antioxidant defense	SOD	↓	●	●	●
	CAT	●	●	●	●
Detoxification response	GST	↑	↓	●	↑
	ABCB	↓	↑	↑	↓
Stress response	HSP70	●	●	●	●
Apoptosis	p53	●	●	↑	↓
Shell biogenesis	CS	●	↑	●	↓
	EP	↓	●	●	●
	CA	↓	●	↑	●
Neuroendocrine signalling	ER1	●	●	●	●
	ER2	●	●	●	●
	5-HTR	↓	●	↑	●

Figure 4.14. Genes analysed with qPCR to evaluate DCF effects on *M. galloprovincialis* larvae. Green arrows indicate upregulation, red arrows indicate downregulation of genes with respect to control conditions. Grey dots indicate that no differences were observed between control conditions and treatment conditions. Image adapted from Balbi et al. (2018).

The β -blocker Propranolol (PROP) was shown to affect larval development at all concentrations tested in the range of 0.01 – 1000 µg/L (Franzellitti et al., 2019). Larvae presented malformation or were arrested at the trochophore stage at all concentrations tested in variable proportion, only the highest concentration tested resulted to induce arrested trochophores as sole phenotype. Genes showed to be impaired after incubation with PROP 0.01 and 1 µg/L at 24 and 48 hpf (Figure 4.15 A). At 24 hpf PROP affected differently gene transcription, by upregulation and downregulation of several genes at both concentrations. At 48 hpf, PROP 0.01 µg/L showed reduced effects but 5-HTR1 was particularly downregulated. On the contrary, 1 µg/L resulted in an upregulation of almost all genes tested (Figure 4.15 A) (Franzellitti et al., 2019).

Franzellitti et al. (2019) also studied the effects of the antiepileptic Carbamazepine (CBZ). CBZ induced a decrease in normal larval development starting from 0.1 µg/L, with larvae bearing malformations. Expression genes levels were also evaluated for CBZ at 24 and 48 hpf. CBZ 0.01 µg/L induced mainly upregulation of gene expression at 24 hpf, whereas antioxidant gene were slightly downregulated at 48 hpf (Figure 4.15 B). Also 1 µg/L induced upregulation at 24 hpf, whereas at 48 hpf downregulation occurred for almost all genes studied (Figure 4.15 B) (Franzellitti et al., 2019).

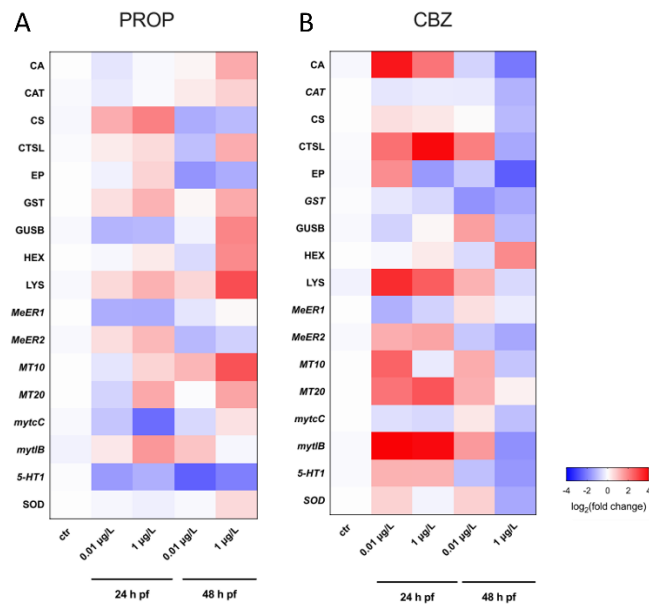


Figure 4.15. Expression profiles of genes listed in Table 4.1 after exposure to propranolol (A) and carbamazepine (B) at 24 and 48 hpf. Red indicates upregulation, blue indicates downregulation. Image taken from Franzellitti et al. (2019).

Recently, *M. galloprovincialis* was shown to be sensitive to exposure to different SSRIs (see Chapter 3). Moreover, *M. galloprovincialis* was shown to be sensitive to Serotonin and Norepinephrine Reuptake Inhibitors (SNRIs), in particular Venlafaxine (VEN) and its metabolite O-desmethylvenlafaxine (ODV) (Rafiq et al., 2023). Both were tested in the range of 0.5 – 500 ng/L. Larval development at 48 hpf was significantly affected by all SSRIs, but not by SNRIs; however, the effects never exceeded 20 % of control values (Rafiq et al., 2023).

5 Aim of the Thesis

As illustrated in the introduction, the mechanisms underlying key steps of bivalve early development, and in particular the transition between the trochophore and the first shelled larva, and its physiological regulation by neuro-endocrine factors are poorly understood.

As described in Chapter 2, the structure of the nervous system in bivalve larvae has been documented, primarily based on the localization of neurotransmitters (serotonin, FMRFamide, and catecholamines). The latter are marked using a non-specific technique, which can also label serotonin and its precursor, 5-hydroxytryptophan. This lack of specificity can lead to results that are challenging to interpret (Kniazkina and Dyachuk, 2022). Moreover, there has been no previous description of the ontogeny of the nervous system using neuronal markers.

Although available data suggest a physiological role for the monoaminergic system in larval development, information on its molecular components and function is still scant. Despite the widespread use of *M. galloprovincialis* as a model organism, limited data exist regarding the presence or absence of genes and proteins associated with the monoaminergic system.

Therefore, the first aim of this thesis is to investigate the monoaminergic system, its characterisation, and its role during embryo-larval development in *M. galloprovincialis*.

The following questions will be addressed:

1. Which components of the monoaminergic system are present in the *M. galloprovincialis* genome?
2. When are these components expressed during the embryo-larval development?
3. In which tissues are these components localised?
4. Can altered concentrations of monoamines and inhibition of monoamine signalling impair normal larval development?

Moreover, as described in Chapter 3, there is increasing evidence that different CEC, both EDCs and PPCPs, including Serotonin Selective Reuptake Inhibitors (SSRIs), can affect *M. galloprovincialis* larval development, potentially acting as neuro-endocrine disruptors (NEDs). This first aim is crucial as it allows the determination of the presence or absence of monoaminergic system components, some of which have already been shown to be impacted by two EDCs (TBA and TBBPA). Most importantly, it enables the identification of the main target of SSRIs: the SERT.

In this light, the present study also aims at identifying monoaminergic components as possible targets for CEC, in particular for SSRI. As discussed in the introduction, the most prevalent SSRIs found in the environment are Fluoxetine (Prozac) and Citalopram (Celexa), which will be both analysed in this thesis.

In particular, these questions will be addressed

1. Are the targets of SSRIs present and conserved in *M. galloprovincialis*?
2. Are there non-specific SSRIs targets present in *M. galloprovincialis*?
3. What is the AOP of SSRIs (i.e.: FLX and CIT)?

The challenge with pharmaceuticals is that they are designed to act on specific targets (enzymes, receptors, transporters) that may be evolutionary conserved in other organisms (Ankley et al., 2007; Duarte et al., 2023; Fabbri and Franzellitti, 2016; Franzellitti et al., 2015, 2013; Gunnarsson et al., 2008). However, to date, there is no information available concerning the presence or absence of SERT in *M. galloprovincialis*.

The results will contribute to identify the molecular targets for SSRI to understand their mode of action and their potential adverse outcome pathway (AOP) in developing larvae.

**6 Aim 1: Ontogeny of the monoaminergic
system during the embryo-larval
development of the Mediterranean mussel
*Mytilus galloprovincialis***

6.1 Material and Methods

6.1.1 Orthology assessment of monoaminergic system elements in *M. galloprovincialis* genome

The monoaminergic system elements in *M. galloprovincialis* were retrieved from the genome assembly (Gerdol et al., 2020, ID: PRJEB24883) by Protein Basic Local Alignment Search Tool – BLAST on Octopus Bioinformatic Server (<https://octopus.obs-vlfr.fr/>), using human (*Homo sapiens*) and fruit fly (*Drosophila melanogaster*) reference sequences as queries (in case of absence of human or fruit fly query sequences, other species available in bibliography were used). Sequences resulting from the BLASTP search (only sequences with a BLAST score \geq 200 were retained for analysis) were subjected to domain analysis using the NCBI Conserved Domain Database (CDD). Only sequences containing the expected functional domains were retained for further analysis. Multiple sequence alignment was performed using ClustalW (BioEdit version 7.0.2) to prepare the data for orthology assessment analysis. Orthology assessment was performed by using Maximum Likelihood (ML) analysis and bootstrap analysis with 1000 replications to assess node support (MEGA-X 10.2.6). Partial deletion and default inference resource usage options were utilized for ML analysis. Substitution model selection and rate estimation were performed for each dataset of protein sequences using the "models" function in MEGA-X. In cases where ML analysis did not yield interpretable results, protein naming and identification were carried out through FASTA sequence alignment using ClustalW (BioEdit); names were given based on presence/absence of amino acids involved in the catalytic site or in ligand binding. In addition to *M. galloprovincialis*, sequences from other species of bivalve molluscs, with public genome repositories in NCBI, were also examined in the process. The test species included: *M. edulis*, *M. coruscus*, *Crassostrea gigas*, *C. virginica*, *Mizuhopecten yessoensis* and *Pecten maximus*, following the selection criteria outlined in Canesi et al. (2022).

6.1.2 Transcriptome analysis for characterizing the ontogeny of the monoaminergic system during *M. galloprovincialis* embryo-larval development

Developmental expression of monoaminergic genes was analysed using the reference developmental transcriptome of the Mediterranean mussel (Miglioli et al., 2024), selecting the libraries collected between 0 to 48 hours post fertilisation (hpf). The raw data were normalized with the DESeq2 R package into log₂ transformed counts per million (CPM) to perform hierarchical clustering of libraries with Pvcust and Principal Component Analysis (PCA) with

factoextra R packages as previously described (Miglioli et al., 2024). Genes of interest were extracted from the counts matrix using the MGAL identifier obtained from the Octopus Bioinformatic Server. For gene expression visualization, gene counts data were normalized by Transcript per Million (TPM). Heatmaps showing the temporal expression dynamics of the genes of interest were generated pheatmap package as previously described (Miglioli et al., 2024) with scaled TPM with respect to the maximum and minimum expression value of a gene (e.g., values between -1 and 1).

6.1.3 Mussel handling, spawning, fertilisation and conservation of larval samples

Sexually mature specimens of *M. galloprovincialis* were sampled from a natural population in the bay of Villefranche-sur-Mer (43.682°N, 7.319°E, France) during the spawning season (January-March 2023). Mussels were acclimatized in flow-through vessels containing filtered natural seawater (0.2 µm Millipore filter), pH 8.0-8.2, 38 ppt salinity, 15°C (Millipore filtered sea water, MFSW) by the Centre de Ressources Biologiques Marines (CRBM) at the Institut de la Mer de Villefranche (IMEV).

Gametes were obtained by inducing spawning with heat shock as previously described (Miglioli et al., 2019). Egg quality and sperm motility were checked by microscopy observations; fertilization and assessment of fertilization success were performed as previously reported (Fabbri et al., 2014; Miglioli et al., 2021a, 2019). After 30 min, fertilized eggs were transferred to 200 mL flasks at a density of 200 larvae/mL and grown in physiological conditions (filtered natural seawater, pH 8.0-8.2, 16°C).

Samples for *in situ* hybridization chain reaction (HCR) were collected at 16, 28 and 48 hpf as follows: larvae were sampled using a 0.2 µm filter and fixed in 4% paraformaldehyde (PFA) in 1× Phosphate Buffered Saline (PBS, 137 mM NaCl, 2.7 mM KCl, 10 mM Na₂HPO₄, 1.8 mM KH₂PO₄, pH 7.4) solution overnight at 4°C. Samples were then washed 3 times for 15 minutes in 1× PBS and stored in 100% methanol at -20°C.

Experiments were also carried out in larvae grown in the presence of agonists and antagonists of the serotonergic and dopaminergic systems. In these experiments, larvae were grown in 24 well plates to perform the 48 h embryotoxicity test (ASTM, 2004). Fertilized eggs were exposed to serotonin (5-HT, stock solution: 100 mM in DMSO, 153-98-0), dopamine (DA, stock solution: 100 mM in DMSO, 62-31-7), methiothepin, a non-selective inhibitor of serotonin receptors, (MT, stock solution 100 mM in DMSO, Sigma-Aldrich 74611-28-2) and SCH 23390,

a selective inhibitor of dopamine receptor 1 (DR1), (SCH, stock solution 50 mM in DMSO, 125941-87-9). All chemicals were diluted in MFSW (Millipore Filtered Seawater) to obtain the final desired concentrations. DMSO (Dimethyl Sulfoxide) at the highest concentration (0.01%) was added to controls. A minimum of four parental pairs were analysed for each condition. Statistical analysis was performed using Kruskal-Wallis test and Dunn test for *post-hoc* comparison with p-values Bonferroni adjustment to show differences between controls and treatments in terms of percentage of normal D-Larvae (ND).

6.1.4 Morphological analysis of larvae

Morphological analyses were performed at 48 hpf: according to the ASTM (2004) larvae were considered normal when they were D-shaped, with a straight hinge and an absence of protruding mantle. Larvae were considered malformed when protruding mantle or/and hinge malformations were present and delayed/arrested when they were at earlier stages (pre-veliger or trochophore) (Fabbri et al., 2014; Miglioli et al., 2021a). Data on larval phenotypes are reported as the percentage of normal or malformed larvae, evaluated in at least 50 larvae per each parental pair and experimental condition. Brightfield images were acquired with 20× objective using the inverted microscope Axio Observer 7.

6.1.5 *In situ* Hybridization Chain Reaction (HCR)

Probe sets for *in situ* HCR were designed using a user-friendly Python interface (https://github.com/rwnull/insitu_probe_generator) and synthesized by OligoPools (Twist Bioscience) as previously described (Miglioli et al., 2024). Amplifiers were purchased from Molecular Instruments (<https://www.molecularinstruments.com>). Synthesis enzyme and degradation enzymes genes were marked with amplifier in yellow (B2¹, ex: 561 nm, em: 572 nm, laser: 552 nm), receptors with amplifier in red (B1, ex: 650 nm, em: 671 nm, laser: 638 nm) and transporters with amplifier in green (B3, ex: 518 nm, em: 543 nm, laser: 488 nm) (see Appendix Table 1 and Appendix Table 2 for probes sequences). To establish the localisation of genes of interest, they were co-labelled with marker genes for specific tissues. These markers are reported in Annex Table 2.

Larval samples stored in methanol at -20°C were rehydrated serially with 1×PBS-TritonX 0.01% (4 washes of 5 minutes each) and then incubated first for 5 minutes (min) and then for 10 min in PBS-TritonX 0.01% at room temperature. Samples were then permeabilized and

¹ Bn° stands for the identifier of the amplifier used.

decalcified for 30 min with Detergent Solution (1% Sodium Dodecyl Sulfate - SDS, 0.005% Tween 20, 50 mM Hydrochloric acid - HCl pH 7.5, 1 mM Ethylenediamine Tetraacetic Acid - EDTA, pH 8, 0.15 M Sodium Chloride - NaCl), washed 2×3 min in PBS-TritonX and then 2×5 min in PBS-TritonX 0.01%. Specimen were pre-hybridised for 30 min at 37 °C in 50 μ L of Hybridization Buffer (30% formamide, 5 \times Saline sodium citrate - SSC, 9 mM citric acid, pH 6, 0.01% Tween 20, 2 mg heparin, 1 \times Denhardt's solution, 10% dextran sulphate).

Hybridization was performed at 37 °C overnight by adding 1 μ L of probe and 49 μ L of Hybridization Buffer (final volume: 50 μ L) to the prehybridization mix (final volume: 100 μ L) as previously described (Miglioli et al., 2024). Larvae were then washed with Washing Solution (30% formamide, 5 \times SSC, 9 mM citric acid, pH 6, 0.01% Tween 20, 2 mg Heparin) once, with the addition of 1.5 volumes of Washing Solution for 15/20 min, then 4×15 min washes always at 37 °C. Samples were then put at room temperature and washed 2×5 min in 5X SSC buffer-Tween 0.1% (SSCTw) and then 2×5 min in 1 \times SSCTw and then 30 minutes in Amplification Buffer (5 \times SSC, 0.01% Tween 20, 10% dextran sulphate) before addition of amplifiers. Amplifiers were prepared as follow: for each well, 2 μ L of hairpin 1 and hairpin 2 for each probe were pipetted in separate 600 μ L tubes, warmed up to 95 °C for 90 seconds and then cooled down to room temperature for 30 min. Hairpins 1 and 2 were then mixed together in Amplification Buffer to reach a final volume of 50 μ L and added directly to the well (final volume: 100 μ L). Hairpins were incubated in a dark room overnight at room temperature. After recovering hairpins, larvae were washed 2×5 min and 2×30 min with 1 \times SSCTw, washed 2×5 min with PBSTw and then incubated 1 μ g/L Hoechst (UV, Ex/Em: 352/461 nm- Hoechst 33342, Invitrogen) in PBSTw. Larvae were then washed 3×5 min in PBSTw and incubated in PBSTw for 30 min at 4°C. At the end, specimens were mounted in the antifading agent CitiFluor AF1 (Agar Scientific) and imaged with a SP8 confocal microscope (Leica Microsystem).

6.1.6 Image acquisition and analysis

Images were taken with SP8 confocal microscope with LasX software with the following settings: three-dimensional acquisition mode (xyz); bidirectional scanning mode, 1024 \times 1024 image format, scanning speed: 600 Hz, pixel size: $\sim 200 \mu\text{m} \times 200 \text{nm}$ and z-stack: z-step size of 0.5 μm for single HCR or 0.8 μm for double/triple HCR. In case of double/triple HCR, line accumulation and frame average were set, respectively, to 3 and to allow a better visualisation of the signal. In presence of both 514 and 546 fluorophores, the sequential mode was used to avoid spillover of the signal coming from each fluorophore. Pictures were taken with 40 \times objective and a minimum of five larvae were analysed for each gene/gene combination.

Images were analysed with Fiji. Function “Math → Subtract” was used when Hoechst autofluorescence was present in probe signal. Process → Subtract Background...” and Gaussian Blur (0.5 μm) were applied to the image to remove background noise and smooth signal. Depending on the type of signal, selective plane projection (selection of specific z-step) or all plane projection (selection of all z-stack, using z-stack → MAX projection) were used to localise the signal and quantify different clusters. Selective plane projection was used to check colocalisation of different genes, with gene signals represented in green and magenta; the resulting white signal indicated overlapping expression. 3D reconstruction was performed with default settings to obtain ventral views. Larvae were oriented all the same by using Image → Transform and then rotated and/or flipped. Larvae were oriented with the dorsal side on the right and the ventral one on the left, anterior part on the top and posterior one on the bottom. Stomodeum (the future mouth) and mouth were ventrally positioned; shell field and hinge were located dorsally. In case of larvae moving during the acquisition process, signals from each channel were aligned using Stackreg (TurboReg) plugin.

Fiji software was used to perform cell counting. Channel containing Hoechst and probe signal were merged. The area of the signal was then cropped, and the stack was converted into a montage, where each image generated represented one stack. Positive nuclei were counted with the point tool by using the counter mode. An example is provided in Supplementary Figure 6.1.

6.2 Results

6.2.1 Characterization of components of the monoaminergic system in *M. galloprovincialis*

To perform the orthology assessment of the components of the monoaminergic system, the following species of bivalve molluscs were used (Table 6.1). Furthermore, the species *H. sapiens* and *D. melanogaster* were used as query sequences.

Order	Family	Species
Mytilida	Mytilidae	<i>Mytilus edulis</i>
Mytilida	Mytilidae	<i>Mytilus coruscus</i>
Ostreida	Ostreidae	<i>Crassostrea gigas</i>
Ostreida	Ostreidae	<i>Crassostrea virginica</i>
Pectinida	Pectinidae	<i>Mizuhopecten yessoensis</i>
Pectinida	Pectinidae	<i>Pecten maximus</i>

Table 6.1. Table of specie used to perform the orthology assessment. Orders and families were retrieved from WoRMS Editorial Board (2024).

6.2.1.1 Synthesis enzymes

Sequences containing the aromatic amino acid hydroxylase (AAAH) domain were analysed (Supplementary Table 6.1). These include three key enzymes: tryptophan hydroxylase (TPH), the rate limiting enzyme for serotonin synthesis; tyrosine hydroxylase (TH), the rate limiting enzyme for dopamine synthesis and phenylalanine hydroxylase (PAH), which synthesizes tyrosine from phenylalanine (Goulty et al., 2023). In *M. galloprovincialis* genome up to four sequences displayed the domain typical of PAH, TH and TPH (Supplementary Table 6.1).

The orthology assessment (Supplementary Figure 6.2) shows that two PAHs, one TH, and one TPH are present in *M. galloprovincialis* genome, like in the other Mytilidae species. In contrast, the other bivalve species analysed (*C. gigas*, *C. virginica*, *M. yessoensis* and *P. maximus*) possess only one PAH. The TPH and PAH groups are sister groups within the same clade, whereas the TH group forms a unique clade that is a sister group of the PAH-TPH clade.

Next, sequences containing the aromatic L-amino acid decarboxylase (AADC) were investigated. Decarboxylases are responsible for removing a carboxyl group during monoamine synthesis (Goulty et al., 2023). This family of enzymes includes: aromatic L-amino acid decarboxylase (AADC, or dopa decarboxylase DDC), the enzyme involved in both serotonin and dopamine synthesis by converting 5-hydroxytryptophan in serotonin and L-DOPA in dopamine; histidine decarboxylase (HDC), which converts histidine to histamine, and tyrosine decarboxylase (TDC), which is responsible for the conversion of tyrosine to tyramine (Goulty et al., 2023; Kuo and Cheng, 2021; Li et al., 2018; Lin et al., 2020; Scammell et al., 2019).

Sequences used for alignment and orthology assessment are reported in Supplementary Table 6.2. Orthology assessment (Supplementary Figure 6.3) shows that there is one decarboxylase for each gene family analysed in all orders of bivalves analysed (Mytilida, Ostreida, Pectinida) and in *H. sapiens* and *D. melanogaster*. This indicates that *M. galloprovincialis* and the other bivalves analysed can synthesise serotonin, dopamine, tyramine and histamine. Groups of gene families are generally well supported (bootstrap values > 70), with the exception of the TDC clade, which is statistically less supported (BP value = 59). From the tree it resulted that the AADC and the HDC are sister groups within the same clade, whereas the TDC appeared to be a sister group of the previous clade but forming a clade on its own.

Sequences containing the typical copper-containing hydroxylase domain were analysed to find the sequences encoding for dopamine- β -hydroxylase (DBH), that catalyse the hydroxylation of dopamine to noradrenaline (or norepinephrine); tyramine- β -hydroxylase, which is involved in the synthesis of octopamine starting from tyramine, and monooxygenase X (DBH-like monooxygenase protein 1 – MOXD1) whose function is still unknown (Goultly et al., 2023; Vendelboe et al., 2016; Xin et al., 2004).

Orthology assessment revealed the presence of one DBH in bivalve molluscs, except for *M. coruscus*, and the presence of several MOXD1 (here called DBH-like) and no TBH (Supplementary Table 6.3, Supplementary Figure 6.4). Results are in line with the recent results reported by Goultly et al., (2023): *D. melanogaster* TBH clusters with DBH present in both bivalves and humans and acts as an outgroup of this clade, since TBH is found only in Ecdysozoa. The DBH/TBH clade is well supported (BP = 75). Moreover, the clade containing the MODX/DBHs-like sequences is also well supported (BP = 99). Of particular interest is the presence of multiple DBHs-like in *M. galloprovincialis* (up to seven different proteins were found), as well as in other Mytilidae species analysed (Supplementary Figure 6.4). The other bivalve species showed a reduced number of DBHs-like proteins: one for *M. yessoensis*, three for *P. maximus* and *C. gigas* and two for *C. virginica* (Supplementary Table 6.3).

Phenylethanolamine-N-methyltransferase (PNMT) is the enzyme responsible for the synthesis of adrenaline from noradrenaline, but no sequences were found in any of the species here analysed, confirming that this enzyme is typical of vertebrates as shown by Goultly et al., 2023.

6.2.1.2 Degradation enzymes

Endogenous and exogenous monoamines are known to be metabolised by monoamine oxidases (MAOs) in vertebrates and invertebrates. Sequences used for orthology assessment are reported

in Supplementary Table 6.5. Orthology assessment did not allow to identify the two isoforms of MOA (MAO-A and MAO-B) in *Mytilus* and other bivalve molluscs, probably due to the fact that one *M. galloprovincialis* sequence displays a galactose mutarose-like additional domain (Supplementary Table 6.5, Supplementary Figure 6.5). As a consequence, multiple sequence alignment was carried out to search for the presence/absence of the amino acids responsible for monoamine catabolism: phenylalanine 208 (F208) for MAO-A, and isoleucine 199 (I199) for MAO-B (Wilson et al., 2020). To perform such analysis, also murine sequences was included (accession number to classify MAOs within their specific isoforms are reported in the Supplementary Table 6.5 alignment). It was found that the two *M. galloprovincialis* MAOs can be classified as MAO-A like (Supplementary Figure 6.6 A) and MAO-B (Supplementary Figure 6.6 B) because the first one shows a similar amino acid (tyrosine) aligning with human and murine MAO-A, whereas the second is a MAO-B because it presents an isoleucine like human and murine MAO-B (see Supplementary Table 6.5). In the other species of bivalve molluscs analysed, at least on MAO or MAO-like was found; for more details see Supplementary Table 6.5.

6.2.1.3 Transporters

Vesicular monoamine transporters (VMATs) belong to the SLC18 family were analysed. Orthology assessment was performed using the sequences reported in Supplementary Table 6.6. Given the absence of specific hit domain for VMAT in bivalve sequences, vesicular acetylcholine transporter sequences (VACHT) were used to better identify VMATs. It was found that all invertebrate species analysed possess one VMAT (Supplementary Figure 6.7), and this in line with previous data reporting the presence of a single VMAT gene in invertebrates (Anne and Gasnier, 2014; Lawal and Krantz, 2013).

Membrane transporters belonging to SLC6 family are the reuptake transporters for serotonin, dopamine, noradrenaline, tyramine and octopamine. This family of transporters belongs to the neurotransmitter: sodium symporters (Goultly et al., 2023; Lai, 2013; Saier, 2000). It must be pointed out that the SLC6 family also includes members involved in the transport of other neurotransmitters and amino acids such as GABA, taurine, glycine (Goultly et al., 2023; Lai, 2013). Orthology assessment was performed using the sequences listed in Supplementary Table 6.7. In *M. galloprovincialis* and in other bivalves analysed, up to two different serotonin reuptake transporters (SERTs) were identified; the cluster of SERTs is, moreover, well supported (BP = 98) (Supplementary Figure 6.8). SERT group appears to be a sister group of the one containing human dopamine and noradrenaline (*HsDAT* and *HsNET*) and octopamine

transporter (OAT), which is, more generally, used for phenolamines (Ribeiro and Patocka, 2013). Also in this case, the group containing human DAT and NET and the typical invertebrate OAT is well supported (BP = 74). A group less supported (BP = 54), containing the protostome invertebrate dopamine transporter (iDAT), is a sister group of the previous clade (Supplementary Figure 6.8). None of the species of bivalve considered showed the presence of noradrenaline reuptake transporter (NET) (Supplementary Figure 6.8). This analysis did not allow to identify a transporter for histamine.

6.2.1.4 Receptors

Monoamines exert their action by binding to their membrane receptors. The majority of monoamines receptors are G-protein-coupled receptors (GPCRs) of class A; however, serotonin represents an exception since it also presents a class of ligand-gated ion receptors classified as Serotonin Receptors 3 (5-HTR3) in vertebrates (Goult et al., 2023).

Orthology assessment was performed for each type of monoamine previously identified.

Serotonin receptors (5-HTRs)

It has been previously shown that bivalve molluscs present at least three different 5-HTRs, in particular: 5-HTR1A1_inv, 5-HTR1A2_inv and 5-HTR7. Orthology assessment revealed the presence of a total of six serotonin receptors (Supplementary Table 6.8, Supplementary Figure 6.9). Each group containing the 5-HTR type is well supported (BP > 70). As shown in the tree (Supplementary Figure 6.9), 5-HTR1, 5-HTR7 and 5-HTR2 are sister groups and form a clade, whereas 5-HTR4 and 5-HTR6 form a different clade and are sister groups within their clade. Consistent with previous studies (Goult et al., 2023), no 5-HTR3 were found in the species analysed, including *D. melanogaster*.

Dopamine receptors (DRs)

In *M. galloprovincialis* only one DR has been so far identified and described (Miglioli et al., 2021b). On the other hand, a recent study showed that the pacific oyster *C. gigas* shows three different DRs: dopamine receptor type 1 (DR1), dopamine receptor type 2 (DR2, or invertebrate dopamine receptor – INDR) and dopamine receptor type 3 (DR3) (Schwartz et al., 2021). To assess the presence of other DRs in *M. galloprovincialis* genome, reference sequences of human, fruit fly and pacific oyster were used (Supplementary Table 6.9, Supplementary Figure 6.10). It was found that *M. galloprovincialis* and the other bivalve species analysed also possess three different DRs, with the exception of *M. coruscus* which lacks DR1 (Supplementary Figure 6.10). As shown in Supplementary Figure 9, DR1 and DR2 are sister group in the same clade,

whereas DR3 clade acts as sister group of DR1-DR2 clade. These data are different from what published by Schwartz et al. (2021), where DR1 and DR3 are sister group within the same clade and DR2/INDR is localised in a different clade. This could be explained by the fact that in that study DRs were analysed together with octopamine and tyramine receptors (OARs, TymRs).

Adrenergic receptors (α -ARs and β -ARs), octopamine receptors (OARs) and tyramine receptors (TARs)

As reported in Supplementary Table 6.10, *Platynereis dumerilii* (annelid) sequences were used as query to identify ARs, since many arthropods lost ARs sequences and thus fruit fly sequences are not available (Bauknecht and Jékely, 2017). Orthology assessment revealed that *M. galloprovincialis* and the other species analysed present both adrenaline and octopamine receptors (OARs) and tyramine receptors (TARs) (Supplementary Figure 6.11). The number of noradrenaline, octopamine and tyramine receptors varies from species to species. The pacific oyster, *C. gigas*, does not show any adrenaline receptors in line with already published data (Bauknecht and Jékely, 2017; Schwartz et al., 2021). Moreover, always in line with bibliography, the bivalve species here analysed lack β -adrenaline receptors, which are found only in chordates (Bauknecht and Jékely, 2017). In *M. galloprovincialis*, two noradrenaline, two octopamine and one tyramine receptors were found (Supplementary Figure 6.11).

Histamine receptors (HSRs)

Information on histamine receptors (HSRs) is very scarce and fragmentary and only recent studies tried to shed some light on their presence/absence in invertebrates: it was reported that HSRs in protostomes are found only in annelids, molluscs and plathelminths (Ravhe et al., 2021). This is the reason why fruit fly sequences could not be used for orthology assessment in *M. galloprovincialis* and other bivalve species here analysed; therefore, reference sequences of the acorn worm *Saccoglossus kowalevskii* (hemichordate) were used (Supplementary Table 6.11). In line with findings of Ravhe et al. (2021), *S. kowalevskii* did not show the presence of HSR subtype 4, which is typical of mammals, but presented orthologs of HSR1-2 and 3. Regarding *M. galloprovincialis* and bivalves here analysed, HSR1 and HSR3 orthologs were found, whereas no HSR2 was found in any species analysed; this could explain why the HSR2 branch forms a clade on its own acting as sister group of the clade containing both HSR1 and HSR3 orthologs (Supplementary Figure 6.12). Branches show good support values (BP > 70). In *M. galloprovincialis* four different HSRs were found: one ortholog to HSR1 and three different HSRs orthologs to HSR3.

In Table 6.2 a summary of orthology assessment results in *M. galloprovincialis* is provided. All the genes that characterise a monoaminergic system (synthesis, degradation, reuptake and receptors) were found for 5-HT, DA and TA but not for NA and OA which lack the reuptake transporter and synthesis enzyme, respectively. MT (Melatonin) and A (Adrenaline) systems were not found in *M. galloprovincialis* genome.

Class	MA	Synthesis	Reuptake	Receptor(s)	Degradation	Storage
Indolamines	5-HT	✓	✓	✓	✓	✓
	MT	✗				
Imidazolamines	HS	✓	✗	✓		
Catecholamines	DA	✓	✓	✓		
	NA	✓	✗	✓		
	A	✗				
Phenolamines	TA	✓	✓	✓		
	OA	✗		✓		

Table 6.2. Schematic table showing the monoaminergic systems found in *M. galloprovincialis* genome through orthology assessment. Green check box indicates the presence of the protein/gene, indicated in the headline for each monoamine, while red box with X indicates its absence.

6.2.2 Developmental expression of monoaminergic genes in *M. galloprovincialis*

The developmental expression dynamics of the monoaminergic genes identified above were analysed using the developmental transcriptome of *M. galloprovincialis* recently published (Miglioli et al., 2024), focusing on stages between 0 and 48 hpf (i.e.: from the unfertilised egg to the D-Veliger stage).

Hierarchical clustering of monoaminergic (MOA) genes expression levels during embryonal development supported two main big clusters (adjusted-unbiased p-values – au >95). The clustering resulted in groups of subsequent developmental timepoints, indicating co-expression and progressive expression of MA genes during specific periods of development (Supplementary Figure 6.13 A). The first major cluster is formed by two clusters: one encompasses the embryonic development phase (phase 1: from 0 to 8 hpf, au = 65), the second one the gastrula stages (phase 2: from 12 to 16 hpf, au = 99). The second major cluster encompassed three phases: the trochophore phase (phase 3: from 20 to 28 hpf, au = 96), the early Veliger phase (phase 4: from 32 to 36 hpf, au = 98) and the D-Veliger phase (phase 5: from 40 to 48 hpf, au = 99).

The correlation between developmental stages and MA genes expression was further analysed with PCA. Principal components (PCs) 1 and 2 covered mostly the total variance of the dataset

(PC1 = 50%, PC2 = 16.5%) and spatially segregated developmental phases previously identified with cluster analysis (Supplementary Figure 6.13 B). Thus, MA gene expression in *M. galloprovincialis* can be correlated with its embryo-larval development identifying five different phases: Embryonic, Gastrula, Trochophore, Early Veliger and D-Veliger phases. Expression dynamics were further visualised by a heatmap, showing that there are genes highly expressed in each phase previously identified (Figure 6.1). AADC, responsible for both serotonin and dopamine synthesis but also involved in other reactions, as well as MAO-B, responsible for the degradation of MA, are highly expressed in eggs, indicating a maternal origin. At 4 hpf, two histamine receptors (HSR3b and HSR3c) displayed high expression; later in Phase 1, at 8 hpf, DR3-like and HDC expression increased. These data indicate that transcripts related to serotonin, dopamine, and histamine synthesis are already present in Phase 1. Phase 2 was characterised by increases in expression of serotonin-related genes. TPH peaked at 16 hpf, while 5-HTR1A2_inv, 5-HTR6-like, and 5-HTR7 reached their highest expression levels during this phase. Additionally, the expression of genes associated with the tyraminergetic system (TDC, TAR1, and OAT) was prominent. Notably, 5-HTR1A2_inv displayed an early increase at 12 hpf, prior to TPH, and DR3-like showed heightened expression at 12 hpf, ahead of other dopaminergic genes. Phase 3 was marked by the rise of 5-HTR2 and SERT2-like, and, interestingly, by iDAT and DR1, which once again preceded the peak of the synthesis enzyme. During phase 4, TH started peaking (36 hpf) as well as DR2 (32 hpf). Phase 5 was mainly characterised by the elevated expression of adrenergic and octopaminergic receptors, as well as all identified DBH-like transcripts.

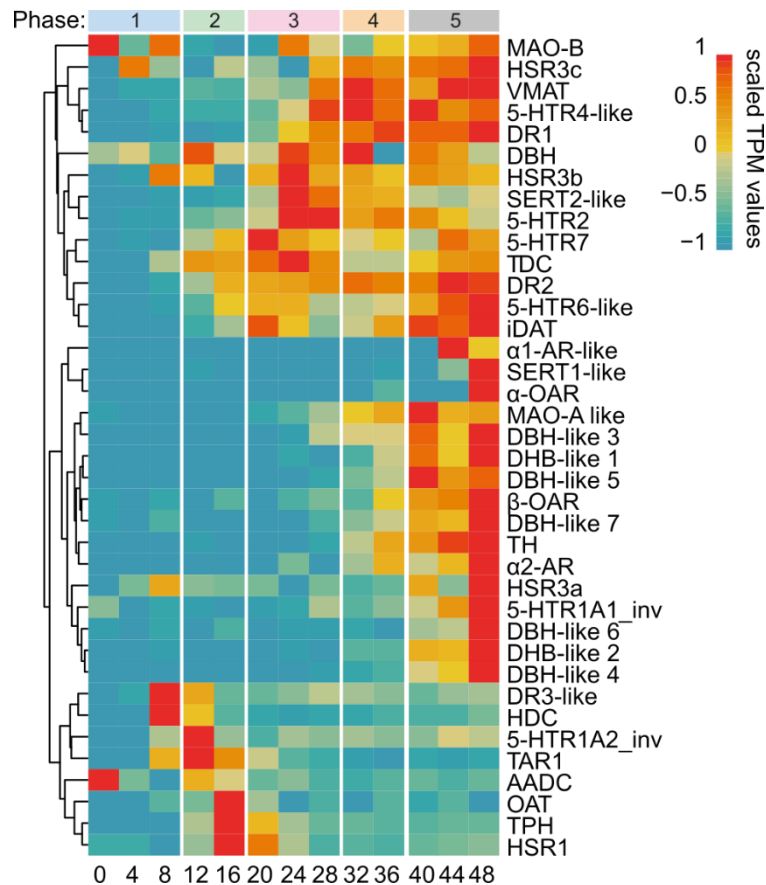


Figure 6.1. Heatmap of developmental expression dynamics of monoaminergic genes. Genes are clustered by rows, with column breaks identifying the five phases. Expression levels are TPM (Transcripts per Million).

Notably, serotonergic and dopaminergic genes exhibit consistent expression profiles throughout embryo-larval development, differently from tyramine and histamine genes, which are mainly expressed during embryonic and gastrula stages, and from adrenergic and octopaminergic genes, whose expression peaked during the last phase: the D-Veliger phase. Surprisingly, high expression of some monoamine receptors was observed before those involved in the synthesis of their respective ligands. Dopamine transporter and receptors (iDAT, DR2, and DR3-like) peaked before TH, 5-HTR1A2_inv peaked before TPH, and AADC before both TPH and TH.

However, the heatmap allowed for checking the expression profile of a gene (peaks, mostly) but not their values of expression. For this reason, receptors and re-uptake transporters peaking before the synthesis enzyme for each monoamine were checked by quantifying their expression profile in terms of TPM. As shown in Fig. 1.2, quantitative data confirm the expression profile data shown in the heatmap (Figure 6.1)

These data may indicate that some serotonin and dopamine receptors and iDAT might have a role in monoamine signalling activated by unspecific ligands at early developmental stages

prior to synthesis of their specific ligands or have a pre-nervous (or morphogenetic) roles (Camicia et al., 2013; de Sa Alves et al., 2009).

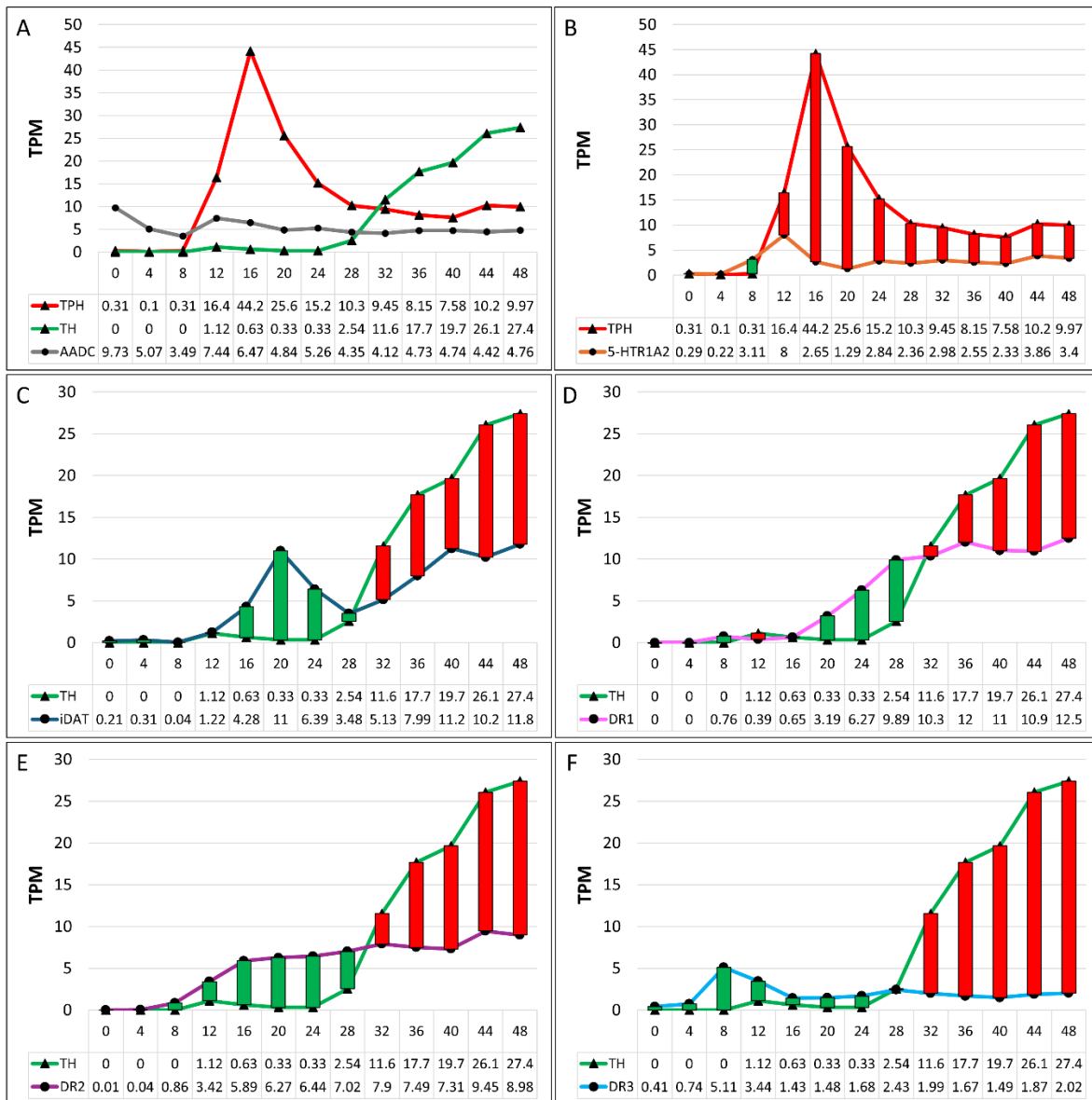


Figure 6.2. Graphs of expression profiles of selected genes in TPM. On the x-axis, the top section represents hours post-fertilisation (hpf), while the bottom section shows TPM values for the genes. Green bars indicate stages where the receptor/transporter is expressed at higher levels than the synthesis enzyme of the monoamine of interest, while red bars indicate the opposite trend, where the synthesis enzyme is expressed more than the receptor/transporter.

Subsequent analysis was focused on serotonergic and dopaminergic systems since all their main components were identified (Table 6.2) and were expressed from gastrula to D-Veliger phases, displaying higher expression levels, in terms of TPM, compared to other monoaminergic genes (see Supplementary Table 6.12). With regards to the TA system, even

if all genes were identified, they were mainly expressed in early embryo-stages (phases 1 and 2) (Figure 6.1).

6.2.3 Spatiotemporal expression of serotonin and dopamine genes during *M. galloprovincialis* embryo-larval development evaluated by HCR: relationship with the neuroendocrine system

6.2.3.1 Spatiotemporal analysis of the pan-neuronal marker 7B2

7B2 (or Secretogranin V) is known to be found in nervous and neuroendocrine tissues of both deuterostome and protostomes (Mbikay et al., 2001; Monjo and Romero, 2015). To assess the spatiotemporal morphology of the neuroendocrine system during *M. galloprovincialis* embryo-larval development, 7B2 was used as marker in larval samples at the gastrula (16 hpf), trochophore (28 hpf) and D-veliger stage (48 hpf) using single HCR. The technique did not allow for the identification of ganglia *sensu stricto* (Richter et al., 2010); therefore, the neural structures identified were considered cluster of neurons.

As shown in Fig. 1.3, 7B2 signal (magenta) at the Gastrula stage displayed two apical clusters: one anterior and one posterior, thus they were named apical-anterior neurons (*aan*) and apical-posterior-neurons (*apn*) (Figure 6.3 A1-B1). At the Trochophore stage, in addition to *aan* and *apn*, a new cluster of neurons appeared: the apical-ventral neurons (*avn*) (Figure 6.3 C-D1). At D-Veliger stage up to four different clusters were identified, and the structure of 7B2 signal became more complex. Two clusters of apical anterior neurons (apical-anterior neurons 1 – *apn1*, and apical-anterior neurons 2 – *apn2*), anterior neurons (*an*) and ventral-posterior neurons (*vpn*) were identified (Figure 6.3E-F1). These clusters showed a bilateral symmetry, in particular the *an* and the *vpn* clusters (Figure 6.3 F-F1).

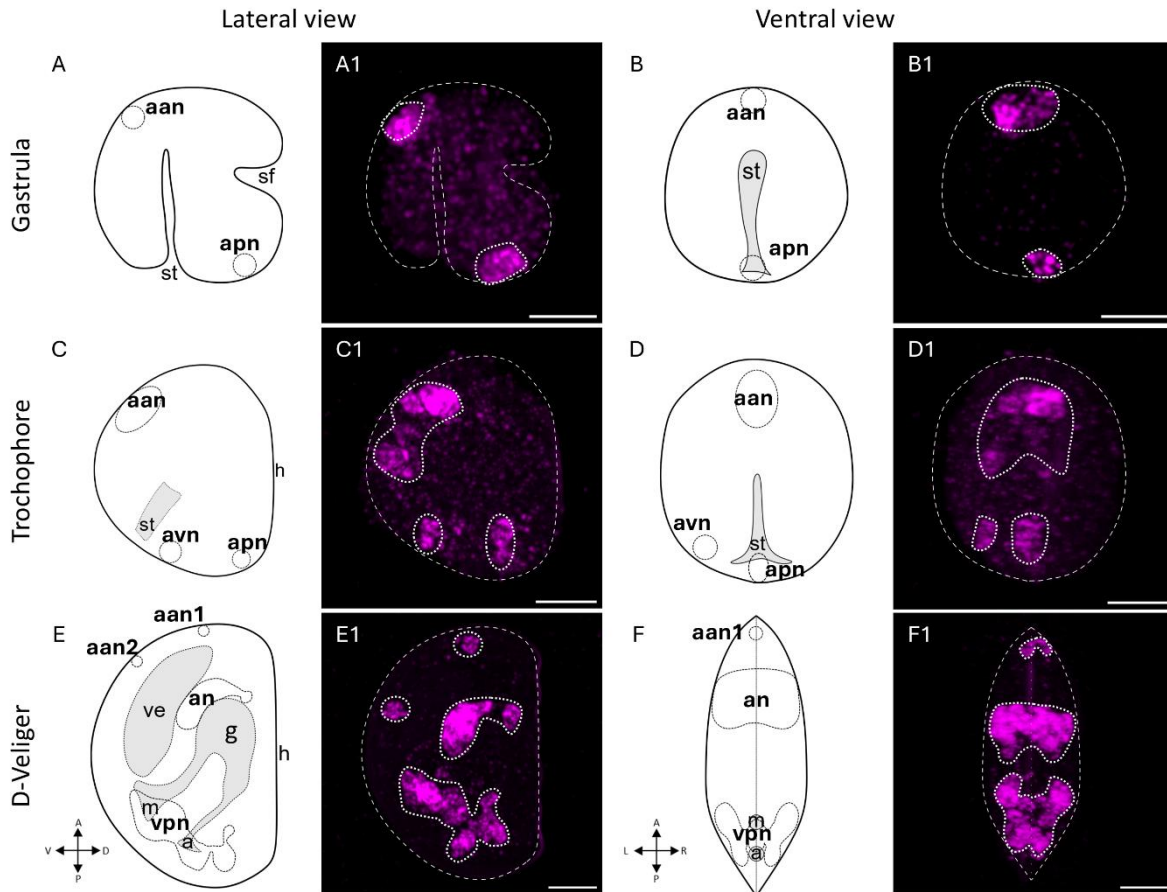


Figure 6.3. Representative images showing the spatiotemporal localization of the pan-neuronal marker 7B2 during *M. galloprovincialis* embryo-larval development.

Each row represents the stages analysed: A-B: Gastrula stage (16 hpf), C-D: Trochophore stage (28 hpf); E-F: D-Veliger stage (48 hpf). In each figure, the larval scheme is represented on the left and the corresponding confocal HCR image on the right. In confocal images clusters are highlighted by a dotted line and the larval body by a dashed line.

A-A1. Schematic representation and maximum plane projection of 7B2 at gastrula stage in lateral view. B-B1. Schematic representation and maximum plane projection of gastrula stage in ventral view. 19 out of 32 larvae presented the two apical clusters: apical-anterior neurons and apical-posterior neurons (*aan*, *apn*; panels A1, B1).

C-C1. Schematic representation and maximum plane projection of trochophore stage in lateral view.

D-D1. Schematic representation and 3D reconstruction of trochophore stage in ventral view. 27 out of 35 larvae analysed presented the three neuronal clusters: *aan*, *apn* and apical-ventral neurons (*avn*) (panels C1, D1).

E-E1. Schematic representation and maximum plane projection of D-Veliger stage in lateral view.

F-F1. Schematic representation and 3D reconstruction of D-Veliger stage in ventral view. 96 out of 116 larvae analysed presented all the clusters: apical anterior neurons1/2 (*aan1/2*), anterior neurons (*an*) and ventral-posterior neurons (*vpn*) (panels E1, F1).

Axis orientation abbreviations: A – anterior, D – dorsal, L – Left, P – posterior, R – right, V – ventral. Anatomical abbreviations: a: anus, g: gut, h: hinge, m: mouth, sf: shell field, st: stomodeum. Scale bar: 20 μ m.

6.2.3.2 Spatiotemporal analysis of serotonin and dopamine producing cells

Serotonin and dopamine producing cells were localised by using specific markers: TPH for 5-HT and TH for DA, the rate limiting enzymes for 5-HT and DA synthesis, respectively. Signal of single HCR of TPH and TH is reported in Supplementary Figure 6.14 and Supplementary Figure 6.15.

Figure 6.4 shows the results of double HCR fluorescence with TPH (green) and 7B2 (magenta) where the overlap of the signals results in a white colour, indicating colocalisation. Serotonin producing cells were first detected at 16 hpf apically, forming a cluster within the *aan* (Figure 6.4 A-B2). Cell counting, performed by merging Hoechst and TPH channels, allowed to identify 3 TPH positive cells (3 ± 0.51 , 24 larvae). At 28 hpf, one TPH cluster was still localised apically within the area of *aan* (Figure 6.3 C-D1), with 4 TPH positive cells (4 ± 0.49 , 29 larvae). At 48 hpf, the TPH signal subsides into the larval body and localises within the *an* (Figure 6.3 E-F1). At this stage, the TPH signal was formed by three clusters, one medial and two lateral (Figure 6.3 F1-F3), and up to 7 cells were positive to TPH (7 ± 0.65 , 52 larvae).

TPH + 7B2

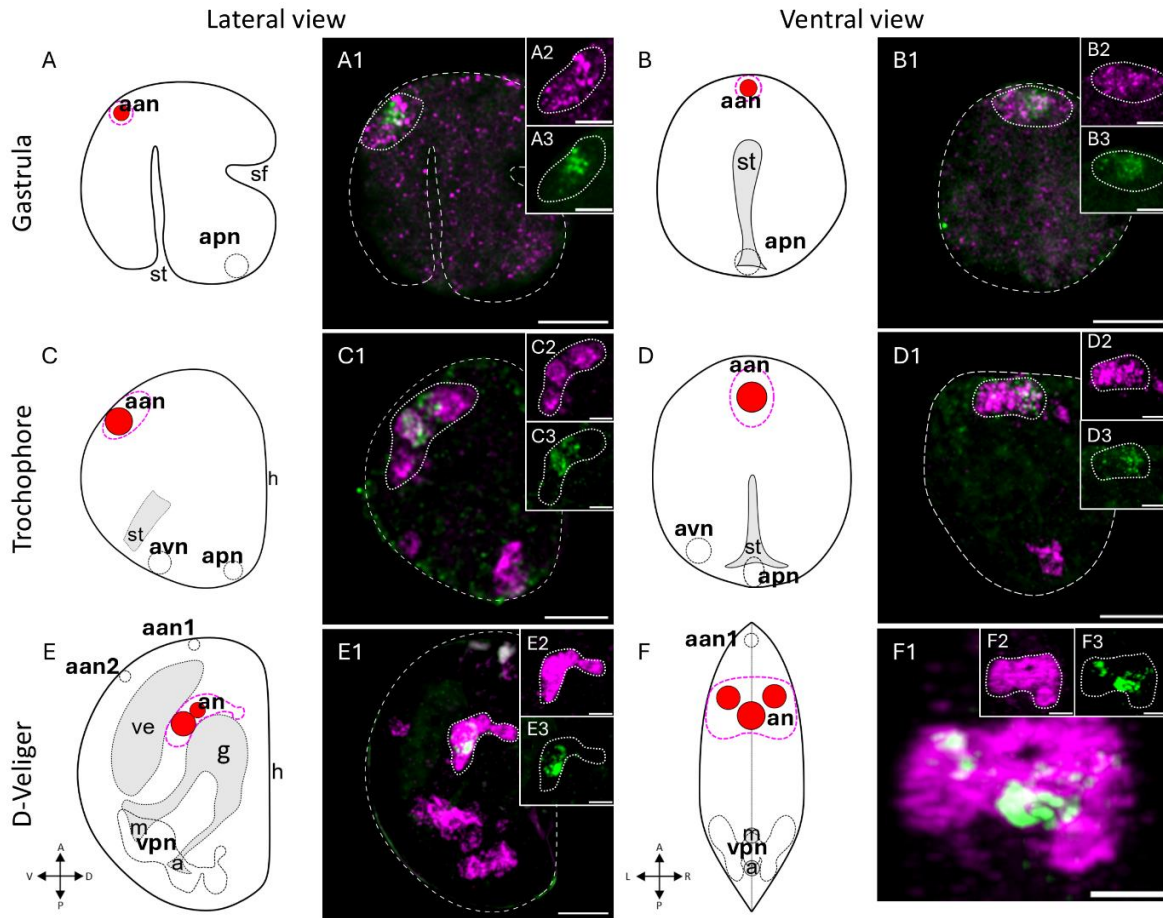


Figure 6.4. Representative images showing the spatiotemporal localisation of serotonin producing cells and 7B2 during *M. galloprovincialis* embryo-larval development. Rows and panels are organised as in Figure 6.3. Double HCR with TPH (B2 amplifier) and 7B2 (B1 amplifier) was used. TPH signal is represented in red and green in scheme and HCR images respectively; 7B2 signal is represented by dotted lines as in Figure 6.3 and in magenta in HCR images. The white colour in confocal images is the result of green and magenta colocalisation.

A-A1. Schematic representation and selective plane projection at Gastrula in lateral view. A2-A3. Magnification of *aan* with 7B2 signal (A2) and TPH signal (A3); the dotted line is the same drawn for 7B2 signal.

B-B1. Schematic representation and selective plane projection at Gastrula stage in ventral view. B2-B3. Magnification of 7B2 (B2) signal of the *aan* and TPH signal (B3). 7 out of 7 larvae showed the colocalisation of TPH within 7B2 (panels A1, B1).

C-C1. Schematic representation and maximum plane projection at Trochophore stage in lateral view. C2 and C3 show the magnification of 7B2 (C2) signal of the *aan* area and the TPH signal (C3).

D-D1. Schematic representation and maximum plane projection at Trochophore stage in ventral view. D2-D3. Magnification of 7B2 signal within the *aan* and TPH. 8 out of 8 larvae showed the colocalisation of TPH within 7B2 (panels C1, D1).

E-E1. Schematic representation and maximum plane projection at D-Veliger stage in lateral view. E2-E3. Magnification of *an* with 7B2 and TPH signals.

F-F1 Schematic representation of D-Veliger stage in ventral view and selective 3D reconstruction of an area. F2-F3. Signal of 7B2 and TPH. 7 out of 7 larvae showed the colocalisation of TPH within 7B2 (panels E1, F1).

Axis orientation abbreviations: A – anterior, D – dorsal, L – Left, P – posterior, R – right, V – ventral.

Anatomical abbreviations: a: anus, g: gut, h: hinge, m: mouth, sf: shell field, st: stomodeum. Scale bars: 20 μm and 10 μm for insets.

Figure 6.5 shows the results of double HCR with TH (green) and 7B2 (magenta). No TH signal was detected at Gastrula stage (Figure 6.5 A-B3), whereas it was detected at Trochophore stage with two lateral clusters, one of them within *avn* (Figure 6.5 C-D3); at this stage, 4 cells resulted to be positive to TH (4 ± 0.61 , 24 larvae). At D-Veliger stage, up to four clusters were identified, with a consistent increase in the number of cells (7 ± 1.41 , 43 larvae) (Figure 6.5 E-F3). These four clusters were symmetrical and bilateral (Figure 6.5 F1, F3) and they were localised within the *vpn* area (Figure 6.5 E1-E3 and F1-F3).

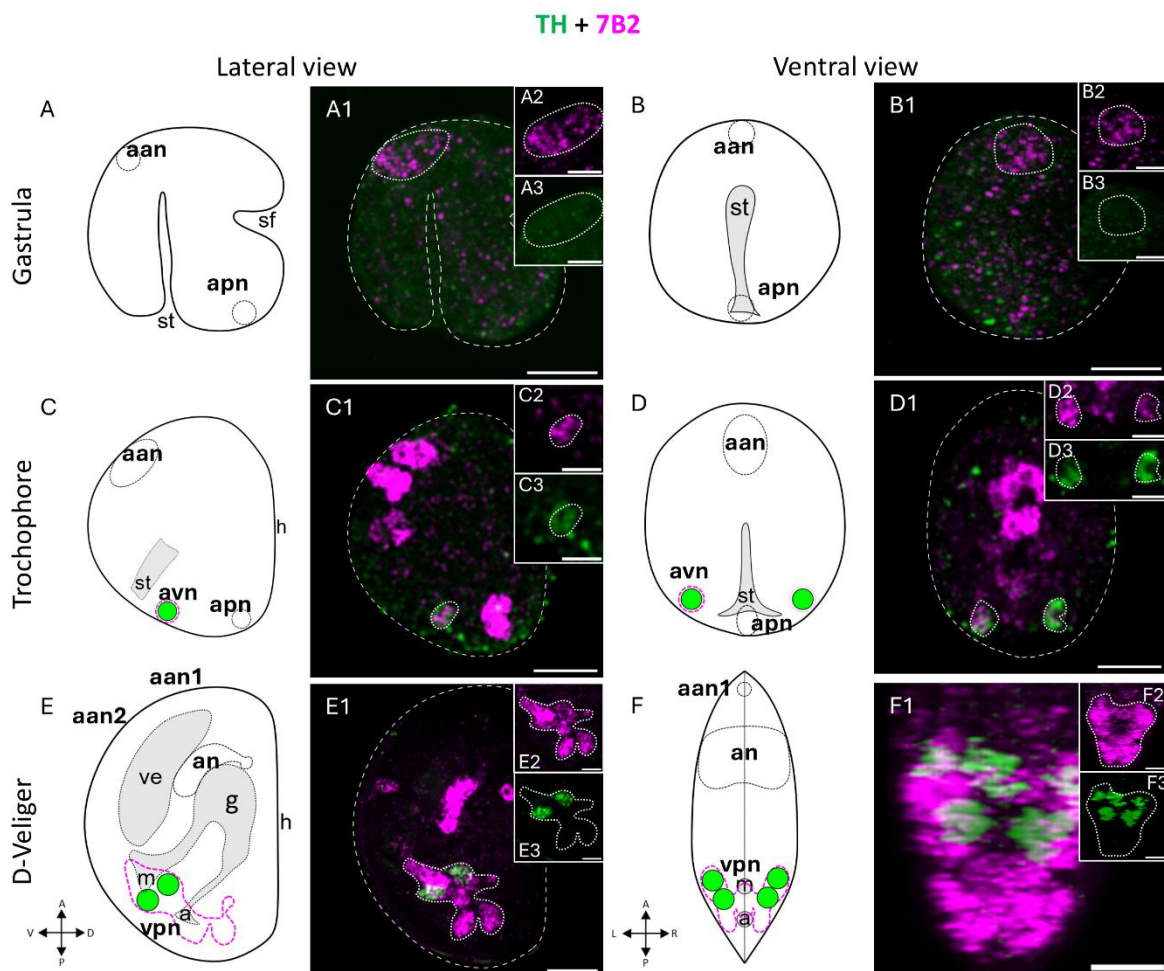


Figure 6.5. Representative images showing the spatiotemporal localisation of dopamine producing cells and 7B2 during *M. galloprovincialis* embryo-larval development. Double HCR with TH (B2 amplifier) and 7B2 (B1 amplifier) was used. TH signal is represented in red and green in scheme and HCR images respectively, 7B2 signal is represented by dotted lines as in Figure 6.3 and in magenta in HCR images. The white colour in confocal images is the result of green and magenta colocalisation.

A-A1. Schematic representation and selective plane projection at Gastrula in lateral view. A2 shows a magnification of *aan* with 7B2 signal and A3 shows the magnification of *aan* with TH signal. The dotted outline is the same one drawn for 7B2 signal. B1-2. Schematic representation and selective plane

projection at Gastrula stage in ventral view. B2 and B3 show the magnification of 7B2 signal and TH signal. 3 larvae were analysed (panels A1, B1).

C-C1. Schematic representation and maximum plane projection at Trochophore stage in lateral view. C2 and C3 show the magnification of 7B2 signal of the *avn* area and the TH signal which is within it.

D-D1. Schematic representation and maximum plane projection at Trochophore stage in ventral view. D2 and D3 show the magnification of 7B2 signal within the *avn* and TH signal within 7B2 area. 7 out of 7 larvae showed TH within *avn* 7B2 area, 5 out of 7 larvae showed the two clusters of TH and only 2 out of 7 larvae showed 2 apical-ventral clusters of 7B2 (panels C1, D1).

E-E1. Schematic representation and maximum plane projection at D-Veliger stage; E2 and E3 show a magnification of *vpn* with 7B2 and TH alone.

F. Schematic representation of ventral view at D-Veliger stage. F1 selective 3D reconstruction of *vpn* area. F2 and F3 show signal of 7B2 and TH on their own. At D-Veliger stage, 6 out of 6 larvae showed TH colocalising within *vpn* area and with 4 clusters (panels E1, F1).

Axis orientation abbreviations: A – anterior, D – dorsal, L – Left, P – posterior, R – right, V – ventral. Anatomical abbreviations: a: anus, g: gut, h: hinge, m: mouth, sf: shell field, st: stomodeum. Scale bars: 20 μ m and 10 μ m for insets.

TPH and TH are necessary but not sufficient for 5-HT and DA synthesis. Indeed, to be synthesised, a second reaction is needed and is catalysed by AADC (see Figure 2.1). As a consequence, colocalisation of AADC was evaluated with either TPH or TH, to assess if this enzyme is found in their same area and, thus, allowing the synthesis of 5-HT and DA. AADC (magenta) was detected from Gastrula to D-Veliger stages showing colocalisation with both TPH and TH (green). Moreover, it was found that AADC signal was present also in other areas of the embryo/larval body (see Supplementary Figure 6.17 and Supplementary Figure 6.18). This widespread localisation could be explained by the affinity of AADC towards a broad range of substrates (e.g.: AADC can convert L-Tyrosine in TA).

6.2.3.3 Spatiotemporal localisation of serotonin and dopamine transporters

Selective reuptake transporters for 5-HT and DA (SERT1-like, SERT2-like and iDAT) were localised during embryo-larval development with single HCR. In line with the RNA-Seq expression profile, SERT1-like could not be detected at both Gastrula and Trochophore stages but at D-Veliger stage only, showing two lateral and symmetrical clusters (Supplementary Figure 6.19). SERT2-like seemed to display an inconspicuous signal at Gastrula stage; at Trochophore stage the signal appeared to be localised at the margins of the larval body, without displaying a specific cluster localisation. At D-Veliger stage a cluster could be identified almost in the centre of the larval body, with the persistence of an inconspicuous signal in the ventral area (Supplementary Figure 6.19). iDAT, in line with the RNA-Seq expression profile, peaked before TH. At both Gastrula and Trochophore stages the signal was localised in non-neuronal areas and in non-dopaminergic areas. At D-Veliger stage two ventral clusters were identified (Supplementary Figure 6.19).

Double HCR with SERTs-like and iDAT (magenta) with their respective synthesis enzymes, TPH and TH respectively (green), was carried out at D-Veliger stage, when all the three reuptake transporters displayed a clear localisation. The results indicate that TPH colocalised in the two lateral symmetrical clusters with SERT1-like, and in the medial cluster with SERT2-like (Figure 6.6). TH displayed colocalisation with iDAT only in the two more ventral clusters (Figure 6.6).

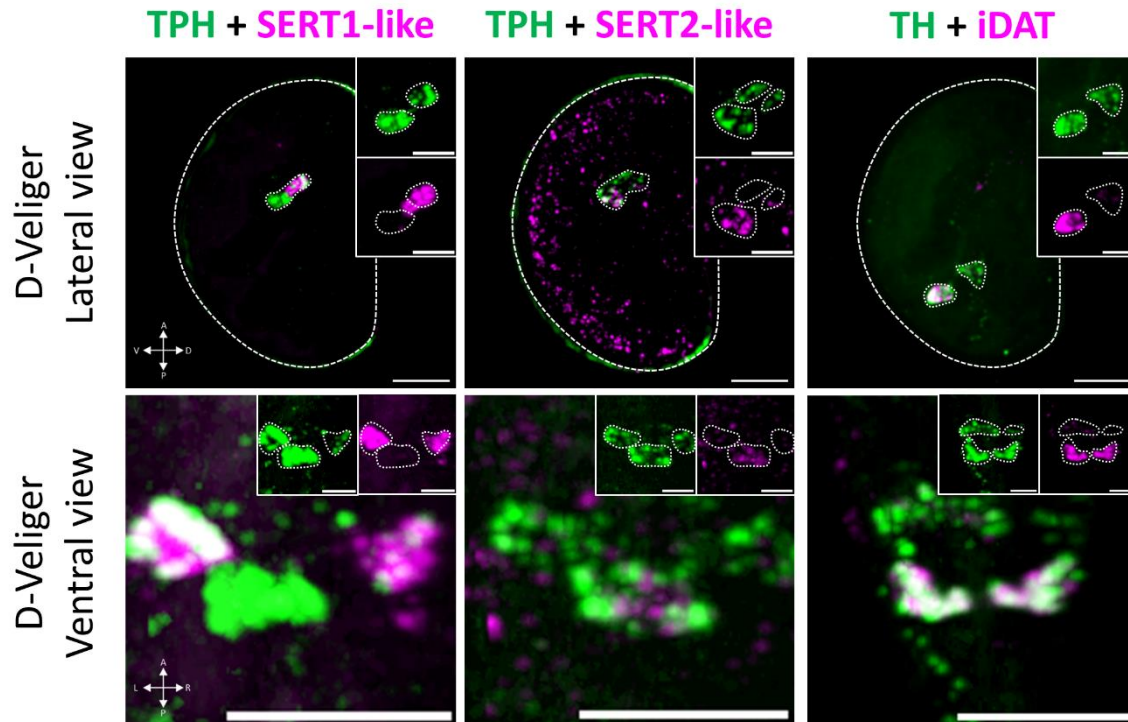


Figure 6.6. Representative images showing the colocalisation of TPH and TH with their reuptake transporters: SERT1-like and SERT2-like for TPH and iDAT for TH. Double HCR was carried out with TPH and TH (B2 amplifier) and transporters (B3 amplifier). Lateral views were realised by maximum-plane projection, ventral view was realised by selective 3D reconstruction. The white colour in confocal images is the result of green and magenta colocalisation. TPH + SERT1-like: 16 out of 20 larvae; TPH + SERT2-like: 5 out of 5 larvae; TH + iDAT: 15 out of 15 larvae displayed colocalisation. Scale bars: 20 μm and 10 μm for insets.

6.2.3.4 Colocalisation of serotonin and dopamine receptors (5-HTRs and DRs) within neural tissue at D-Veliger stage

5-HTRs and DRs localisation expression patterns were first investigated at 48 hpf, as all receptors displayed distinct and consistent localisation patterns across larvae at this stage, allowing for the discrimination of receptors forming clusters in specific tissues. Additionally, this analysis helped to identify which receptors are located within, near, or distant from the cluster where their ligand is synthesised. In this section, the localisation of 5-HTRs and DRs (green) with 7B2 (magenta) will be shown.

5-HTRs and DRs displayed both a neuronal and non-neuronal localisation. In particular, 5-HTR1A2_inv (which shows the same expression pattern of 5-HTR1A1_inv at 48 hpf), 5-HTR6-like and DR3-like are exclusively neuronal (Figure 6.7 A-C). 5-HTR1A2_inv displayed two clusters, one localised within the *an* and the other one localised within the *vpn* (Figure 6.7 A). 5-HTR6 like displayed just one posterior cluster within the *vpn* (Figure 6.7 B). DR3-like showed three clusters, one localised in the *an* and the others two localised in the *vpn* (Figure 6.7 C).

5-HTR4-like, 5-HTR7 and DR1 displayed both a neuronal and non-neuronal localisation (Figure 6.7 D-F). 5-HTR4-like showed, as well as 5-HTR6-like and DR3-like, a posterior cluster within the *vpn*. In addition, 5-HTR4-like also localised in a non-neuronal area above the region of the *an* (Figure 6.7 D). 5-HTR7 displayed two neuronal clusters, one within the *an* and one within the *vpn*; the posterior neuronal cluster showed the same localisation of the ones of 5-HTR4-like and 5-HTR6-like (Figure 6.7 E). DR1 showed an area at the shell margins, an area that should be where the mouth is (according to Miglioli et al. (2024)) and a cluster posterior to the *an* (Figure 6.7 F).

The only receptor analysed displaying exclusively a non-neuronal localisation was DR2. Its two clusters localised nearby hinge margins (one anterior and posterior) (Figure 6.7 G).

5-HTR2 did not display a clear localisation pattern at 48 hpf (data not shown).

For a better visualisation of the signal of the receptors here analysed, see Supplementary Figure 6.16.

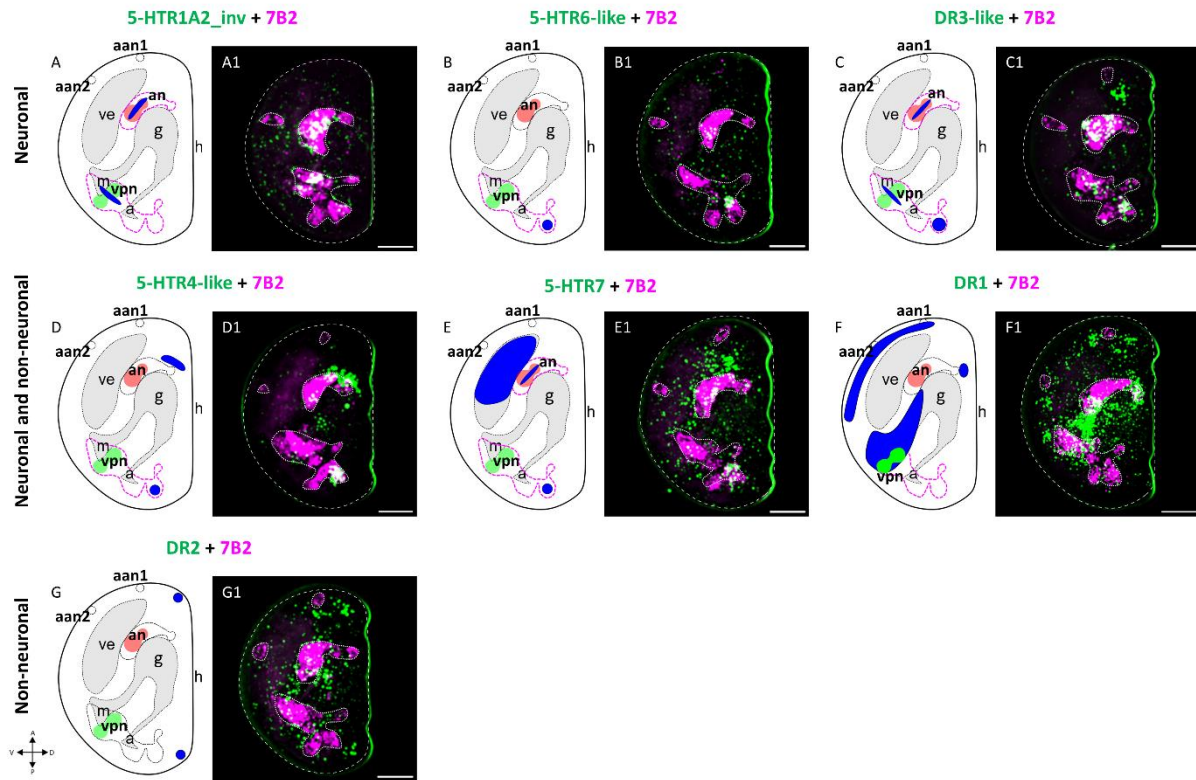


Figure 6.7. Representative images showing the localisation of 5-HTRs and DRs (green) at D-Veliger stage (48 hpf) within or outside the 7B2 (magenta) areas. In each figure, the larval scheme is represented on the left and the corresponding confocal HCR image on the right. Double HCR was carried out: receptors were all marked with amplifier B1, 7B2 was analysed with amplifier B3. The white colour in confocal images is the result of green and magenta colocalisation. The nervous tissue regions are outlined with dotted lines in schemes and represented in magenta in confocal images, while the receptor localisation observed via HCR is indicated by blue areas in schemes and in green in confocal images. Serotonin synthesis site is marked in pale red, and dopamine synthesis sites are marked in pale green in schemes. In confocal images, the larval body is highlighted by a dashed outline. HCR pictures are maximum plane projections. Rows from top to bottom: exclusively neuronal localisation, neuronal and non-neuronal localisation, exclusively non-neuronal localisation. 7 larvae were analysed for each receptor.

Axis orientation abbreviations: A – anterior, D – dorsal, P – posterior, V – ventral.

Anatomical abbreviations: a: anus, g: gut, h: hinge, m: mouth. Scale bars = 20 μm .

6.2.3.5 Colocalisation of 5-HTR1A2_inv and 5-HTR7 with TPH

5-HTR1A2_inv and 5-HTR7 displayed clusters within *an*, where serotonin producing cells are localised (Figure 6.7); colocalisation was thus investigated by double HCR with TPH. The results are reported in Figure 6.8 (green for TPH and magenta for 5-HTR1A2_inv and 5-HTR7)

5-HTR1A2_inv showed a broad area of signal at Gastrula, especially dorsally, that was localised within TPH area (Figure 6.8 A-B3). At Trochophore stage, two clusters were observed: one anterior, within TPH area (Figure 6.8 C1-C3 and D1-D3), and one posterior. Also, in D-Veliger, two clusters were present: one anterior and one ventral-posterior (Figure

6.8 E-E1). The anterior cluster, that was previously shown to be within the *an* area, showed colocalisation with TPH (Figure 6.8 E1-E3 and F1-F3). At this stage, 5-HTR1A2_inv showed co-localisation with all the three TPH clusters (Figure 6.8 F2-F3).

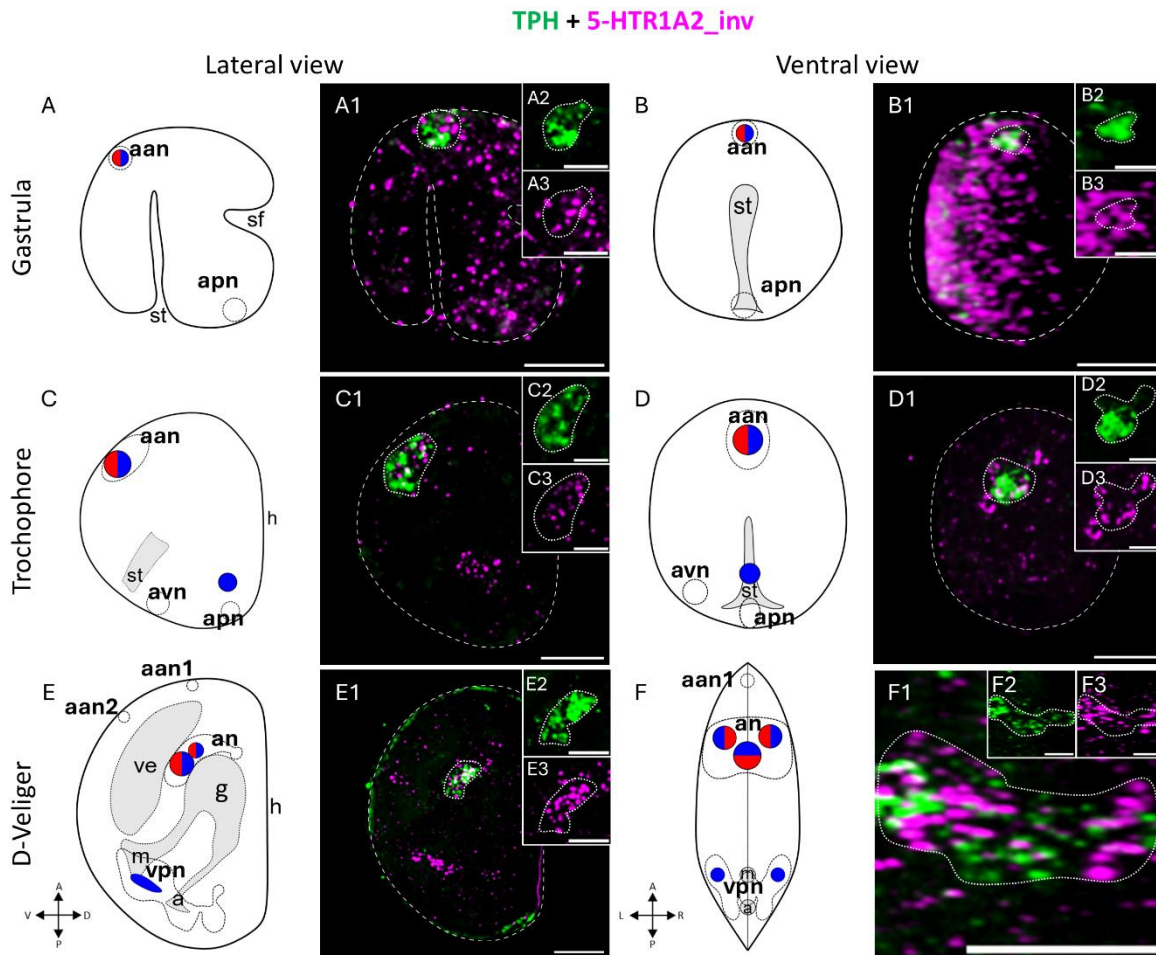


Figure 6.8. Representative images showing the spatiotemporal localisation of 5-HTR1A2_inv within serotonin producing cells during *M. galloprovincialis* embryo-larval development. Double HCR with 5-HTR1A2_inv (B1 amplifier) and TPH (B2 amplifier) was used. TPH signal is represented in red in schemes and in green in HCR pictures, 5-HTR1A2_inv signal is represented in blue and in magenta in schemes and HCR pictures, respectively. 7B2 areas are present in schemes and identified by areas with dotted lines. The panel is organised as Figure 6.3. The white colour in confocal images is the result of green and magenta colocalisation.

A-A1. Schematic representation and selective plane projection at Gastrula in lateral view. A2 shows a magnification TPH signal, A3 shows the magnification with 5-HTR1A2_inv signal; the dotted outline is the same one drawn for TPH signal.

B-B1. Schematic representation and selective plane projection at Gastrula stage in ventral view. B2 and B3 show the magnification of TPH signal and 5-HTR1A2_inv signal. 3 out of 3 larvae analysed displayed colocalization (panels A1-B1).

C-C3. Schematic representation and maximum plane projection at Trochophore stage in lateral view. C2 and C3 show the magnification of TPH signal and the 5-HTR1A2_inv signal which is within it.

D-D1. Schematic representation and maximum plane projection at Trochophore stage in ventral view. D2 and D3 show the magnification of TPH signal and 5-HTR1A2_inv signal within TPH area. 4 out of 4 larvae displayed colocalisation (panels C1-D1).

E-E1. Schematic representation and maximum plane projection at D-Veliger stage. E2 and E3 show a magnification of TPH and 5-HTR1A2_inv alone.

F. Schematic representation of ventral view at D-Veliger stage. F2 selective 3D reconstruction of an area. F2 and F3 show signal of TPH and 5-HTR1A2_inv on their own. 4 out of 5 larvae displayed colocalisation (panels E1-F1).

Axis orientation abbreviations: A – anterior, D – dorsal, L – Left, P – posterior, R – right, V – ventral. Anatomical abbreviations: a: anus, g: gut, h: hinge, m: mouth, sf: shell field, st: stomodeum. Scale bars: 20 μ m and 10 μ m for inset pictures.

5-HTR7 signal was observed at both Gastrula and Trochophore stages (Figure 6.9 A-D3), with a broad apical-ventral area and a posterior area clearly identified at Trochophore stage. Colocalisation with TPH resulted difficult to establish, given the wide apical-ventral area covered by 5-HTR7. Figure 6.9 shows that a partial colocalisation is present at Gastrula stage (A-B3) but is absent at Trochophore stage (C-D3). At the D-Veliger stage, 5-HTR7 showed a colocalisation with TPH only within the two bilateral clusters and not with TPH medial cluster (Figure 6.9 E1-E3 and F1-F3, respectively).

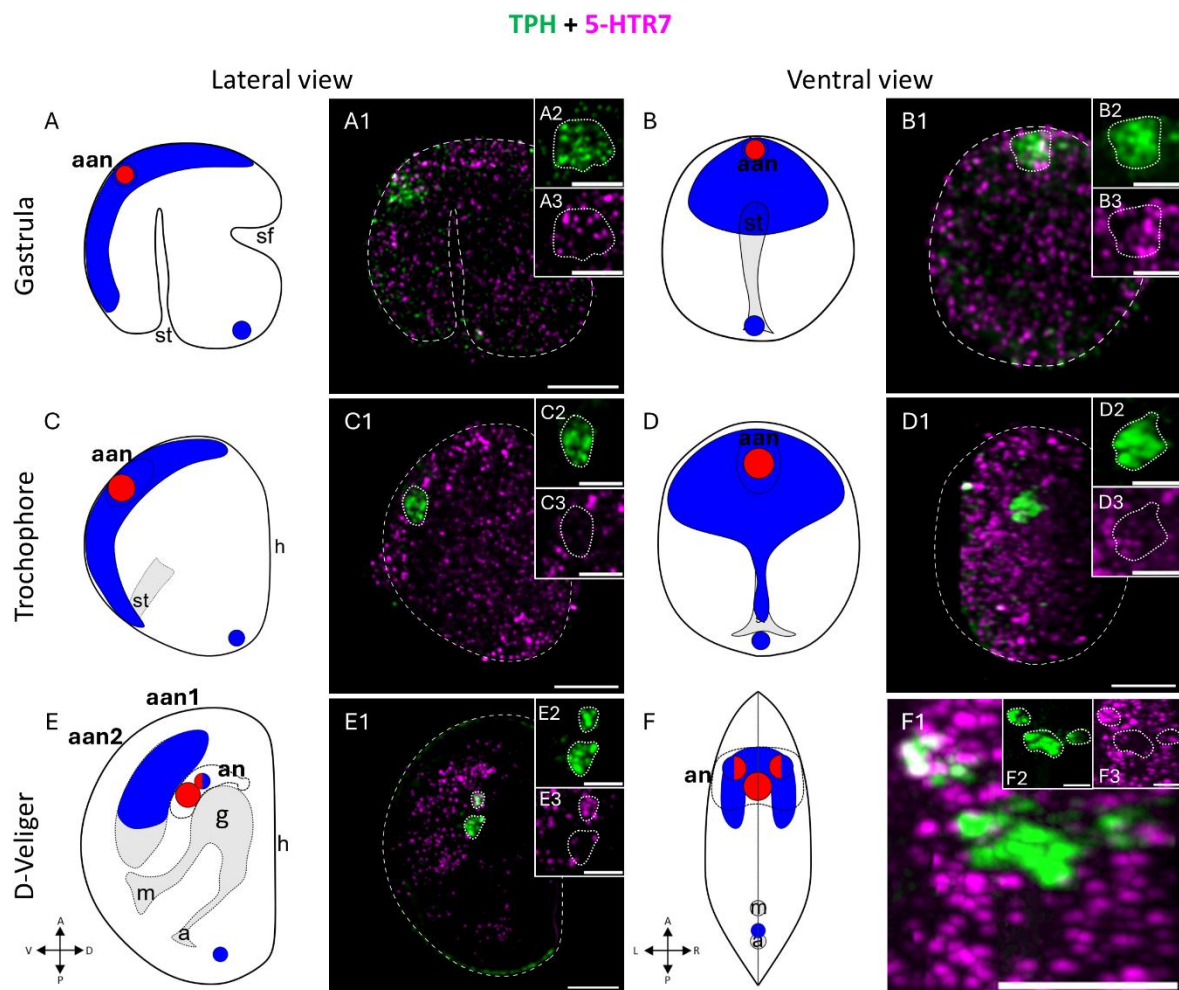


Figure 6.9. Representative images showing the spatiotemporal localisation of 5-HTR7 within serotonin producing cells during *M. galloprovincialis* embryo-larval development. Double HCR with 5-HTR7 (B1 amplifier) and TPH (B2 amplifier) was used. 5-HTR7 signal is represented in blue in schemes and in

green in HCR pictures, TPH is red in schemes and green in confocal images, 7B2 signal is represented by dotted areas in schemes and in magenta in HCR pictures. Panels are organised as in Figure 6.3. The white colour in confocal images is the result of green and magenta colocalisation.

A-A1. Schematic representation and selective plane projection at Gastrula in lateral view. A2-A3 shows a magnification of TPH and 5-HTR7 signals.

B1-2. Schematic representation and selective plane projection at Gastrula stage in ventral view. B2-B3 show the magnification of TPH and 5-HTR7 signals. 6 out of 6 larvae displayed colocalisation (panels A1-B1).

C1-2. Schematic representation and maximum plane projection at Trochophore stage in lateral view. C2-C3. Magnification of TPH and the 5-HTR7 signals.

D1-2. Schematic representation and maximum plane projection at Trochophore stage in ventral view. D2-D3. Magnification of TPH and 5-HTR7 signals. 5 out of 5 larvae were analysed and displayed this pattern (panels C1-D1).

E-E1 Schematic representation and maximum plane projection at D-Veliger stage. E2-E3. Magnification of TPH and 5-HTR7 signals.

F. Schematic representation of ventral view at D-Veliger stage. F1 selective 3D reconstruction of TPH area. F2-F3. TPH and 5-HTR7 signals. 15 out of 15 larvae displayed colocalisation (panels E1-F1).

Axis orientation abbreviations: A – anterior, D – dorsal, L – Left, P – posterior, R – right, V – ventral. Anatomical abbreviations: a: anus, g: gut, h: hinge, m: mouth, sf: shell field, st: stomodeum. Scale bars: 20 µm and 10 µm for inset pictures.

6.2.3.6 Colocalisation of DR1 and DR3-like with TH

As previously shown in Figure 6.5, no TH signal was detectable at Gastrula stage. DR1 and DR3-like were thus analysed at later stages to check their possible colocalisation with TH. TH (green) colocalised with DR1 (magenta) at both Trochophore (Figure 6.10 A1-A3) and D-Veliger stage (Figure 6.10 B1-B3) stages. DR1 showed also areas near and outside TH area at both stages (Figure 6.10 A1 and B1). On the contrary, no colocalisation was found for DR3-like (magenta) in either stage analysed (Figure 6.10 C1-C3 and D1-D3).

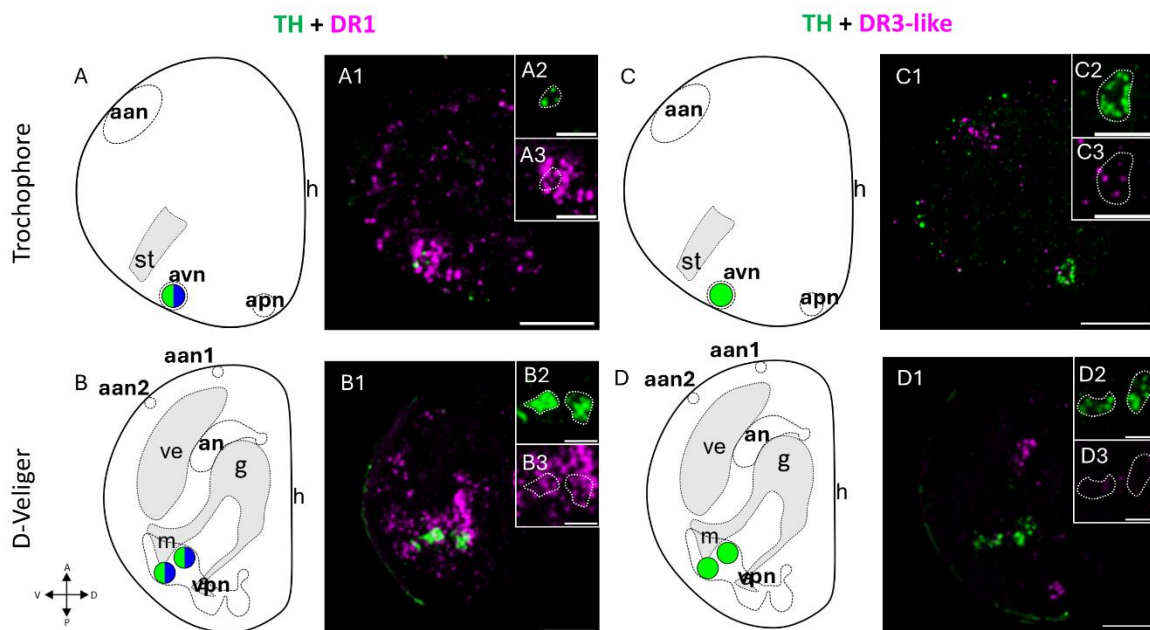


Figure 6.10. Representative images showing the colocalisation of TH with DR1 and DR3-like at Trochophore (28 hpf) and D-Veliger (48 hpf) stages. Double HCR was carried out using TH with B2 amplifier and DRs with B1 amplifier. Organisation of rows from top to bottom: TH + DR1 and TH 9 DR3-like. TH is presented in green in both schemes and confocal images, receptors are blue and magenta in schemes and confocal images respectively. The white colour in confocal images is the result of green and magenta colocalisation.

A-A1. Schematic representation and selective plane projection at Trochophore stage in later view. A2 shows the magnification of TH signal and A3 of DR1. 15 out of 15 larvae displayed colocalisation.

B-B1. Schematic representation and selective plane projection at D-Veliger stage in lateral view. B2-B3 show the magnification of TH signal and DR1 signals. 13 out of 13 larvae displayed colocalisation.

C-C1. Schematic representation and selective plane projection at Trochophore stage in later view. C2-C3 show the magnification of TH and DR1 signals. 5 larvae were analysed.

D-D1. Schematic representation and selective plane projection at D-Veliger stage in lateral view. D2-D3 show the magnification of TH signal and DR1 signals. 14 larvae were analysed.

Axis orientation abbreviations: A – anterior, D – dorsal, L – Left, P – posterior, R – right, V – ventral.

Anatomical abbreviations: a: anus, g: gut, h: hinge, m: mouth, st: stomodeum. Scale bars: 20 µm and 10 µm for inset pictures.

6.2.3.7 Localisation of 5-HTRs within neuronal and ciliated tissues

Localisation of 5-HTR1A2_{inv} and 5-HTR6-like receptors (green) within neuronal tissues was investigated by double HCR with 7B2 (magenta). These two receptors were chosen because they displayed a complete neuronal localisation at D-Veliger stage (see Figure 6.7).

5-HTR1A2_{inv} signal at Gastrula stage was found within *an*, where serotonin producing cells are present (Figure 6.11 A-B3). At Trochophore stage the anterior and apical clusters were found to localise within *aan*; moreover, a posterior cluster appeared but it did not colocalise within *apn* but outside them, thus indicating the presence of both neuronal and non-neuronal clusters. At D-Veliger stage two clusters were found, one anterior within *an* and one ventral-posterior within the more ventral and apical area of *vpn*. The clusters within the *an* showed a bilateral profile and were localised within all *an* area (Figure 6.11 F1-F3); the cluster localised in the *vpn* area resulted to be bilateral and symmetrical in the more anterior area of *vpn* (Figure 6.10 F1, F4 and F5).

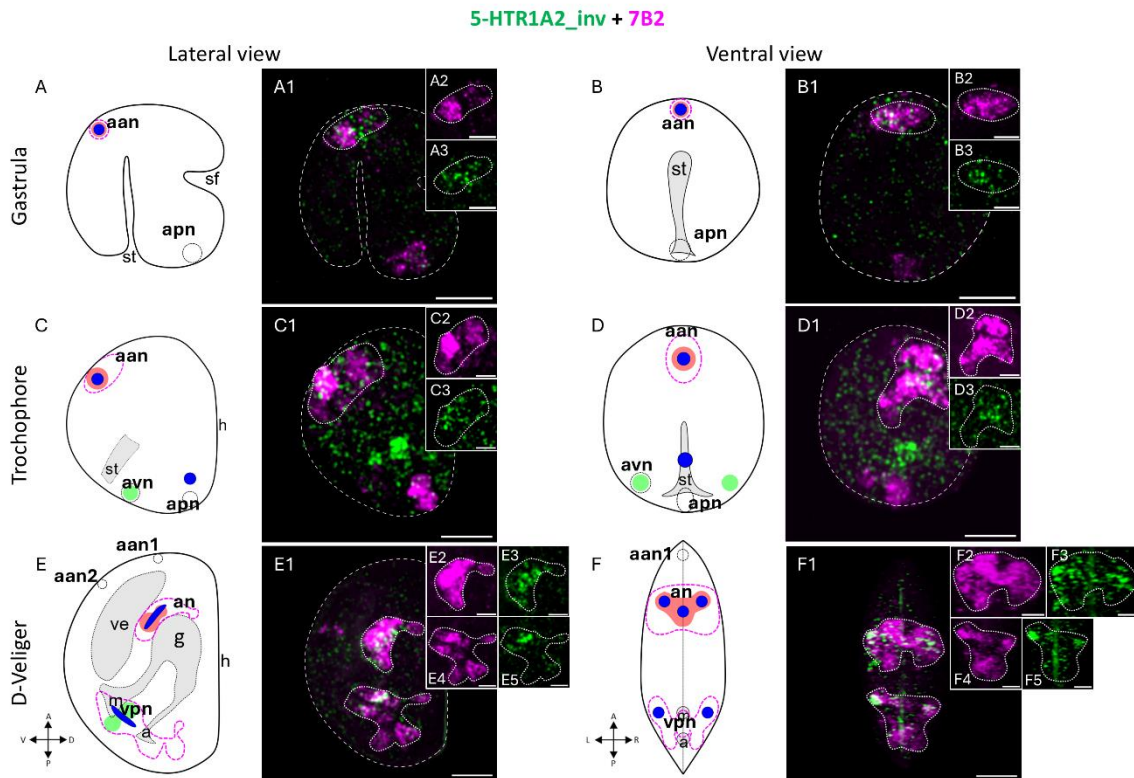


Figure 6.11. Representative images showing the spatiotemporal localisation of 5-HTR1A2_inv within 7B2. Double HCR was performed using 5-HTR1A2_inv (B1 amplifier) and 7B2 (B3 amplifier). Panels are arranged as in Figure 6.3. In the schemes, sites of synthesis of serotonin and dopamine are shown in pale red and green, respectively. The white colour in confocal images is the result of green and magenta colocalisation.

A1-2. Schematic representation and selective plane projection at Gastrula in lateral view. A2-A3 shows a magnification of TPH and 5-HTR1A2_inv signals.

B-B1. Schematic representation and selective plane projection at Gastrula stage in ventral view. B2-B3 show the magnification of TPH and 5-HTR1A2_inv signals. 7 out of 7 larvae displayed colocalisation (panels A1, B1).

C-C1. Schematic representation and maximum plane projection at Trochophore stage in lateral view. C2-C3. Magnification of TPH and the 5-HTR1A2_inv signals.

D-D1. Schematic representation and maximum plane projection at Trochophore stage in ventral view. D2-D3. Magnification of TPH and 5-HTR1A2_inv signals. 6 out of 6 larvae displayed colocalisation (panels C1, D1).

E-E1 Schematic representation and maximum plane projection at D-Veliger stage. E2-E3. Magnification of 7B2 and 5-HTR1A2_inv signals of *an* area. E4-E5. Magnification of 7B2 and 5-HTR1A2_inv of *vpn* area.

F-F1. Schematic representation and 3D reconstruction of D-Veliger in ventral view. F2-F3. Magnification of 7B2 and 5-HTR1A2_inv signals of *an* area. F4-F5. Magnification of 7B2 and 5-HTR1A2_inv signals of *vpn* area. 7 out of 7 larvae displayed colocalization (panels F1, E1).

Axis orientation abbreviations: A – anterior, D – dorsal, L – Left, P – posterior, R – right, V – ventral. Anatomical abbreviations: a: anus, g: gut, h: hinge, m: mouth, sf: shell field, st: stomodeum. Scale bars: 20 μ m and 10 μ m for inset pictures.

5-HTR6-like showed a neuronal localization in all stages studied (Figure 6.12). At Gastrula stage it was detected within *apn* area (Figure 6.12 A1-A3 and B1-B3) and the cluster here identified remained posterior and localised within *apn* also at Trochophore stage (Figure 6.12

C1-C3 and D1-D3). At D-Veliger stage, the posterior cluster was localised within the more posterior area of *vpn* (Figure 6.12 E1-E3 and F1-F3) as previously shown (Figure 6.7 B).

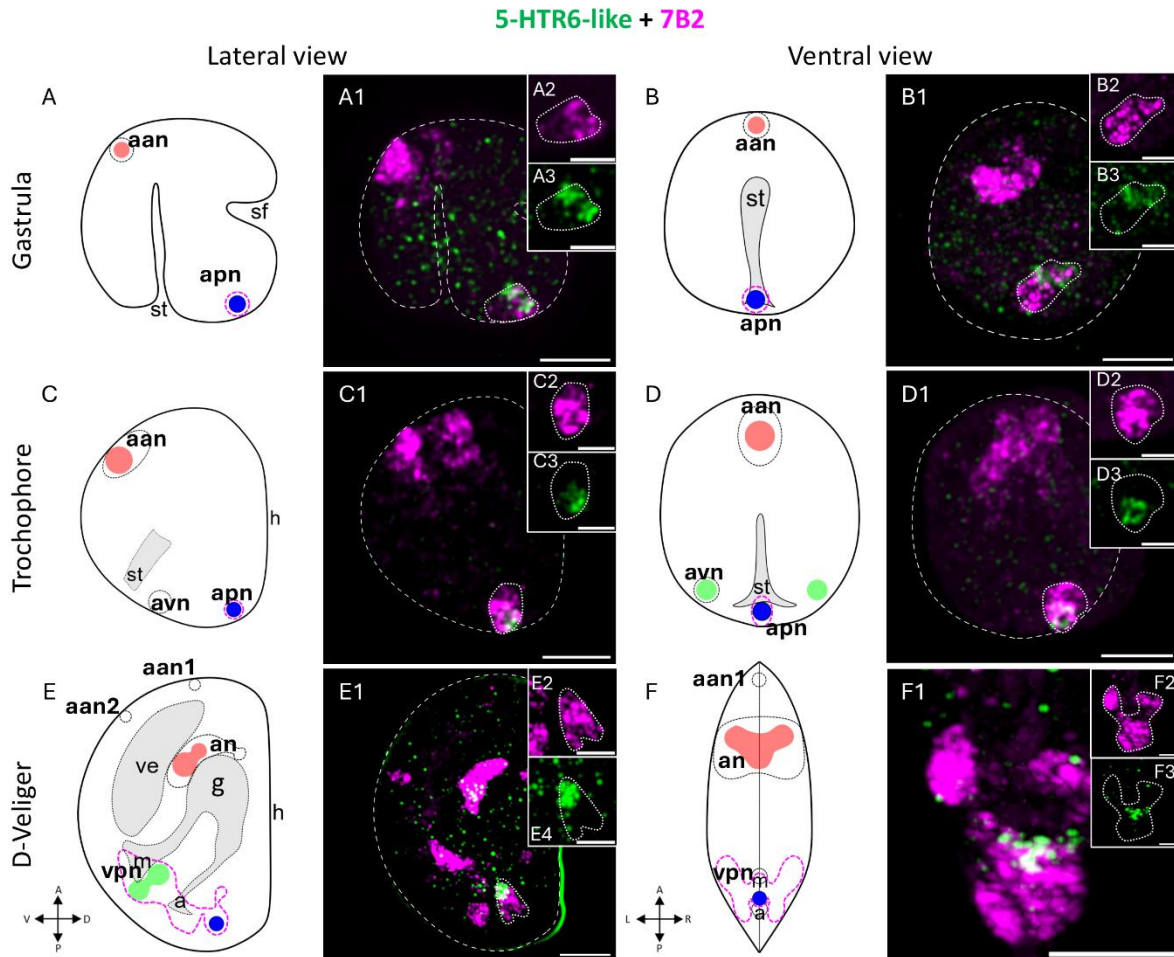


Figure 6.12. Representative images of the spatiotemporal localisation of 5-HTR6-like within 7B2. Double HCR was performed using 5-HTR6-like (B1 amplifier) and 7B2 (B3 amplifier). Panels are arranged as in Figure 6.3. 5-HTR6-like is in green and blue in confocal images and schemes, respectively; 7B2 in magenta in confocal images highlighted by dotted lines in schemes. In the schemes, sites of synthesis of serotonin and dopamine are shown in pale red and green, respectively. The white colour in confocal images is the result of green and magenta colocalisation.

A-A1. Schematic representation and selective plane projection at Gastrula in lateral view. A2 shows a magnification of *apn* with 7B2 and 5-HTR6-like signals.

B-B1. Schematic representation and selective plane projection at Gastrula stage in ventral view. B2 and B3 show the magnification of 7B2 signal and 5-HTR6-like signals of the *apn*. 7 out of 7 larvae displayed colocalisation (panels A1, B1).

C-C1. Schematic representation and maximum plane projection at Trochophore stage in lateral view. C2 and C3 show the magnification of 7B2 and 5-HTR6-like signals of the *apn*.

D-D1. Schematic representation and maximum plane projection at Trochophore stage in ventral view. D2 and D3 show the magnification of 7B2 and 5-HTR6-like signals of *apn*. 7 out of 7 larvae displayed colocalisation (panels C1, D1).

E-E1. Schematic representation and maximum plane projection at D-Veliger stage; E2 and E3 show a magnification of *vpn* with 7B2 and TH alone.

F. Schematic representation of ventral view at D-Veliger stage. F1 selective 3D reconstruction of *vpn* area. F2 and F3 show signal of 7B2 and TH on their own. 6 out of 6 larvae showed TH colocalising within *vpn* area and with 4 clusters. 5 out of 7 larvae displayed colocalization (panels E1, F1). Axis orientation abbreviations: A – anterior, D – dorsal, L – Left, P – posterior, R – right, V – ventral. Anatomical abbreviations: a: anus, g: gut, h: hinge, m: mouth, sf: shell field, st: stomodeum. Scale bars: 20 μm and 10 μm for insets.

Double HCR was also utilized to investigate the colocalisation of 5-HTR7 (green) with tektin (magenta), a tissue marker for the ciliated epithelium (Miglioli et al., 2024; Piovani et al., 2023), because this receptor displayed a broad cluster at D-Veliger stage near shell margins (see Figure 6.7). Tektin was shown to be present already at Gastrula stage (16 hpf), anteriorly and posteriorly, forming the apical and posterior tufts. At Trochophore stage (28 hpf) the signal expanded and tektin marked the prototroch, the ciliary band that divides, approximately, the larval body in two; furthermore, tektin formed two islets in proximity of the stomodeum and the region of the future anus. At D-Veliger stage (44 hpf) the prototroch was completely internalised and gave rise to the velum and tufts were observed in proximity to the mouth and anus (Miglioli et al., 2024). For more information, check out Chapter 4, section 4.3.2.

5-HTR7 was found to colocalise with tektin at all the stages here analysed. At Gastrula stage, 5-HTR7 colocalised within the apical tuft (*at*), with a posterior islet of ciliated epithelium and with the broad anterior-ventral area of signal of tektin (Figure 6.13 A-B1). At Trochophore stage, 5-HTR7 localised within the anterior apical tuft, the prototroch (*pt*) and the posterior islet of ciliated epithelium that will identify, later on, the anus. At D-Veliger stage, 5-HTR7 was localised in the velum, the internalised prototroch, and in the anal tuft located posteriorly (Figure 6.14 E-F1).

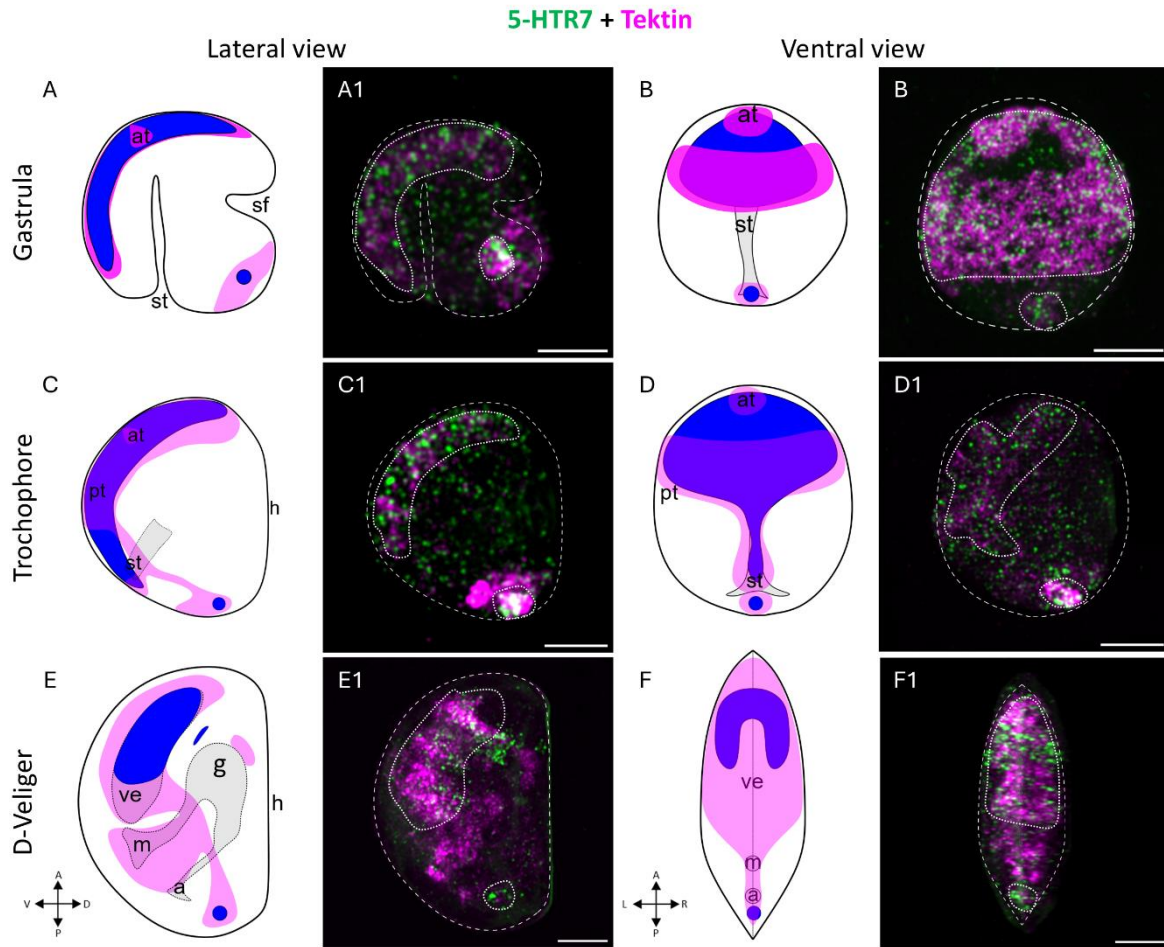


Figure 6.13. Representative images of the spatiotemporal localisation of 5-HTR7 within ciliated epithelium. Double HCR was performed using 5-HTR7 (B1 amplifier) and Tektin (B2 amplifier). 5-HTR7 is represented with blue areas in schemes and in green in HCR images; Tektin is represented in magenta in both schemes and HCR images. Panels are organised as in Figure 6.3. The white colour in confocal images is the result of green and magenta colocalisation.

A-B1. Schematic representation and maximum plane projection at Gastrula stage in lateral (A-A1) and ventral (B-B1) view. 7 out of 7 larvae displayed colocalisation (panels A1, B1).

C-D1. Schematic representation and maximum plane projection at Trochophore stage in lateral (C-C1) and ventral (D-D1) view. 8 out of 8 larvae displayed colocalisation (panels C1, D1).

E-E1. Schematic and maximum plane projection at D-Veliger stage in lateral view. F-F1. Schematic and 3D reconstruction at D-Veliger stage in ventral view. 7 out of 7 larvae displayed colocalisation (panels E1, F1).

Axis orientation abbreviations: A – anterior, D – dorsal, L – Left, P – posterior, R – right, V – ventral. Anatomical abbreviations: a: anus, at: apical tuft, g: gut, h: hinge, m: mouth, pt: prototroch, sf: shell field, st: stomodeum. Scale bar: 20 μ m.

6.2.3.8 Localisation of DR1 within ciliated tissue

At Gastrula stage, no DR1 signal could be detected, in line with the RNA-Seq expression profile (Figure 6.14 A1, B1). DR1 signal (green) was detected at Trochophore stage in different areas.

Two clusters were localised within tektin area (magenta): a conspicuous cluster was localised in an area corresponding to the stomodeum and another one at the level of the apical tuft. A third

cluster was under the prototroch area (Figure 6.14 C-D1). At the D-Veliger stage, DR1 signal localised within different areas marked by tektin: in the velum, at the level of the oral tuft and in the dorsal region of the ciliated stomach (Figure 6.14 E-F1).

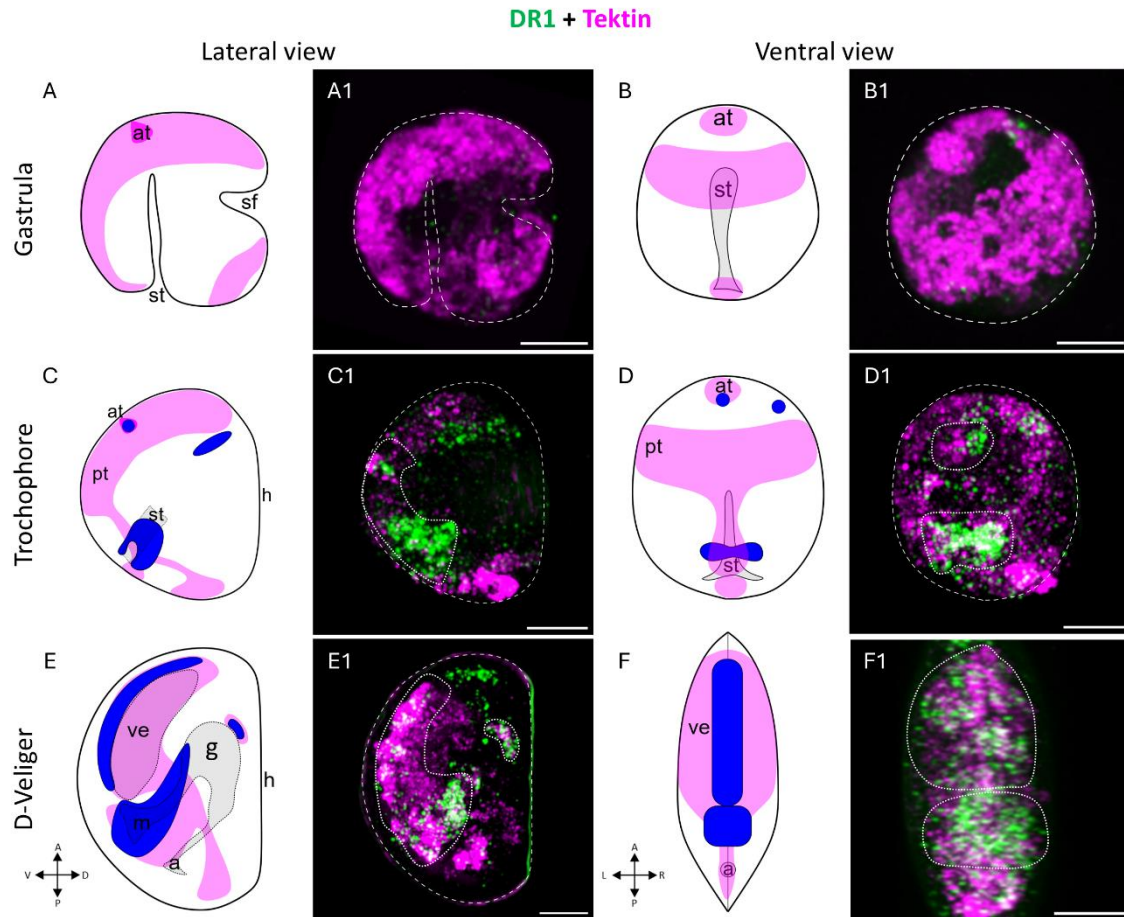


Figure 6.14. Representative images of the spatiotemporal localisation of DR1 within ciliated epithelium. Double HCR was carried out using DR1 (amplifier B1 and Tektin (amplifier B2). DR1 is represented with blue areas in schemes and in green in HCR images; Tektin is represented in magenta in both schemes and HCR images. Panels are organised as in Figure 6.3.

A-B1. Schematic representation and maximum plane projection at Gastrula stage in lateral (A-A1) and ventral (B-B1) view. 3 larvae were analysed. The white colour in confocal images is the result of green and magenta colocalisation.

C-D1. Schematic representation and maximum plane projection at Trochophore stage in lateral (C-C1) and ventral (D-D1) view. 7 out of 7 larvae displayed colocalisation.

E-E1. Schematic and maximum plane projection at D-Veliger stage in lateral view. F-F1. Schematic and 3D reconstruction at D-Veliger stage in ventral view. 7 out of 7 larvae displayed colocalisation.

Axis orientation abbreviations: A – anterior, D – dorsal, L – Left, P – posterior, R – right, V – ventral. Anatomical abbreviations: a: anus, at: apical tuft, g: gut, h: hinge, m: mouth, pt: prototroch, sf: shell field, st: stomodeum. Scale bar: 20 μ m.

6.2.3.9 Localisation of DBHs-like

The DBH previously identified and localised through chromogenic *in situ* hybridisation was found to cluster within the clade of DBHs-like and was called DBH4-like (Miglioli et al.,

2021b). Three DBHs-like were analysed at D-Veliger, because their expression profiles peaked at 48 hpf, during the D-Veliger phase (phase 5, see Figure 6.1). They were found to localise centrally and dorsally, near the hinge (Supplementary Figure 6.20 A-C). The localisation of one of them (DBH5-like) in the larval body suggested that they should be localised in an area that should correspond to the stomach (Supplementary Figure 6.20 C1), thus in a non-neuronal area. Even though the existence of this enzyme is known even in humans, at the state of art there is no clue about its function(s) (Goultly et al., 2023; Xin et al., 2004).

6.2.4 Effects of treatment with exogenous monoamines and pharmacological inhibitors of 5-HTRs and DRs on D-Veliger phenotypes (48 hpf)

Once established the presence of all the main components of serotonergic and dopaminergic system in early larval stages of *M. galloprovincialis*, the effects of exogenous serotonin and dopamine were tested on early larval development at pharmacological concentrations as in oyster larvae (Liu et al., 2020). The endogenous levels of these two monoamines in the haemolymph of adult bivalves are in the nM range, and about 30 times higher for serotonin than dopamine (Fabbri et al., 2024).

Addition of exogenous 5-HT to fertilized eggs induced a significant reduction in the percentage of normal D-Veliger larvae from 1 μ M (p-value < 0.001). At 1 and 10 μ M 5-HT about 35% of D-larvae were normal. Among abnormal larvae, the most recurring phenotypes were protruding mantle (PM) and malformed hinge (MH) (Figure 6.15 A).

In contrast, exogenous dopamine affected normal larval development only at the highest concentration tested (10 μ M), reducing the percentage of normal D-larvae up to 50% (p-value < 0.01). In these conditions, most abundant phenotypes were PM, MH and AT (arrested trochophore) (Figure 6.15 B).

Treatment with Methiothepin, a non-selective inhibitor of 5-HTRs, induced a significant, but small decrease (about -30%) in the percentage of normal D-larvae at 1 μ M (p-value < 0.001). The most recurring phenotypes at 1 μ M were PM and MH. Lower concentrations (0.01 and 0.1 μ M) were ineffective. In contrast, higher concentrations of Methiothepin (10 μ M) were embryotoxic since no viable larvae were detected (Figure 6.15 C).

Finally, the effects of SCH 23390 (a selective inhibitor of DR1) were evaluated. SCH induced a significant decrease in normal larval development from 1 μ M (p-value < 0.001) with MH being the most abundant phenotype. Moreover, 5 μ M induced developmental arrest, with 100% of larvae represented by arrested trochophores (p-value < 0.01) (Figure 6.15 D).

The results indicate that exposure to serotonin induced a clear dose dependent effect on larval development, whereas dopamine was apparently ineffective below high concentrations. Inhibitors for both receptors were embryotoxic at highest concentrations, indicating that both 5-HTRs and DR1 are crucial to mussel larval development. A generally stronger effect was observed with SCH 23390 with respect to methiothepin.

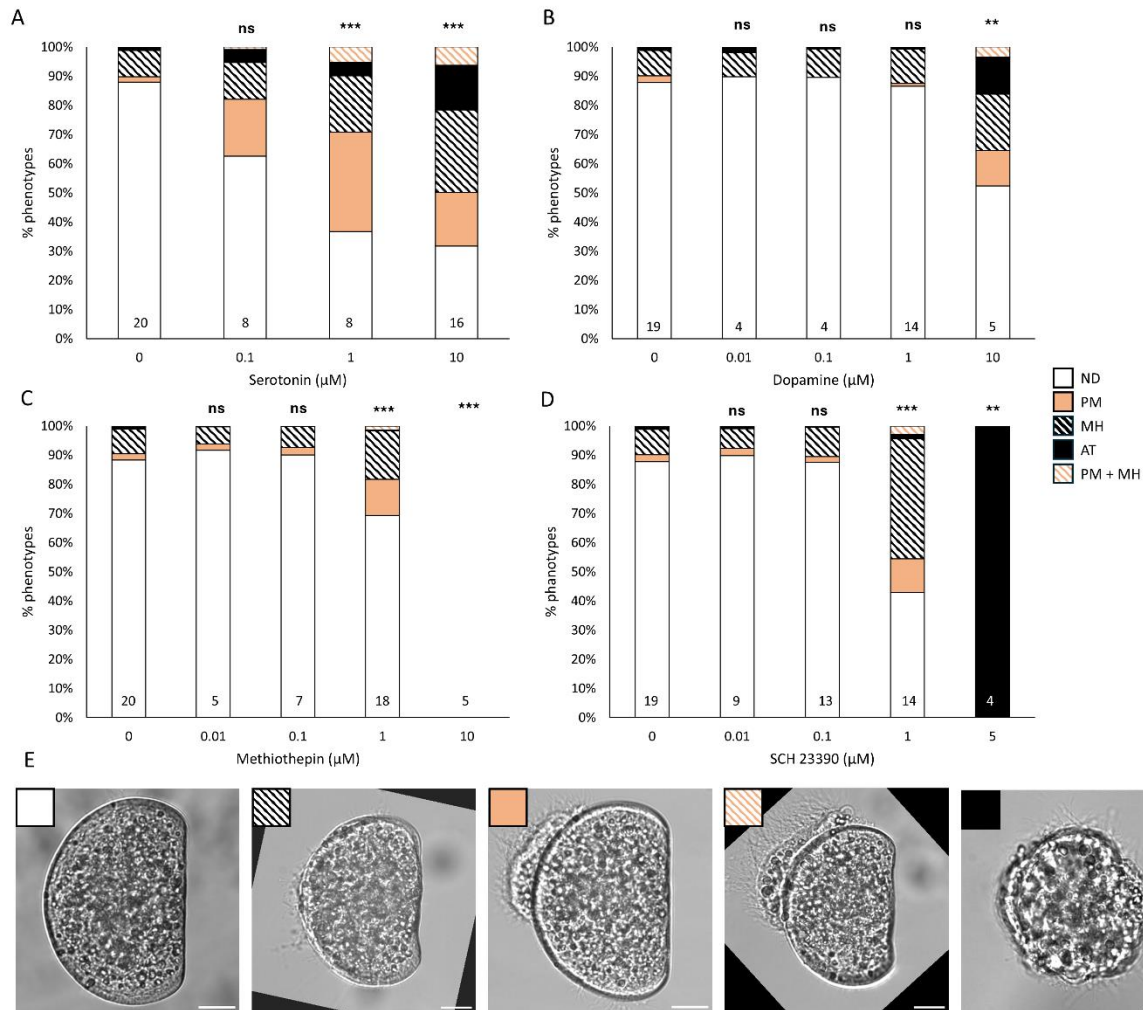


Figure 6.15. A-D. Bar plots showing the percentage of phenotypes in controls and in samples treated with 5-HT, DA, Methiothepin and SCH 23390 at 48 hpf. Asterisks indicate p-values statistical significance (p-value < 0.001 = ***, 0.001 < p-value < 0.01 = **, 0.01 < p-value < 0.05 = *, p-value > 0.05 = ns). Numbers at the bottom of the bar indicate the number of parental pairs analysed per each condition. E. Phenotypes shown by larvae: white Normal D-Larvae (ND), black bars malformed hinge (MH), orange protruding mantle (PM), orange bars protruding mantle + malformed hinge (PM +MH) and black arrested trochophore (AT). Scale bar: 20 μm.

6.3 Discussion

In this study, the characterisation of the monoaminergic (MA) system in bivalves was performed through various experimental approaches using the Mediterranean mussel, *M. galloprovincialis*, as a model organism. *In silico* analyses of the genome and transcriptome were carried out to identify the presence of components of each monoaminergic system and to examine their expression during embryo-larval development. The spatiotemporal evolution of the main components of the monoaminergic system was investigated by single and double HCR at different developmental stages: Gastrula (16 hpf), Trochophore (28 hpf) and D-Veliger (48 hpf).

6.3.1 Six monoaminergic systems may be present in the *M. galloprovincialis* genome

Up to date, very scarce information was available regarding the presence of monoaminergic genes in *M. galloprovincialis*, with only three serotonin and one dopamine receptors, one synthesis enzyme each for dopamine and adrenaline synthesis, identified so far (Canesi et al., 2022; Miglioli et al., 2021b).

In line with a recent study showing that monoaminergic systems are typical of Bilateria (Goulty et al., 2023), the present study identified six out of eight monoaminergic systems in *M. galloprovincialis* genome: components of the serotonin (5-HT), dopamine (DA), noradrenaline (NA), tyramine (TA), octopamine (OA) and histamine (HS) systems were found (Table 6.2).

6.3.1.1 Synthesis enzymes

The synthesis enzymes involved in 5-HT (Tryptophan Hydroxylase – TPH and Aromatic L-Amico Acid Decarboxylase – AADC), DA (Tyrosine Hydroxylase – TH, and AADC), HS (Histidine Decarboxylase – HDC), TA (Tyrosine Decarboxylase – TDC) and NA (Dopamine- β -Hydroxylase – DBH) were identified in the *M. galloprovincialis* genome (from Supplementary Figure 6.2 to Supplementary Figure 6.4). In contrast, the enzyme responsible for the conversion of tyramine to octopamine, Tyramine- β -Hydroxylase – TBH, was not identified, in line with the findings of Goulty et al. (2023) indicating its presence only in Ecdysozoa. Bioinformatic analyses did not identify the synthesis enzyme for melatonin. Analysis of copper containing hydroxylases revealed the presence of the synthesis enzyme for adrenaline (DBH) and several copies of MOXD/DBH-like (up to seven in *M. galloprovincialis*; Supplementary Figure 6.4). These results are also in line with data published by Goulty et al. (2023). Additionally, other bivalves analysed presented multiple sequence

copies of DBH-like enzymes; this could be explained by the genome duplication process documented for Mytilidae but also for bivalves in general (Corrochano-Fraile et al., 2022). For OA synthesis, see BOX.1.

BOX 1. How is octopamine synthesised in non-Ecdysozoa?

As previously mentioned, OA synthesis occurs *via* TBH; however, this enzyme is exclusively present in Ecdysozoa (Goultly et al., 2023), raising intriguing question about the synthesis of OA in other animal groups. It is known that AO is present in both invertebrates and vertebrates, even if in traces in the latter ones (Mell and Carpenter, 1980). In molluscs the presence of octopamine was identified fluorometric detection (Erspamer and Boretti, 1951; Mell and Carpenter, 1980; Pryce et al., 2015). More recent works assessed *via* bioinformatic techniques the presence of octopamine receptors and transporters in non Ecdysozoa invertebrates (Bauknecht and Jékely, 2017; Camicia et al., 2022; Goultly et al., 2023; Ribeiro and Patocka, 2013; Schwartz et al., 2021). This collective evidence suggests that OA is indeed present and synthesized in these organisms. Although OA and NA are derived from two different substrates, they show an almost identical structure, except for a hydroxyl group present only in NA (see Figure 2.1). In the last century, some research groups found that TA and OA are present and synthesised in mice, rat and human brains (Boulton and Wu, 1973, 1972; Carlsson and Waldeck, 1964). In vertebrates, it appears that DBH plays a crucial role in the synthesis of OA (Carlsson and Waldeck, 1964; Pryor et al., 2016). In the planarian *Dugesia japonica* a gene responsible for OA synthesis, named TBH, was identified. The RNA interference targeting this gene resulted in decreased OA without affecting NA, suggesting that this gene was necessary for OA synthesis (Nishimura et al., 2008). A more recent study used the *Dj*TBH to investigate the genes in the new *de novo* genome sequencing of *Lymnaea stagnalis*, identifying a sequence that clustered with *Dj*TBH and was designated as TBH. This cluster, however, formed a sister group with vertebrate DBH (Sadamoto et al., 2012). In this study, the sequence from *L. stagnalis* was used in orthology assessment for copper-containing hydroxylase and it was clustering with mollusc DBHs rather than with *D. melanogaster* TBH. These results corroborate the findings by Goultly et al., (2023) where TBH was found only for Ecdysozoa. Considering the molecular similarity of NA and OA, the information from *in vivo* and *in vitro* in vertebrates, and the recent studies of RNA interference and bioinformatics, it could be possible to speculate that all Bilateria, excluding Ecdysozoa, can synthesise OA by using the same enzyme responsible for the conversion of DA to NA: DBH.

6.3.1.2 Degradation enzymes

Although monoamine oxidases (MAOs) do not represent the major degradation pathway in invertebrates (Finberg and Rabey, 2016; Sloley, 2004), two sequences were identified in the *M. galloprovincialis* genome, named as MAO-A like and MAO-B, based on the presence of identical or similar amino acids responsible for the reaction catalysis (Supplementary Figure 6.6) (Wilson et al., 2020). These results are supported by data from Goulty et al. (2023), which noted that MAOs are present across Bilateria.

6.3.1.3 Transporters

This study revealed the presence of one vesicular monoamine transporter (VMAT) and several membrane transporters of the SLC6 family in *M. galloprovincialis*. Specifically, two SERT-like transporters, one iDAT and one OAT were identified (Supplementary Figure 6.7, Supplementary Figure 6.8). The presence of two SERT-like transporters could be ascribed to the process of genome duplication, as suggested for DBH-like enzymes. The DAT identified clustered with invertebrates sequences (iDAT), consistent with existing literature (Camicia et al., 2022; Goulty et al., 2023).

Notably, no specific transporter for tyramine was identified, reinforcing the hypothesis that OAT is used for phenolamines, thus TA and OA (Caveney et al., 2006; Ribeiro and Patocka, 2013). Moreover, the absence of a histamine transporter reinforces the debate on its presence in both vertebrates and invertebrates (Ribeiro and Patocka, 2013).

Interestingly, no NET was found in any of the species analysed, in accordance with previous data suggesting that OAT is invertebrate-specific while NET is vertebrate-specific (Adamo, 2008; Caveney et al., 2006; Ribeiro and Patocka, 2013). In the absence of NET, OAT could perform the clearance of NA, given its demonstrated affinity towards TA, OA, DA and NA in *Lumbricus terrestris* and in Arthropoda (Caveney et al., 2006).

6.3.1.4 Receptors

GPCRs were identified in the *M. galloprovincialis* genome for 5-HT, DA, NA, TA, OA and HS. In this study new serotonin receptors (5-HTRs) belonging to different families were identified (Supplementary Figure 6.9), thereby expanding the existing knowledge of 5-HTRs in *M. galloprovincialis* (Canesi et al., 2022). The absence of 5-HTR3 (ion-gated channels) aligns with previous findings in invertebrates (Goulty et al., 2023). Three different dopamine receptors (DRs) were identified (Supplementary Figure 6.10), and data align with previous findings published for the Pacific oyster, *C. gigas*, with a DR, named DR2, belonging to the clade of Invertebrate Dopamine Receptor (INDR) (Schwartz et al., 2021). Concerning NA, TA

and OA receptors (ARs, TARs and OARs, see Supplementary Figure 6.11), two ARs belonging to the family of $\alpha 1$ and $\alpha 2$ adrenergic receptors were found; no β -AR could be identified in line with previous findings, showing that β -ARs are restricted to chordates (Bauknecht and Jékely, 2017; Goultly et al., 2023). Data of TARs and OARs are align with previously published data, with no TAR type 2 receptor reported in Mollusca (Bauknecht and Jékely, 2017). Four HS receptors (HSRs) were found, restricted to the family of HSR1 and HSR3 (Supplementary Figure 6.12), aligning with previous findings (Ravhe et al., 2021).

6.3.2 Expression profiles of serotonin and dopamine gene suggest that they might have several key roles during *M. galloprovincialis* embryo-larval development

The analysis of expression dynamics of monoaminergic genes during embryo-larval development of *M. galloprovincialis* (from 0 to 48 hpf) identified five distinct phases of gene expression from early embryo (Phase 1), Gastrula (Phase 2), Trochophore (Phase 3), Early Veliger (Phase 4) and D-Veliger (Phase 5) Notably, 5-HT and DA related genes were primarily expressed from Phase 2 (corresponding to 16 hpf). (Figure 6.1). Moreover, these genes exhibited quantitatively higher expression values compared to other identified monoaminergic genes, suggesting that they may represent the primary monoaminergic systems involved in embryo-larval development.

The expression profiles of other monoaminergic components support this hypothesis. Histamine and octopamine genes were predominantly expressed during Embryonic and Gastrula phases (Phases 1 and 2), whereas noradrenaline and octopamine receptors were restricted to D-Veliger phase (Phase 5).

Interestingly, AADC expression was detected as early as the egg stage, preceding that of TPH and TH. This finding indicates maternal transmission of the capacity to synthesize 5-HT and DA during early embryonic development. The role of serotonin in embryo development of different invertebrate species has been described. In sea urchin embryos 5-HT was detected first in the micromeres (8-16 cell stages) and then in the macromeres during the blastula stage (Buznikov et al., 2001). In bivalve molluscs, 5-HT was detected at four and eight blastomere stages and during the blastula phase in *M. trossulus* (Ivashkin et al., 2012). In *Lymnaea stagnalis* the intracellular 5-HT concentration was found to be pivotal for maintaining a spiral cleavage pattern. Alterations in 5-HT concentration lead to a disruption of the spiral cleavage pattern leading to a complete malformed gastrula (Bogomolov and Voronezhskaya, 2022). In

both sea urchins and molluscs, 5-HT was synthesised in the zygote and blastomeres, acting as an intracellular regulator and local hormone.

In early developmental stages, 5-HT appears to play a crucial role in cell proliferation and migration. Specifically, it interacts with cytoskeletal components (microfilaments in the cortical contractile ring, microfilaments of filopodia involved in blastomeres adhesion and structure involved in mitotic spindle orientation) (Buznikov et al., 1996; Lauder, 1993). In the blastula of sea urchins, 5-HT has been suggested to promote ciliary activity, facilitating cells to move in the blastocoel and initiating the invagination of the ectoderm, marking the beginning of gastrulation (Buznikov et al., 2001, 1996; Lauder, 1993). Also in mammalian embryos, 5-HT was shown to influence proliferation of early embryonic cells through a signalling independent from GPCRs, including intracellular receptors and a process termed serotonylation (Cikos et al., 2011).

Also DA has been detected in eggs of echinoderms and bivalve molluscs (*M. yessoensis* and *Crenoiyrilus grayanus*) (Buznikov, 1984; Khotimchenko, 1991) and during cleavage stages (from 4 cells to blastula) in *M. trossulus* (Ivashkin et al., 2012). DA appeared to be the only monoamine found in eggs of bivalve molluscs and echinoderms, suggesting a possible role in regulating oogenesis and, possibly, embryonic development. In echinoderms, DA was localised in vesicular structures within ectodermal cells at early developmental stages; addition of exogenous DA resulted in cytostatic effects, inhibiting cleavage division at concentrations ranging from 100 to 400 μ M (Buznikov, 1984). In sea urchins, DA was found to promote the embryonic cleavage through adenylyl cyclase (Buznikov et al., 2001, 1996). The regulatory effects of DA are believed to involve dopamine amides intracellular binding sites (Buznikov et al., 2001; Khotimchenko, 1991).

The zygote represents an autocrine system, while the developing embryo a semi-autocrine system, where neurotransmitters retain their intracellular roles and act also through their receptors localised on the cell membrane (Buznikov et al., 1999). These findings indicate that both 5-HT and DA have pre-nervous roles, also referred to as morphogenetic roles, as they regulate developmental processes independently of their neurotransmission activities (Camicia et al., 2013).

In the present work, data are reported on the time course of expression of enzymes involved in 5-HT and DA synthesis in *M. galloprovincialis* embryos. The peak expression of AADC at the egg stage (0 hpf), indicating a maternal origin, likely helps regulating initial 5-HT and DA

levels in the first embryo stages. TPH and TH expression peaks occur later (at 16 and 36 hpf, respectively).

This pattern aligns with the time course of expression of three serotonin receptors (5-HTR1A2_inv, 5-HTR6-like, 5-HTR7) across embryo/larval development. 5-HTR1A2_inv peaked before TPH (12 hpf), while 5-HTR6-like and 5-HTR7 began to increase at 16 hpf, coinciding with TPH peak (Figure 6.1). HCR data confirm that these three receptors were detected at the Gastrula stage (16 hpf) and indicate that their localization is in tissues characterised by a neuroendocrine and ciliated epithelium signature, supporting the hypothesis of a pre-nervous role of 5-HT during the first stages of development.

Similarly, dopaminergic components, including iDAT, DR2 and DR3-like peaked before TH during the Embryonic and Gastrula phases (Phase 1 and 2, Figure 6.1), suggesting that DA might also play a pre-nervous role in *M. galloprovincialis* embryos. However, their exact localisation could not be identified.

The discrepancy between expression of synthesis enzymes and that of some receptors, suggests that some 5-HTRs and DRs could be involved in sensing the environment and responding to environmental cues, especially indole compounds and their derivatives (Kumar et al., 2021; Tomberlin et al., 2017). Indole, a derivative of tryptophan, is widespread in living organisms and in the environment as it is produced by free living bacteria, plants and bacteria flora in animals (Kumar et al., 2021; Tomberlin et al., 2017). Most studies have focused on insects and *C. elegans*, where indole and its derivatives are known to influence several behaviours such as feeding, mating and oviposition (Kumar et al., 2021). Mussels, specifically, have been observed to respond to indole and its derivatives produced by bacteria, which serve as antifouling agents by inhibiting larval settlement (Kumar et al., 2021). These compounds are known to act on the monoaminergic system, with 5-HTRs serving as primary target. The binding of indole to 5-HTRs was reported to influence animal behaviour, especially gut motility and food intake (Tomberlin et al., 2017). Additionally, indole and its derivatives were reported to bind also to α 1-AR and DRs (de Sa Alves et al., 2009; Tomberlin et al., 2017). These findings support the hypothesis that 5-HTRs and DRs, expressed prior to 5-HT and DA synthesis, could be involved in early environmental sensing to regulate embryo-larval behaviour.

In addition to this, this discrepancy could be explained by recent findings in *D. melanogaster* and chicken embryos. Indeed, it was found that in *D. melanogaster* two subtypes of 5-HTR2, namely 5-HTR2A and 5-HTR2B, are involved in regulating the activation of Myosin II during gastrulation (Karki et al., 2023). In chicken embryos 5-HTR2A and 5-HTR2B were shown to

be pivotal during gastrulation by regulating levels and activation of Myosin II (Karki et al., 2023). It could be possible that also in *M. galloprovincialis* embryos 5-HTRs could have morphogenetic roles based on these findings. In addition to this, in the frog embryos of *Xenopus*, 5-HT was shown to regulate left-right asymmetry by displaying an asymmetric localisation and through serotonergic and gap-junctions signalling (Vandenberg et al., 2014, 2013).

Regarding the later developmental stages, specifically the Trochophore and Veliger, 5-HT and DA components showed further upregulation and secondary expression peaks. Specifically, 5-HTR6-like and 5-HTR7 remained upregulated following the Gastrula phase (Trochophore, Early Veliger and D-Veliger), while 5-HTR1A2_inv exhibited a second increase in expression during the D-Veliger phase (Figure 6.1). Moreover, 5-HTR2 and 5-HTR4-like increased their expression during the Trochophore phase and showed upregulation in the two subsequent phases. In contrast, 5-HTR1A1_inv stood out as the only 5-HTR expressed exclusively during a single phase: the D-Veliger (Figure 6.1). The serotonin reuptake transporter (SERTs) appeared after the peak of TPH: SERT2-like was upregulated from Trochophore to D-Veliger phases, whereas SERT1-like peaked only during the D-Veliger phase (48 hpf) (Figure 6.1). Regarding DA components, iDAT also showed upregulation following the peak of TH (at 36 hpf), and both DR1 and DR2 were upregulated from the Trochophore to D-Veliger phases (Figure 6.1). The emergence of new components and the continuous upregulation of 5-HT and DA transcripts suggest their roles in the development of the larval stages, as well as in the potential transition between trochophore and veliger.

This hypothesis is consistent with the pharmacological results obtained in this study. Incubation with exogenous 5-HT and DA affected larval development, with 5-HT being more effective than DA, which reduced the percentage of normal D-larvae only at high concentrations (Figure 6.15 A, B). Treatment with methiothepin, a non-selective inhibitor of 5-HTRs, weakly affected larval development at 1 μ M and was completely toxic at 10 μ M, with no viable larvae detected, suggesting that methiothepin may not be selective for *M. galloprovincialis* 5-HTRs. Conversely, larvae treated with SCH 23390 were strongly affected at 1 μ M and displayed developmental arrest when incubated at 5 μ M.

5-HT and DA play a critical role in larval development and the transition from trochophore to veliger in *C. gigas*. In this species both 5-HT and DA modulate shell biogenesis through a TGF- β SMAD pathway, regulating the expression of tyrosinase and chitinase (two genes involved in the deposition of the organic shell matrix) (Liu et al., 2020).

In two polychaete species, *Phyllidoce maculata* and *P. dumerilii*, exposure to high 5-HT concentrations led to developmental retardation, malformations and chaotic arrangement of nerve fibres with chaotic sprouting of nerve fibres resulting in a dose dependent manner (Nezlin and Voronezhskaya, 2017). On the contrary, trochophore larvae of *C. gigas* incubated with 100 μM 5-HT and 1 μM DA exhibited an accelerated growth rate compared to larvae grown under control conditions (Liu et al., 2020). The effects displayed after 5-HT exposure align with the results obtained for *P. maculata* and *P. dumerilii* where malformation were detected following incubation with exogenous 5-HT. Caution is needed when comparing results of *C. gigas* with respect to results presented here because oyster larvae were treated once they reached the stage of trochophore, leading to different findings. This difference may arise because, at the trochophore stage, the 5-HT and DA components involved in larval development are already present and expressed. Consequently, the addition of exogenous monoamines may impact larval development differently, altering the responses elicited.

In invertebrates, methiothepin appears to act as an effective non-selective antagonist, inhibiting 5-HTR1, 5-HTR2, and 5-HTR7 in arthropods, nematodes, and molluscs, though there appears to be species-specific variability (Tierney, 2018). The addition of 10 μM methiothepin to *C. gigas* trochophore larvae inhibited the calcified shell deposition (Liu et al., 2020). Experiments on *P. maculata* and *P. dumerilii* showed that incubation with mianserin, a selective antagonist of 5-HTR2, led to either no effect on larval development or complete toxicity (100 μM and 20 μM infective, 200/500 μM and 50 μM completely toxic for *P. maculata* and *P. dumerilii* respectively). These findings led Nezlin and Voronezhskaya (2017) to suggest that these substances may lack specificity for invertebrate 5-HTRs. Consistent with the results on polychaetes, methiothepin appears to be either ineffective or toxic on *M. galloprovincialis* larvae.

C. gigas larvae treated with 10 μM SCH 23390 exhibited inhibited formation of the calcified shell (Liu et al., 2020). Previous studies on *M. galloprovincialis* demonstrated that DR1 inhibition with 0.5 μM SCH23390 interfered with the shell biogenesis process (Miglioli et al., 2021b). These findings highlight the importance of DA signalling through DR1 in ensuring normal larval development and shell biogenesis process. *M. galloprovincialis* appears to be more sensitive than *C. gigas*, as concentrations of 0.5 μM and 1 μM were sufficient to affect larval development, while 5 μM led to an arrest in development.

In conclusion, both transcriptomic and pharmacological results suggest that 5-HT and DA play a key role in larval development and shell biogenesis. Specifically, 5-HT and DR1 seem to be

pivotal for larval development and shell biogenesis. The effects of DA are less pronounced compared to 5-HT, possibly due to the expression profile of iDAT. In contrast, methiothepin appears to lack selectivity towards *M. galloprovincialis* 5-HTRs.

6.3.3 Expansion of neuronal clusters highlights growing complexity in *M. galloprovincialis* embryo-larval development

This study shows for the first time the neuroendocrine system of *M. galloprovincialis* during embryo-larval development using 7B2 as marker. The first clusters identified appeared anterior-apically (*aan*) at Gastrula stage (16 hpf) and its signal increased in term of clusters at Trochophore stage (28 hpf). At this stage, two other clusters of neurons appeared (*avn* and *apn*). By 48 hpf the structure of the nervous system became more complex, with the appearance of two large clusters, the *an* and *vpn*, which displayed a bilateral and symmetrical pattern. Two more clusters (*aan1* and *aan2*) were also identified.

The nervous system of the Trochophore stage of *C. gigas* was recently analysed using *in situ* hybridisation techniques (chromogenic and HCR). Analysis with the pan-neuronal marker 7B2 allowed the identification of two clusters: one apical and one posterior (Piovani et al., 2023). The localisation of these clusters appears similar to the findings presented here, where the apical cluster, referred to as the apical organ (AO), likely corresponds to *aan*, and the posterior cluster aligns with *apn*. However, no ventral cluster was detected in the trochophore of the Pacific oyster (Piovani et al., 2023). These differences might be attributed to differences in developmental timing or the technique used to study 7B2: in this study HCR was employed, while in Piovani et al., (2023) the gene 7B2 was analysed by chromogenic *in situ* hybridisation (ISH). HCR has a better resolution compared to ISH. The nomenclature of clusters in this study was based on their position in the larval body. Based on its position, it is possible that what is described as *aan* corresponds to the AO described by Piovani et al., (2023).

At the D-Veliger stage, no data using pan-neuronal markers are available for bivalve molluscs. Sparse data exist for other lophotrochozoans. At D-Veliger stage *an* and *vpn* exhibited a bilateral and symmetrical signal (Figure 6.16). This structure is reminiscent of the nervous system described in *Schmidtea polychroa* and *P. dumerilii* (Achim et al., 2018; Monjo and Romero, 2015). Late stage *S. polychroa* showed two lateral and ventral stripes of signal and a notable concentration of signal at the anterior pole (Figure 6.16) using Elav as marker (Monjo and Romero, 2015). In *P. dumerilii*, 7B2 signal was found only anterior-ventrally marking the apical organ (AO). The nervous system was more clearly visualised using a different neuronal marker (Rab3), which displayed a bilateral and symmetrical pattern resembling the *an* and *vpn*

observed at 48 hpf. The anterior cluster marked by Rab3 was localised in the same region as the 7B2 signal; Rab3 also revealed a more posterior cluster with a butterfly-like structure similar to *vpn* (Figure 6.16) (Achim et al., 2018). Despite differences in developmental stages, these organisms share a ventral nervous system characteristic of protostomes (Nieder, 2021).

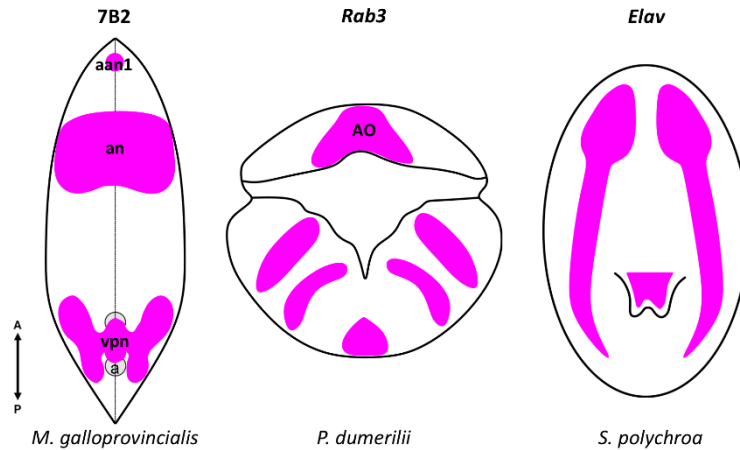


Figure 6.16. Comparison of nervous system structure in *M. galloprovincialis* at D-Veliger stage with larval stages of *P. dumerilii* and *S. polychroa*. Larvae are shown in ventral view evaluated with different neuronal markers. The signal of each marker is represented by magenta areas.

6.3.4 Serotonin and dopamine producing cells occur in different neuronal clusters that could correspond to the AO/CG and PG

Localisation of TPH and TH allowed the identification of cells involved in 5-HT and DA production, respectively. TPH was detectable already at Gastrula stage (16 hpf), in contrast to TH that was detected from Trochophore stage (28 hpf). The differences in the time of detection were in line with the expression profiles shown in the transcriptome (Figure 6.1, Figure 6.2). TPH was localised within the *aan* at 16 and 28 hpf and within the *an* at 48 hpf; TH was localised within the *avn* and *vpn* at 28 and 48 hpf, respectively. Overall, the results clearly indicate that 5-HT and DA producing cells are localised in two different neuronal areas.

Data of TPH localisation are in line with data previously obtained using the immunocytochemistry technique in *M. galloprovincialis* (Miglioli et al., 2021a). The first two 5-HT-*lir* cells were shown to appear at 24 hpf; at 28 hpf the number increased up to three, four at 32 hpf, and seven at 48 hpf. With the HCR technique three TPH positive cells were counted already at 16 hpf, four at 28 hpf and seven at 48 hpf. Variations in the number of cells and the timing of detection should be attributed to the differences in the technique used (immunocytochemistry vs HCR).

5-HT and catecholamines were localised in several species of bivalves (*Acila insignis*, *Azumapecten farreri*, *Crassostrea gigas*, *Dreissena polymorpha*, *M. trossulus* and *Spisula sybillae*) during larval development using the immunocytochemistry technique for 5-HT and the induced autofluorescence technique for catecholamines. Data on the following species at different stages of development are reported in Figure 1.4 (Kniazkina and Dyachuk, 2022; Miglioli et al., 2021b; Nikishchenko et al., 2023; Nikishchenko and Dyachuk, 2024; Pavlicek et al., 2018; Voronezhskaya et al., 2008; Yurchenko et al., 2018; Yurchenko and Dyachuk, 2022). In contrast to all other bivalves, *A. insignis* is characterised by the presence of a short pelagic larval period and the larva is called pericalymma, which has been defined as a modified Veliger by Nikishchenko and Dyachuk (2024), thus data regarding its neurodevelopment are put in the schemes of Veliger stages. Neurons are reported to appear first at the Trochophore stage in a non-paired sensory structure called the Apical Organ (AO), a structure formed of neurons bearing cilia (Kniazkina and Dyachuk, 2022; Yurchenko et al., 2019). Neurons of the AO were found to be positive to 5-HT- and FMRFamide-like immunoreactive (*lir*).

The areas here identified as *aan* at Trochophore stage and *an* at D-Veliger stage could correspond to the AO and AO/CG, given its apical and anterior position at Trochophore stage and its relocation in the larval body at D-Veliger stage, respectively. The AO is characterised by the presence of different transmitters, including 5-HT, FMRFamide and acetylcholine (Yurchenko et al., 2019). 5-HT-*lir* cells were reported to localise in the AO of the bivalves *A. farreri*, *C. gigas*, *D. polymorpha*, *M. trossulus*, *S. sybillae* and in the Scaphopoda *Antalis entails* and in the pericalymma of *A. insignis*. In all the species analysed the AO was shown to still be positive to 5-HT during developmental progression: in bivalve molluscs and in *A. entails* it was shown that the AO subsided into the larval body forming the AO/CG (Kniazkina and Dyachuk, 2022; Pavlicek et al., 2018; Voronezhskaya et al., 2008; Yurchenko et al., 2018). In this study it was shown that TPH signal was first apical and then it underwent an internalisation into the larval body. Given the molecular signature of *aan/an*, it should correspond to the forming AO at 16 and the AO at 28 hpf, and to the AO/CG described in other molluscs at 48 hpf.

The nomenclature AO/CG is maintained because the fate of the AO, once it is internalised, is not very clear. A recent study showed that AO is still present at Pediveliger stage of different bivalves species (Nikishchenko et al., 2023); furthermore Nielsen (2005) described the CG as a paired structure forming lateral to the AO. This observation seems to be confirmed by the data here presented. TPH formed one cluster at 16 and 28 hpf, at 48 hpf it was possible to identify three different clusters: one medial cluster and two lateral and symmetrical clusters. Moreover,

the two lateral clusters appeared to be to SERT1-like, which appeared only in Phase 5 of development, peaking at 48 hpf (Figure 6.1). So far AO/CG has never been described with pan-neuronal markers but only by immunocytochemistry techniques. These findings suggest that AO subsided into the larval body and its structures increased in complexity after migration.

In contrast to other bivalves, *M. galloprovincialis* was positive to TPH and 5-HT just in the area of AO-AO/CG; on the contrary *C. gigas*, *D. polymorpha* and *S. sybillae* showed 5-HT-*lir* structures outside the AO/CG; in *D. polymorpha* one neuron was accessory (stomatogastric neuron, *sgn*) and disappeared during late development, on the contrary, *S. sybillae* *sgn* neurons remained during development, and *C. gigas* showed 5-HT-*lir* also in the PG. These differences could be attributed to species variabilities.

TPH was studied in the larva of *P. dumerilii* and it was found to localise within the area of 7B2 (Achim et al., 2018) and in the adult gastropod *Berghia stephanieae* cell transcriptome, TPH clustered with 7B2 (Ramirez et al., 2024), thus corroborating the findings presented here, that is serotonin producing neurons possess a neuroendocrine identity.

TH was localised ventrally at both 28 and 48 hpf. Comparison with the bivalve species above mentioned is more difficult in this case, first of all because the technique used is not dopamine-specific, and secondly because not all of the bivalves mentioned were investigated for catecholamine-positive cells, except for *A. farreri* and *M. trossulus*. Data for *M. galloprovincialis* are available: TH was studied by chromogenic *in situ*, and the localisation is in line with the data reported here (Miglioli et al., 2021b). With the HCR technique it was possible to assess that DA producing cells increased with time: from four at 28 hpf to seven/eight at 48 hpf. In *A. farreri* and *M. trossulus* CA positive cells were localised within the velum and near the esophagus and stomach (Kniazkina and Dyachuk, 2022; Voronezhskaya et al., 2008) and only at D-Veliger stage. At Pediveliger stage, CAs were found in the PG and VG of *M. trossulus* (Voronezhskaya et al., 2008). Such discrepancies should be attributable to the different techniques used.

TH was studied in the planaria *S. polychroa* and the signal was found at both early and late stages of development within the nervous system area (Monjo and Romero, 2015). However, a comparison in terms of localisation with *Mytilus* is not possible due to differences in the structure of the larval body plan. Nevertheless, TH was analysed in the larva of *P. dumerilii*, and it was found to be localised in the area of the pan-neuronal marker, both anteriorly and posteriorly, thus covering a greater area compared to *M. galloprovincialis* (Achim et al., 2018).

Nonetheless, even if there was no colocalisation in other species with 7B2, the results obtained here suggest that dopamine producing cells also have a neuroendocrine identity.

A recent article studied the neurotransmitters identity of the ganglia of the mussel *Crenomytilus grayanus* (Kotsyuba et al., 2020). Among the neurotransmitters studied, there were 5-HT and DA (using immunocytochemistry against TH). Their results showed that 5-HT is found in the adult CPG and PG but not in the VG. On the contrary, TH is found in all adult ganglia, with higher density in the PG. These data could allow for the identification of the destiny of *vpn*. TH was the only monoamine synthesizing enzyme localised in the *vpn*. Only in *M. edulis* CA were found to be localised within ganglia: within the PG at the D-Veliger stage and within PG and VG at the Pediveliger stage. Given the localisation of CAs in *M. edulis* and the presence of TH in all ganglia of *C. grayanus*, it could be possible that *vpn* would give rise to the future PG and VG given its positivity to TH.

6.3.5 Localisation of 5-HTRs and DRs: potential implications in synaptic and neuroendocrine functions

This study revealed that certain receptors, such as 5-HTR1A2_{inv}, 5-HTR7, and DR1, colocalise with their respective synthesis enzymes (TPH and TH). However, these same receptors also exhibit clusters or regions that do not show colocalisation, like the other receptors examined. These findings align with the dual role of monoamines, which act both as neurotransmitters and neuromodulators in neuroendocrine systems (Fabbri et al., 2024; Malagoli and Ottaviani, 2017; Seralini and Jungers, 2021).

The anterior cluster of 5-HTR1A2_{inv} colocalised within the TPH area from Gastrula to D-Veliger stages (Figure 6.8). Conversely, 5-HTR7 and TPH colocalised only at D-Veliger stage, exclusively in the two lateral clusters of TPH (Figure 6.9). The remaining clusters/areas of these two 5-HTRs were distant from the site of synthesis, with the ventral-posterior cluster of 5-HTR1A2_{inv} located in the *vpn* area at the D-Veliger stage, and 5-HTR7 within the ciliated epithelium from Gastrula to D-Veliger (Figure 6.13). 5-HTR6-like was localised only within the neuroendocrine tissue from Gastrula to D-Veliger (*apn* at Gastrula and Trochophore, and *vpn* at D-Veliger) (Figure 6.12), whereas 5-HTR4-like localised in the *vpn* and in a non-neuronal area at the D-Veliger stage near AO/CG, suggesting a potential paracrine role for this latter cluster (Figure 6.7).

Regarding DRs, only DR1 exhibited partial colocalization with TH at Trochophore and D-Veliger stages, in contrast to DR3-like, which did not show any colocalisation (Figure 6.10).

At D-Veliger stage, DR2 was localised near the anterior and posterior hinge margins, while DR3-like displayed bilateral and symmetrical clusters within the *an* and *vpn* (Figure 6.7).

In mammals, 5-HTRs type 1A are classified based on their localisation in autoreceptors and heteroreceptors (Altieri et al., 2012). Autoreceptor display a somatodendritic localisation in the serotonin producing neurons, exerting local negative feedback in response to the local release of 5-HT by inhibiting the rate firing (thus reducing 5-HT release), synthesis and turnover (Altieri et al., 2012; Brady et al., 2012; Hoyer, 2019a). The data presented in this study align with those reported in mammals, suggesting that 5-HTR1A2_inv may function as both an autoreceptor and a heteroreceptor. Moreover, in vertebrates, a study showed that 5-HTR7 interacts with 5-HTR1A by forming heterodimers involved in modulation of intracellular signalling (Quintero-Villegas and Valdés-Ferrer, 2022). This could explain the presence of both 5-HTR1A2_inv and 5-HTR7 in the lateral clusters of TPH at 48 hpf. However, distinct from 5-HTR1, so far 5-HTR7 and DR1 have not been identified as autoreceptors in mammals; thus, the results presented here suggest the possibility that this role may be specific to invertebrates. Further studies are needed to confirm this hypothesis, as current data do not provide direct evidence for such a function.

Interestingly, 5-HTR1A2_inv is localised within *vpn* area, where dopaminergic neurons are present, and DR3-like is located within *an*, where there are serotonergic neurons. These data suggest a potential reciprocal control between 5-HT and DA. In vertebrates, 5-HTR1A seems to regulate DA release (Alex and Pehek, 2007). In mammals, DRs belonging to the family of D₂-like receptors (DR2, DR3, and DR4 for humans) are known to regulate serotonergic neurons (Aman et al., 2007; Monti and Jantos, 2008). The DR3-like identified here groups with the human DR2, DR3 and DR4, thus belonging to the family of D₂-like. Therefore, this suggests that 5-HTR1A2_inv and DR3-like could modulate dopaminergic and serotonergic neurons, respectively, similar to what happens in mammals, in a neuroendocrine context.

In conclusion, the localisation of 5-HTRs and DRs throughout development, along with their spatial relationship to the synthesis enzyme, indicates their potential involvement in synaptic and neuroendocrine functions. Furthermore, the localisation of 5-HTR1A2_inv and DR3-like suggests a possible reciprocal regulation between the serotonin and dopamine systems.

6.4 Supplementary Tables

Species	BDAAAH tree	ID NCBI	Domain
<i>Homo sapiens</i>	<i>Hs</i> TPH1	NP_004170.1	Trp_5_monoox
	<i>Hs</i> TPH2	NP_775489.2	Biopterin_H, ACT super family
	<i>Hs</i> TH	NP_000351.2	Biopterin_H, ACT_TH, TOH_N
	<i>Hs</i> PAH	NP_000268.1	Phe4hydrox_tetr
<i>Drosophila melanogaster</i>	<i>Dm</i> TPH	NP_612080.1	Trp_5_monoox
	<i>Dm</i> TH	NP_476897.1	Tyr_3_monoox
	<i>Dm</i> PAH	NP_523963.2	Phe4hydrox_tetr
<i>Mytilus galloprovincialis</i>	<i>Mg</i> TPH	VDI27042.1	Biopterin_H, ACT super family
	<i>Mg</i> TH	VDI80387.1	Biopterin_H, ACT super family
	<i>Mg</i> PAH1	VDI22208.1	arom_aa_hydroxylase family
	<i>Mg</i> PAH2	VDI56986.1	Biopterin_H, ACT super family
<i>Mytilus edulis</i>	<i>Me</i> TPH	CAG2197326.1	Biopterin_H, ACT super family
	<i>Me</i> TH	CAG2223525.1	Biopterin_H, ACT super family
	<i>Me</i> PAH1	CAG2249523.1	arom_aa_hydroxylase family
	<i>Me</i> PAH2	CAG2192858.1	Biopterin_H, ACT super family
<i>Mytilus coruscus</i>	<i>Mc</i> TPH	CAC5389082.1	Biopterin_H, ACT super family
	<i>Mc</i> TH	CAC5425702.1	Biopterin_H, ACT super family
	<i>Mc</i> PAH1	CAC5395754.1	arom_aa_hydroxylase family
	<i>Mc</i> PAH2	CAC5395750.1	Biopterin_H, ACT super family
<i>Pecten maximus</i>	<i>Pm</i> TPH	XP_033740032.1	Trp_5_monoox super family
	<i>Pm</i> TH	XP_033740979.1	Biopterin_H, ACT super family
	<i>Pm</i> PAH1	XP_033740976.1	arom_aa_hydroxylase family
<i>Mizuhopecten yessoensis</i>	<i>My</i> TPH	XP_021359444.1	Biopterin_H, ACT super family
	<i>My</i> TH	XP_021366851.1	Biopterin_H, ACT super family
	<i>My</i> PAH1	XP_021366786.1	arom_aa_hydroxylase family
<i>Crassostrea gigas</i>	<i>Cg</i> TPH	XP_011438860.1	Biopterin_H, ACT super family
	<i>Cg</i> TH	XP_011440999.1	Biopterin_H, ACT super family
	<i>Cg</i> PAH1	XP_011448508.2	Biopterin_H, ACT super family
<i>Crassostrea virginica</i>	<i>Cv</i> TPH	XP_022338844.1	Biopterin_H, ACT super family
	<i>Cv</i> TH	XP_022288025.1	Biopterin_H, ACT super family
	<i>Cv</i> PAH1	XP_022291726.1	Biopterin_H, ACT super family
<i>Vibrio vulnificus</i>	<i>Vv</i> PAH	NP_762419.1	phhA

Supplementary Table 6.1. List of sequences used for orthology assessment of biopterin dependent aromatic amino acids hydroxylase (BDAAAH). The first column reports the complete species name, the second column the abbreviations used in the tree; the third column protein NCBI accession number and the fourth the proteins domain found on NCBI Conserved Domain Database (CDD) are listed. Query sequences from human and fruit fly were retrieved from Siltberg-Liberles et al., 2008; PAH from *V. vulnificus* was used to root the tree as indicated by Candy and Collet, 2005.

Species	AADC tree	ID NCBI	Domain
<i>Homo sapiens</i>	<i>Hs</i> AADC	AAP35655.1	Pyridoxal_deC
	<i>Hs</i> HDC	NP_002103.2	Pyridoxal_deC
	<i>Hs</i> GAD1	NP_000808.2	Pyridoxal_deC
	<i>Hs</i> GAD2	NP_000809.1	Pyridoxal_deC
<i>Drosophila melanogaster</i>	<i>Ds</i> AADC	CAA28022.1	Pyridoxal_deC
	<i>Ds</i> TDC	NP_610226.2	Pyridoxal_deC
	<i>Ds</i> HDC	NP_001260856.1	Pyridoxal_deC
<i>Mytilus galloprovincialis</i>	<i>Mg</i> AADC	VDI21287.1	Pyridoxal_deC
	<i>Mg</i> TDC	VDI46831.1	Pyridoxal_deC
	<i>Mg</i> HDC	VDI74570.1	Pyridoxal_deC
<i>Mytilus edulis</i>	<i>Me</i> AADC	CAG2229905.1	AAT_I_super family
	<i>Me</i> HDC	CAG2237808.1	Pyridoxal_deC
<i>Mytilus coruscus</i>	<i>Mc</i> AADC	CAC5399292.1	Pyridoxal_deC
	<i>Mc</i> HDC	CAC5419651.1	Pyridoxal_deC
<i>Pecten maximus</i>	<i>Pm</i> AADC	XP_033732723.1	Pyridoxal_deC
	<i>Pm</i> TDC	XP_033763259.1	Pyridoxal_deC
	<i>Pm</i> HDC	XP_033726247.1	Pyridoxal_deC + pnk super family
<i>Mizuhopecten yessoensis</i>	<i>My</i> AADC	XP_021349019.1	Pyridoxal_deC
	<i>My</i> TDC	XP_021353126.1	Pyridoxal_deC
	<i>My</i> HDC	XP_021366630.1	Pyridoxal_deC
<i>Crassostrea gigas</i>	<i>Cg</i> AADC	XP_011417382.2	Pyridoxal_deC
	<i>Cg</i> TDC	XP_011449820.2	Pyridoxal_deC
	<i>Cg</i> HDC	XP_034320494.1	Pyridoxal_deC
<i>Crassostrea virginica</i>	<i>Cv</i> AADC	XP_022324359.1	Pyridoxal_deC
	<i>Cv</i> HDC	XP_022307816.1	Pyridoxal_deC

Supplementary Table 6.2. List of sequences used for orthology assessment of aromatic L-amino acid decarboxylase. The table structure is the same as that of Tab. 1. Glutamate Decarboxylases (GADs) were used as an outgroup. Asterisks in the table indicate presence in the protein of an additional domain. Humans and fruit fly reference sequences of AADC were retrieved from Lin et al., 2020 and those of HDC and GAD were retrieved directly from NCBI.

Species	DBH-TBH tree	NCBI ID	Domain
<i>Homo sapiens</i>	<i>Hs</i> DBH	EAW88099.1	Cu2_monoox_C, Cu2_monooxygen, DOMON
	<i>Hs</i> MOXD1	Q6UVY6	Cu2_monoox_C, Cu2_monooxygen, DOMON_DOH
	<i>Hs</i> PAM	P19021	NHL_PAL_like, Cu2_monooxygen, Cu2_monoox_C
<i>Mus musculus</i>	<i>Mm</i> MOXD1	NP_067484.2	Cu2_monoox_C, Cu2_monooxygen, DOMON_DOH
<i>Drosophila melanogaster</i>	<i>Dm</i> TBH	NP_001284996.1	Cu2_monoox_C, Cu2_monooxygen, DOMON
<i>Lymnaea stagnalis</i>	<i>Ls</i> DBH	BAM35937.1	Cu2_monoox_C, Cu2_monooxygen, DOMON_DOH
<i>Litopenaus vannamei</i>	<i>Lv</i> DBH-like	ANA78437.1	Cu2_monoox_C, Cu2_monooxygen, DOMON_DOH
<i>Azumapecten farreri</i>	<i>Af</i> DBH-like	ADP08787.1	Cu2_monoox_C, Cu2_monooxygen, DOMON_DOH
<i>Mytilus galloprovincialis</i>	<i>Mg</i> DBH	VDI40652.1	Cu2_monoox_C, Cu2_monooxygen, DOMON
	<i>Mg</i> DBH-like1	VDI39903.1	Cu2_monoox_C, Cu2_monooxygen, DOMON_DOH
	<i>Mg</i> DBH-like2	VDI67128.1	Cu2_monoox_C, Cu2_monooxygen, DOMON_DOH
	<i>Mg</i> DBH-like3	VDH93561.1	Cu2_monoox_C, Cu2_monooxygen, DOMON_DOH
	<i>Mg</i> DBH-like4	VDI71937.1	Cu2_monoox_C, Cu2_monooxygen, DOMON_DOH
	<i>Mg</i> DBH-like5	VDH89228.1	Cu2_monoox_C, Cu2_monooxygen
	<i>Mg</i> DBH-like6	VDH89227.1	Cu2_monoox_C, Cu2_monooxygen, DOMON_DOH
	<i>Mg</i> DBH-like7	VDH89226.1	Cu2_monoox_C, Cu2_monooxygen, DOMON_DOH
<i>Mytilus edulis</i>	<i>Me</i> DBH	CAG2241177.1	Cu2_monoox_C, Cu2_monooxygen, DoH
	<i>Me</i> DBH-like1	CAG2228505.1	Cu2_monoox_C, DOMON_DOH, Cu2_monooxygen
	<i>Me</i> DBH-like2	CAG2227288.1	Cu2_monoox_C, Cu2_monooxygen, DOMON_DOH
	<i>Me</i> DBH-like3	CAG2243417.1	Cu2_monoox_C, DOMON_DOH, Cu2_monooxygen
	<i>Me</i> DBH-like4	CAG2243415.1	Cu2_monoox_C, DOMON_DOH, Cu2_monooxygen
	<i>Me</i> DBH-like5	CAG2223451.1	Cu2_monooxygen, Cu2_monoox_C super family, DOMON_DOH
	<i>Me</i> DBH-like6	CAG2223452.1	Cu2_monoox_C, Cu2_monooxygen, DOMON_DOH, DOMON_DOH, Cu2_monoox_C super family, Cu2_monooxygen super family
<i>Mytilus coruscus</i>	<i>Mc</i> DBH-like1	CAC5419594.1	Cu2_monoox_C, DOMON_DOH, Cu2_monooxygen
	<i>Mc</i> DBH-like2	CAC5419592.1	Cu2_monoox_C, DOMON_DOH, Cu2_monoox_C super family
	<i>Mc</i> DBH-like4	CAC5384613.1	Cu2_monooxygen, Cu2_monoox_C super family, DOMON_DOH
	<i>Mc</i> DBH-like5	CAC5382674.1	Cu2_monooxygen, Cu2_monoox_C super family
	<i>Mc</i> DBH-like6	CAC5382672.1	Cu2_monoox_C, Cu2_monoox_C, Cu2_monooxygen, Cu2_monooxygen, DOMON_DOH, DOMON_DOH
	<i>Pm</i> DBH	XP_033732438.1	Cu2_monoox_C, Cu2_monooxygen, DOMON_DOH
<i>Pecten maximus</i>	<i>Pm</i> DBH-like1	XP_033727585.1	Cu2_monoox_C, Cu2_monooxygen, DOMON_DOH
	<i>Pm</i> DBH-like2	XP_033732845.1	Cu2_monoox_C, Cu2_monooxygen, DOMON_DOH
	<i>Pm</i> DBH-like3	XP_033727736.1	Cu2_monoox_C, Cu2_monooxygen, DOMON_DOH
	<i>Pm</i> DBH-like4	XP_033727736.1	Cu2_monoox_C, Cu2_monooxygen, DOMON_DOH

<i>Mizuhopecten yessoensis</i>	<i>My</i> DBH	XP_021341155.1	Cu2_monoox_C, Cu2_monooxygen, DOMON_DOH
	<i>My</i> DBH-like	XP_021377609.1	Cu2_monoox_C, Cu2_monooxygen, DOMON_DOH
<i>Crassostrea gigas</i>	<i>Cg</i> DBH	XP_011429599.3	Cu2_monoox_C, Cu2_monooxygen, DOMON_DOH
	<i>Cg</i> DBH-like1	XP_034303478.1	Cu2_monooxygen, Cu2_monooxygen, Cu2_monoox_C, Cu2_monoox_C super family, DOMON_DOH, DOMON_DOH
	<i>Cg</i> DBH-like2	XP_034303477.1	Cu2_monooxygen, Cu2_monooxygen, Cu2_monoox_C, Cu2_monoox_C super family, DOMON_DOH, DOMON_DOH
<i>Crassostrea virginica</i>	<i>Cv</i> DBH	XP_022328150.1	Cu2_monoox_C, Cu2_monooxygen, DOMON_DOH
	<i>Cv</i> DBH-like1	XP_022324691.1	Cu2_monooxygen, Cu2_monooxygen, Cu2_monoox_C, Cu2_monoox_C super family, DOMON_DOH, DOMON_DOH
	<i>Cv</i> DBH-like2	XP_022320601.1	Cu2_monooxygen, Cu2_monoox_C super family, DOMON_DOH, DOMON_DOH

Supplementary Table 6.3. List of sequences used for orthology assessment of copper containing hydroxylase. Humans, murine and fruit fly reference sequences of DBH/TBH were retrieved from Xu et al., 2018 & 2016. Other reference sequences from other invertebrates species (gastropod, crustacean and bivalve) were retrieved from different publication (Cheng et al., 2016; Sadamoto et al., 2012). Peptidylglycine alpha-hydroxylating monooxygenase (PAM) was used as outgroup and the sequence was retrieved on NCBI.

Species	MAO tree	NCBI ID	Domain
<i>Homo sapiens</i>	<i>Hs</i> MAO-A	NP_000231.1	YobN
	<i>Hs</i> MAO-B	NP_000889.3	YobN
	<i>Hs</i> SMOX	NP_787033.1	PLN02568 super family
<i>Mus musculus</i>	<i>Mm</i> SMOX	NP_663508.1	PLN02568 super family
<i>Mytilus galloprovincialis</i>	<i>Mg</i> MAO1	VDI35724.1	galactose_mutarotase_like, YobN
	<i>Mg</i> MAO2	VDI72060.1	YobN
<i>Mytilus edulis</i>	<i>Me</i> MAO1	CAG2225782.1	YobN
	<i>Me</i> MAO2	CAG2201179.1	YobN
<i>Mytilus coruscus</i>	<i>Mc</i> MAO	CAC5413206	YobN
<i>Pecten maximus</i>	<i>Pc</i> MAO	XP_033759977.1	YobN
<i>Mizuhopecten yessoensis</i>	<i>My</i> MAO1	XP_021339456.1	YobN
	<i>My</i> MAO2	XP_021339606.1	YobN
<i>Crassostrea gigas</i>	<i>Cg</i> MAO1	NP_001292240.1	YobN
	<i>Cg</i> MAO2	XP_034329734.1	YobN
<i>Crassostrea virginica</i>	<i>Cv</i> MOA	XP_022288515.1	YobN

Supplementary Table 6.4. List of sequences used for orthology assessment of monoamine oxidases (MAOs). Humans MAOs were used as reference sequences retrieved from Wilson et al., 2020 (here the updated sequences of the human MAOs were used, sequences were found through BLASTP in NCBI using the sequences reported in the previous cited paper as query).. Human and murine Spermine Oxidase (SMOX) were used as outgroup retrieved from Salvi and Tavladoraki, 2020 (human sequence was retrieved from NCBI though BLASTP using murine SMOX as query).

Species	MAOs alignment	ID NCBI
<i>Homo sapiens</i>	<i>Hs</i> MAO-A	NP_000231.1
	<i>Hs</i> MAO-B	NP_000889.3
<i>Mus musculus</i>	<i>Mm</i> MAO-A	NP_776101.3
	<i>Mm</i> MAO-B	NP_766366.2
<i>Mytilus galloprovincialis</i>	<i>Mg</i> MAO-A like	VDI35724.1
	<i>Mg</i> MAO-B	VDI72060.1
<i>Mytilus edulis</i>	<i>Me</i> MAO-like 1	CAG2225782.1
	<i>Me</i> MAO-like 2	CAG2201179.1
<i>Mytilus coruscus</i>	<i>Mc</i> MAO-A like	CAC5413206.1
<i>Pecten maximus</i>	<i>Pm</i> MAO-A	XP_033759977.1
<i>Mizuhopecten yessoensis</i>	<i>My</i> MAO-A 1	XP_021339456.1
	<i>My</i> MAO-A 2	XP_021339606.1
<i>Crassostrea gigas</i>	<i>Cg</i> MAO-A 1	NP_001292240.1
	<i>Cg</i> MAO-A 2	XP_034329734.1
<i>Crassostrea virginica</i>	<i>Cv</i> MAO-A	XP_022288515.1

Supplementary Table 6.5. MAOs sequences classification based on presence/absence of conserved amino acids in their sequences. In case of similar amino acid, sequences were named *MAO-A/B like*, in case of non-conserved amino acids sequences were named *MAO-like*.

Species	VMAT tree	NCBI ID	Domain
<i>Homo sapiens</i>	<i>Hs</i> VMAT1	NP_001129163.1	MFS_SLC18A1_2_VAT1_2
	<i>Hs</i> VMAT2	NP_003045.2	MFS_SLC18A1_2_VAT1_2
	<i>Hs</i> VChT	NP_003046.2	MFS_SLC18A3_VChT
<i>Drosophila melanogaster</i>	<i>Dm</i> VMAT	AAX52708.1	MFS_SLC18A1_2_VAT1_2
	<i>Dm</i> VChT	AAF55587.2	MFS_SLC18A3_VChT
	<i>Dm</i> portabella	AAF56164.2	MFS_SLC18A1_2_VAT1_2
<i>Mytilus galloprovincialis</i>	<i>Mg</i> VMAT	VDI69536.1	MFS super family
	<i>Mg</i> VChT	VDI82944.1	MFS super family
<i>Mytilus edulis</i>	<i>Me</i> VMAT	CAG2199852.1	MFS_SLC18A1_2_VAT1_2
<i>Mytilus coruscus</i>	<i>Mc</i> VMAT	CAC5411616.1	MFS_SLC18A1_2_VAT1_2
<i>Pecten maximus</i>	<i>Pc</i> VMAT	XP_033756792.1	MFS_SLC18A1_2_VAT1_2
<i>Mizuhopecten yessoensis</i>	<i>My</i> VMAT	XP_021371911.1	MFS_SLC18A1_2_VAT1_2
<i>Crassostrea gigas</i>	<i>Cg</i> VMAT	XP_011418922.1	MFS_SLC18A1_2_VAT1_2
<i>Crassostrea virginica</i>	<i>Cv</i> VMAT	XP_022338792.1	MFS_SLC18A1_2_VAT1_2
<i>Apis mellifera</i>	<i>Am</i> portabella	XP_001122029.1	MFS super family

Supplementary Table 6.6. List of sequences used for orthology assessment of VMATs. The table structure is the same of Tab. 1. Humans and fruit fly VMATs were used as reference proteins; Portabella transporters were used as outgroup. Reference sequences were retrieved from Lawal and Krantz, 2013.

Species	SLC6A tree	ID NCBI	Domain
<i>Homo sapiens</i>	<i>Hs</i> SERT	NP_001036.1	SLC6sbd_SERT,5HT_transport_N
	<i>Hs</i> DAT	NP_001035.1	SLC6sbd_DAT1
	<i>Hs</i> NET	NP_001034.1	SLC6sbd_NET
<i>Drosophila melanogaster</i>	<i>Dm</i> SERT	NP_001369117.1	SLC6sbd_SERT-like
	<i>Dm</i> DAT	NP_001261026.1	SLC6sbd_SERT-like_u1
<i>Lumbricus terrestris</i>	<i>Lt</i> OAT	ABG91820.1	SLC6sbd_SERT-like
<i>Mytilus galloprovincialis</i>	<i>Mg</i> SERT1	VDI80712.1	SLC5-6 like_sbd super family
	<i>Mg</i> SERT2	VDI80716.1	SLC5-6 like_sbd super family, CLET, CLET super family
	<i>Mg</i> OAT	VDI21627.1	SLC5-6 like_sbd super family
	<i>Mg</i> DAT	VDI13252.1	SLC5-6 like_sbd super family
<i>Mytilus edulis</i>	<i>Me</i> SERT1	CAG2225029.1	SLC5-6 like_sbd super family
	<i>Me</i> SERT2	CAG2225028.1	SLC5-6 like_sbd super family, CLET
	<i>Me</i> OAT	CAG2238301.1	SLC5-6 like_sbd super family
	<i>Me</i> DAT	CAG2231692.1	SLC5-6 like_sbd super family
<i>Mytilus coruscus</i>	<i>Mc</i> SERT1	CAC5404890.1	SLC5-6 like_sbd super family
	<i>Mc</i> SERT2	CAC5404892.1	SLC6sbd_SERT-like
	<i>Mc</i> OAT	CAC5357485.1	SLC5-6 like_sbd super family
	<i>Mc</i> DAT	CAC5415933.1	SLC5-6 like_sbd super family
<i>Pecten maximus</i>	<i>Pc</i> SERT1	XP_033748230.1	SLC5-6 like_sbd super family
	<i>Pc</i> SERT2	XP_033747389.1	SLC6sbd_SERT-like
	<i>Pc</i> OAT	XP_033754663.1	SLC5-6 like_sbd super family
	<i>Pc</i> DAT	XP_033747446.1	SLC5-6 like_sbd super family
<i>Mizuhopecten yessoensis</i>	<i>My</i> SERT1	XP_021349756.1	SLC5-6 like_sbd super family
	<i>My</i> SERT2	XP_021340900.1	SLC5-6 like_sbd super family
	<i>My</i> OAT	XP_021352717.1	SLC5-6 like_sbd super family
	<i>My</i> DAT	XP_021374721.1	SLC5-6 like_sbd super family
<i>Crassostrea gigas</i>	<i>Cg</i> SERT1	XP_011448899.1	SLC5-6 like_sbd super family
	<i>Cg</i> SERT2	XP_034298933.1	SLC6sbd_SERT-like
	<i>Cg</i> OAT	XP_034317982.1	SLC5-6 like_sbd super family
	<i>Cg</i> DAT	XP_034337145.1	SLC5-6 like_sbd super family
<i>Crassostrea virginica</i>	<i>Cv</i> SERT1	XP_022339634.1	SLC5-6 like_sbd super family
	<i>Cv</i> SERT2	XP_022335714.1	SLC5-6 like_sbd super family, CLET, CLET super family
	<i>Cv</i> DAT	XP_022342062.1	SLC5-6 like_sbd super family
<i>Symbiobacterium thermophilum</i>	<i>St</i> TnaT	WP_011194576.1	SLC6sbd_u1
<i>Aquifex aeolicus</i>	<i>Aa</i> LeuT	WP_010881359.1	LeuT-like_sbd
<i>Fusobacterium nucleatum</i>	<i>Fn</i> Tyl1	WP_011015963.1	SLC6sbd_Tyl1-Like

Supplementary Table 6.7. List of sequences used for orthology assessment of SLC6 transporters. Bacterial transporters were used as outgroup and reference sequences of human, fruit fly and earthworm (no OAT has been detected in fruit fly) were retrieved from Camicia et al., 2022.

Species	5-HTRs tree	NCBI ID	Domain
<i>Homo sapiens</i>	<i>Hs</i> 5-HTR1A	P08908	7tmA_5-HT1A_vertibrates
	<i>Hs</i> 5-HTR2	P28223	7tmA_5-HT2A
	<i>Hs</i> 5-HTR4	Q13639	7tmA_5-HT4
	<i>Hs</i> 5-HTR5	P47898.1	7tmA_5-HT5
	<i>Hs</i> 5-HTR6	P50406.1	7tmA_5-HT6
	<i>Hs</i> 5-HTR7	P34969	7tmA_5-HT7
	<i>Hs</i> RhodR	AAC31763	7tmA_MWS_opsin, Rhodopsin_N
<i>Drosophila melanogaster</i>	<i>Dm</i> 5-HTR1A1_inv	P28286	7tmA_5-HT1A_invertebrates, 7tm_GPCRs super family
	<i>Dm</i> 5-HTR1A2	P28285	7tmA_5-HT1A_invertebrates, 7tm_GPCRs super family
	<i>Dm</i> 5-HTR2	NP_001262373.1	7tmA_5-HT2_insect-like, 7tm_GPCRs super family
	<i>Dm</i> 5-HTR7	P20905	7tmA_5-HT7
	<i>Dm</i> FMRFaR	Q9VZW5	7tmA_FMRFamide_R-like
<i>Mytilus galloprovincialis</i>	<i>Mg</i> 5-HTR1A1_inv	VDI18290.1	7tmA_5-HT1A_invertebrates
	<i>Mg</i> 5-HTR1A2_inv	VDI79810.1	7tmA_5-HT1A_invertebrates
	<i>Mg</i> 5-HTR2	VDI68244.1	7tmA_5-HT2
	<i>Mg</i> 5-HTR4-like	VDI23809.1	7tm_GPCRs super family
	<i>Mg</i> 5-HTR6-like	VDI08258.1	7tm_GPCRs super family
	<i>Mg</i> 5-HTR7	VDI03255.1	7tmA_5-HT7
<i>Mytilus edulis</i>	<i>Me</i> 5-HTR1A1_inv	CAG2244063.1	7tmA_5-HT1A_invertebrates
	<i>Me</i> 5-HTR1A2_inv	CAG2184416.1	7tmA_5-HT1A_invertebrates
	<i>Me</i> 5-HTR2	CAG2241697.1	7tmA_5-HT2
	<i>Me</i> 5-HTR4-like	CAG2236894.1	7tm_GPCRs super family
	<i>Me</i> 5-HTR6-like	CAG2227698.1	7tm_GPCRs super family
<i>Mytilus coruscus</i>	<i>Mc</i> 5-HTR1A1_inv	CAC5401894.1	7tmA_5-HT1A_invertebrates
	<i>Mc</i> 5-HTR1A2_inv	CAC5414895.1	7tmA_5-HT1A_invertebrates
	<i>Mc</i> 5-HTR2	CAC5372018.1	7tmA_5-HT2
	<i>Mc</i> 5-HTR4-like	CAC5420242.1	7tm_GPCRs super family
	<i>Mc</i> 5-HTR6-like	CAC5407614.1	7tm_GPCRs super family
	<i>Mc</i> 5-HTR7	CAC5361060.1	7tmA_5-HT7
<i>Pecten maximus</i>	<i>Pc</i> 5-HTR1A1_inv	XP_033761462.1	7tmA_5-HT1A_invertebrates
	<i>Pc</i> 5-HTR1A2_inv	XP_033762204.1	7tmA_5-HT1A_invertebrates
	<i>Pc</i> 5-HTR2	XP_033761220.1	7tm_GPCRs super family, 7tm_GPCRs super family
	<i>Pc</i> 5-HTR4-like	XP_033756774.1	7tm_GPCRs super family
	<i>Pc</i> 5-HTR6-like	XP_033763972.1	7tm_GPCRs super family
	<i>Pc</i> 5-HTR7	XP_033756397.1	7tmA_5-HT7
<i>Mizuhopecten yessoensis</i>	<i>My</i> 5-HTR1A1_inv	XP_021376348.1	7tmA_5-HT1A_invertebrates
	<i>My</i> 5-HTR1A2_inv	XP_021373779.1	7tmA_5-HT1A_invertebrates
	<i>My</i> 5-HTR2	XP_021356297.1	7tm_GPCRs super family
	<i>My</i> 5-HTR4-like	XP_021369092.1	7tm_GPCRs super family
	<i>My</i> 5-HTR6-like	XP_021369720.1	7tm_GPCRs super family
	<i>My</i> 5-HTR7	XP_021371611.1	7tmA_5-HT7
<i>Crassostrea gigas</i>	<i>Cg</i> 5-HTR1A1_inv	XP_011455576.1	7tmA_5-HT1A_invertebrates
	<i>Cg</i> 5-HTR1A2_inv	XP_011450089.1	7tmA_5-HT1A_invertebrates

	<i>Cg</i> 5-HTR2	XP_011430856.2	7tmA_5-HT2
	<i>Cg</i> 5-HTR4	XP_011430667.2	7tmA_5-HT4
	<i>Cg</i> 5-HTR6-like	XP_011444450.2	7tm_GPCRs super family
	<i>Cg</i> 5-HTR7	XP_011451539.2	7tmA_5-HT7
<i>Crassostrea virginica</i>	<i>Cv</i> 5-HTR1A1_inv	XP_022307411.1	7tmA_5-HT1A_invertebrates
	<i>Cv</i> 5-HTR1A2_inv	XP_022308516.1	7tmA_5-HT1A_invertebrates
	<i>Cv</i> 5-HTR2	XP_022343922.1	7tmA_5-HT2
	<i>Cv</i> 5-HTR4	XP_022341057.1	7tmA_5-HT4
	<i>Cv</i> 5-HTR6-like	XP_022344621.1	7tm_GPCRs super family
	<i>Cv</i> 5-HTR7	XP_022288073.1	7tmA_5-HT7

Supplementary Table 6.8. List of sequences used for orthology assessment of 5-HTRs. Reference sequences of human, fruit fly and outgroup were retrieved from Canesi et al. (2022); the other 5-HTRs protein sequences were retrieved from NCBI. Sequences presenting a nonspecific hit domain were called *5-HTRx-like*.

Species	DRs tree	NCBI ID	Domain
<i>Homo sapiens</i>	<i>Hs</i> DR1	NP_000785.1	7tmA_D1A_dopamine_R
	<i>Hs</i> DR2	NP_000786.1	7tmA_D2_dopamine_R
	<i>Hs</i> DR3	NP_000787.2	7tmA_D3_dopamine_R
	<i>Hs</i> DR4	NP_000788.2	7tmA_D4_dopamine_R
	<i>Hs</i> DR5	NP_000789.1	7tm_GPCRs super family
<i>Drosophila melanogaster</i>	<i>Dm</i> DR1	CAA54451.1	7tmA_Ap5-HTB1-like
	<i>Dm</i> DR2/INDR	AAC47161.1	7tmA_Dop1R2-like
	<i>Dm</i> DR3	AAN15955.1	7tmA_D2-like_dopamine_R, 7tm_GPCRs super family
	<i>Dm</i> GluR	AHN58219.1	Periplasmic_Binding_Protein_type1 super family
<i>Mytilus galloprovincialis</i>	<i>Mg</i> DR1	VDI52979.1	7tmA_Ap5-HTB1-like
	<i>Mg</i> DR2/INDR	VDI46294.1	7tmA_Dop1R2-like
	<i>Mg</i> DR3	VDI63946.1	7tm_GPCRs super family, 7tm_GPCRs super family*
<i>Mytilus edulis</i>	<i>Me</i> DR1	CAG2208947.1	7tmA_Ap5-HTB1-like
	<i>Me</i> DR2/INDR	CAG2191779.1	7tmA_Dop1R2-like
	<i>Me</i> DR3	CAG2199322.1	7tm_GPCRs super family, 7tm_GPCRs super family*
<i>Mytilus coruscus</i>	<i>Mc</i> DR2/INDR	CAC5395991.1	7tmA_Dop1R2-like
	<i>Mc</i> DR3	CAC5377743.1	7tm_GPCRs super family, 7tm_GPCRs super family*
<i>Pecten maximus</i>	<i>Pm</i> DR1	XP_033756542.1	7tmA_Ap5-HTB1-like
	<i>Pm</i> DR2/INDR	XP_033757324.1	7tmA_Dop1R2-like
	<i>Pm</i> DR3	XP_033758528.1	7tm_GPCRs super family, 7tm_GPCRs super family*
<i>Mizuhopecten yessoensis</i>	<i>My</i> DR1	XP_021361185.1	7tmA_Ap5-HTB1-like
	<i>My</i> DR2/INDR	XP_021340507.1	7tmA_Dop1R2-like
	<i>My</i> DR3	XP_021359917.1	7tm_GPCRs super family, 7tm_GPCRs super family*
<i>Crassostrea gigas</i>	<i>Cg</i> DR1	EKC33807.1	7tmA_Ap5-HTB1-like
	<i>Cg</i> DR2/INDR	XP_011448304.1	7tmA_Dop1R2-like
	<i>Cg</i> DR3	XP_034304151.1	7tmA_D2-like_dopamine_R
<i>Crassostrea virginica</i>	<i>Cv</i> DR1	XP_022341991.1	7tmA_Ap5-HTB1-like
	<i>Cv</i> DR2/INDR	XP_022345762.1	7tmA_Dop1R2-like
	<i>Cv</i> DR3	XP_022326371.1	7tmA_D2-like_dopamine_R

Supplementary Table 6.9. List of sequences used for orthology assessment of DRs. Reference sequences of human, fruit fly and outgroup were retrieved from (Schwartz et al., 2021). Asterisks in the table indicate the absence of the specific domain (i.e.: 7tm_GPCRs super family) or the presence in the protein of an additional domain. Sequences presenting a nonspecific hit domain were called DRx-like.

Species	ARs-OARs-TARs tree	NCBI ID	Domain
<i>Homo sapiens</i>	Hs α 1A-AR	P35348	7tmA_alpha1A_AR
	Hs α 1B-AR	P35368	7tmA_alpha1B_AR
	Hs α 1D-AR	P25100	7tmA_alpha1D_AR
	Hs α 2A-AR	P08913	7tmA_alpha2A_AR, PHA03307 super family
	Hs α 2B-AR	P18089	7tmA_alpha2B_AR
	Hs α 2C-AR	P18825	7tmA_alpha2C_AR
	Hs 5-HTR1A	P08908	7tmA_5-HT1A_vertebrates
<i>Drosophila melanogaster</i>	Dm α -OAR	AAC17442.1	7tmA_Octopamine_R
	Dm β -OAR	Q4LBB9.2	7tmA_DmOct-betaAR-like
	Dm TAR1	BAB71788.1	7tmA_tyramine_octopamine_R-like, 7tm_GPCRs super family
<i>Platynereis dumerilii</i>	Pd α 1-AR	APC23842.1	7tm_GPCRs super family
	Pd α 2-AR	APC23843.1	7tmA_alpha2_AR, 7tm_GPCRs super family
<i>Mytilus galloprovincialis</i>	Mg α 1-AR	VDI56181.1	7tm_GPCRs super family
	Mg α 2-AR	VDI47615.1	7tmA_alpha2_AR
	Mg α -OAR	VDI46334.1	7tmA_octopamine_R
	Mg β -OAR	VDH94544.1	7tmA_DmOct-betaAR-like
	Mg TAR1	VDI38207.1	7tm_GPCRs super family
<i>Mytilus edulis</i>	Me α 2-AR	CAG2200960.1	7tm_GPCRs superfamily
	Me α -OAR	CAG2213059.1	7tmA_Octopamine_R
	Me β -OAR	CAG2243062.1	7tmA_DmOct-betaAR-like
	Me TAR1	CAG2256422.1	7tm_GPCRs superfamily
<i>Mytilus coruscus</i>	Mc α 1-AR	CAC5425975.1	7tm_GPCRs superfamily
	Mc α 2-AR	CAC5360115.1	7tm_GPCRs superfamily
	Mc α -OAR	CAC5418640.1	7tmA_Octopamine_R
	Mc TAR1	CAC5376693.1	7tm_GPCRs superfamily
<i>Pecten maximus</i>	Pc α 1-AR	XP_033757493.1	7tm_GPCRs superfamily
	Pc α 2-AR	XP_033757424.1	7tm_GPCRs superfamily, Stathmin super family
	Pc α -OAR	XP_033757191.1	7tmA_Octopamine_R
	Pc β -OAR	XP_033757386.1	7tmA_DmOct-betaAR-like
	Pc TAR1	XP_033757501.1	7tm_GPCRs superfamily
<i>Mizuhopecten yessoensis</i>	My α 1-AR	XP_021358894.1	7tm_GPCRs superfamily
	My α 2-AR	XP_021369427.1	7tmA_alpha2_AR
	My α -OAR	XP_021355583.1	7tmA_Octopamine_R
	My β -OAR	XP_021378407.1	7tmA_DmOct-betaAR-like
	My TAR1	XP_021350693.1	7tm_GPCRs superfamily
<i>Crassostrea gigas</i>	Cg α 1-AR	XP_019921211.1	7tm_GPCRs superfamily

	Cg α 2-AR	XP_01143377 5.2	7tmA_alpha2_AR
	Cg TAR1	XP_01145130 9.2	7tmA_tyramine_octopamine_R-like
<i>Crassostrea virginica</i>	Cv α 1-AR	XP_02233857 9.1	7tmA_amine_R-like
	Cv α 2-AR	XP_02233549 6.1	7tmA_alpha2_AR, 235kDa-fam super family
	Cv β -OAR	XP_02228628 4.1	7tmA_DmOct-betaAR-like
	Cv TAR1	XP_02228637 2.1	7tmA_tyramine_octopamine_R-like

Supplementary Table 6.10. List of sequences used for orthology assessment of noradrenaline, tyramine and octopamine receptors. Reference sequences of human, fruit fly and clam worm and outgroup (*Hs* 5-HTR1A) were retrieved from Bauknecht and Jékely, 2017.

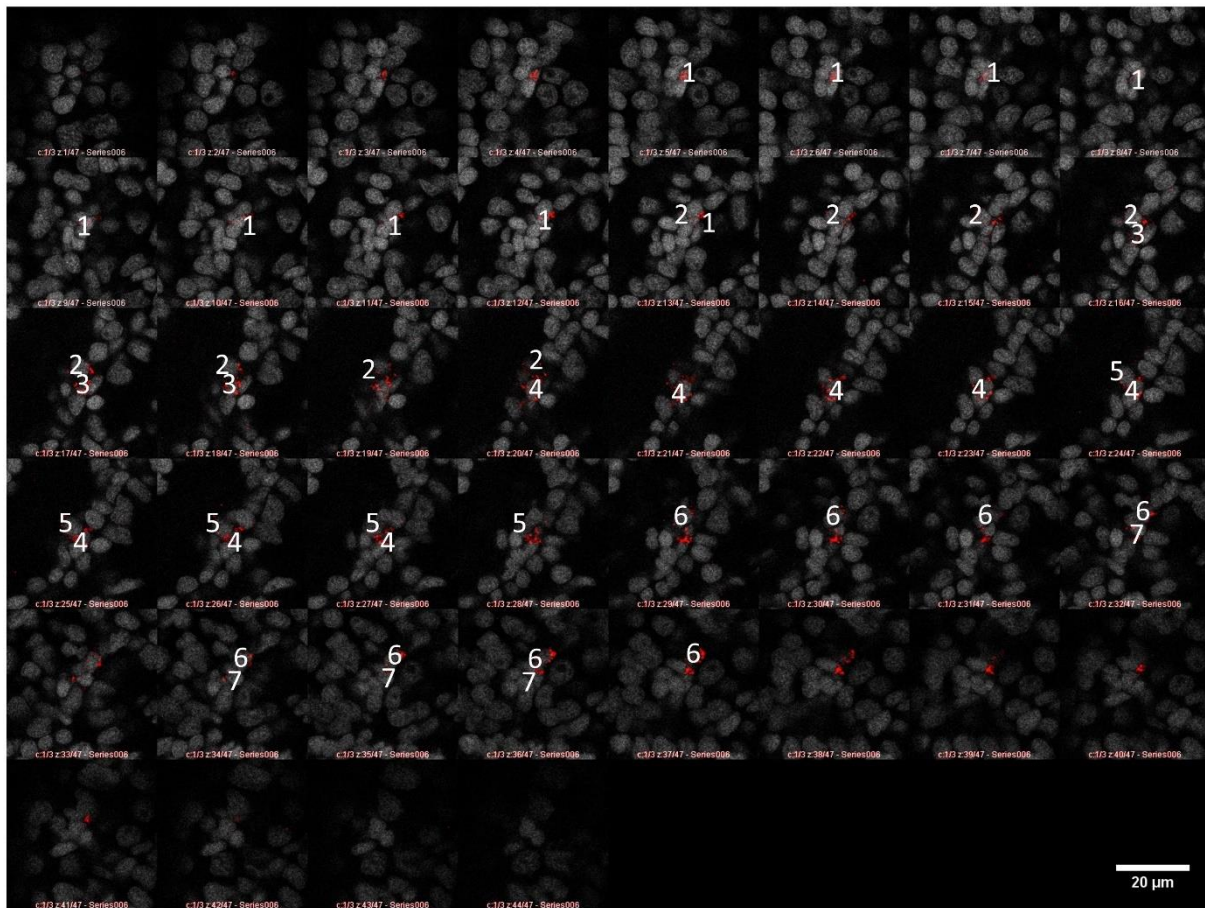
Species	Tree HRs	ID NCBI	Domain
<i>Homo sapiens</i>	<i>Hs</i> HSR1	NP_001091683.1	7tmA_Histamine_H1R
	<i>Hs</i> HSR2	P25021	7tmA_Histamine_H2R
	<i>Hs</i> HSR3	XP_005260323.1	7tmA_Histamine_H3R
	<i>Hs</i> HSR4	NP_067637.2	7tmA_Histamine_H4R
	<i>Hs</i> 5-HTR1A	P08908.3	7tmA_5-HT1A Vertebrates
<i>Rattus norvegicus</i>	<i>Rn</i> HSR1	P31390.1	7tmA_Histamine_H1R
	<i>Rn</i> HSR2	P25102.1	7tmA_Histamine_H2R
	<i>Rn</i> HSR3	NP_445958.1	7tmA_Histamine_H3R
	<i>Rn</i> HSR4	NP_571984.2	7tm_GPCRs super family
<i>Saccoglossus kowalevskii</i>	<i>Sk</i> HSR1a	XP_002734542.1	7tm_GPCRs super family, 7tm_GPCRs super family
	<i>Sk</i> HSR2a	XP_006815469.1	7tm_GPCRs super family
	<i>Sk</i> HSR2c	XP_006822831.1	7tm_GPCRs super family
	<i>Sk</i> HSR2b	XP_002734602.2	7tm_GPCRs super family
	<i>Sk</i> HSR2d	XP_006821795.1	7tm_GPCRs super family
	<i>Sk</i> HSR3a	XP_006813134.1	7tm_GPCRs super family
	<i>Sk</i> HSR3c	XP_002736401.1	7tm_GPCRs super family
	<i>Sk</i> HSR3b	XP_002736922.1	7tmA_Histamine_H3R_H4R
<i>Mytilus galloprovincialis</i>	<i>Mg</i> HSR1	VDI72281.1	7tm_GPCRs super family, 7tm_GPCRs super family
	<i>Mg</i> HSR3a	VDI51385.1	7tm_GPCRs super family
	<i>Mg</i> HSR3b	VDH98688.1	7tm_GPCRs super family
	<i>Mg</i> HSR3c	VDI68841.1	7tm_GPCRs super family
<i>Mytilus edulis</i>	<i>Me</i> HSR1	CAG2218007.1	7tm_GPCRs super family, 7tm_GPCRs super family
	<i>Me</i> HSR3a	CAG2199989.1	7tm_GPCRs super family, Herpes_BLLF1 super family
	<i>Me</i> HSR3b	CAG2194047.1	7tm_GPCRs super family
	<i>Me</i> HSR3c	CAG2219105.1	7tm_GPCRs super family
	<i>Me</i> HSR3d	CAG2217793.1	7tm_GPCRs super family
	<i>Me</i> HSR3e	CAG2248932.1	7tm_GPCRs super family
<i>Mytilus coruscus</i>	<i>Mc</i> HSR1	CAC5407822.1	7tm_GPCRs super family, 7tm_GPCRs super family
	<i>Mc</i> HSR3a	CAC5381873.1	7tm_GPCRs super family
	<i>Mc</i> HSR3b	CAC5408573.1	7tm_GPCRs super family
	<i>Mc</i> HSR3c	CAC5414181.1	7tm_GPCRs super family
	<i>Mc</i> HSR3d	CAC5403000.1	7tm_GPCRs super family
<i>Pecten maximus</i>	<i>Pm</i> HSR1	XP_033745642.1	7tm_GPCRs super family, 7tm_GPCRs super family
	<i>Pm</i> HSR3	XP_033742805.1	7tm_GPCRs super family
<i>Myzohopecten yessoensis</i>	<i>My</i> HSR1	XP_021351022.1	7tm_GPCRs super family, 7tm_GPCRs super family
	<i>My</i> HSR3	OWF39279.1	7tm_GPCRs super family
<i>Crassostrea gigas</i>	<i>Cg</i> HSR1	XP_034307059.1	7tm_GPCRs super family, 7tm_GPCRs super family
	<i>Cg</i> HSR3a	XP_034300264.1	7tmA_Histamine_H3R_H4R
	<i>Cg</i> HSR3b	XP_034300265.1	7tmA_Histamine_H3R_H4R
	<i>Cg</i> HSR3c	XP_011445390.3	7tmA_Histamine_H3R_H4R
	<i>Cg</i> HSR3d	XP_034300263.1	7tmA_Histamine_H3R_H4R
<i>Crassostrea virginica</i>	<i>Cv</i> HSR1	XP_022301907.1	7tm_GPCRs super family, 7tm_GPCRs super family
	<i>Cv</i> HSR3a	XP_022319992.1	7tmA_Histamine_H3R_H4R
	<i>Cv</i> HSR3b	XP_022328449.1	7tmA_Histamine_H3R_H4R

Supplementary Table 6.11. List of sequences used for orthology assessment of histamine receptors (HSRs). Reference sequences of human, rat and *S. kowalevskii* (no evidence of histamine receptors in fruit fly) were retrieved from Ravhe et al., 2021. Given the fact that HSRs are GPCRs, human 5-HTR1A was used as outgroup.

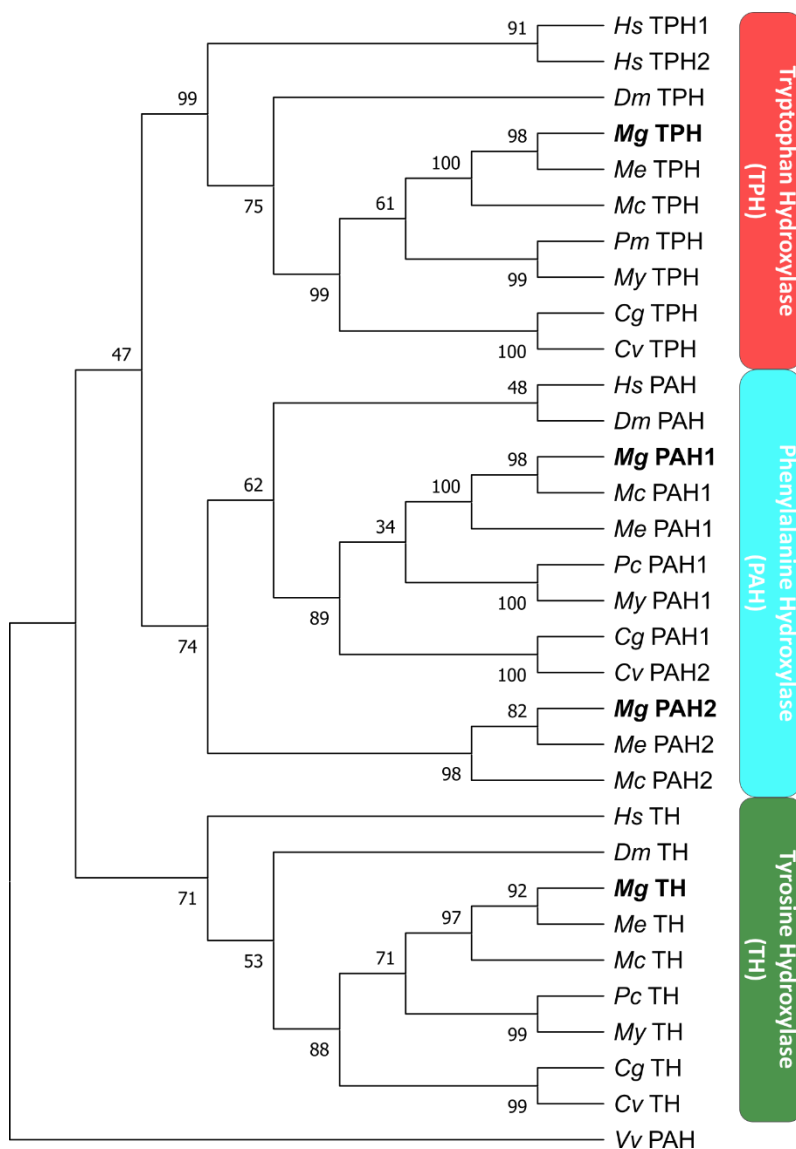
Gene	0	4	8	12	16	20	24	28	32	36	40	44	48
TPH	0.31	0.1	0.31	16.41	44.17	25.6	15.19	10.25	9.45	8.15	7.58	10.23	9.97
AADC	9.73	5.07	3.49	7.44	6.47	4.84	5.26	4.35	4.12	4.73	4.74	4.42	4.76
SERT1-like	0	0	0	0.13	0	0	0	0	0.05	0.08	0.07	0.59	2.09
SERT2-like	0.14	0	0.5	0.27	0.74	2.86	7.74	6.57	4.97	4.87	3.2	2.76	3.62
5-HTR1A1_inv	1.52	0.72	0.9	0.82	0.61	0.82	0.92	1.88	1.22	1.52	2.17	3.08	4
5-HTR1A2_inv	0.29	0.22	3.11	8	2.65	1.29	2.84	2.36	2.98	2.55	2.33	3.86	3.4
5-HTR2	0	0.19	0.28	0.97	1.17	1.9	4.2	4.07	2.9	3.45	3.1	2.3	1.91
5-HTR4-like	0.07	0.06	0.14	0.19	0.21	0.35	0.67	1.3	1.34	1.16	1.32	1.03	1.19
5-HTR6-like	0	0.11	0.57	1.92	6	7.18	7.06	4.47	4.78	5.37	7.27	10.49	11.46
5-HTR7	0.12	0.33	0.22	1.73	2.64	4.34	2.96	2.48	2.14	2.35	1.67	3.65	2.98
TH	0	0	0	1.12	0.63	0.33	0.33	2.54	11.57	17.68	19.65	26.07	27.4
DAT-like	0.21	0.31	0.04	1.22	4.28	10.98	6.39	3.48	5.13	7.99	11.25	10.23	11.78
DR1	0	0	0.76	0.39	0.65	3.19	6.27	9.89	10.34	12.03	11.03	10.93	12.5
DR2	0.01	0.04	0.86	3.42	5.89	6.27	6.44	7.02	7.9	7.49	7.31	9.45	8.98
DR3	0.41	0.74	5.11	3.44	1.43	1.48	1.68	2.43	1.99	1.67	1.49	1.87	2.02
DBH	0.29	0.4	0.17	0.77	0.42	0.37	0.81	0.63	0.85	0	0.7	0.58	0.34
α 1-AR-like	0	0	0	0	0	0	0	0	0	0	0	0.15	0.08
α 2-AR	0	0	0	0	0	0	0.06	0	0.08	0.14	0.1	0.14	0.23
α -OAR	0	0	0	0	0	0	0	0	0	0.03	0	0	0.16
β -OAR	0.12	0	0.21	0.07	0.57	0	0.51	0.78	0.52	1.55	2.17	2.4	3.08
OAT	0	0	0.16	0.22	0.86	0.31	0	0.14	0	0.17	0.07	0.15	0
TyrDC	0.25	0.28	2.16	3.98	3.76	4.59	5.38	4.07	2.42	2.45	2.93	3.85	4.15
TymR1	0	0	3.92	6.31	4.81	2.85	1.08	0.75	0.33	0.14	0.5	0.36	0.6
HDC	0	0	2.62	1.48	0.46	0.23	0.14	0.23	0.18	0.41	0.38	0.43	0.64
HR1-like	0.08	0.09	0	0.22	0.68	0.56	0.27	0.09	0.13	0.1	0.16	0.18	0.2
HR3a-like	0	0.1	0.29	0.13	0.11	0.11	0	0.12	0.06	0.1	0.29	0.13	0.45
HR3b-like	0	0.12	2.27	1.59	0	1.68	2.77	1.84	1.91	1.5	2.04	1.93	1.62
HR3c-like	0	0.36	0.14	0	0.18	0.14	0	0.27	0.35	0.33	0.36	0.37	0.43
MAO-A-like	2.44	1.67	1.19	0.82	1.09	4.61	7.9	15.07	22.48	27.82	41.54	26.53	29.21
MAO-B	1.28	0.58	1.14	0.45	0.39	0.43	1.12	0.81	0.62	0.84	0.87	0.93	1.18
VMAT	0	0.4	0.35	0.86	0.62	1.65	1.27	3.56	4.25	3.7	2.92	4.34	4.22
DHB1-like	0	0	0	0	0	0	0.02	0	0.03	0.11	0.2	0.12	0.24
DHB2-like	0	0	0.03	0.02	0	0	0.03	0	0.09	0.09	0.29	0.27	0.47
DBH3-like	0.06	0	0	0	0	0	0.18	1.37	1.54	1.51	2.8	1.68	3.19
DBH4-like	0	0	0.23	0.07	0	0	0	0.42	0.87	1.46	4.45	4.8	9.52
DBH5-like	0.09	0.97	1.02	0.69	0.46	0.57	3.38	15.33	45.36	76.17	182.04	127.7	162.36
DBH6-like	0.13	0.04	0.19	0	0.35	0	0.15	0.12	0.25	0.08	0.92	1.1	2.59
DBH7-like	0.06	0	0.24	0	0	0	0	0.21	0.42	0.7	0.99	0.89	1.53

Supplementary Table 6.12. Table of Transcript Per Million (TPM) values of all monoaminergic genes identified from 0 to 48 hpf. In the first column genes name are reported, in the other columns TPM values for each sampling time are reported.

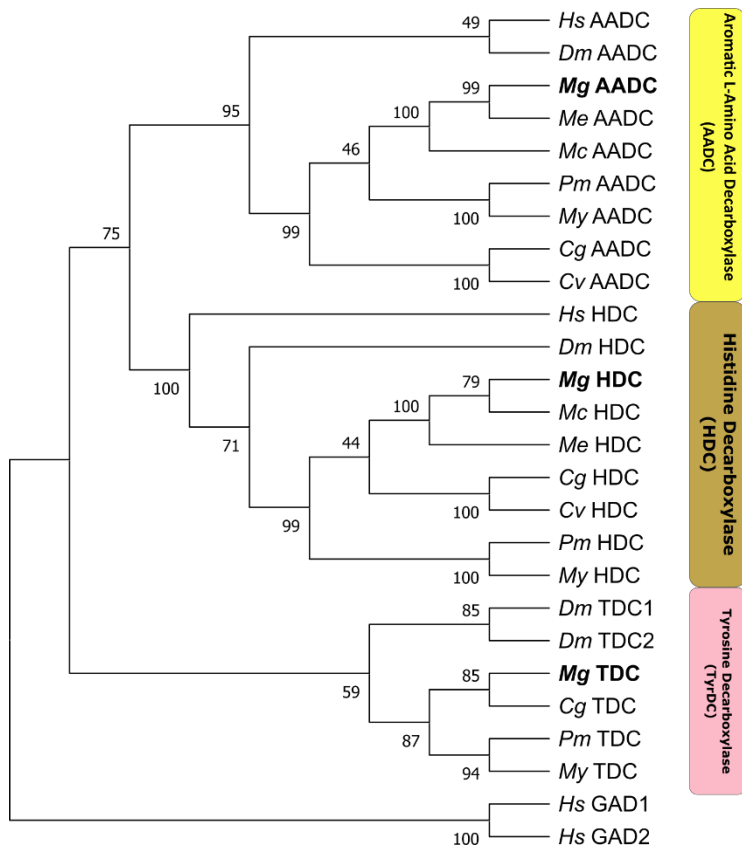
6.5 Supplementary Figures



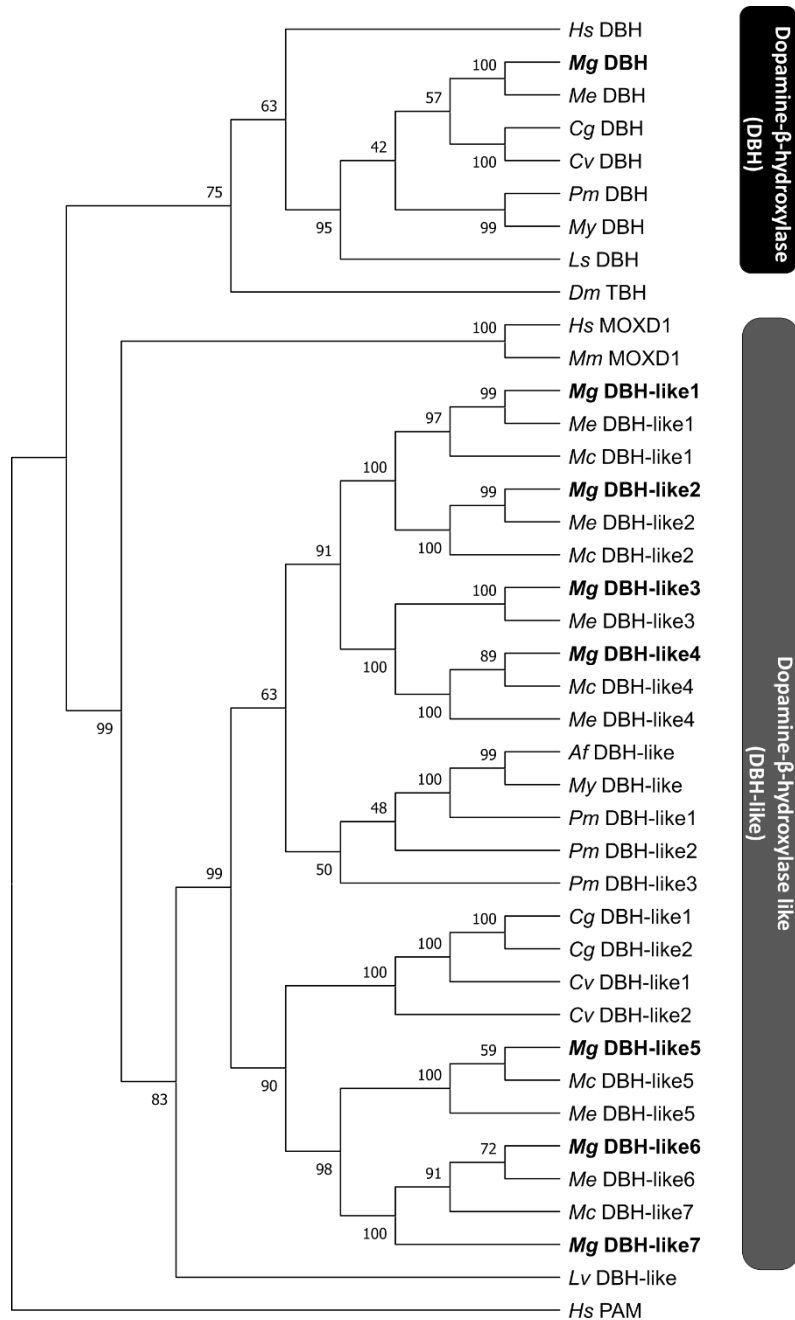
Supplementary Figure 6.1. Counting of Tryptophan Hydroxylase (TPH) positive cells in a 48 hpf D-Veliger in control conditions. The figure shows a montage of sequential z-stacks of TPH signal (green) and Hoechst (grey) merged together. The area containing the probe signal was cropped from the entire larva. Numbers indicate the numbers of positive cells appearing in sequential stacks. Scale bar: 20 μm.



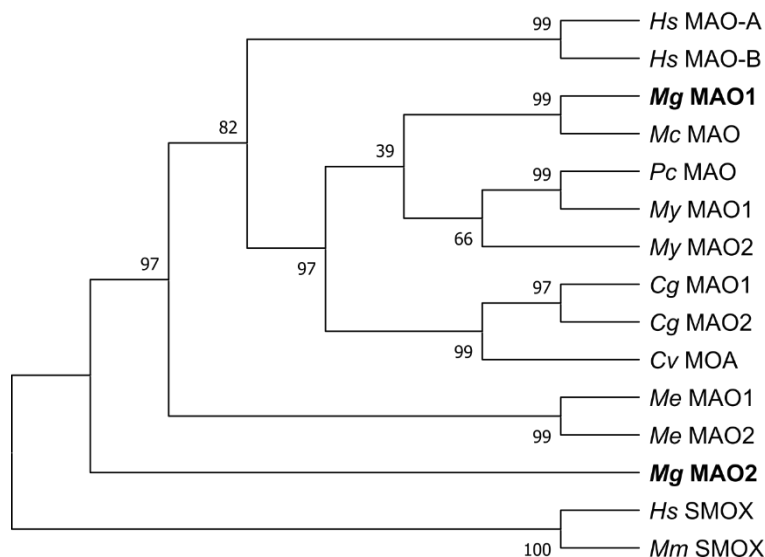
Supplementary Figure 6.2. Tree of BDAAAH proteins identified in bivalves. The tree was realised by using Maximum Likelihood method and Le Gascuel model; bootstraps values were inferred from 1000 replicates. Initial tree(s) for the heuristic search were obtained automatically by applying Neighbor-Join and BioNJ algorithms to a matrix of pairwise distances estimated using the JTT model, and then selecting the topology with superior log likelihood value. A discrete Gamma distribution was used to model evolutionary rate differences among sites (5 categories (+G, parameter = 0.8349)). This analysis involved 32 amino acid sequences. All positions with less than 85% site coverage were eliminated. Tryptophan Hydroxylase (TPH) is highlighted in red, Phenylalanine Hydroxylase (PAH) in sky blue and Tyrosine Hydroxylase (TH) in green. Abbreviations of species and enzymes can be found in Supplementary Table 6.1. *M. galloprovincialis* sequences are highlighted in bold.



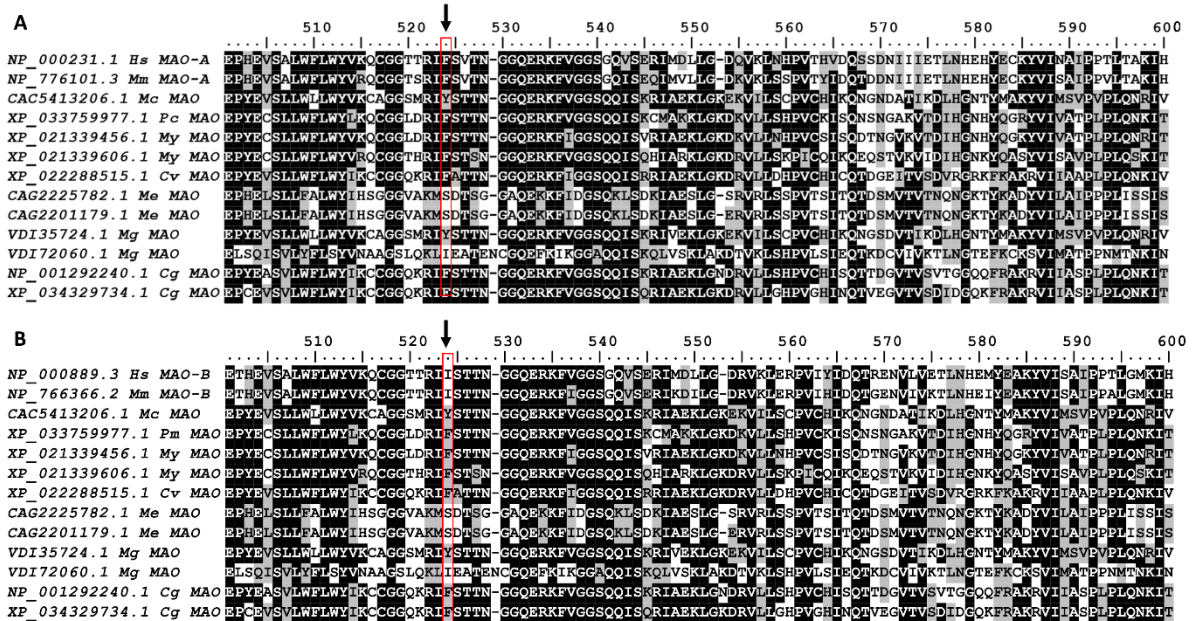
Supplementary Figure 6.3. Tree of AADC proteins in bivalves. The tree was realised by using Maximum Likelihood method and Le Gascuel model; bootstraps values were inferred from 1000 replicates. Initial tree(s) for the heuristic search were obtained automatically by applying Neighbor-Join and BioNJ algorithms to a matrix of pairwise distances estimated using the JTT model, and then selecting the topology with superior log likelihood value. A discrete Gamma distribution was used to model evolutionary rate differences among sites (5 categories (+G, parameter = 1.0119)). This analysis involved 26 amino acid sequences. All positions with less than 85% site coverage were eliminated. Aromatic L-Amino Acid Decarboxylase (AADC) is highlighted in yellow, Histidine Decarboxylase (HDC) in brown and Tyrosine Decarboxylase (TyrDC) in rose. Abbreviations of species and enzymes can be found in Supplementary Table 6.2. *M. galloprovincialis* sequences are highlighted in bold.



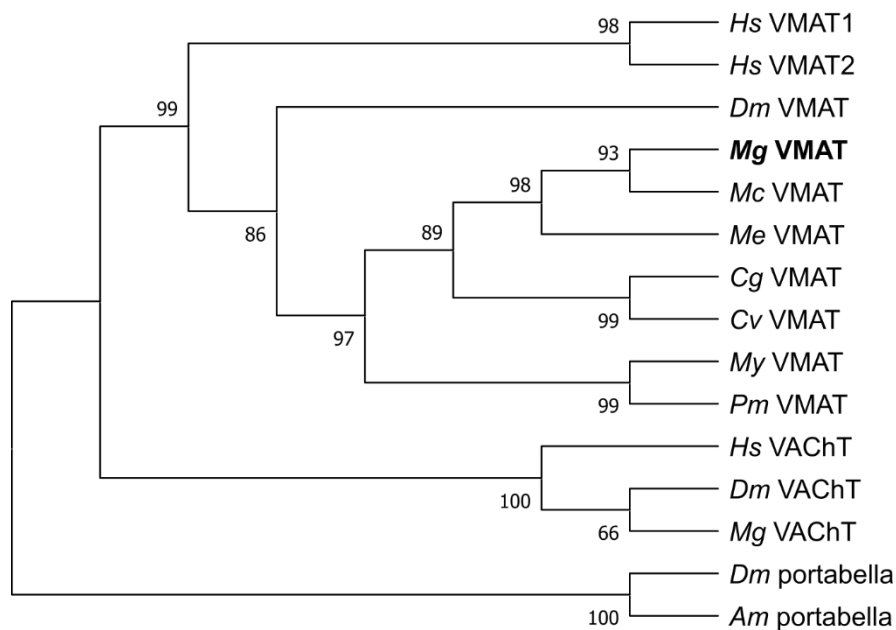
Supplementary Figure 6.4. Tree of copper-containing hydroxylase proteins. The tree was realised by using Maximum Likelihood method and Le Gascuel model; bootstraps values were inferred from 1000 replicates. Initial tree(s) for the heuristic search were obtained automatically by applying Neighbor-Join and BioNJ algorithms to a matrix of pairwise distances estimated using the JTT model, and then selecting the topology with superior log likelihood value. A discrete Gamma distribution was used to model evolutionary rate differences among sites (5 categories (+G, parameter = 1.2529)). The rate variation model allowed for some sites to be evolutionarily invariable ([+I], 0.56% sites). This analysis involved 40 amino acid sequences. All positions with less than 85% site coverage were eliminate. Dopamine- β -Hydroxylase (DBH) is highlighted in black, Dopamine- β -Hydroxylase-like (DBH-like) in dark grey. Abbreviations of species and enzymes can be found in Supplementary Table 6.3. *M. galloprovincialis* sequences are highlighted in bold.



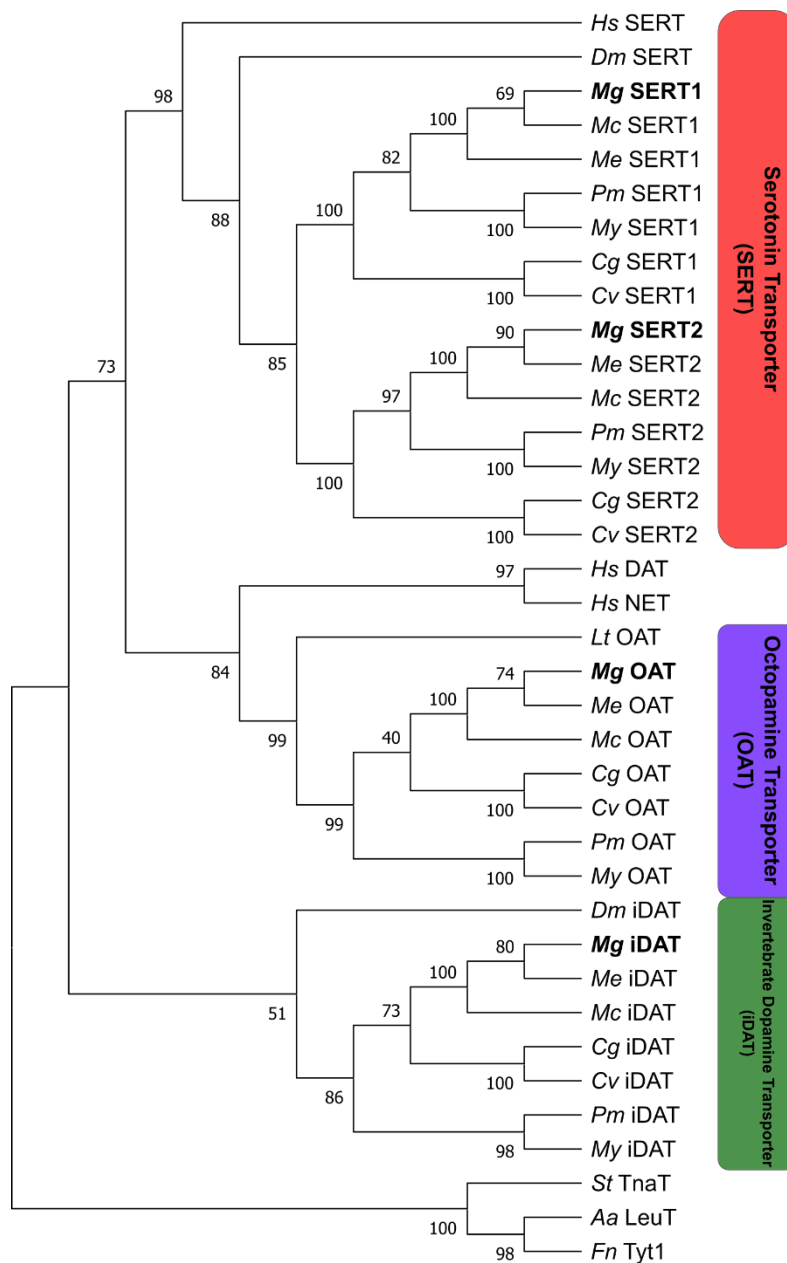
Supplementary Figure 6.5. Tree of MAOs. The tree was realised by using Maximum Likelihood method and Le Gascuel model; bootstraps values were inferred from 1000 replicates. nitial tree(s) for the heuristic search were obtained automatically by applying Neighbor-Join and BioNJ algorithms to a matrix of pairwise distances estimated using the JTT model, and then selecting the topology with superior log likelihood value. A discrete Gamma distribution was used to model evolutionary rate differences among sites (5 categories (+G, parameter = 1.1999)). This analysis involved 15 amino acid sequences. All positions with less than 85% site coverage were eliminated. Abbreviations of species and enzymes can be found in Supplementary Table 6.4. *M. galloprovincialis* sequences are highlighted in bold.



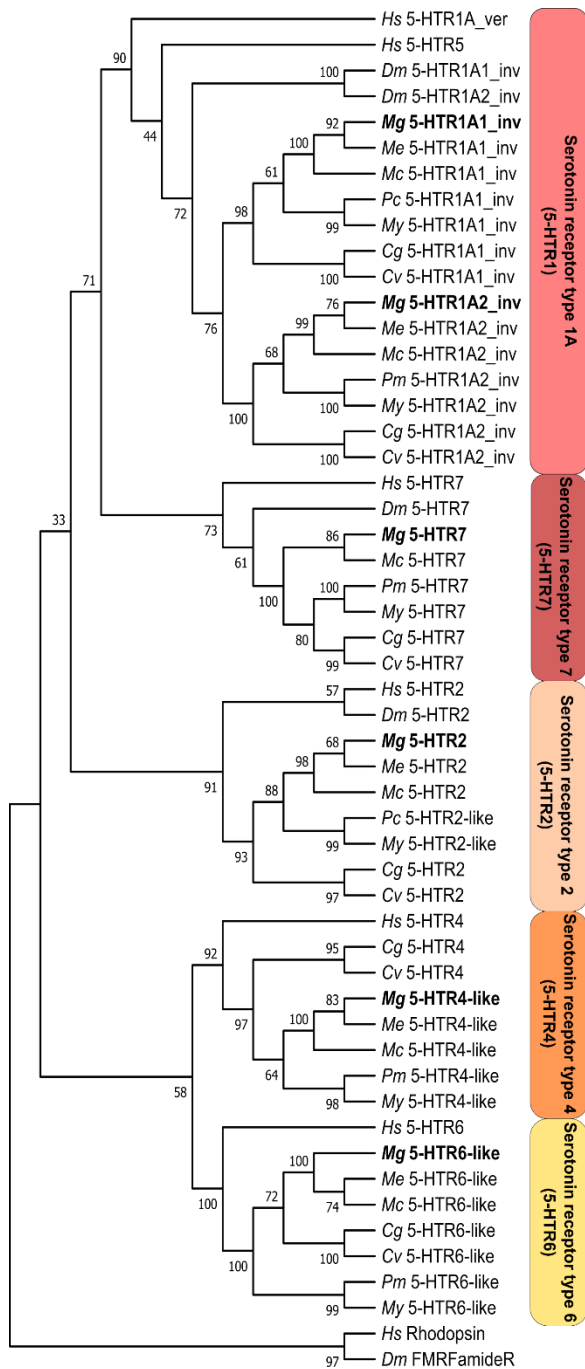
Supplementary Figure 6.6. Insight of MAOs multiple sequences alignment. A-B. Sequences alignment with human and murine MAO-A and MAO-B respectively. Black arrow and red box indicate F208 and I199. Black shading indicates identical amino acids, grey shading similar amino acids, absence of shading indicates that amino acids are not conserved. Abbreviations of species and enzymes can be found in Supplementary Table 6.5. *M. galloprovincialis* sequences are highlighted in bold.



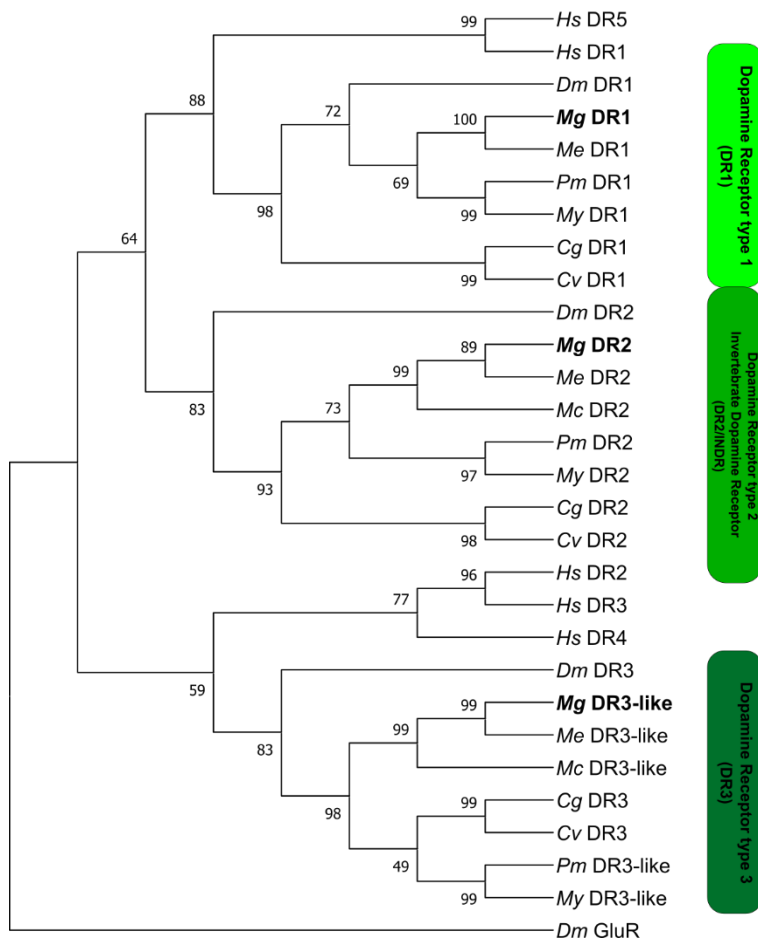
Supplementary Figure 6.7. Tree of VMATs proteins. The tree was realised by using Maximum Likelihood method and Le Gascuel model; bootstraps values were inferred from 1000 replicates. Initial tree(s) for the heuristic search were obtained automatically by applying Neighbor-Join and BioNJ algorithms to a matrix of pairwise distances estimated using the JTT model, and then selecting the topology with superior log likelihood value. A discrete Gamma distribution was used to model evolutionary rate differences among sites (5 categories (+G, parameter = 0.9514)). This analysis involved 15 amino acid sequences. All positions with less than 85% site coverage were eliminated. Abbreviations of species and enzymes can be found in Supplementary Table 6.6. *M. galloprovincialis* sequences are highlighted in bold.



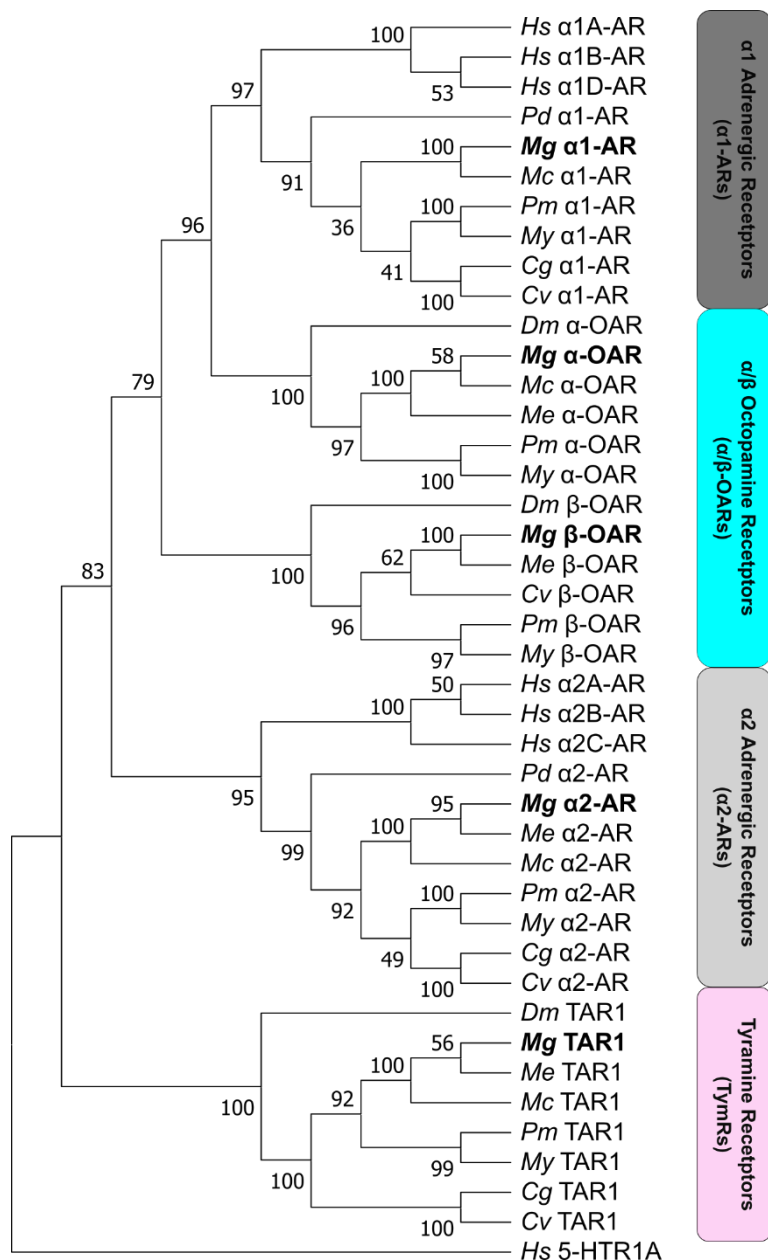
Supplementary Figure 6.8. Tree of SLC6 proteins. The tree was realised by using Maximum Likelihood method and Le Gascuel model; bootstraps values were inferred from 1000 replicates. Initial tree(s) for the heuristic search were obtained automatically by applying Neighbor-Join and BioNJ algorithms to a matrix of pairwise distances estimated using the JTT model, and then selecting the topology with superior log likelihood value. A discrete Gamma distribution was used to model evolutionary rate differences among sites (5 categories (+G, parameter = 1.1173)). The tree is drawn to scale, with branch lengths measured in the number of substitutions per site. This analysis involved 37 amino acid sequences. Serotonin Reuptake Transporter (SERT) is highlighted in red, Octopamine Transporter (OAT) in violet and invertebrate Dopamine Reuptake Transporter (iDAT) in green. Abbreviations of species and enzymes can be found in Supplementary Table 6.7. *M. galloprovincialis* sequences are highlighted in bold.



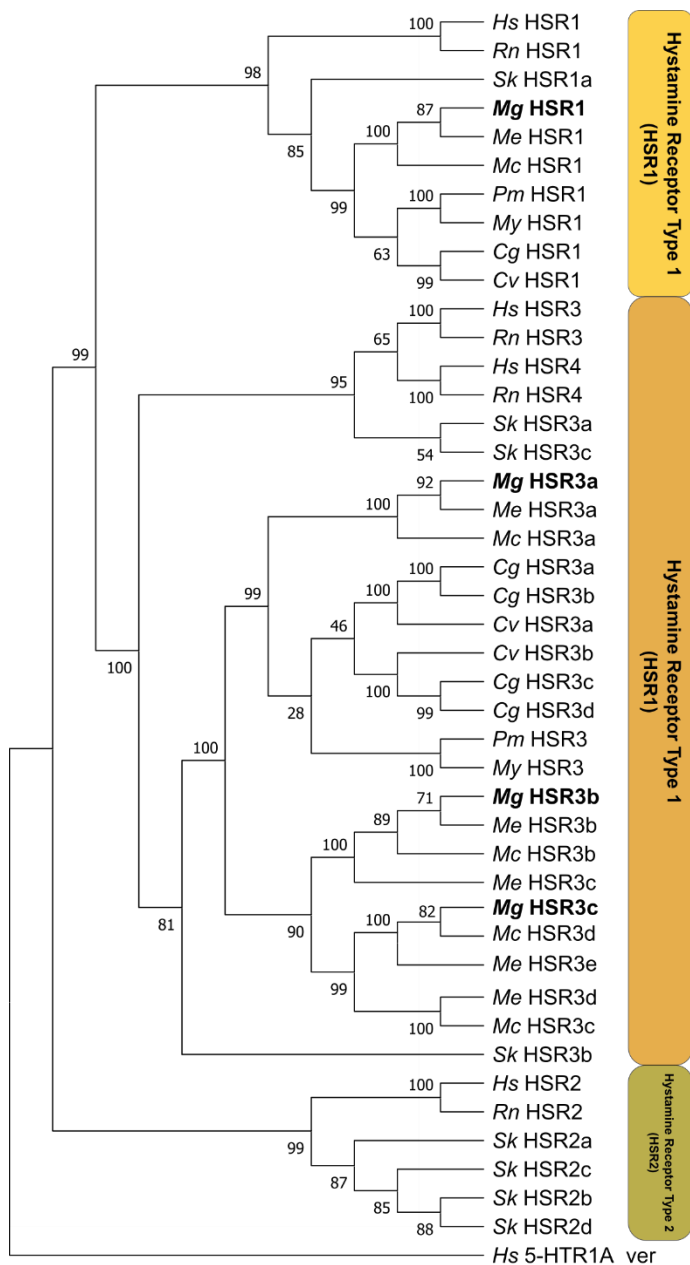
Supplementary Figure 6.9. Tree of 5-HTRs. The tree was realised by using Maximum Likelihood method and Le Gascuel model; bootstraps values were inferred from 1000 replicates. Initial tree(s) for the heuristic search were obtained automatically by applying Neighbor-Join and BioNJ algorithms to a matrix of pairwise distances estimated using the JTT model, and then selecting the topology with superior log likelihood value. A discrete Gamma distribution was used to model evolutionary rate differences among sites (5 categories (+G, parameter = 0.8278)). The rate variation model allowed for some sites to be evolutionarily invariable ([+I], 0.66% sites). This analysis involved 59 amino acid sequences. All positions with less than 85% site coverage were eliminated. 5-HTRs types are highlighted by different shades of red, orange and yellow. Abbreviations of species and enzymes can be found in Supplementary Table 6.8. *M. galloprovincialis* sequences are highlighted in bold.



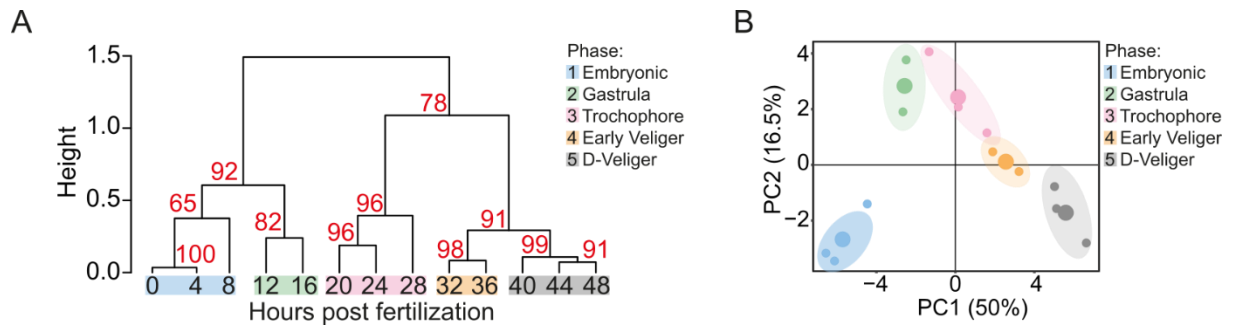
Supplementary Figure 6.10. Tree of DRs. The tree was realised by using Maximum Likelihood method and Le Gascuel model; bootstraps values were inferred from 1000 replicates. Initial tree(s) for the heuristic search were obtained automatically by applying Neighbor-Join and BioNJ algorithms to a matrix of pairwise distances estimated using the JTT model, and then selecting the topology with superior log likelihood value. A discrete Gamma distribution was used to model evolutionary rate differences among sites (5 categories (+G, parameter = 2.3432)). This analysis involved 29 amino acid sequences. All positions with less than 85% site coverage were eliminated. DRs types are highlighted by different shades of green. Abbreviations of species and receptors can be found in Supplementary Table 6.9. *M. galloprovincialis* sequences are highlighted in bold.



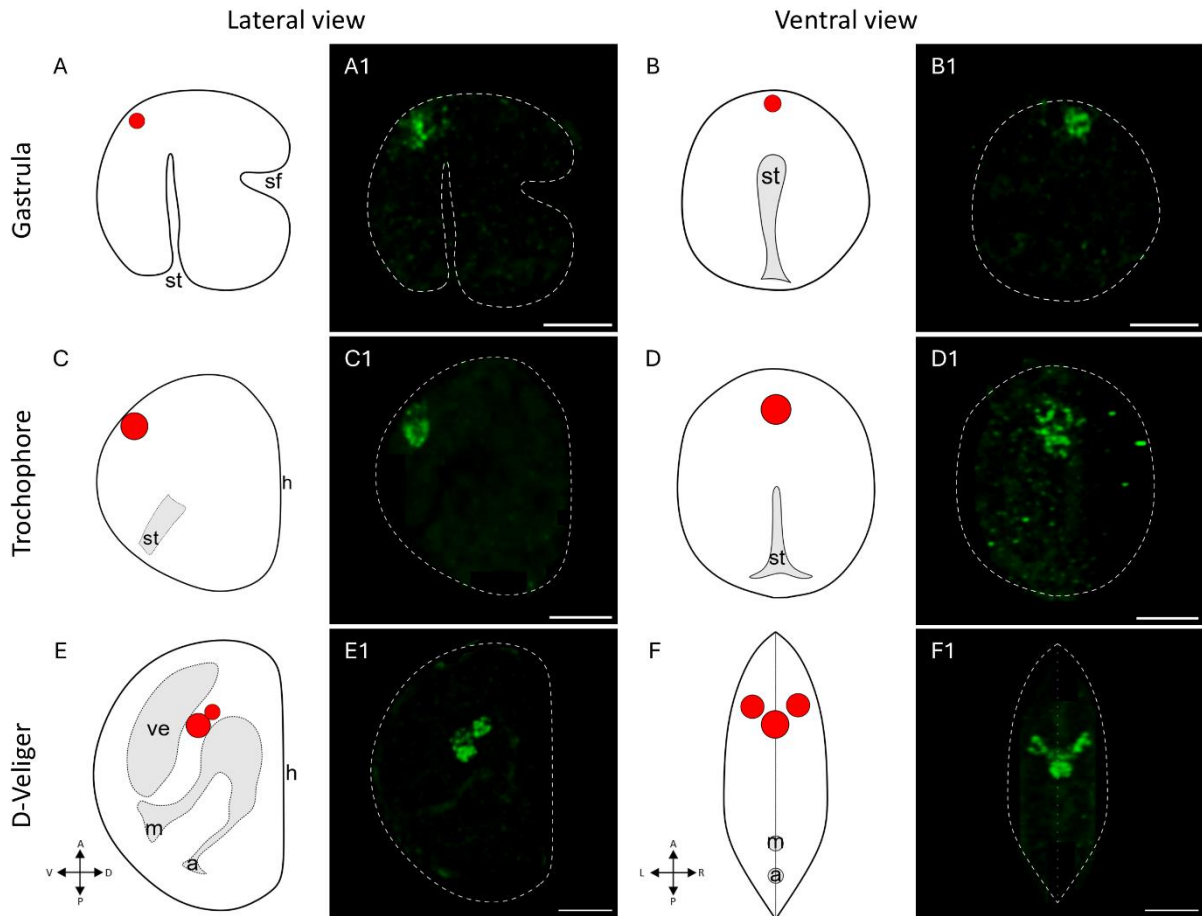
Supplementary Figure 6.11. Tree of adrenergic, octopaminergic and tyraminerpic receptors. The tree was realised by using Maximum Likelihood method and Le Gascuel model; bootstraps values were inferred from 1000 replicates. Initial tree(s) for the heuristic search were obtained automatically by applying Neighbor-Join and BioNJ algorithms to a matrix of pairwise distances estimated using the JTT model, and then selecting the topology with superior log likelihood value. A discrete Gamma distribution was used to model evolutionary rate differences among sites (5 categories (+G, parameter = 2.3316)). This analysis involved 42 amino acid sequences. All positions with less than 85% site coverage were eliminated. OARs are highlighted in sky blue, ARs in light grey and TARs in pink. Abbreviations of species and enzymes can be found in Supplementary Table 6.10. *M. galloprovincialis* sequences are highlighted in bold.



Supplementary Figure 6.12. Tree of HSRs. The tree was realised by using Maximum Likelihood method and Le Gascuel model; bootstraps values were inferred from 1000 replicates. Initial tree(s) for the heuristic search were obtained automatically by applying Neighbor-Join and BioNJ algorithms to a matrix of pairwise distances estimated using the JTT model, and then selecting the topology with superior log likelihood value. A discrete Gamma distribution was used to model evolutionary rate differences among sites (5 categories (+G, parameter = 3.2968)). The rate variation model allowed for some sites to be evolutionarily invariable ([+I], 2.24% sites). The tree is drawn to scale, with branch lengths measured in the number of substitutions per site. This analysis involved 44 amino acid sequences. All positions with less than 85% site coverage were eliminated. HSRs different types are highlighted by different shades of orange. Abbreviations of species and HSRs can be found in Supplementary Table 6.11. *M. galloprovincialis* sequences are highlighted in bold.



Supplementary Figure 6.13. Developmental expression dynamics of monoaminergic genes. A. Hierarchical clustering of MA genes from 0 to 48 hpf. Five phases were identified: phase 1 Embryonic (0 to 8 hpf), phase 2 Gastrula (12 to 16 hpf), phase 3 Trochophore (24 to 28 hpf) and phase 4 Early Veliger (32 to 36 hpf) and phase 5 D-Veliger (40 to 48 hpf). The numbers in red represent approximate unbiased p-value (au). B. Principal Component Analysis (PCA) biplot of MA genes in each sample analysed, samples were renamed in function of the phase identified in the hierarchical clustering. Ellipses highlight the five developmental clusters (corresponding to the phases 1, 2, 3, 4 and 5).



Supplementary Figure 6.14. Representative images of single HCR of TPH signal during embryo-larval development. Panels are organised as in Figure 6.3.

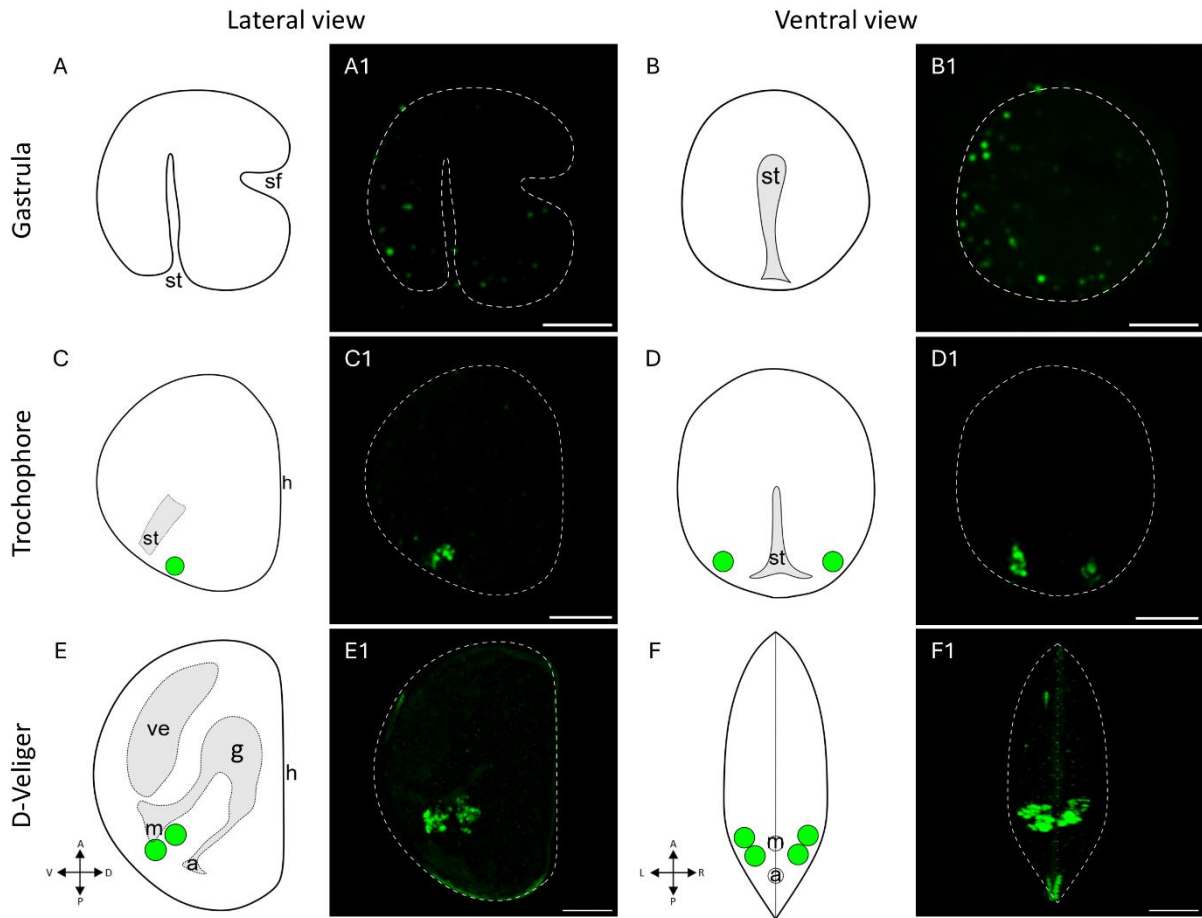
A-B1. Schematic representations and confocal images of TPH signal at Gastrula stage. 5 out of 5 larvae displayed signal.

C-D1. Schematic representations and confocal images of TPH signal at Trochophore stage. 5 out of 5 larvae displayed signal.

E-E1. Schematic representation and confocal image of TPH signal at D-Veliger stage in lateral view.

F-F1. Schematic representation and 3D reconstruction of TPH signal at D-Veliger stage in lateral view. 27 out of 30 larvae displayed the three clusters.

Axis orientation abbreviations: A – anterior, D – dorsal, L – Left, P – posterior, R – right, V – ventral. Anatomical abbreviations: a: anus, g: gut, h: hinge, m: mouth, sf: shell field, st: stomodeum. Scale bar: 20 μ m.



Supplementary Figure 6.15. Representative images of single HCR of TH signal during embryo-larval development. Panels are organised as in Figure 6.3.

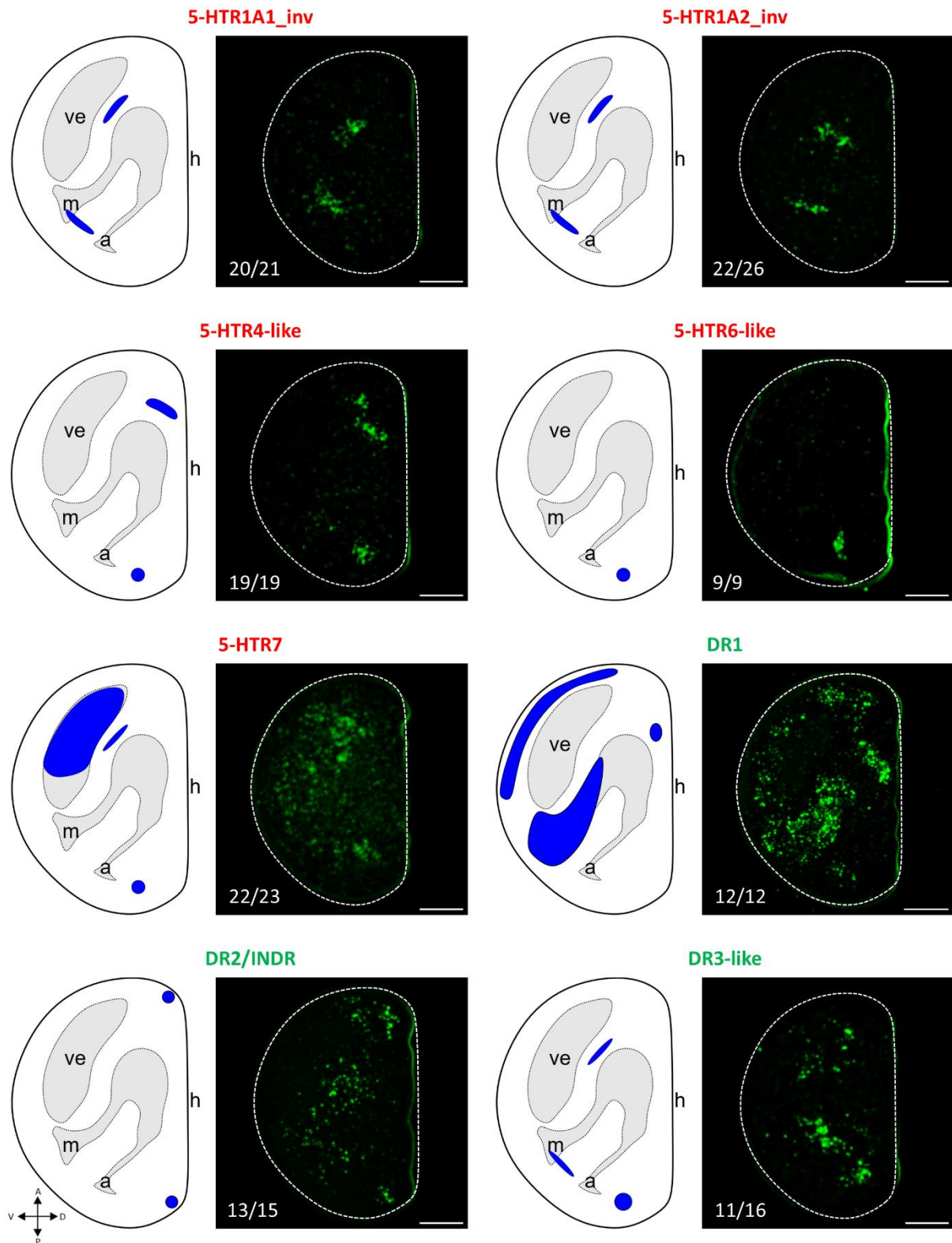
A-B1. Schematic representations and confocal images of TPH signal at Gastrula stage. 5 out of 5 larvae displayed no signal.

C-D1. Schematic representations and confocal images of TPH signal at Trochophore stage. 11 out of 11 larvae displayed the reported signal.

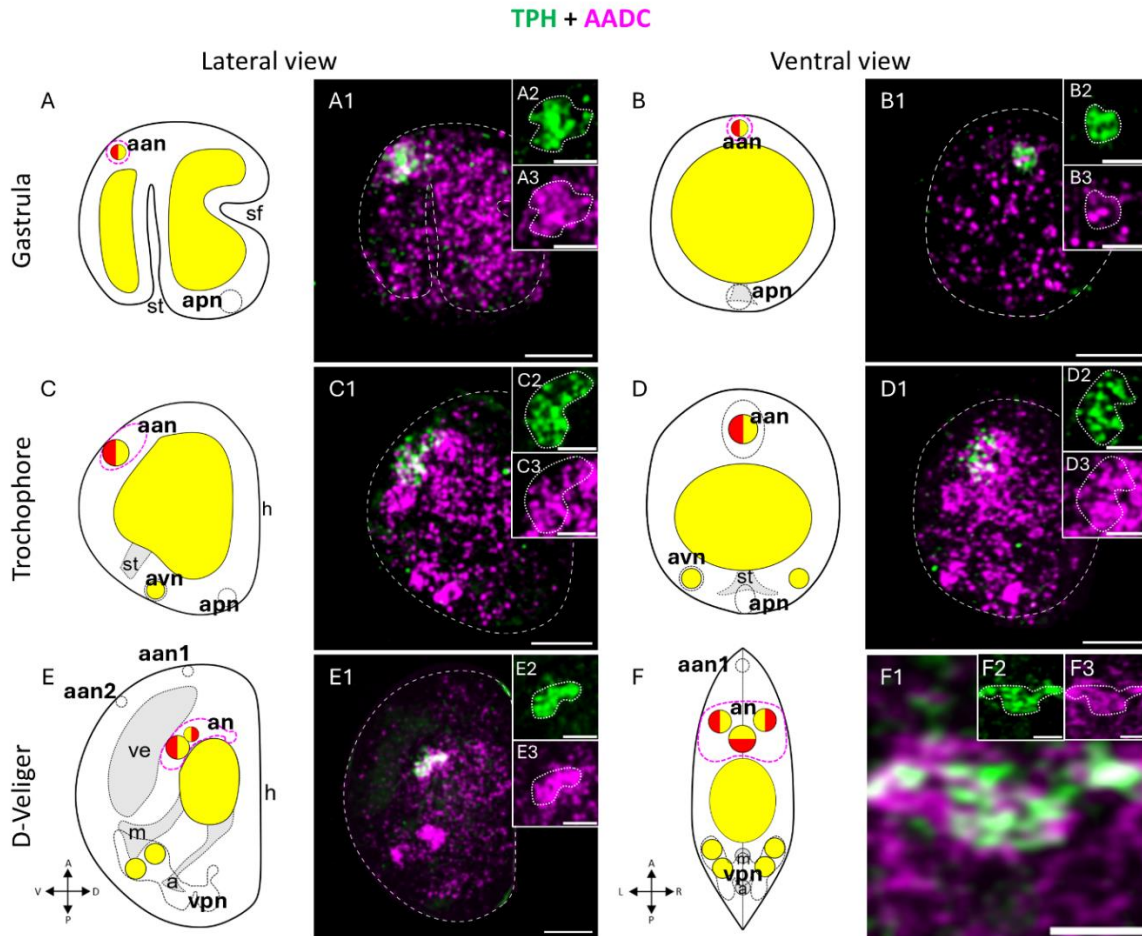
E-E1. Schematic representation and confocal image of TPH signal at D-Veliger stage in lateral view.

F-F1. Schematic representation and 3D reconstruction of TPH signal at D-Veliger stage in lateral view. 24 out of 37 larvae displayed the four clusters. Axis orientation abbreviations: A – anterior, D – dorsal, L – Left, P – posterior, R – right, V – ventral.

Anatomical abbreviations: a: anus, g: gut, h: hinge, m: mouth, sf: shell field, st: stomodeum. Scale bar: 20 μ m.



Supplementary Figure 6.16. Representative images of single HCR of the 5-HTRs (red title) and DRs (green title) analysed. For each confocal images a scheme representing the signal is reported on the left. The number of larvae presenting the signal drawn in the scheme is reported on the left corner of confocal images. Scale bar: 20 μ m.



Supplementary Figure 6.17. Spatiotemporal localisation of AADC and TPH during *M. galloprovincialis* embryo-larval development. Doble HCR with AADC (B1 amplifier) and TPH (B2 amplifier) was conducted. AADC signal is represented in yellow in schemes and in magenta in HCR pictures, TPH signal is represented in red in schemes and in green in HCR pictures. 7B2 area is represented in schemes by dotted lines and by neuronal clusters names. The white colour in confocal images is the result of green and magenta colocalisation.

A-A1. Schematic representation and maximum plane projection at Gastrula in lateral view. A2 and A3 show the magnification of TPH signal and the AADC signal, the dotted line represents TPH signal in this inset and in the ones shown after.

B-B1. Schematic representation and maximum plane projection at Gastrula stage in ventral view. B2 and B3 show the magnification of TPH signal and the AADC signal. 7 out of 7 larvae presented the colocalisation TPH-AADC (panels A1, B1).

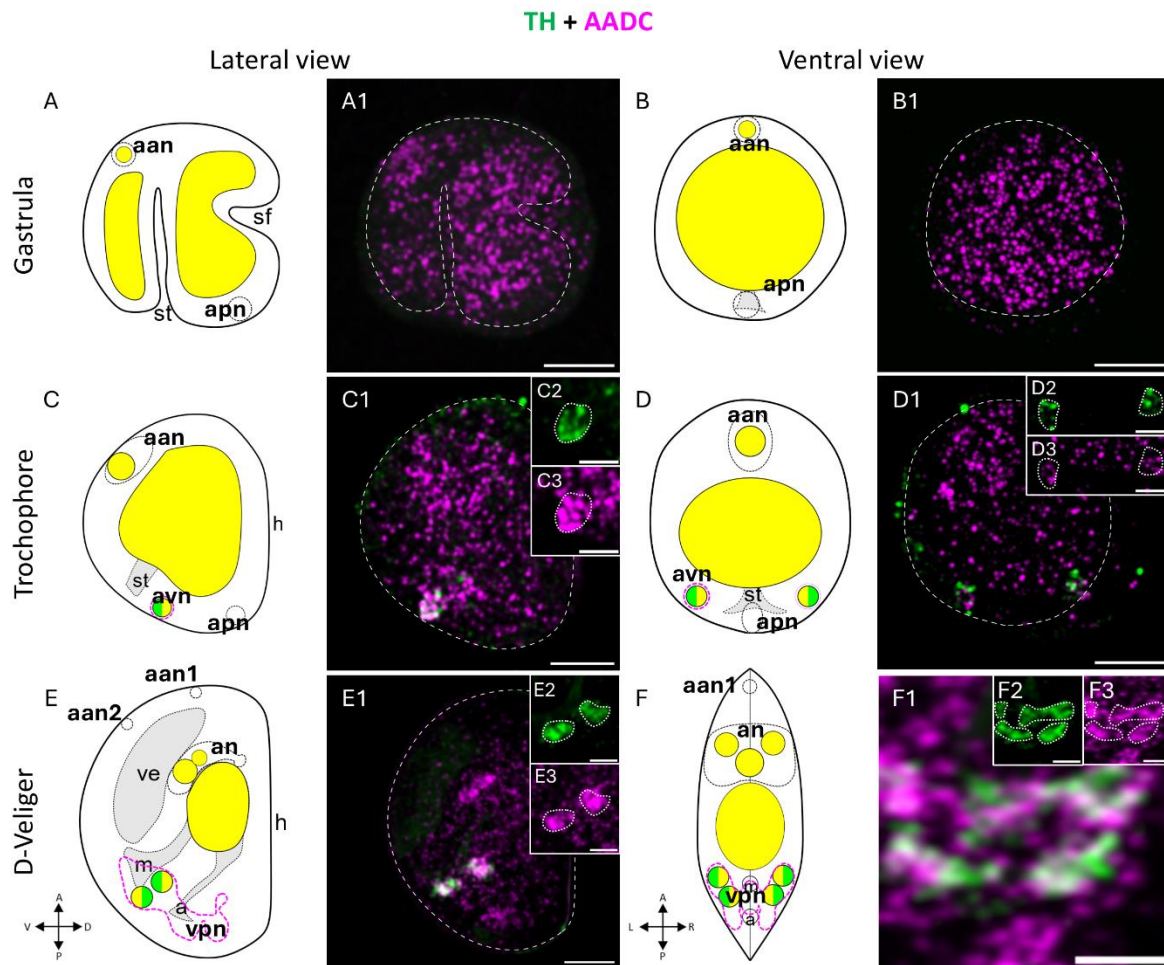
C-C1. Schematic representation and maximum plane projection at Trochophore stage in lateral view. C2 and C3 show the magnification of TPH signal and the AADC signal.

D-D1. Schematic representation and selective plane projection at Trochophore stage in ventral view. D2 and D3 show the magnification of TPH signal and AADC. 8 out of 8 larvae presented the colocalisation of TPH-AADC (panels C1, D1).

E-E1. Schematic representation and maximum plane projection at D-Veliger stage; E2 and E3 show a magnification of TPH and AADC.

F. Schematic representation of ventral view at D-Veliger stage. F1 selective 3D reconstruction of TPH area. F2 and F3 show signal of TPH and AADC. 8 out of 8 larvae showed colocalisation of TPH-AADC (panels E1, F1).

Axis orientation abbreviations: A – anterior, D – dorsal, L – Left, P – posterior, R – right, V – ventral. Anatomical abbreviations: a: anus, h: hinge, m: mouth, sf: shell field, st: stomodeum. Scale bars: 20 µm and 10 µm for inset pictures.



Supplementary Figure 6.18. Spatiotemporal localisation of AADC and TH during *M. galloprovincialis* embryo-larval development. Double HCR with TH (B2 amplifier) and AADC (B1 amplifier) was used. TH signal is represented in green in both schemes and HCR images; AADC signal is represented in yellow and in magenta in schemes and HCR images, respectively. 7B2 area is represented in schemes by dotted lines and by neuronal clusters names. The white colour in confocal images is the result of green and magenta colocalisation.

A-A1. Schematic representation and maximum plane projection at Gastrula in lateral view.

B-B1. Schematic representation and maximum plane projection at Gastrula stage in ventral view. 7 larvae were analysed (panels A1, B1).

C-C1. Schematic representation and maximum plane projection at Trochophore stage in lateral view. C2 and C3 show the magnification of TH signal and the AADC signal, the dotted line represents TH signal in this inset and in the ones shown after.

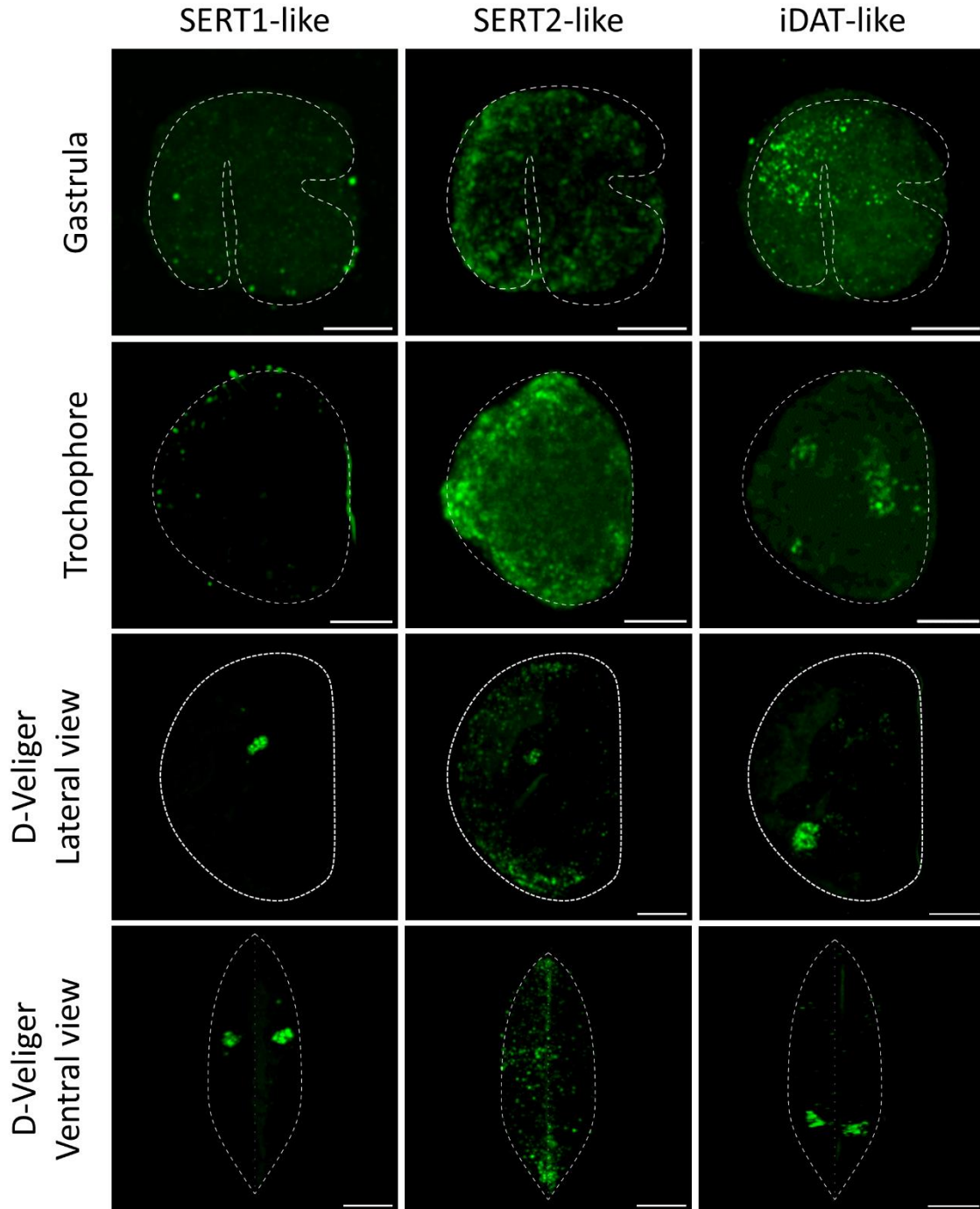
D-D1. Schematic representation and selective plane projection at Trochophore stage in ventral view. D2 and D3 show the magnification of TH signal and AADC. 6 out of 7 larvae presented the two clusters colocalising with AADC (panels C1, D1).

E-E1. Schematic representation and maximum plane projection at D-Veliger stage; E2 and E3 show a magnification of TH and AADC.

F. Schematic representation of ventral view at D-Veliger stage. F1 selective 3D reconstruction of TH area. F2 and F3 show signal of TH and AADC. 5 out of 9 larvae presented the four TH clusters and, as consequence, the respectively AADC clusters (panels E1, F1).

Axis orientation abbreviations: A – anterior, D – dorsal, L – Left, P – posterior, R – right, V – ventral.

Anatomical abbreviations: a: anus, h: hinge, m: mouth, sf: shell field, st: stomodeum. Scale bars: 20 µm and 10 µm for inset pictures.



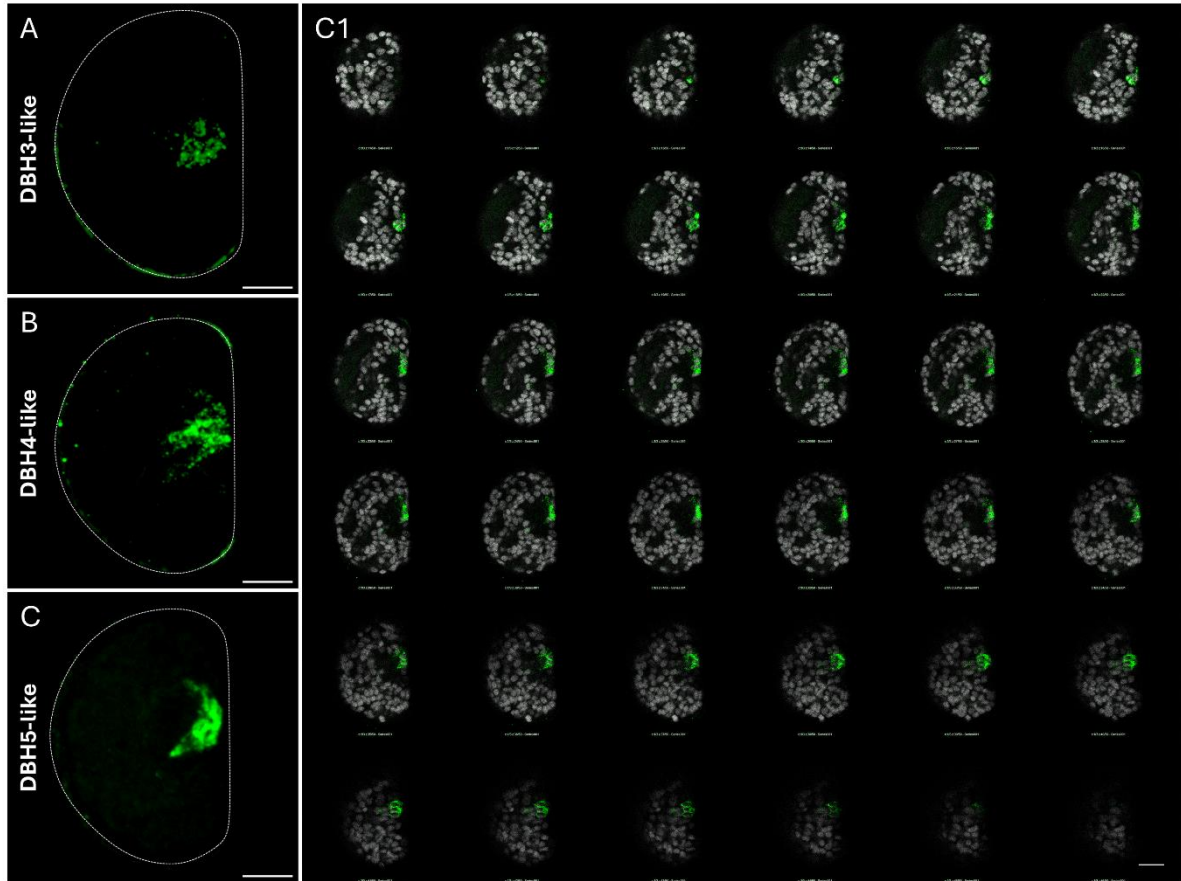
Supplementary Figure 6.19. Spatiotemporal localisation of serotonin and dopamine selective reuptake transporters. Rows organisation from top to bottom: Gastrula (16 hpf), Trochophore (28 hpf), D-Veliger (48 hpf) first in lateral and then ventral view.

SERT1-like: 3 larvae analysed (16 hpf), 5 larvae analysed (28 hpf) and 30 out of 30 larvae displayed the two clusters (48 hpf).

SERT2-like: 5 larvae analysed (16 hpf), 11 larvae analysed (28 hpf) and 17 out of 17 larvae displayed the middle cluster (48 hpf).

iDAT: 12 out of 16 displayed the anterior cluster (16 hpf), 8 out of 12 larvae displayed the clusters (28 hpf) and 34 out of 47 larvae displayed the two ventral clusters (48 hpf).

Scale bar: 20 μ m.



Supplementary Figure 6.20. Localisation of three DBHs-like at D-Veliger (48 hpf) stage. A, B, C. Maximum plane projection of DBH3-like, DBH4-like and DBH5-like. C1. Montage of DBH5-like signal (in green) and Hoechst (in grey). 15 larvae were analysed for each transcript. Scale bars: 20 μ m.

**7 Aim 2: Sensitivity of *M. galloprovincialis*
early development to fluoxetine and
citalopram as model SSRIs**

7.1 Materials and Methods

7.1.1 Analysis of human and mussel SERT sequences

Human and mussel SERT sequences were aligned and analysed using BioEdit (version 5.0.9) and ClustalW multiple alignment was performed using default settings. Amino acids involved in binding SSRIs (citalopram, fluoxetine and paroxetine) were retrieved from Andersen et al. (2014, 2010, 2009) and Coleman et al. (2016).

7.1.2 Mussel handling, spawning, fertilisation and conservation

See the previous section 6.1.3 page 66.

7.1.3 Exposure conditions

Fertilised eggs were exposed to the SSRIs fluoxetine (((±)-N-Methyl-γ-[4-(trifluoromethyl)phenoxy]benzenepropanamine hydrochloride, 56296-78-7) and citalopram (1-[3-(Dimethylamino)propyl]-1-(4-fluorophenyl)-1,3-dihydro-5-isobenzofurancarbonitrile hydrobromide, 59729-32-7). Chemicals were purchased from Sigma Aldrich. A stock solution was prepared at a concentration of 2 g/L dissolved in dimethyl sulfoxide (DMSO) and stored at -20°C. All chemicals were diluted in MFSW to obtain the final desired concentrations: 1, 10 and 100 µg/L. DMSO at the highest concentration (0.005%) was added to controls. The 48-hour embryotoxicity test (ASTM, 2004) was carried out in 50 mL flasks. Six parental pairs were analysed for each dilution. See the previous chapter for larval growth conditions.

7.1.4 Morphological analysis of larvae

See the previous section 6.1.4 page 67. A minimum of 100 larvae per condition were analysed.

7.1.5 Statistical analysis

Data were analysed using RStudio (2024.04.2). All data were tested for normality using the Shapiro-Wilk normality test and for homoscedasticity using the Bartlett Test of Homogeneity of Variances. When data did not show a normal distribution, Kruskal-Wallis test was performed followed by Dunn's test with Bonferroni correction method *post-hoc* comparisons. In the case of data displaying normal distribution and variance homogeneity, one-way ANOVA was carried out.

7.1.6 Retrieval of Nose Resistant to Fluoxetine (nrf) proteins in *Mytilus galloprovincialis* genome

NRFs proteins in *M. galloprovincialis* were retrieved from the genome assembly (Gerdol et al., 2020, ID: PRJEB24883 by Protein Basic Local Alignment Search Tool – BLAST on Octopus

Bioinformatic Server (<https://octopus.obs-vlfr.fr/>), using roundworm (*Caenorhabditis elegans*) nrf-6 reference sequence as query (AAD51972.1). Sequences resulting from the BLASTP with a BLAST score ≥ 200 were retained and were subjected to domain analysis using the NCBI Conserved Domain Database (CDD). Only sequences containing the expected functional domains were retained.

7.1.7 Retrieval of Nose Resistant to Fluoxetine (nrf) proteins in other bilaterian organism models

C. elegans reference protein nrf-6 was used to find orthologs across different animal species belonging to the group of Bilateria: *D. melanogaster*, *S. purpuratus*, *C. intestinalis* and *D. rerio*. BLASTP was performed on NCBI (<https://www.ncbi.nlm.nih.gov/>) for all species mentioned.

7.1.8 Analysis of expression profile of nrf transcripts in *M. galloprovincialis* transcriptome

See the previous section 6.1.2 page 65.

7.1.9 HCR

See the previous section 6.1.5 page 67. See Annex for nrf probes sequences.

7.1.10 Image acquisition and analysis

Images were taken with SP8 confocal microscope with LasX software with the following settings: three-dimensional acquisition mode (XYZ); bidirectional scanning mode, 1024 × 1024 image format, scanning speed: 600 Hz, pixel size: ~ 200 nm × 200 nm and z-stack: z-step size of 0.8 μm . Pictures were taken with a 40× objective. TPH expression was analysed on 15 larvae per condition at the highest concentration of SSRIs tested (100 $\mu\text{g/L}$) on three different parental pairs. For cell counting protocol, see the previous section 6.1.6 page 68.

7.2 Results

7.2.1 Analysis of presence/absence of conserved amino acids involved in SSRIs binding

The sixteen amino acids of human SERT involved in binding citalopram, fluoxetine and paroxetine are listed in Table 7.1.

Amino acids	Abbreviations	FLX	CIT	PAR
Tyr95	Y95	●	●	●
Asp98	D95	●	●	●
Ile168	I168	●	●	
Ala169	A169		●	●
Ile172	I172	●	●	●
Ala173	A173		●	●
Tyr176	Y176		●	●
Asn177	N177	●	●	
Phe335	F335		●	●
Phe341	F341	●	●	●
Ser438	S438		●	
Thr439	T439		●	●
Leu443	L443			●
Glu493	E493	●		●
Thr497	T497		●	●
Val501	V501		●	●

Table 7.1. Human SERT amino acids involved in the binding of fluoxetine (FLX), citalopram (CIT) and paroxetine (PAR). Points indicate the amino acids involved in the binding of the SSRI. Data were retrieved from Andersen et al. (2014) for FLX, from Andersen et al. (2010, 2009) and Coleman et al. (2016) for CIT and from Coleman et al. (2016) for PAR.

The sixteen amino acids involved in the binding of the three SSRIs are localised within different transmembrane (TM) helices, in particular: TM1, TM3, TM6, TM8 and TM10 except for Glu493 that is localised in an extracellular domain, as shown in Figure 7.1. Multiple sequence alignment allowed to identify the presence/absence of the amino acids listed in Table 7.1 in the SERTs protein sequences of *M. galloprovincialis*. Of the sixteen amino acids involved in SSRI binding, thirteen of them are conserved: D95, I168, A169, I172, Y176, N177, F335, F341, S438, T439, L443, E493 and V501 (Figure 7.1).

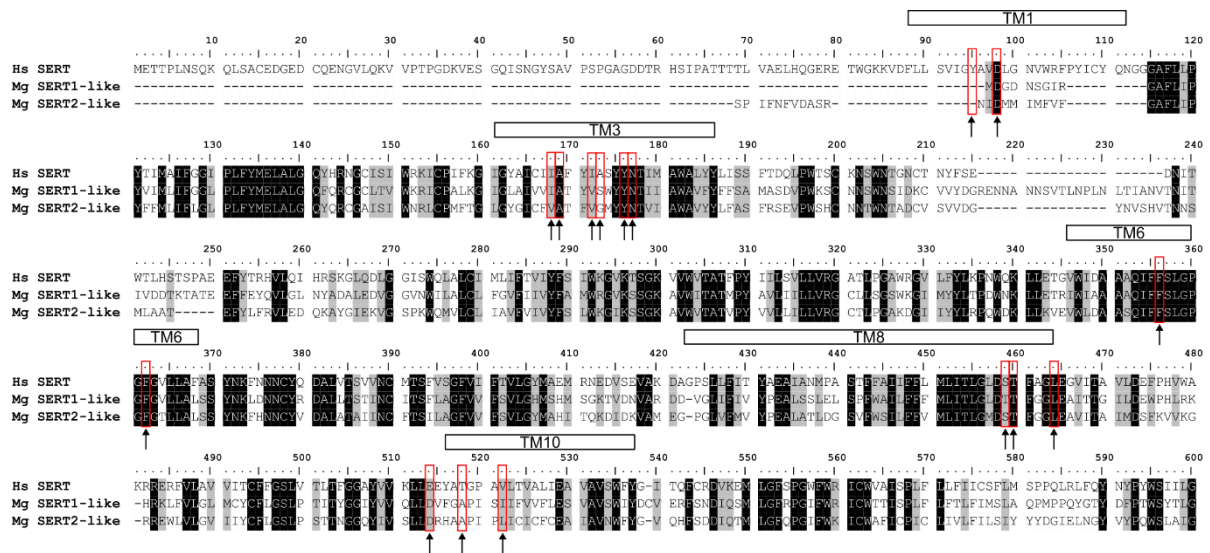


Figure 7.1. Amino acid sequence alignment of human Serotonin Re-Uptake Transporter (*Hs SERT*) and the two SERTs identified in *M. galloprovincialis* (*Mg SERT1-like* and *Mg SERT2-like*). Identical amino acids are highlighted in black, and similar amino acids in grey. Putative binding sites of Fluoxetine (FLX), Citalopram (CIT) and Paroxetine (PAR) are highlighted by red boxes. Black boxes and the arrows beneath them indicate the transmembrane (TM) localisation of amino acids based on data retrieved from Coleman et al. (2016) and UniProt (<https://www.uniprot.org/>).

Eight amino acids are identical (D98, A169, Y176, N177, F335, F341, T439 and L443) and five are similar (I168V for SERT2-like, I172V for both *Mg SERTs*, S438T for SERT1-like, E493D and V501I for both SERTs). Concerning I168, it is identical in *Mg SERT1-like* but similar in SERT2-like (Val, V) and S438 is identical in SERT2-like and similar in SERT1-like (Thr, T) (see Table 7.2 for a better visualisation).

Amino acids	Abbreviations	Mg SERT1-like	Mg SERT2-like
Tyr95	Y95	-	-
Asp98	D98	D	D
Ile168	I168	I	V
Ala169	A169	A	A
Ile172	I172	V	V
Ala173	A173	S	G
Tyr176	Y176	Y	Y
Asn177	N177	N	N
Phe335	F335	F	F
Phe341	F341	F	F
Ser438	S438	T	S
Thr439	T439	T	T
Leu443	L443	L	L
Glu493	E493	D	D
Thr497	T497	A	A
Val501	V501	I	L

Table 7.2. Summary showing similarities and differences between the two *Mg* SERT-like transporters. A black background indicates identical amino acids and a grey background similar amino acids.

Overall, the results indicate that thirteen out of sixteen amino acids are conserved in *M. galloprovincialis* sequences, in particular: Asp98, Ile168, Ala169, Ile172, Tyr176, Asn177, Phe335, Phe341, Ser438, Thr439, Leu443 and Glu493.

As previously shown in the first section of results and discussion, SERT-like transporters are expressed at different times during *M. galloprovincialis* larval development. In particular, SERT2-like peaked during Trochophore phase (Phase 3) at 24 hpf, whereas SERT1-like during D-Veliger phase (Phase 5) at 48 hpf. For better visualisation, their quantitative expression profiles expressed in TPM are reported in Supplementary Figure 7.1.

7.2.2 Effects of fluoxetine (FLX) and citalopram (CIT) on larval development

The results of the 48-h embryotoxicity test showed that FLX (Figure 7.2 A) affected larval development slightly but significantly only at the highest concentration tested (100 µg/L) (about – 20% with respect to control, p -value < 0.05), with malformed hinge (MH) representing the most abundant phenotype. On the other hand, although CIT induced a small decrease in the percentage of normal larvae, no significant effects were observed at any concentration tested (Figure 7.2 B) did not significantly affect larval development at any concentration tested (p -value > 0.05).

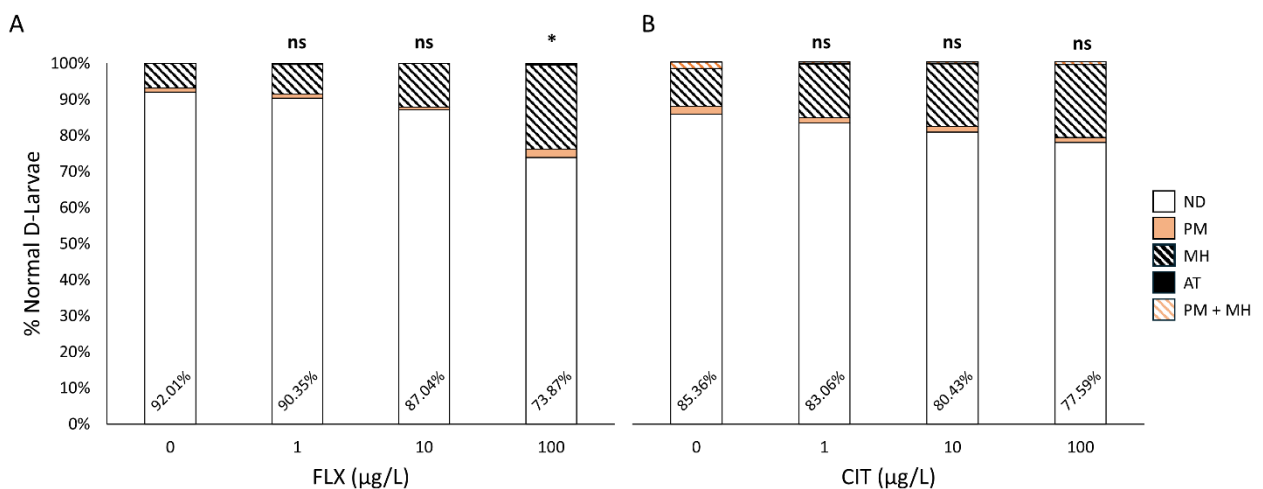


Figure 7.2. Effect of FLX (A) and CIT (B) on *M. galloprovincialis* development in the 48-h larval assay. Bar plots show the percentage of Normal D-Larvae (ND, percentage indicated at the bottom of the bars), and the occurrence in percentage of other phenotypes: malformed hinge (MH), protruding mantle (PM), arrested trochophore (AT) and protruding mantle + malformed hinge (PM + MH). Statistical analyses were conducted on 6 different parental pairs. FLX data were analysed with Kruskal Wallis test plus Dunn's test *post-hoc* comparison ($0.01 < p$ -value < 0.05). CIT data were analysed by one-way ANOVA.

7.2.3 Effects on serotonin synthesis enzyme Tryptophan Hydroxylase (TPH)

TPH was used as marker of the monoaminergic system to assess the possible effects of the two SSRIs tested. Number of TPH positive cells was counted on larvae treated with FLX and CIT (100 µg/L) at 48 hpf (D-Veliger). Positive cells were counted by merging the Hoechst and probe channels as described in materials and methods. In control larvae, the number of TPH cells was 7 ± 0.83 (90 larvae). As it is possible to see from Figure 7.3 A, B, FLX and CIT induced a shift towards an inferior number of cells. The effect is stronger in FLX treated larvae than in CIT treated larvae, with a percentage of larvae bearing 6 and 5 cells of 44% and 24%, respectively (Figure 7.3 A). The same effect was present in CIT treated larvae but less visible because larvae displayed a broader range of TPH positive cells (from 4 to eight); in particular: 31%, 33% and

2% of larvae showed 6, 5 and 4 positive TPH cells (Figure 7.3 B). The decrease induced by treatments was statistically significant (p -value > 0.01) as shown in the violin plots; FLX treated larvae displayed 6 ± 0.90 TPH positive cells (45 larvae), CIT 6 ± 0.95 TPH positive cells (45 larvae) (Figure 7.3 A1, B1). The results indicate that both FLX and CIT exposure can affect the synthesis of serotonin.

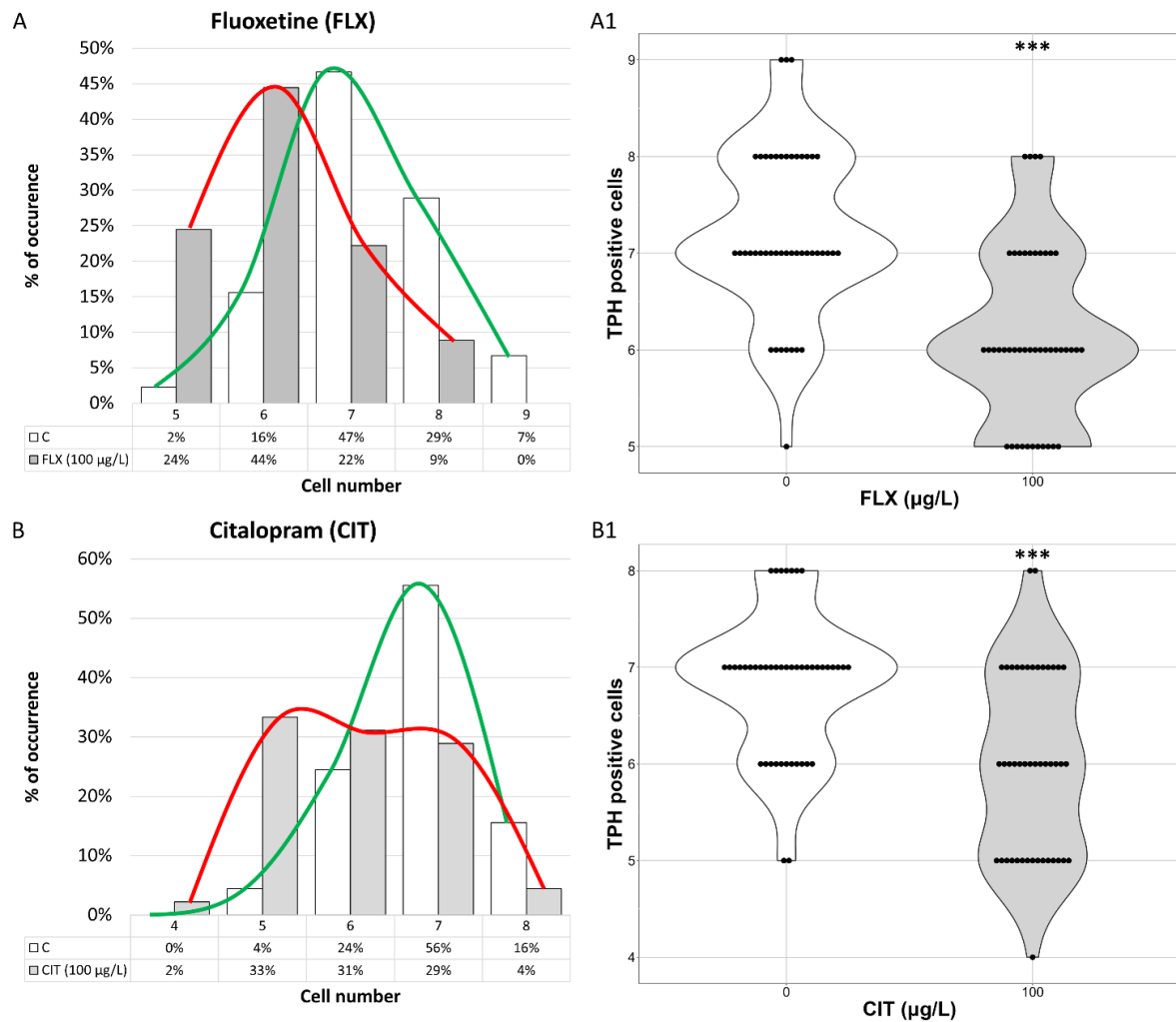


Figure 7.3. Effects of FLX and CIT 100 µg/L on TPH expression. Bar plots showing the occurrence of TPH positive cells in larvae treated with FLX (A) and CIT (B). The green and red curves indicate the distribution of data in control and treated larvae, respectively. Violin plots showing the effects of FLX (A1) and CIT (B1) at 100 µg/L on TPH signal. Statistical analysis was conducted on 3 different parental pairs. FLX and CIT data were analysed with Kruskal-Wallis test (p -value < 0.001). Dots in the violin plot indicate the number of cells counted in each image analysed (15 larvae per condition).

Overall, these data indicate that both SSRIs can affect early larval development in *M. galloprovincialis* through dysregulation of the serotonergic system. However, both the effect on larval phenotypes and on TPH positive cells were small, indicating a little sensitivity towards concentrations of SSRIs much higher than those present in the environment, indicating some

resistance of mussel embryo/larval stages to SSRI exposure. This possibility was explored by investigating the presence of Nose Resistant to Fluoxetine (nrf) proteins in *M. galloprovincialis*.

7.2.4 Presence of Nore Resistant to Fluoxetine (nrf) proteins in *M. galloprovincialis* and other bilaterian species

The NRF domain was identified in 19 sequences retrieved in *M. galloprovincialis* genome using BLASTP. This domain is associated either with an OafA domain or with an Acyl_transf_3 domain (Table 7.3). Sequences bearing the NRF domain, and the other two associated domains, were identified also in the other species analysed except for *H. sapiens*, where no protein with the NRF domain could be identified. BLASTP allowed to identify 12 sequences in *D. melanogaster* and *S. purpuratus*, 19 sequences in *B. floridae*, 3 in *C. intestinalis* and 1 in *D. rerio* (their accession numbers and domains are reported in Supplementary Table 13).

Therefore, among the invertebrate species considered, *M. galloprovincialis* was one of those expressing the higher number of nfr sequences.

Name	NCBI ID	Domains
nrf-1	VDI45122.1	NRF; OafA
nrf-2	VDI26244.1	NRF; Acyl_transf_3
nrf-3	VDI43809.1	OafA; NRF; OafA super family
nrf-4	VDI33667.1	NRF; OafA
nrf-5	VDI15781.1	OafA; NRF
nrf-6	VDI62592.1	NRF; OafA
nrf-7	VDI29520.1	OafA; NRF
nrf-8	VDI58070.1	NRF; OafA
nrf-9	VDI79433.1	NRF; Acyl_transf_3
nrf-10	VDH90651.1	NRF; OafA
nrf-11	VDI83770.1	NRF; OafA
bnrf-12	VDI83771.1	OafA; NRF
nrf-13	VDI21431.1	NRF; OafA
nrf-14	VDI35887.1	OafA; NRF
nrf-15	VDH89138.1	NRF; OafA
nrf-16	VDI72520.1	OafA; NRF superfamily
nrf-17	VDI74052.1	OafA; NRF
nrf-18	VDI44792.1	OafA; NRF
nrf-19	VDI42167.1	NRF; Acyl_transf_3 superfamily

Table 7.3. List of nrf proteins identified through BLASTP in the *M. galloprovincialis* genome. Names were given based on the order of finding. NCBI ID and domains are listed in columns two and three, respectively.

7.2.5 Expression of nrf proteins during *M. galloprovincialis* embryo-larval development

The expression of nrf transcripts was analysed during the embryo-larval development of *M. galloprovincialis*, using the recently published transcriptome (Miglioli et al., 2024). Expression profiles were analysed between 0 and 48 hpf (i.e.: from the unfertilised egg to the D-Veliger stage).

The developmental expression dynamics of nrf genes were analysed first through hierarchical clustering, which allowed for the identification of two major clusters ($au \geq 90$) (Supplementary Figure 7.2 A). The first major cluster formed a cluster on its own, whereas the second major cluster was formed by four subclusters. The first major cluster ($au = 93$) encompassed the Embryonic phase (Phase 1: from 0 to 16 hpf). The second major cluster ($au = 95$) encompassed four subsequent clusters: the Early Trochophore phase (Phase 2: from 20 to 24 hpf, $au = 99$) the Mature Trochophore phase (Phase 3: from 28 to 32 hpf, $au = 93$), the Early Veliger phase (Phase 4: from 36 to 40 hpf, $au = 89$) and the D-Veliger phase (Phase 5: from 44 to 48 hpf, $au = 98$). It was thus possible to identify five different phases based on the differential expression of nrf genes. The PCA analysis corroborated previous findings and covered mostly the total variance of the dataset (PC1 = 63.1% and PC2 17.6%) (Supplementary Figure 7.2 B). Expression dynamics were further analysed by realising a heatmap. This visualisation reinforced previous analyses by showing that there are genes highly expressed in each phase previously identified (Figure 7.4). During the Embryonic phase, five nrf genes displayed upregulation (nrf-4, nrf-5, nrf-14, nrf16, nrf-17 and nrf-19); during the following two phases, Early and Late Trochophore phases, three nrf genes were upregulated (nrf-7, nrf-18 and nrf-19). The two Veliger phases (Early and D-Veliger phases) showed a second peak of nrf-7, nrf-14 and nrf-18; moreover, up to eleven genes were upregulated during these two phases (nrf-1, nrf-2, nrf-3, nrf-6, nrf-8, nrf-9, nrf-10, nrf-11, nrf-12, nrf-13 and nrf-15).

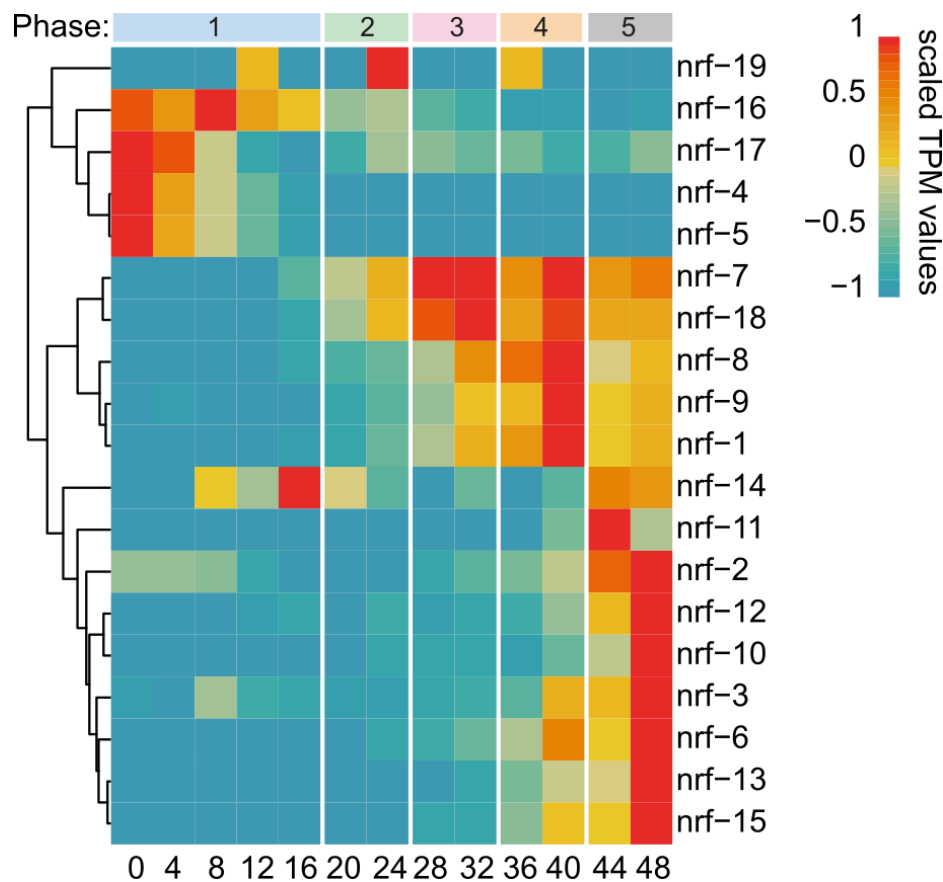


Figure 7.4. Heatmap of developmental expression dynamics of nrf genes. Genes are clustered by rows, with column breaks identifying the five phases, which are indicated above the columns. Expression levels in TPM (Transcripts per Million) values scaled by the maximum and minimum value of each row (gene).

7.2.6 Localisation of four nrf genes at D-Veliger stage (48 hpf)

Even though several nrf genes were shown to peak during Phase 5, four nrf genes were analysed based on their higher TPM values at 48 hpf as best candidates for HCR analysis and, therefore, their localisation in the larval body (see Supplementary Figure 7.3). The genes chosen were: nrf-1, nrf-2, nrf-6 and nrf-9.

The nrf transcripts, nrf-1, nrf-6 and nrf-9 displayed a cluster localised dorsally near the centre of the hinge, whereas nrf-2 displayed a widespread signal localised ventrally, presumably in the velum area (Figure 7.5). To better understand the localisation of nrf-1, nrf-2 and nrf-9, montages with Hoechst signal were realised. Nrf-1, nrf-6 and nrf-9 localised near cavities of the larval body of the D-Veliger that could represent oesophagus and stomach areas, and thus largely localised in the digestive system (Supplementary Figure 7.4).

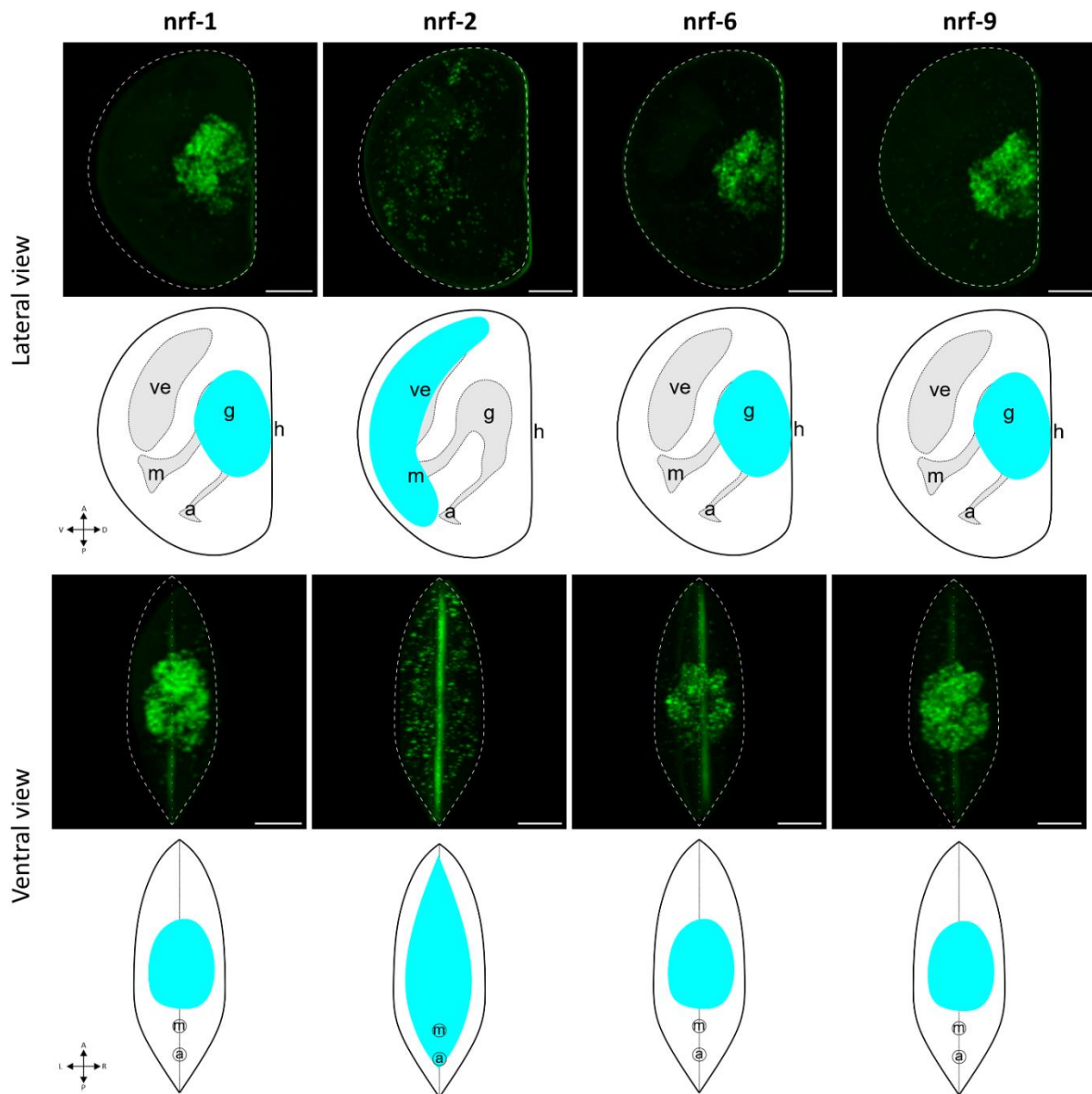


Figure 7.5. Localisation of *nrf* genes at D-Veliger stage (48 hpf). The first two rows show the confocal images obtained with maximum plane projection and corresponding schemes, with signal schematised in cyan and lateral view. The last two rows show the 3D reconstruction of confocal images and their corresponding schemes in ventral view.

Axis abbreviation: A: anterior, D: dorsal, L: left, P: posterior, R: right, V: ventral.

Anatomical abbreviations: a: anus, g: gut, h: hinge, m: mouth. Scale bar: 20 μ m.

7.3 Discussion

7.3.1 SSRIs may bind to SERT-like transporters of *M. galloprovincialis*

SSRIs are designed to bind the human serotonin reuptake transporter (SERT) resulting in inhibiting the recycling of 5-HT and increasing the 5-HT concentration at the synaptic level (Andersen et al., 2014, 2009; Zhou et al., 2009). However, SERT's inhibition mechanisms were reported to be poorly understood (Andersen et al., 2010, 2009). Crystallography experiments allowed to identify the amino acids of human SERT involved in binding different SSRIs (i.e.: FLX, CIT and PAR) and to understand which are pivotal for the binding through mutagenesis experiments (Andersen et al., 2014, 2010, 2009; Coleman et al., 2016).

Sequence analysis of human and mussel SERTs showed that the amino acids involved in binding CIT, FLX and PAR are conserved in *M. galloprovincialis* SERT-like transporters protein sequences. Six out of seven of the amino acids involved in binding FLX are conserved in *M. galloprovincialis* sequences; Tyr97 is not present in any of the two SERT-like transporter sequences. Regarding CIT, eleven out of fourteen amino acids are present and conserved except for Ala173 and Thr497, with the latter replaced by an Ala in both SERT-like transporter sequences. PAR shows twelve amino acids involved in binding human SERT and ten are conserved in *M. galloprovincialis* except for Ala173 and Thr497 as it is for CIT (Table 7.4).

Amino acids	Abbreviations	<i>Mg</i> SERT1-like	<i>Mg</i> SERT2-like	FLX	CIT	PAR
Tyr95	Y95	-	-	●	●	●
Asp98	D95	D	D	●	●	●
Ile168	I168	I	V	●	●	
Ala169	A169	A	A		●	●
Ile172	I172	V	V	●	●	●
Ala173	A173	S	G		●	●
Tyr176	Y176	Y	Y		●	●
Asn177	N177	N	N	●	●	
Phe335	F335	F	F		●	●
Phe341	F341	F	F	●	●	●
Ser438	S438	T	S		●	
Thr439	T439	T	T		●	●
Leu443	L443	L	L			●
Glu493	E493	D	D	●		●
Thr497	T497	A	A		●	●
Val501	V501	I	L		●	●

Table 7.4. Schematic table showing the amino acids conserved between human and mussel sequences and the amino acids involved in binding FLX, CIT and PAR. Green dots indicate that amino acids are conserved, and red dots indicate that amino acids are not conserved.

Point mutations in human SERT showed that the most important amino acids involved in FLX binding are Tyr95, Asp98, Ile168, Ile172 and Asn177 (Andersen et al., 2014). Indeed, substitution of Tyr95 with alanine or valine, Asp98 with glutamate, Ile172 with methionine and glutamine and N177 with serine induced a loss of potency for fluoxetine, whereas substitution of Ile168 with phenylalanine increased FLX potency (Andersen et al., 2014). This experiment was conducted also to show the pivotal amino acids involved in CIT binding which are: Tyr95, Asp98, Ile172, Asn177, Phe341 and Ser438 (Andersen et al., 2010). Substitution of Tyr95 to valine, glutamine and alanine, Asp98 to glutamate, Ile172 to phenylalanine and glutamate, Ile177 to serine, Phe341 to tyrosine and Ser438 to threonine reduced significantly citalopram potency (Andersen et al., 2010).

The pivotal amino acids involved in FLX binding are conserved and identical in both *M. galloprovincialis* SERT-like transporter sequences, except for Tyr95 which was not found in any of the two sequences. These results suggest that *M. galloprovincialis* SERT-like transporters can bind FLX. The same suggestions can be made for CIT, whose pivotal amino acids involved in binding human SERT are conserved and identical in SERT2-like, and SERT1-like displays a similar amino acid at the position of human Ser438: threonine.

From the results of these *in silico* analysis it is possible to argue that SSRIs may bind to SERT-like transporters of *M. galloprovincialis*, confirming that the targets of SSRIs are conserved. This information is of pivotal importance for assessing the conceptual model of the “mode-of-action” (MOA) to assess the environmental risks of pharmaceuticals, in this case of SSRIs (Ankley et al., 2010, 2007). Moreover, the identification of specific targets in *M. galloprovincialis* can help to better understand the adverse outcome pathway caused by SSRIs, where the molecular initiating event is the binding of SSRIs to mussel SERTs-like (Ankley et al., 2010; Hutchinson et al., 2013).

7.3.2 Effect of Fluoxetine (FLX) and Citalopram (CIT) on D-Larvae phenotypes

Even though the primary target of SSRIs is conserved in *M. galloprovincialis* SERT-like protein sequences (thirteen out of sixteen amino acids involved in binding SSRIs in humans), the results of exposure to FLX and CIT showed that larvae were weakly affected by concentration in the order of $\mu\text{g/L}$. FLX induced a reduction of about 30% in normal D-Larvae was significant for

FLX only at the highest concentration tested (100 µg/L), whereas no significant decrease was observed in larvae treated with CIT, and the highest concentration resulted in a reduction in normal D-Larvae of about 8%. By scoring phenotypes, it was found that the highest concentrations of FLX caused malformations, namely malformed hinge.

A recent study showed that environmental concentrations of FLX and CIT in *M. galloprovincialis* larvae at 48 hpf caused small decreases in the percentage of normal D-Larvae (Rafiq et al., 2023). In particular, FLX caused a dose-dependent reduction in normal D-Larvae of 11% at 100, 200 and 500 ng/L; the CIT response was not dose-dependent, with significant reduction in normal D-Larvae observed at 25, 100 and 500 ng/L, with a maximum of 20% of reduction, but not at 50 and 250 ng/L (Rafiq et al., 2023). CIT was shown to cause abnormalities (Rafiq et al., 2023), and this is in line with the data shown here, where the most abundant phenotype was represented by malformed hinge. On the contrary, FLX was previously shown to induce delay in development, namely arrested trochophore (Rafiq et al., 2023), whereas the results of the present study showed that malformed hinge was the most abundant phenotype. Differences could be explained by the differences in mussel sources: in this study, mussels were collected directly from a natural population from the bay in Villefranche-sur-Mer, in the study of Rafiq et al. (2023), adult mussels were collected from an aquaculture farm in the Adriatic sea. However, both studies showed that larvae were weakly sensitive to FLX and CIT.

It is important to note that while the higher levels of FLX and CIT tested here did not cause significant effects when evaluated in isolation, they may still have an impact when present at lower concentrations as part of a mixture of contaminants, as it occurs in the environment. Therefore, further studies are needed to assess the potential synergies between SSRIs and other contaminants (Duarte et al., 2023; Rafiq et al., 2023).

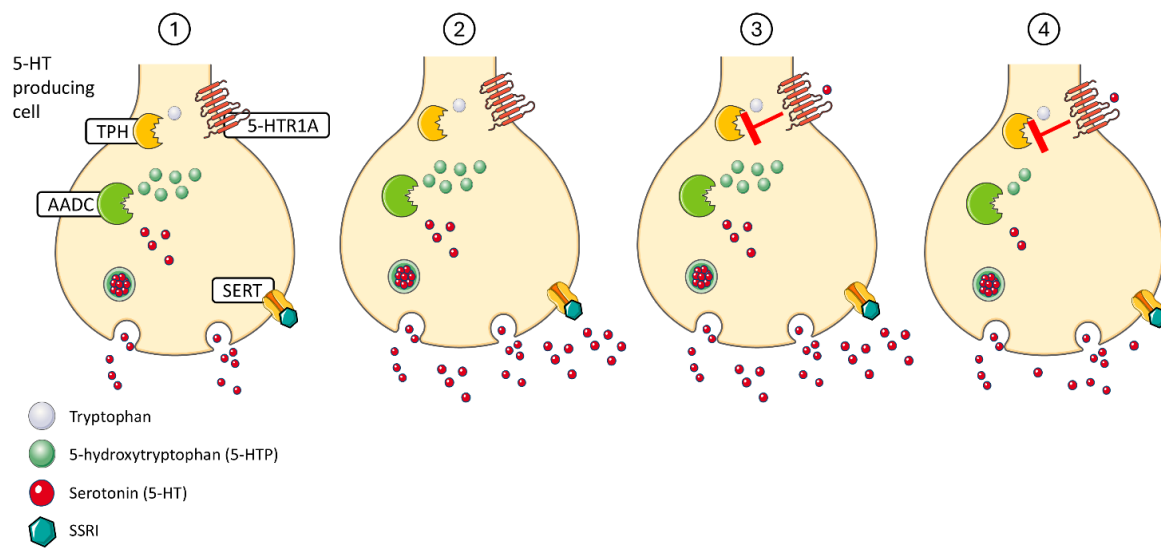
7.3.3 Serotonin Reuptake Transporters do not represent unique targets of SSRI

Choy and Thomas (1999) reported in humans that FLX does not only target SERT protein but interferes also with cytochrome P450 (CYP 450). Additionally, several studies showed that 5-HTRs may represent other targets of SSRIs in both humans and *C. elegans* acting as either agonists or antagonists depending on the receptor subtype (Kullyev et al., 2010; Sghendo and Mifsud, 2012; Sohel et al., 2024). Specifically, 5-HTR1A appears to act as a non-direct target of FLX; more details on this topic are provided in BOX 2.

BOX 2: 5-HTR1A: a non-direct target of SSRIs that modulates serotonergic neuron activity

In the past century, SSRIs gained particular attention in the scientific literature due to their ability to increase 5-HT levels within a few hours of treatment, yet require two to four weeks to be effective in alleviating symptoms of depression (Choy and Thomas, 1999). It is assumed that such a delay in the effectiveness of SSRI treatment is due to a mechanism of negative feedback mediated by 5-HTR type 1A, which acts as an autoreceptor in serotonergic neurons when localised in the somatodendritic region (Esteban et al., 1999; Moret and Briley, 1992). In mammals, 5-HTR1A autoreceptors exert negative feedback in response to the local 5-HT release by inhibiting the rate firing (and consequently 5-HT release), synthesis, and turnover (Altieri et al., 2012; Brady et al., 2012; Hoyer, 2019a).

In rats, stimulation of the 5-HTR1A autoreceptor with the agonist, 8-hydroxy-2-(di-npropylamino)tetralin (8-OH-DPAT) led to a decrease of 5-hydroxytryptophan (5-HTP), the product of TPH activity, suggesting that 5-HTR1A autoreceptor stimulation not only reduces the serotonergic neurons firing rate but also inhibits TPH, the enzyme responsible for converting tryptophan to 5-HTP (Invernizzi et al., 1991). Experiments with SSRIs in rats (FLX, CIT and zimelidine, the latter no more commercialised (Mulinari, 2015)) measured 5-HTP concentrations, the precursor of 5-HT, following treatment with NSD 1015, an inhibitor of Aromatic L-Amino Acid Decarboxylase (AADC, responsible for the conversion of 5-HTP into 5-HT) (Esteban et al., 1999; Moret and Briley, 1992). Acute exposure (2 h) to these SSRIs resulted in a decrease in 5-HTP concentration, suggesting an inhibition of TPH (Esteban et al., 1999; Moret and Briley, 1992). In rats chronically exposed to SSRIs (21 days), the decrease in 5-HTP concentration decreased until day 3, then 5-HTP levels began to recover (Esteban et al., 1999; Moret and Briley, 1992). This time-dependent loss in the ability to decrease the synthesis of 5-HT suggests the induction of a desensitisation process of 5-HTR1A autoreceptors, corresponding to a down-regulation of the inhibitory feedback mechanism regulating 5-HT synthesis (Esteban et al., 1999; Moret and Briley, 1992). In this context, 5-HTR1A and TPH seem to be a non-direct target of SSRIs. For a deeper understanding of the mechanism induced by acute exposure to SSRIs, see Box Figure 7.1.



Box Figure 7.1. Schematic representation of the reduction of 5-hydroxytryptophan (5-HTP) in 5-HT producing cells induced by treatment with SSRIs. 1. Addition of the SSRI, which binds to SERT. 2. SSRI inhibits the reuptake of 5-HT leading to an increase in 5-HT concentration at the synaptic level. 3. 5-HT binds to 5-HTR1A autoreceptor, which inhibits TPH. 4. TPH inhibition results in a decrease in 5-HTP concentration. Images adapted from Servier Medical Art, licensed under CC BY 4.0 (<https://smart.servier.com>).

Data found in rats appear to align with results shown here, suggesting that even in *M. galloprovincialis* the two 5-HTRs type 1A identified (5-HTR1A1_inv and 5-HTR1A2_inv), which display colocalisation within TPH area, could act as autoreceptors. Indeed after 48 h of exposure to 100 µg/L FLX and CIT, a decrease in TPH expression was observed in treated larvae. This could align with a reduced production of 5-HTP, thus mitigating the effects of increased 5-HT synaptic levels. When *M. galloprovincialis* larvae were treated with exogenous 5-HT, the phenotypes displayed were more severe than those caused by incubation with FLX and CIT, resulting in fewer than 50% normal D-larvae. The most abundant phenotypes were protruding mantle and malformed hinge. However, it must be considered that by adding exogenous 5-HT, the concentration likely increases throughout the entire larval body, whereas in larvae treated with SSRIs, the 5-HT concentration may increase only in the area of serotonin producing cells. This localised increase in 5-HT concentration might result in a milder phenotype compared to a more widespread rise in 5-HT levels. Moreover, it should be noted that the 5-HT concentrations tested and found effective (1 and 10 µM) were more than 2 and 20 times higher in terms of µg/L (212.68 µg/L and 2126.8 µg/L) compared to the FLX and CIT concentrations tested. In contrast, 0.1 µM 5-HT (21.268 µg/L) induced no significant effects on D-Veliger larvae. However, a direct comparison between these treatments is not possible, as the local concentration of 5-HT after SSRI exposure remains unknown.

Further experiments are crucial to explore these mechanisms, particularly the decrease of 5-HTP and increase of 5-HT concentration after SSRI exposure. High-Performance Liquid Chromatography (HPLC) could be used to measure 5-HTP and 5-HT concentrations in larvae; in fact, HPLC coupled with Mass Spectrometry (MS) has already been employed to analyse lipid composition in *M. galloprovincialis* larvae (Balbi et al., 2023b).

7.3.4 Expression of nfr proteins suggests a role in larval development and transport of SSRIs

In this study, 19 different proteins were identified and share similarities with the NRF proteins identified in *C. elegans*. As in *C. elegans*, these proteins display the domain called NRF, along with an additional domain: either the Peptidoglycan/LPS O-acetylase domain or the Acyltransferase domain (Choy et al., 2006; Choy and Thomas, 1999). Transcriptomic and HCR analyses revealed, for the first time, the expression and localisation of nfr transcripts during embryo-larval development of a bivalve mollusc. Nfrs are differentially expressed during *M. galloprovincialis* embryo-larval development, with up to six genes expressed during embryonic and gastrula stages (Embryonic phase, Figure 7.4) and up to fifteen genes expressed during larval development (Early- and Mature Trochophore, Early- and D-veliger phases, Figure 7.4). HCR analysis at D-Veliger stage (48 hpf) revealed that three of these transcripts (nfr-1, nfr-6 and nfr-9, which peaked during the early- and D-Veliger phases) localised in the region of the gut cavity (Figure 7.5). Just one of the nfr protein here analysed seemed to be localised in what should correspond to the velum area (Figure 7.5) (Miglioli et al., 2024).

This study showed that proteins sharing the NRF domain were present in the genome of various organisms across different evolutionary levels (*D. melanogaster*, *S. purpuratus*, *B. lanceolatum*, *C. intestinalis* and *D. rerio*) but not in humans (Figure 7.6), consistent with earlier findings by Choy and Thomas (1999). Interestingly, among all the species analysed, *M. galloprovincialis* and *B. floridae* display the highest number of nfr proteins. However, due to the limited information available on these proteins, it is difficult to establish a possible evolutionary process. Nonetheless, the data suggest a reduction in the number of these proteins in chordates (Figure 7.6).




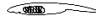




Dueterostomia	Chordata	Vertebrata	<i>H. sapiens</i>		<input type="checkbox"/>	0
			<i>D. rerio</i>		<input checked="" type="checkbox"/>	1
		Urochordata	<i>C. intestinalis</i>		<input checked="" type="checkbox"/>	3
			Cephalochordata	<i>B. floridae</i>		<input checked="" type="checkbox"/>
Ambulacraria	Echinodermata	<i>S. purpuratus</i>		<input checked="" type="checkbox"/>	12	
Protostomia	Lophotrochozoa	Mollusca	<i>M. galloprovincialis</i>		<input checked="" type="checkbox"/>	19
	Ecdysozoa	Arthropoda	<i>D. melanogaster</i>		<input checked="" type="checkbox"/>	12
		Nematoda	<i>C. elegans</i>		<input checked="" type="checkbox"/>	7

Figure 7.6. Table of presence/absence and number of nrf genes/proteins across different species at different evolutionary levels.

This work is the first to show that nrf genes are expressed during the embryo-larval development of a bivalve mollusc. Interestingly, a recent study identified a transcript corresponding to these genes, expressed exclusively in the sporocyst stage of the human parasite *Schistosoma mansoni* (plathelminth), but not in other developmental stages (miracidium, schistosomulum and adult) (Diaz Soria et al., 2024). However, there are no current insights into their potential role during early developmental stages.

Information on the possible role of nrf genes/proteins remains limited to *C. elegans*. Nrfs were first discovered and characterised by Choy and Thomas (1999) while investigating other possible targets of FLX. In *C. elegans* exposed to FLX, the animals exhibited behavioural phenotypes such as nose contraction and egg laying, with the nose contraction independent of any increase in serotonin levels (Choy and Thomas, 1999). By generating mutant lineages, Choy and Thomas (1999) identified seven genes that conferred partial resistance to fluoxetine, hence named Nose Resistant to Fluoxetine. These genes were also responsible for resistance to PAR and Clomipramine (a tricyclic antidepressant). Initial research on two of these genes revealed that both encoded twelve transmembrane domain proteins (Choy and Thomas, 1999). The nrf genes were studied in terms of spatial localisation (nrf-5, nrf-6 and ndg-4), and two were found to be localised in both the hypodermis of the nose and the intestine (nrf-6 and ndg-4), and one localised exclusively in the intestine (nrf-5) (Choy et al., 2006; Choy and Thomas, 1999). The localisation in the intestine aligns with HCR results here shown. Subsequent studies focused on the analysis of the product of nrf-5, which displayed similarity to human proteins involved in the immune system, cholesterol metabolism and transport. Sequence analysis predicted nrf-5 to be a secreted molecule, likely promoting the recognition of apoptotic cells and facilitating the transport of lipoproteins associated with cholesterol by binding to their lipid moieties (Choy et al., 2006; Watts and Browse, 2006; Zhang et al., 2012). Additionally, the

ability to transfer lipidic molecules was also predicted for *nrf-6* and *ndg-4* (Watts and Browse, 2006). Taken together, these findings suggest that these proteins play a role in the transport of yolk proteins, polyunsaturated fatty acids (PUFAs), and cholesterol by binding to their lipid moieties (Choy et al., 2006; Watts and Browse, 2006; Zhang et al., 2012). This function suggests they may also participate in the transport of FLX within the organism (Watts and Browse, 2006); indeed SSRIs, SNRIs and tricyclic antidepressants are amphipathic molecules (Kapoor et al., 2019), crucial characteristic for their transport through lipid-binding proteins such as *nrf*.

Although the functional characterisation of *nrf* proteins was not performed in this study, evidence from *C. elegans* suggests that if similar mechanisms operate in *M. galloprovincialis*, it could be plausible that *nrf* proteins bind and transport FLX across membranes. Furthermore, *nrf* proteins in *C. elegans* were shown to give resistance to PAR as well, suggesting that they may recognise and interact with various SSRIs, not just FLX.

7.3.5 Possible Molecular Initiating Events (MIEs) and Adverse Outcome Pathway (AOP) caused by SSRIs in *M. galloprovincialis*

SSRIs here analysed may bind to *M. galloprovincialis* SERT-like transporters. Moreover, a second possible target could be represented by *nrf* proteins as previously found in *C. elegans* (Choy et al., 2006; Choy and Thomas, 1999; Zhang et al., 2012). In addition to this, a third possible target is represented by 5-HTRs, even though it is still unknown how SSRIs bind to 5-HTRs (Kullyev et al., 2010). Thus, three possible molecular initiating events (MIEs) may be induced by FLX and CIT in *M. galloprovincialis* by binding SERTs-like, *nrf* proteins and 5-HTRs (Figure 7.7).

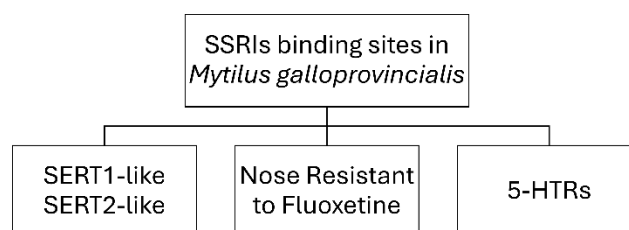


Figure 7.7. Schematic representation of the molecular initiating events (MIEs) of SSRIs in *M. galloprovincialis*.

Given the MIEs of SSRIs and the effects described in *C. elegans* and in rats after exposure to SSRIs, a tentative Adverse Outcome Pathway (AOP) of FLX and CIT in *M. galloprovincialis* is schematised in Figure 7.8. The first step is the Molecular Initiating Event (MIE) which consists of the binding of FLX and CIT to SERTs-like, and, perhaps, to nrf and 5-HTRs. However, the binding sites of SSRIs to nrf and 5-HTRs are not known, thus a question mark is reported in their respective MIE box (Figure 7.8).

Our results show that both FLX and CIT led to a decrease in the number of TPH positive cells. It could be possible that, after the MIE, the key event is represented by disruption of serotonin signalling during development, resulting in malformed larvae (Figure 7.8).

The weak effects observed for FLX and CIT could potentially be explained by the temporal expression patterns of the two SERT-like transporters during development. As shown in the previous chapter, the first SERT to be expressed is the SERT2-like, which peaked during the Trochophore phase (24 hpf), while the SERT1-like peaked later, during the D-Veliger phase (48 hpf). Since proteomic data on SERT-like transporters expression are unavailable, it can be hypothesised that if the protein only begins to appear in larvae after the RNA peak, the actual targets of SSRIs might not be expressed until the trochophore stage. This would limit the potential interaction of FLX and CIT towards their targets, thereby reducing their overall effects. In contrast, different nrf transcripts were already expressed in the egg and others appeared and peaked throughout embryo-larval development. It could be possible that some nrf products could be already present at the egg stage and in the following embryonic stages. If these proteins are involved in the transport of FLX and CIT, amphipathic molecules containing a hydrophobic body, these compounds should be less available in developing tissues of *M. galloprovincialis* embryo-larvae, thus preventing adverse effects. In this case, nrf proteins could protect from partially lipophilic xenobiotics, which would explain the weak effects induced by both SSRIs tested even at high concentrations (max 100 µg/L). Nevertheless, further experiments are required to confirm these hypotheses and the possible AOP caused by FLX and CIT in *M. galloprovincialis*.

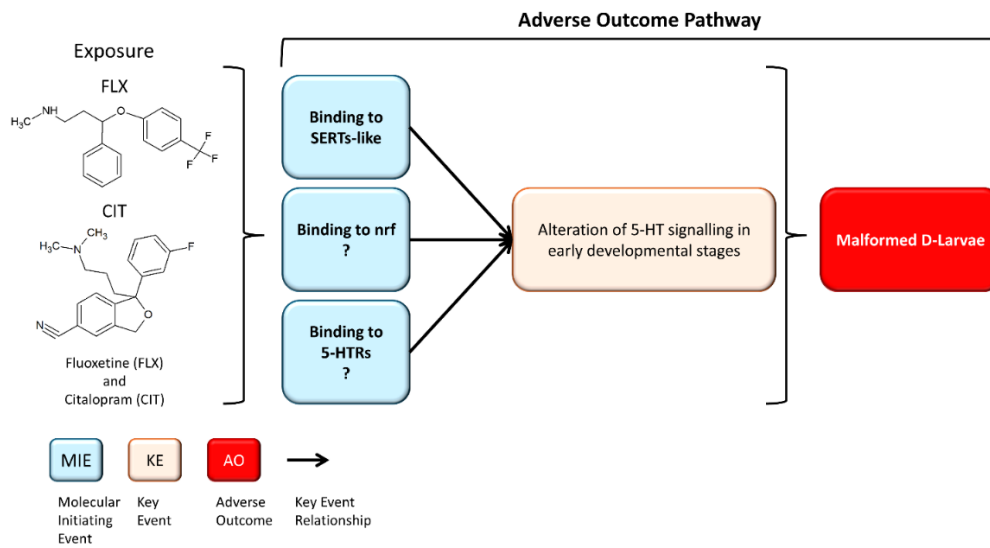


Figure 7.8. Schematic representation of the possible AOP caused by FLX and CIT in *M. galloprovincialis* larvae. The colour coding of boxes is described in the image legend.

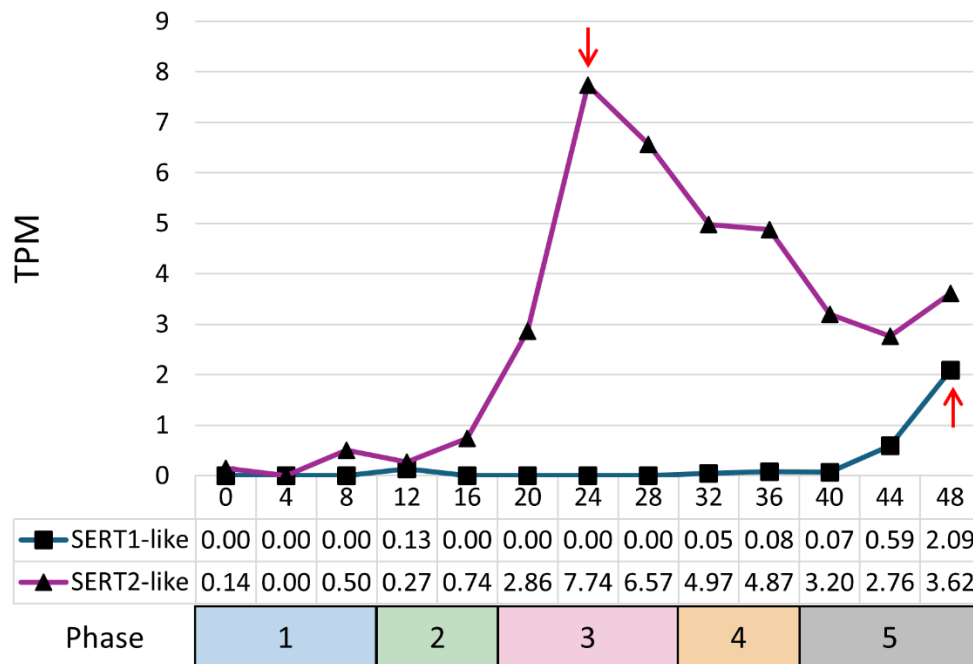
7.4 Supplementary Table

Species	NCBI ID	Domain
<i>D. melanogaster</i>	NP_001285060.1	NRF; OafA
	NP_608323.1	NRF; OafA
	NP_608590.2	NRF; OafA
	NP_727670.1	NRF; OafA
	NP_650959.2	NRF; OafA
	NP_001259710.1	NRF; OafA
	NP_651159.3	NRF; OafA
	NP_651158.1	NRF; OafA
	NP_001286373.1	NRF; OafA
	NP_996269.2	OafA; NRF
	NP_651160.3	NRF; OafA
	NP_001284731.1	NRF; OafA
<i>S. purpuratus</i>	XP_030831669.1	OafA; NRF
	XP_030831493.1	OafA; NRF
	XP_030851059.1	OafA; NRF
	XP_001198703.3	OafA; NRF
	XP_030830004.1	Acyl_transf_3; NRF
	XP_030841635.1	Acyl_transf_3; NRF
	XP_030840416.1	OafA; NRF
	XP_030841026.1	Acyl_transf_3
	XP_792732.4	OafA; NRF
	XP_030829546.1	OafA; NRF super family
	XP_011672917.2	OafA; NRF super family
XP_011672918.2	OafA; NRF	
<i>B. lanceolatum</i>	XP_035683589.1	NRF; OafA
	XP_035698599.1	NRF; OafA
	XP_035683620.1	NRF; OafA
	XP_035700320.1	NRF; OafA
	XP_035658030.1	NRF; OafA
	XP_035700321.1	NRF; OafA
	XP_035686734.1	NRF; OafA
	XP_035678860.1	NRF; OafA
	XP_035692129.1	NRF; OafA
	XP_035696988.1	Acyl_transf_3; NRF
	XP_035696984.1	Acyl_transf_3; NRF
	XP_035696985.1	Acyl_transf_3; NRF
	XP_035687103.1	OafA; NRF
	XP_035687102.1	NRF; OafA
	XP_035687461.1	NRF; OafA
	XP_035660415.1	NRF; OafA super family

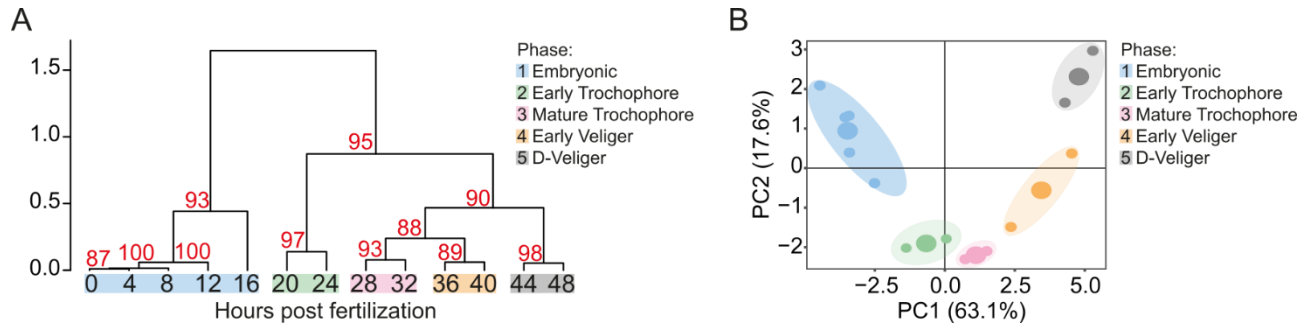
	XP_035657996.1	NRF
	XP_035690037.1	NRF
	XP_035683600.1	NRF
<i>C. intestinalis</i>	XP_002128751.1	OafA; NRF
	XP_009862304.1	NRF; OafA
	XP_026692261.1	NRF; OafA; OafA super family
<i>D. rerio</i>	XP_021324686.1	OafA; NRF
<i>H. sapiens</i>	-	-

Supplementary Table 13. List of nrf proteins identified through BLASTP in different bilaterian species.

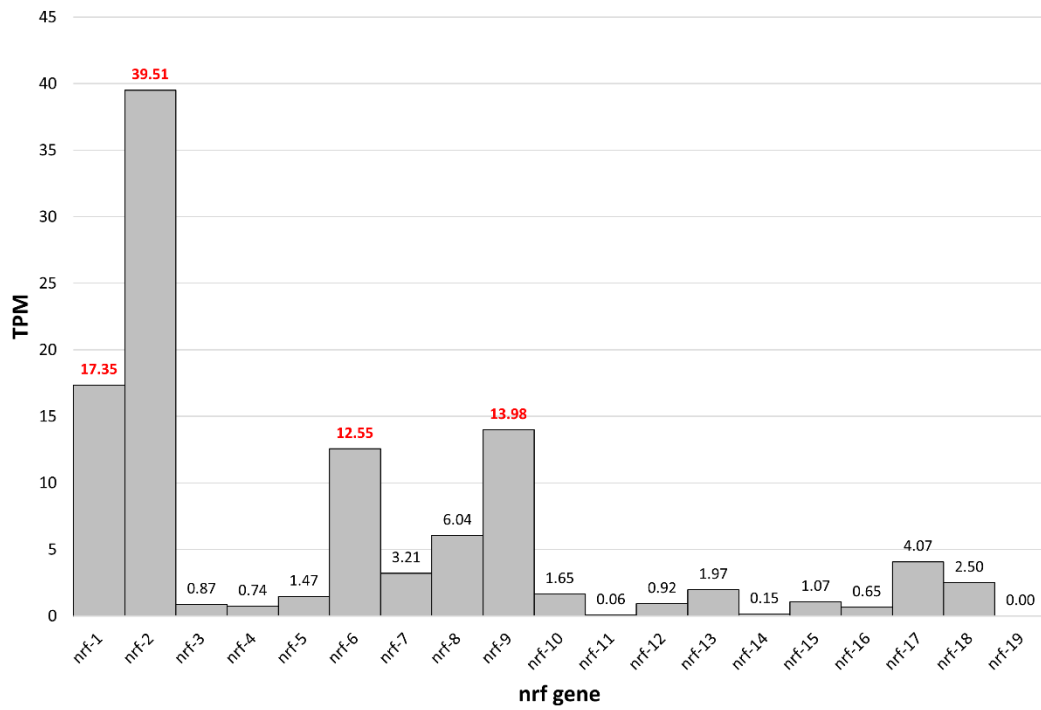
7.5 Supplementary Figures



Supplementary Figure 7.1. Graph showing the expression profiles (in TPM) of SERT1-like (blue) and SERT2-like (violet) during *M. galloprovincialis* embryo-larval development. TPM values are reported for each transcript under the hours post fertilisation (from 0 to 48 hpf). Phases previously identified are reported: Phase 1 = Embryonic Phase (0-8 hpf); Phase 2 = Gastrula Phase (12-16 hpf); Phase 3 = Trochophore Phase (20-28 hpf); Phase 4 = Early Veliger Phase (32-36 hpf); Phase 5 = D-Veliger Phase (40-48 hpf). Red arrows indicate the peak of expression of the two SERTs-like: at 48 hpf for SERT1-like and 24 hpf for SERT2-like.

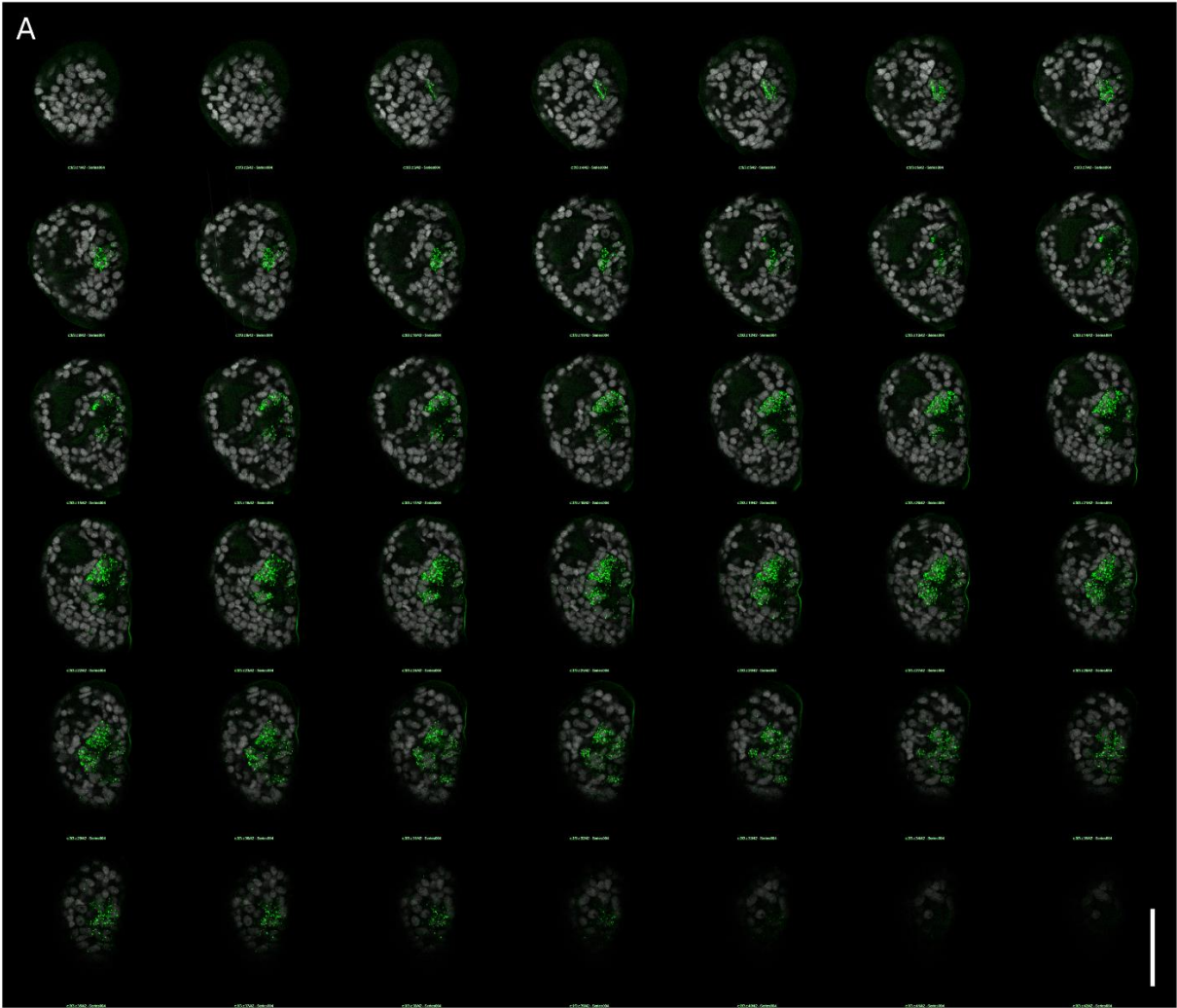


Supplementary Figure 7.2. Developmental expression dynamics of *nrf* genes. A. Hierarchical clustering of *nrf* genes from 0 to 48 hpf. Five phases were identified: phase 1 Embryonic (0 to 16 hpf), phase 2 Early Trochophore (20 to 24 hpf), phase 3 Mature Trochophore (28 to 32 hpf) and phase 4 Early Veliger (36 to 40 hpf) and phase 5 D-Veliger (44 to 48 hpf). The numbers in red represent approximate unbiased p-value (au). B. Principal Component Analysis (PCA) biplot of *nrf* genes in each sample analysed, samples were renamed in function of the phase identified in the hierarchical clustering. Ellipses highlight the five developmental clusters (corresponding to the phases 1, 2, 3, 4 and 5).

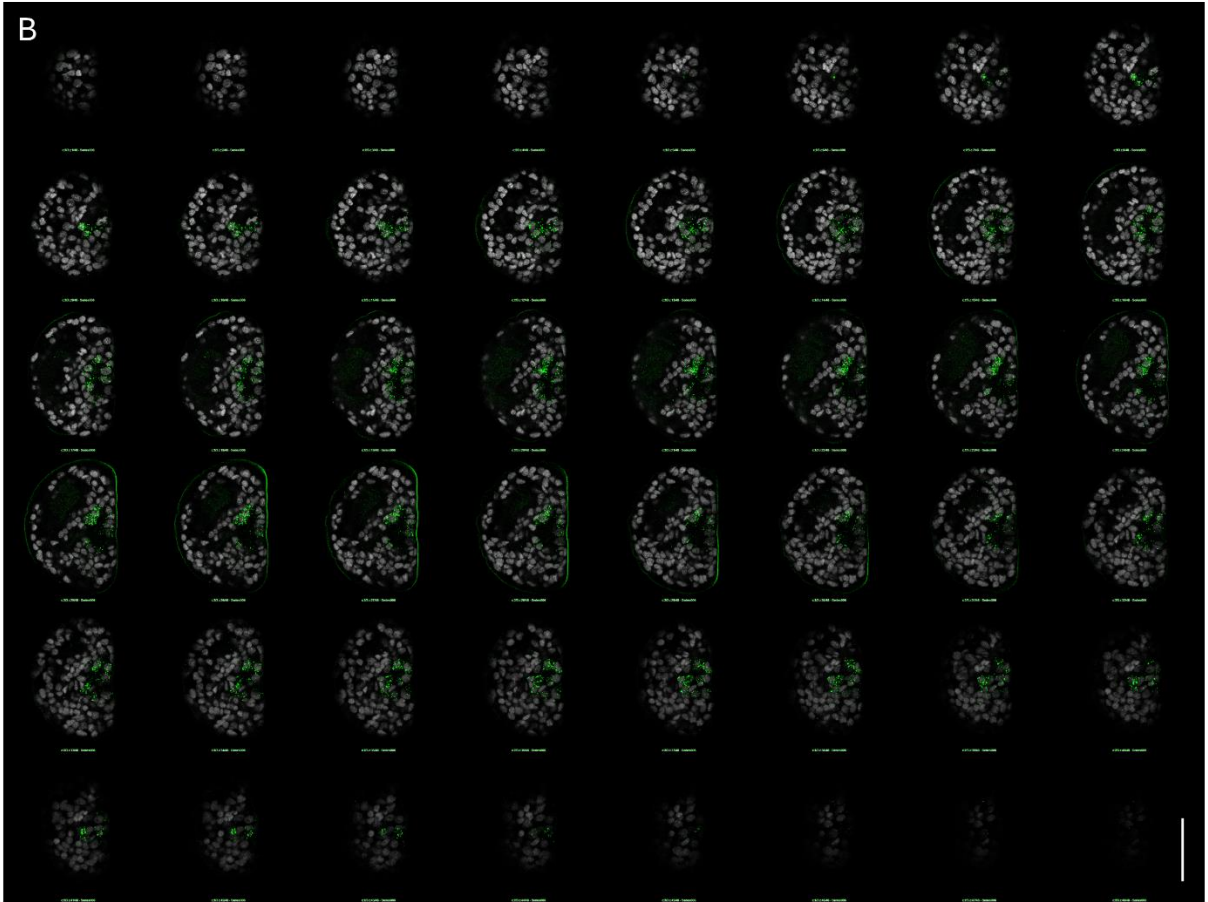


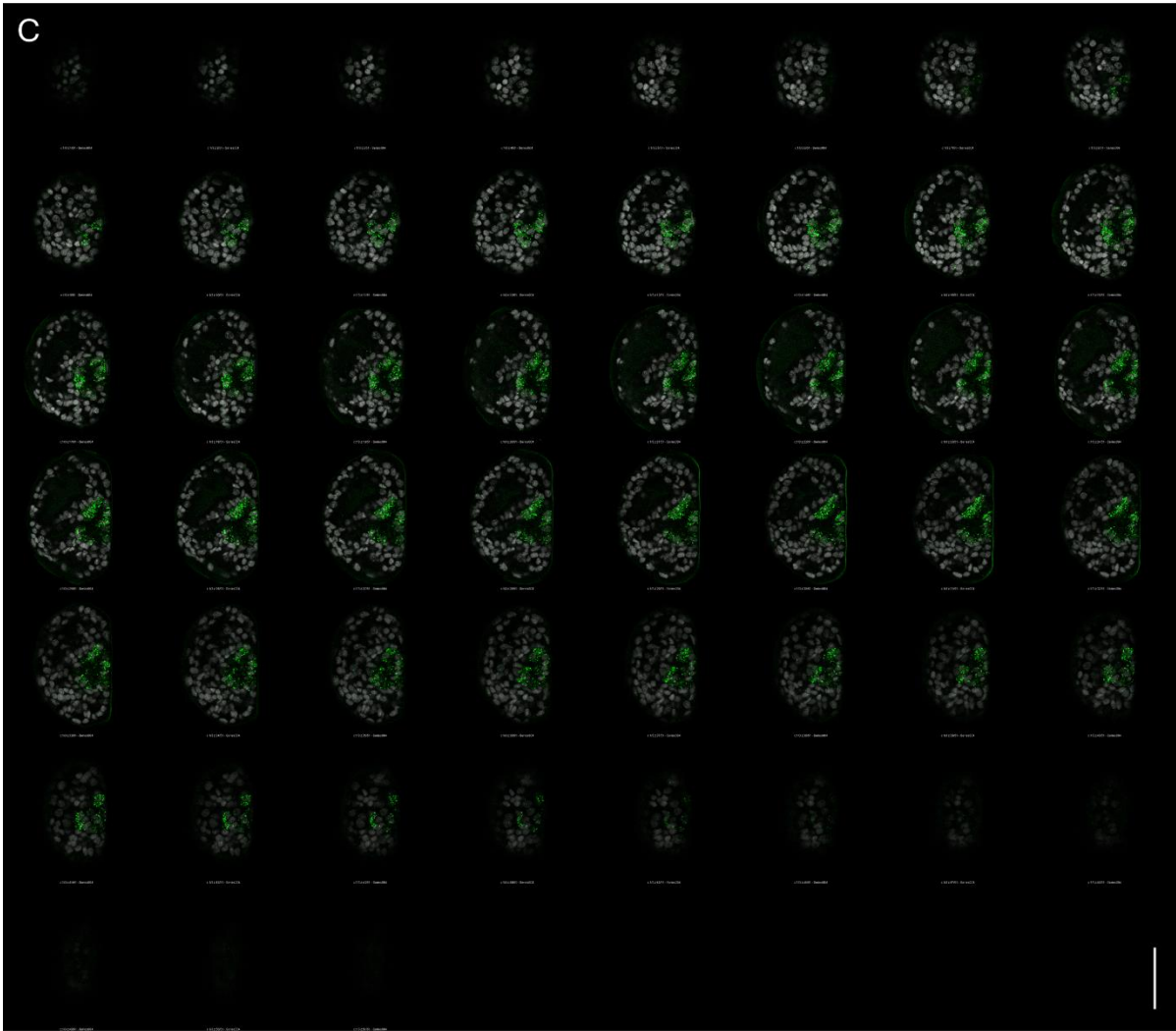
Supplementary Figure 7.3. Barplot showing the TPM values of the nineteen nrf genes identified at D-Veliger stage (48 hpf). Values at the bottom of the bars indicate the TPM value of each gene. Values in bold and in red highlight the gene chosen for HCR analysis.

A



B





Supplementary Figure 7.4. Localisation of nrf-1 (A), nrf-6 (B) and nrf-9 (C) in the larval body of D-veliger larvae (48 hpf). Montages show the nrf signal in green and Hoechst signal in grey. Scale bars: 50 μm .

8 Conclusions and future perspectives

1. Characterisation of the monoaminergic system in *M. galloprovincialis*

This work presents the first comprehensive study of the monoaminergic system in the Mediterranean mussel, *M. galloprovincialis*, with a focus to early developmental stages. Six out of the eight monoaminergic systems were found in *M. galloprovincialis* genome, which aligns with a recent published phylogenetic analysis (Goultly et al., 2023).

The expression analysis of the identified monoaminergic genes during embryo-larval development suggests a specific involvement of serotonin and dopamine, which stand out as the main systems expressed. Serotonin producing cells emerge at early stage, at Gastrula (16 hpf) in the area corresponding to the AO/CG, whereas dopamine producing cells appear later, at Trochophore stage (28 hpf) in an area corresponding to pedal ganglia PG.

Both neural and non-neural localisation of serotonin and dopamine receptors suggests that 5-HT and DA regulate developmental and physiological larval process mainly through neuroendocrine pathways.

Pharmacological experiments emphasised the fundamental role of 5-HT and DA, as the concentrations of 5-HT and the activity of the DR1 emerged as key players during the embryo-larval development of *M. galloprovincialis*.

The elevated expression of Aromatic L-Amino Acid Decarboxylase (AADC) at the egg stage, an enzyme involved in the synthesis of both 5-HT and DA, suggests a possible morphogenetic role for these two monoamines, potentially regulating cell cleavage.

Furthermore, expression of 5-HTRs and DRs prior to synthesis of 5-HT and DA in the growing embryo-larva raises the possibility of a non-neuronal role for these receptors, which could be involved in environmental sensing. In particular, these receptors may interact with exogenous ligands representing environmental clues, such as indole and its derivatives (Tomberlin et al., 2017). In addition to this, 5-HTRs could be involved in morphogenetic roles by regulating cell contractility and left-right patterning (Karki et al., 2023; Levin et al., 2006; Vandenberg et al., 2013).

Moreover, a potential mutual regulation between serotonin and dopamine producing cells could be hypothesised, with the two monoaminergic systems reciprocally controlling each other at the D-Veliger stage (48 hpf).

The characterisation of serotonin and dopamine components conducted in this study may contribute to a better understanding of their roles and help distinguishing the involvement of different receptor types in various processes occurring during embryo-larval development.

Future studies employing receptor-specific inhibitors and/or gene knockout experiments would be necessary to understand the precise roles of these receptors. Additionally, assessing the specificity of serotonin and dopamine receptors towards different ligands, including exogenous ligands present in the marine environment, could further elucidate their potential role in environmental sensing. To achieve this, competitive binding assays could be employed (Cao et al., 2020). Once the characterisation is accomplished, it would be interesting to create null mutants for each receptor to better understand their role in embryo-larval development of *M. galloprovincialis*, shedding thus more light on their possible morphogenetic function(s) in early developmental stages and their involvement in larval development.

2. Environmental implications

Monoamines, especially 5-HT and DA, appear to be pivotal for the larval development of bivalve molluscs, namely in the Pacific oyster, *C. gigas*, and in the Mediterranean mussel, to ensure proper shell biogenesis and larval development. Early larval stages of marine calcifying embryos are particularly sensitive to environmental stressors, such as ocean acidification, pollution, urbanisation, nutrient enrichment, sedimentation and parameters related to the ongoing global change (Balbi et al., 2017a; Miglioli et al., 2021a; Przeslawski et al., 2015). Among these, acidification, and exposure to contaminants have been shown to disrupt 5-HT and DA components, resulting in alterations of the molecular processes involved in shell biogenesis (Balbi et al., 2018, 2016; Liu et al., 2020; Miglioli et al., 2021a, 2021b).

Bivalve molluscs include species of ecological and economical importance, and they are used worldwide as sentinel organisms for monitoring marine pollution. Among mussels, the genus *Mytilus* is commonly used in biomonitoring marine pollution with a multi-biomarker approach. *M. galloprovincialis* is a key species in the Mediterranean and, along with other species, is used in acute (48 h) embryo toxicity essay (Balbi et al., 2017b; Fabbri et al., 2014; FAO, 2022; Miglioli et al., 2019). Given this context, understanding the onset of the monoaminergic system as possible target of pollutants and environmental changes is crucial to shed light on the potential targets for neuroendocrine disruption.

Among pollutants, contaminants of emerging concern (CEC) are raising particular attention, because they have now been recognised or suspected to be present in the environment and may

represent a threat to organisms (Sauvé and Desrosiers, 2014). Among CEC, pharmaceuticals are compounds designed to act on specific target (enzyme, receptor or transporter) that can be evolutionary conserved in other organisms (Ankley et al., 2010; Gunnarsson et al., 2008). Thus, information from mammals can be integrated to assess the potential environmental risks of pharmaceuticals through the conceptual model of known as “mode-of-action” (MOA) (Ankley et al., 2010). Among pharmaceuticals, Selective Serotonin Reuptake Inhibitors (SSRIs) are designed to bind to the serotonin reuptake transporter (SERT), inhibiting the recycling of 5-HT, and thereby increasing its concentration at the synaptic level (Andersen et al., 2014, 2009; Zhou et al., 2009).

In this study, thirteen out of sixteen amino acids involved in SSRIs binding (namely Citalopram – CIT, Fluoxetine - FLX, and Paroxetine – PAR) were found to be conserved in *M. galloprovincialis* SERT-like transporters suggesting that the two transporters identified may bind SSRIs. Furthermore, *in silico* analysis of the genome revealed the presence of non-selective targets of SSRIs: nineteen Nose Resistant to Fluoxetine (nrf) proteins, first identified in *Caenorhabditis elegans*, and serotonin receptors (5-HTRs) (Choy and Thomas, 1999; Kullyev et al., 2010). These potential targets were shown to be expressed during embryo-larval development of *M. galloprovincialis*. However, exposure to high concentrations of FLX and CIT did not strongly affect larval phenotypes, suggesting some mechanisms of resistance.

In this regard, one of the novelties of the present work is also represented by the identification of nrf proteins in mussel larvae. Nrf proteins were reported in *C. elegans* to act as binding and transporter proteins of lipidic molecules. In this light, the nrf proteins identified in mussel genome and their expression across early developmental stages, with localization near the digestive system indicate that these proteins could have a crucial role in *M. galloprovincialis* embryo-larval development. Characterising these proteins in terms of structure and function is thus required to understand if they might act in transport of SSRIs, which could explain the weak effect observed at high concentrations. Furthermore, it is also necessary to assess whether *M. galloprovincialis* 5-HTRs can bind to SSRIs and, if so, what responses are elicited.

This finding underlines particularly the need of drug elucidation, which refers to “the process of understanding the mechanisms of action of marketed drugs by studying their novel effects in model organisms” (Dwyer et al., 2014). *M. galloprovincialis* could represent a good model for screening and shedding light on the mode of action, targets and pathway affected by pharmaceuticals.

In conclusion, this study represents a significant advancement in understanding the monoaminergic system in *M. galloprovincialis*, revealing the presence of various monoaminergic systems and their potential crucial role in embryo-larval development. The results obtained offer new insights into the functions of serotonin and dopamine, highlighting their importance in regulating developmental processes and responding to environmental stressors. Additionally, the integration of data on the binding of SSRIs to serotonin receptors, transporters, nrf proteins and 5-HTRs may lay the groundwork for future research on the effects of SSRIs, and, potentially, other CEC on bivalves.

Annex

<i>Mg</i> annotation	Sequence ID	Amplifier	Probe sequence
<i>Mg</i> HTR1A1_inv	5- MGAL_10B032935	B1	GAGGAGGGCAGCAAACGGAAAAACAATATTTTATGAAAAGCGTG T
			TCTCTGCGATTTTTGTGAGTATTTGTAGAAGAGTCTTCCTTTACG
			GAGGAGGGCAGCAAACGGAAATAGGATTCAGCAAACCTATTA T
			AACTCGGGACTAAAAATTGTGTAAATAGAAGAGTCTTCCTTTACG
			GAGGAGGGCAGCAAACGGAATAGGCGGAAATTCATATTGCCTA A
			CCAACCAAAGCACTATCGAATGTAATAGAAGAGTCTTCCTTTACG
			GAGGAGGGCAGCAAACGGAACAACCAGCAAACAATGTATGCACC T
			TCCAATTAAGCTATCAGAAAAATTAGAAGAGTCTTCCTTTACG
			GAGGAGGGCAGCAAACGGAACCTCAGTTTCATTCTAATTTTT
			ATTATTCCAAGAGTCCGAGCTGCTTTAGAAGAGTCTTCCTTTACG
			GAGGAGGGCAGCAAACGGAAAAATCACCTTTGGTGTTGGAACCTG
			TTGCGCGTTTAGCTTTAGCAGCAATTAGAAGAGTCTTCCTTTACG
			GAGGAGGGCAGCAAACGGAAGTTGTCGTTCTTGCTGAACCTCCG
			TACCAAAGCATTTGAATGAACTTTTTAGAAGAGTCTTCCTTTACG
			GAGGAGGGCAGCAAACGGAATCAACGTTATGTCTGTTGAACAC G
			ACCATTCCATTGCACGAAGTTTCGTTAGAAGAGTCTTCCTTTACG
			GAGGAGGGCAGCAAACGGAATTAAGAACTACTTTTTGCAAGATC
			GACCATTAATAGGTGATGGCGGTGCTAGAAGAGTCTTCCTTTACG
			GAGGAGGGCAGCAAACGGAATTTATGAAAGTTTTCCGCCGAATT
			AACATTCCTGTTAGCCCGTATTGTTAGAAGAGTCTTCCTTTACG
			GAGGAGGGCAGCAAACGGAATAAATAATTAACATTACAACCTGTT G
			GATCTTGCTACTTGAAAAATTTAATAGAAGAGTCTTCCTTTACG
			GAGGAGGGCAGCAAACGGAACGGTGTAACGTCTATTTGGCTAAT
			AGTAAAAGGCACCAATTGTTGAAAATAGAAGAGTCTTCCTTTACG
			GAGGAGGGCAGCAAACGGAATGCATCGTCTTCCAACCAACAA A
			ACATTTTCCCGTGAATTCAGGCGCATAGAAGAGTCTTCCTTTACG
			GAGGAGGGCAGCAAACGGAACATGCCATGGCGATCATCAGCAGA A
			GGAATAGAAATAAACATTCCAACGTAGAAGAGTCTTCCTTTACG
			GAGGAGGGCAGCAAACGGAACAATGTTTGTAAACAGCCCAATATC G
			GCCTTGCAGTTCGATTTCTGATATATAGAAGAGTCTTCCTTTACG
			GAGGAGGGCAGCAAACGGAAGAAGATGTACAACACAAGACATC A
			AACAGATATTGCAACAAGATGTAATAGAAGAGTCTTCCTTTACG
			GAGGAGGGCAGCAAACGGAACCTAAAAACCACTTCACTAACC T
			GATATCCACATATCACAGACTTCACTAGAAGAGTCTTCCTTTACG
			GAGGAGGGCAGCAAACGGAATGGCTACCATCAGGTCCGCTACAG C
			ACACTACACTTAACGGCATCTAATAAGAAGAGTCTTCCTTTACG

			GAGGAGGGCAGCAAACGGAATGCAAGTTTTCTCCAGAATAATA
			AGATAATATCAAATAGTTCGCAACATAGAAGAGTCTTCCTTTACG
			GAGGAGGGCAGCAAACGGAAGTGGCTAATATCATTAGTCCTAATA
			GCTATCACAAAGACATTTCCGATTATAGAAGAGTCTTCCTTTACG
			GAGGAGGGCAGCAAACGGAATTTTGATTTGTGGACCACCAATTTT
			CGGAAGTCCGACTAAATGTGCAATAGAAGAGTCTTCCTTTACG
			GAGGAGGGCAGCAAACGGAAGTTGTATTGTAATAATGTTGTTAAT
			TGGTGTTCCTGTATTTTCTTGGTAGAAGAGTCTTCCTTTACG
			GAGGAGGGCAGCAAACGGAATCCCCATGTTTCATGTAGCTTCAA
			GCGTGTTAATATTTGCTTCATTAAGTAGAAGAGTCTTCCTTTACG
			GAGGAGGGCAGCAAACGGAAGGAATCTTACAAATATCGTTCGCA
			A ATCACACTCTGCTTATATGCTCCTGTAGAAGAGTCTTCCTTTACG
			GAGGAGGGCAGCAAACGGAACGTTTCGATTGCAACCTGATTGCGT
			GATTGCCTGGTGAATCTTACAAATTAGAAGAGTCTTCCTTTACG
			GAGGAGGGCAGCAAACGGAACCTTATGTGTAATGGAATTTGAAG
			A AGATGAATTTTGACCCGATAATCCATAGAAGAGTCTTCCTTTACG
			GAGGAGGGCAGCAAACGGAACAAAAGGGAGCAGTGAAGCAAT
			AA ATTATTGCATGGAAGCGTAACAGTTTAGAAGAGTCTTCCTTTACG
			GAGGAGGGCAGCAAACGGAACACCTGTAATAATTCCAAGAACCC
			G AAAATGGAAGCCAGCAGGCGATAAATAGAAGAGTCTTCCTTTACG
			GAGGAGGGCAGCAAACGGAATTTTGCTTTTCTCATTTTCTCTTTA
			TGCCTTACGTTCTCGTTTCATTTTATAGAAGAGTCTTCCTTTACG
			GAGGAGGGCAGCAAACGGAATTATTGTTTTCTGAAGATGTTTTCG
			TCTTTAATTTGATTTCTTTACTGCTAGAAGAGTCTTCCTTTACG
			GAGGAGGGCAGCAAACGGAATTGTGCGCACTGTTAAGTATTTGAG
			TTAGTGGTTTGTTAAATGAATACACTAGAAGAGTCTTCCTTTACG
			GAGGAGGGCAGCAAACGGAATAGCTGATAATCGGTAGGAACAGT
			T AGAATCAGATATGTTTCCAGTCCCGTAGAAGAGTCTTCCTTTACG
			GAGGAGGGCAGCAAACGGAACAAGACCCGTTATATACAGTGAAG
			C GTGTTTTCAAATTCAGGTCCATTTATAGAAGAGTCTTCCTTTACG
			GAGGAGGGCAGCAAACGGAATATGATGTGTAGTGACATCAGCGT
			T CTTGACTGACGTCCTCCGGATGATAGAAGAGTCTTCCTTTACG
			GAGGAGGGCAGCAAACGGAAGTACTTCCACTACTACTAAAATGC
			AATAGTCTGACATGGAATTGGTCTGTAGAAGAGTCTTCCTTTACG
			GAGGAGGGCAGCAAACGGAATATATTTTATAATTCAAAATAACA
			TTACGAATCCTCGATCTTGCAGCTGTAGAAGAGTCTTCCTTTACG
			GAGGAGGGCAGCAAACGGAACAGTGGAAAGAAGTGTATGCGT
			A GAATCATAGGACAATAAAAAGCGCCTAGAAGAGTCTTCCTTTACG
			GAGGAGGGCAGCAAACGGAATTCGGGGTGTCTCTCTTTTTTC
Mg HTR1A2_inv	5- MGAL_10B063464	B1	

			TTGACTGATTAACAATTCCCAACATAGAAGAGTCTTCCTTTACG
			GAGGAGGGCAGCAAACGGAAACAGATACAATCCAACTATAACA A
			CCAAATAGAGGTGTGATAGAAATTATAGAAGAGTCTTCCTTTACG
			GAGGAGGGCAGCAAACGGAATTCGAATATAATCAATGTTGATAC
			TTATTAGTATTTGTTTTGCACAACGTAGAAGAGTCTTCCTTTACG
			GAGGAGGGCAGCAAACGGAAAAGATGCAGTATAGATGCCGTGCA G
			CCAAAACCGATCCAACGAAATTGCATAGAAGAGTCTTCCTTTACG
			GAGGAGGGCAGCAAACGGAACATAGTTCTGAGCCGAGGTACCAG A
			AGAACATCAAAAGATACCCACATATTAGAAGAGTCTTCCTTTACG
			GAGGAGGGCAGCAAACGGAAGCATAACTAAAACGGCTACCATTA A
			CACTCACCTGGTTGACGACACTTATTAGAAGAGTCTTCCTTTACG
			GAGGAGGGCAGCAAACGGAAGTTTGACACTCCTTGACAGACTGCGT
			GGTAACTGCTAAGGACAGAATTAATAGAAGAGTCTTCCTTTACG
			GAGGAGGGCAGCAAACGGAATTTCCAAGTATCGTCGAAAAGTATC A
			AAAACGATAGCAGCAATCACAAAAATAGAAGAGTCTTCCTTTACG
			GAGGAGGGCAGCAAACGGAAGGAGCTGGTTGGATAGTACTGAT C
			GCATGGTGTCTCTAAGCTAACAGTATAGAAGAGTCTTCCTTTACG
			GAGGAGGGCAGCAAACGGAAGTTTTACGTTGAAGCGTATCATATT
			TTACTTAAACATCCAACGTGGACCCTAGAAGAGTCTTCCTTTACG
			GAGGAGGGCAGCAAACGGAATAAATGTTTTGTTAAACATGGTATA
			AAAGTATTAGCTTTTTAAAGGTCATTAGAAGAGTCTTCCTTTACG
			GAGGAGGGCAGCAAACGGAAGCCAAGCCATACGAAAAGTTGAAAT C
			GATAGGATTGATTGTGCTTGATAAGTAGAAGAGTCTTCCTTTACG
			GAGGAGGGCAGCAAACGGAAAAGGCTGAAGTTATGTTGACGATG A
			GTCTGACTAAAGAAGCATTTACTACTAGAAGAGTCTTCCTTTACG
			GAGGAGGGCAGCAAACGGAATAAATACTATTCTATGACTTTTGA
			ATGGTGCCAGCAGACTACAAATATTAGAAGAGTCTTCCTTTACG
			GAGGAGGGCAGCAAACGGAATTTTATCTCGCTCTTTAAGCTCC
			TTTCTGTTCACTGTAACATCATCTTAGAAGAGTCTTCCTTTACG
			GAGGAGGGCAGCAAACGGAAGCTGAGGGACTTGACAAATTAAG T
			TGATGTTCTTTATCAGTCTAGATATAGAAGAGTCTTCCTTTACG
			GAGGAGGGCAGCAAACGGAACCTTCTGTGAATGATACACAGAAC A
			CCTTTTATCCATTTACTGTTTAGTAGAAGAGTCTTCCTTTACG
			GAGGAGGGCAGCAAACGGAAAAGATACGGGGTATTCTTTTGAAT A
			CTTGTCAGGTGACACATCTCCTGGATAGAAGAGTCTTCCTTTACG
			GAGGAGGGCAGCAAACGGAATTTCTACCTGGCTTTCTACCTATCA
			AAAGTTAAGCTGGGACGTAATCGCTTAGAAGAGTCTTCCTTTACG
			GAGGAGGGCAGCAAACGGAACAATACTCCATTCCGAGATGTCA G
			GTGAAAAGTATTATCGGCATTCCCTAGAAGAGTCTTCCTTTACG
Mg 5-HTR2	MGAL_10B049511	B1	GAGGAGGGCAGCAAACGGAAGGAGCTGGTTGGATAGTACTGAT C
			GCATGGTGTCTCTAAGCTAACAGTATAGAAGAGTCTTCCTTTACG
			GAGGAGGGCAGCAAACGGAAGTTTTACGTTGAAGCGTATCATATT
			TTACTTAAACATCCAACGTGGACCCTAGAAGAGTCTTCCTTTACG
			GAGGAGGGCAGCAAACGGAATAAATGTTTTGTTAAACATGGTATA
			AAAGTATTAGCTTTTTAAAGGTCATTAGAAGAGTCTTCCTTTACG
			GAGGAGGGCAGCAAACGGAAGCCAAGCCATACGAAAAGTTGAAAT C
			GATAGGATTGATTGTGCTTGATAAGTAGAAGAGTCTTCCTTTACG
			GAGGAGGGCAGCAAACGGAAAAGGCTGAAGTTATGTTGACGATG A
			GTCTGACTAAAGAAGCATTTACTACTAGAAGAGTCTTCCTTTACG
			GAGGAGGGCAGCAAACGGAATAAATACTATTCTATGACTTTTGA
			ATGGTGCCAGCAGACTACAAATATTAGAAGAGTCTTCCTTTACG
			GAGGAGGGCAGCAAACGGAATTTTATCTCGCTCTTTAAGCTCC
			TTTCTGTTCACTGTAACATCATCTTAGAAGAGTCTTCCTTTACG
			GAGGAGGGCAGCAAACGGAAGCTGAGGGACTTGACAAATTAAG T
			TGATGTTCTTTATCAGTCTAGATATAGAAGAGTCTTCCTTTACG
			GAGGAGGGCAGCAAACGGAACCTTCTGTGAATGATACACAGAAC A
			CCTTTTATCCATTTACTGTTTAGTAGAAGAGTCTTCCTTTACG
			GAGGAGGGCAGCAAACGGAAAAGATACGGGGTATTCTTTTGAAT A
			CTTGTCAGGTGACACATCTCCTGGATAGAAGAGTCTTCCTTTACG
			GAGGAGGGCAGCAAACGGAATTTCTACCTGGCTTTCTACCTATCA
			AAAGTTAAGCTGGGACGTAATCGCTTAGAAGAGTCTTCCTTTACG
			GAGGAGGGCAGCAAACGGAACAATACTCCATTCCGAGATGTCA G
			GTGAAAAGTATTATCGGCATTCCCTAGAAGAGTCTTCCTTTACG

			GAGGAGGGCAGCAAACGGAATTGGACAGGTTTTCGACTCAACGAT
			TGATTGAAATCGTACATATGGACGGTAGAAGAGTCTTCCTTTACG
			GAGGAGGGCAGCAAACGGAACCTCTTTGACACTTTTTAGACTGTC
			CTCATTATAGGTTTACCATTATGATTAGAAGAGTCTTCCTTTACG
			GAGGAGGGCAGCAAACGAAAATAAAATCATGATGAAAAGTGGAA
			TGAGTAAATACAAAGTTATACTGTATAGAAGAGTCTTCCTTTACG
			GAGGAGGGCAGCAAACGAAAAAATGTTTGTGCTTAGAACACA
			GAAAGCACATATTGATCCATATATCTAGAAGAGTCTTCCTTTACG
			GAGGAGGGCAGCAAACGAAAACAAATCCTAGAATTGTAATCGGG
			CTCCACTTAAATATTTGACTCGTTAGAAGAGTCTTCCTTTACG
			GAGGAGGGCAGCAAACGGAATTATTATTTTTAATATCACAACAGT
			ATATTGTGACTGCTATAACCCATACTAGAAGAGTCTTCCTTTACG
			GAGGAGGGCAGCAAACGGAATCGTATAGCCATGAATCTTTCAAGT
			TGATTTATTACGGTTTGAAAGAGGTTAGAAGAGTCTTCCTTTACG
			GAGGAGGGCAGCAAACGGAAGTGCACATGAAGACATCAGCAGTC
			ATCGTACATAAATGAAGTATAGAAGTAGAAGAGTCTTCCTTTACG
			GAGGAGGGCAGCAAACGAAAACCACTGACCTGTAAATTCATTAAT
			AAAAATCACAAGAAGACTGGTCCAAATAGAAGAGTCTTCCTTTACG
			GAGGAGGGCAGCAAACGAAAAGTAAGTCAGTCACAGCGGAGAGA
			GCTAAGTGGCATAACTATAACACACTAGAAGAGTCTTCCTTTACG
			GAGGAGGGCAGCAAACGGAACGTTTTCTCCATAGATATAGCCATA
			AGAAAGTAATTGGTCACAGTTTGAATAGAAGAGTCTTCCTTTACG
			GAGGAGGGCAGCAAACGGAATTATCAACGGAGACCATAGTAATA
			CAAGTATATTTCCAGCAATTTCAAATAGAAGAGTCTTCCTTTACG
			GAGGAGGGCAGCAAACGGAATTTGTTGAGTTGGATGAATCGTT
			CCAGTTATACTCGGTCTCCATGCTATAGAAGAGTCTTCCTTTACG
			GAGGAGGGCAGCAAACGGAATATTCTGTTCCATTCTTTTACTAA
			TGGTTCAGCAGTAAATCCCATTGTATAGAAGAGTCTTCCTTTACG
			GAGGAGGGCAGCAAACGAAAAGACATTTCTGTAATAGGACTATG
			TTCATAAGTACTTCCGGCACTGAAGTAGAAGAGTCTTCCTTTACG
			GAGGAGGGCAGCAAACGGAATGTAAATGAACATCGGAATTGTCA
			TCATGGTTCAATGAAGAATTATTCGTAGAAGAGTCTTCCTTTACG
			GAGGAGGGCAGCAAACGGAAGAAGACTCCTTGGCATACTTTAAATGT
			TGTTGAATATGTCATCATTATACTCTAGAAGAGTCTTCCTTTACG
			GAGGAGGGCAGCAAACGGAATCTATTAATTTGATGAAAGGAA
			TAAACGTTTGAATGCTGTTTTGTATTAGAAGAGTCTTCCTTTACG
			GAGGAGGGCAGCAAACGGAACAAATCGCTGTTGTAAGAAAGTGCA
			TTAAGCATTGAATTAACATATCCCATAGAAGAGTCTTCCTTTACG
			GAGGAGGGCAGCAAACGGAACAATATTCAGTATGAAAATGGAA
			A
Mg 5-HTR4-like	MGAL_10B069739	B1	GAGGAGGGCAGCAAACGAAAAGACATTTCTGTAATAGGACTATG
			TTCATAAGTACTTCCGGCACTGAAGTAGAAGAGTCTTCCTTTACG
			GAGGAGGGCAGCAAACGGAATGTAAATGAACATCGGAATTGTCA
			TCATGGTTCAATGAAGAATTATTCGTAGAAGAGTCTTCCTTTACG
			GAGGAGGGCAGCAAACGGAAGAAGACTCCTTGGCATACTTTAAATGT
			TGTTGAATATGTCATCATTATACTCTAGAAGAGTCTTCCTTTACG
			GAGGAGGGCAGCAAACGGAATCTATTAATTTGATGAAAGGAA
			TAAACGTTTGAATGCTGTTTTGTATTAGAAGAGTCTTCCTTTACG
			GAGGAGGGCAGCAAACGGAACAAATCGCTGTTGTAAGAAAGTGCA
			TTAAGCATTGAATTAACATATCCCATAGAAGAGTCTTCCTTTACG
			GAGGAGGGCAGCAAACGGAACAATATTCAGTATGAAAATGGAA
			A

			G A A G C T T A T A T C C G A T C A A A G G A T C T A G A A G A G T C T T C C T T T A C G
			G A G G A G G G C A G C A A A C G G A A A G T G A T T G T C T T G G C G G C T T C G T T
			G C A G A C A C A A A A G C A A C C C A T A A T A T A G A A G A G T C T T C C T T T A C G
			G A G G A G G G C A G C A A A C G G A A T G T A A A T G A G C T T C T A A A C T A T G G
			A C G C T T A G T T T A C C T T T T T A T G T T T A G A A G A G T C T T C C T T T A C G
			G A G G A G G G C A G C A A A C G G A A A T A T C T T T A T A T T G C T T A G A A T T A G
			G T T G C G C T T G C T T T C T G G C T A C T T G T A G A A G A G T C T T C C T T T A C G
			G A G G A G G G C A G C A A A C G G A A T G A G C A A A T T A T C G A A A A T G G T T T
			G T A T A G C A G G A A T G T A A A A A G C T A T A T A G A A G A G T C T T C C T T T A C G
			G A G G A G G G C A G C A A A C G G A A G G C G G A A A A A G G C A A T C A T G C A G T
			T A C T A T G A A T C C A C A A A C T T C T T C A T T A G A A G A G T C T T C C T T T A C G
			G A G G A G G G C A G C A A A C G G A A A A T T G G A A G A A A T G A T A T G A A A A
			T C G A T T C C A A T G A G A T T C C A T T T A A A T A G A A G A G T C T T C C T T T A C G
			G A G G A G G G C A G C A A A C G G A A T C C A A T G A T G G T T T T G C T T A T T C G T
			C G T T A T C C A A C A A G C A G C C A A C A T T T A G A A G A G T C T T C C T T T A C G
			G A G G A G G G C A G C A A A C G G A A T A C C G G T C T A T C G C T A A A C A T G A A
			A T G T A A A A A T G G C C G A C A T A T A G C T A T A G A A G A G T C T T C C T T T A C G
			G A G G A G G G C A G C A A A C G G A A C A T C A A G A C T T G T A G T C A C T A G A C
			A G C A T G A T G G A T G T C G T C G T G A A C A T T A G A A G A G T C T T C C T T T A C G
			G A G G A G G G C A G C A A A C G G A A G T T A T A T T G T T G A T A T A T T C C A A A T
			A T C T T T A C C T A G C T G C C A C A C T T T A T A G A A G A G T C T T C C T T T A C G
			G A G G A G G G C A G C A A A C G G A A G C A A C C G A T A G G G A C A C A A C G A A T
			G A T T A C A A A T A C G G C C A C C A A T A A A T T A G A A G A G T C T T C C T T T A C G
			G A G G A G G G C A G C A A A C G G A A T G T A T A C C G C T A T T A T A A C T A A A G
			C T A G T T A T T G T C T G A A G A C G T T T A T G T A G A A G A G T C T T C C T T T A C G
			G A G G A G G G C A G C A A A C G G A A T G T C A A T A C T G C C G T C A A G A A A T A
			C A C C A C C A G C T G T C A A A A G T G G A A A G T A G A A G A G T C T T C C T T T A C G
			G A G G A G G G C A G C A A A C G G A A C C G G C A A C A T T T G C G A G T A T T C C T C
			G T T T C T T G G T C C A G A A A C G G T G G A G T A G A A G A G T C T T C C T T T A C G
<i>Mg 5-HTR6-like</i>	MGAL_10B033325	B1	G A G G A G G G C A G C A A A C G G a a T C T T G G A C T T T C C T G A A A G T G T T T C
			T T T T C T T A A T G G A A A C T G T T T A C A C t a G A A G A G T C T T C C T T T A C G
			G A G G A G G G C A G C A A A C G G a a A T T G C T T T T G A C G T A C A C C T T C C T G A
			G T T T T A A A G T A T G G A C A A C C G G T t a G A A G A G T C T T C C T T T A C G
			G A G G A G G G C A G C A A A C G G a a G A T T A A T T A A A C T G T T A C A A A T A A C C
			C T C G C A T G A A T A A A G G A T A T A T T A T t a G A A G A G T C T T C C T T T A C G
			G A G G A G G G C A G C A A A C G G a a C G G A A C A C A T T C A C A G A C C G A T T C G
			C C A T A C A A A T G C T A C A A A A C T T T A t a G A A G A G T C T T C C T T T A C G
			G A G G A G G G C A G C A A A C G G a a G T A A C A A C A T A T G C T A C A A C T A T A A
			A T G T T T G T A A T A A A A A A T G G C G C C C t a G A A G A G T C T T C C T T T A C G

			GAGGAGGGCAGCAAACGGaaAAGGTTCTCGAACATGTTTGGAAGT
			CTAATGTTACAGTTGCCTTATGAGTtaGAAGAGTCTTCCTTTACG
			GAGGAGGGCAGCAAACGGaaAACCATTAAGTTCTACAAATAAT
			GTTCTTTCTAATAATACGTTGCTTtaGAAGAGTCTTCCTTTACG
			GAGGAGGGCAGCAAACGGaaTAATACAACACAAGAGCTATTATTA
			TGTCTTTTAGCTTCTTTTGACTCTtaGAAGAGTCTTCCTTTACG
			GAGGAGGGCAGCAAACGGaaTAAACGCATACGGTACTCACTAT
			GAATTAGAATTGTAAGTGTGGAAGtaGAAGAGTCTTCCTTTACG
			GAGGAGGGCAGCAAACGGaaTGTCAAATCTTCAGTGTAGGTAAA
			CAGACATTGTGGTTTATTACTGATTtaGAAGAGTCTTCCTTTACG
			GAGGAGGGCAGCAAACGGaaACAAATGAAGAGAAAATTGCAATTC
			GGATTATGAAGTCCACTTATTATTGtaGAAGAGTCTTCCTTTACG
			GAGGAGGGCAGCAAACGGaaGACGATGTGTAATAATAGTTTTATA
			AAGCAGCTAGAAGCATGTATAGCGtaGAAGAGTCTTCCTTTACG
			GAGGAGGGCAGCAAACGGaaGTCGATACTAATTAACACACATTT
			GAGTGGAGTCATAATGGAAATATATtaGAAGAGTCTTCCTTTACG
			GAGGAGGGCAGCAAACGGaaAACGAGACCCAAATGGAACAAAAT
			G
			ACAGAAGCGCTAGTCAACATCACATtaGAAGAGTCTTCCTTTACG
			GAGGAGGGCAGCAAACGGaaCGTTTATTGCAGCCGGAATCATGAC
			GATGTAAAATCCATTCACCAAAAATtaGAAGAGTCTTCCTTTACG
			GAGGAGGGCAGCAAACGGaaTAATGAAAGTATAAACATATTAGAG
			GGTGCCAAACAATAAATCGGCCAAataGAAGAGTCTTCCTTTACG
			GAGGAGGGCAGCAAACGGaaGCTACTAAAACAATAACATTACCAA
			GTTCTTAGTTTTTTGTTTCGATGTCAtaGAAGAGTCTTCCTTTACG
			GAGGAGGGCAGCAAACGGaaCACATCCTGTGCCTATATTTTCAGA
			TTGTCATGGTAATGATAAAAAATAataGAAGAGTCTTCCTTTACG
			GAGGAGGGCAGCAAACGGaaTCCTATATTCAATCCGTGACTGTTA
			AATCACAGTTTTGACGGCGCCTCTtaGAAGAGTCTTCCTTTACG
			GAGGAGGGCAGCAAACGGaaACACACATGCTATTTTCGCACGTTA
			TTTGACAAATAATTCTGGTTCTCAataGAAGAGTCTTCCTTTACG
			GAGGAGGGCAGCAAACGGaaAAGTTCCTTTAATTTCTGGTAAACT
			TTTGAATTTAGTAGTTATGTTGAGtaGAAGAGTCTTCCTTTACG
Mg 5-HTR7	MGAL_10B020631	B1	GAGGAGGGCAGCAAACGGAAATTTCTCTAAATGAACTTCCGTGCGA
			TACTTTACTTTTCAGAAGGCGTCGAATAGAAGAGTCTTCCTTTACG
			GAGGAGGGCAGCAAACGGAAAGTAGGAGGTCGTAAACAATCTCTC
			A
			TGACTGTGCTATCGAACAACCGACGTAGAAGAGTCTTCCTTTACG
			GAGGAGGGCAGCAAACGGAAAGCTTTCTGAACGAATTCTCACATT
			TAGGATCTGGTCCATATTGCTCGACTAGAAGAGTCTTCCTTTACG
			GAGGAGGGCAGCAAACGGAACTTGAAAGGAGTTCGAAAATCCCT
			G
			TCCCTTGCAACGCAAGCATAATATTTAGAAGAGTCTTCCTTTACG

			GAGGAGGGCAGCAAACGAAAATGAATTAAGTATCCTAGCCAA T
			AACCTTGCCTAGATCACTGGGTTTCATAGAAGAGTCTTCCTTTACG
			GAGGAGGGCAGCAAACGGAACGTTATCTTCTACGAATGGTCTAAT
			AGACACTTATCATGTGGATTGGAATTAGAAGAGTCTTCCTTTACG
			GAGGAGGGCAGCAAACGGAACGCCGTAATCCACCCATTATAAAT
			GGCAAGAATAAAAAATGGCAACCAATAGAAGAGTCTTCCTTTACG
			GAGGAGGGCAGCAAACGGAATGCCAGATGATCTACGACCTTTTG
			AGTGTTTTAATAGCCTTCGAATCTTTAGAAGAGTCTTCCTTTACG
			GAGGAGGGCAGCAAACGGAATTTGAATTGAAGCACTATTTTTTGC
			AAATACTTTTAAGTGTAATCTACGTAGAAGAGTCTTCCTTTACG
			GAGGAGGGCAGCAAACGGAATTCCTATGGCAACCATTCTTTACG
			CATTTCTACTCTTTTCATCTTCATCTTAGAAGAGTCTTCCTTTACG
			GAGGAGGGCAGCAAACGGAATCAACAGAATTCGTCTTTACTCTAT
			CCGTTAGGTAAAACAGTACATCCCGTAGAAGAGTCTTCCTTTACG
			GAGGAGGGCAGCAAACGGAACAATACTGCCAAGCTGATTTGTACT
			AGTAATGAGCATTGCTTTGGACTTTTAGAAGAGTCTTCCTTTACG
			GAGGAGGGCAGCAAACGGAACATATTCTGTAGTAAACTGCCAAC A
			TTTTTTGCTAATCGAGAAGATACTCTAGAAGAGTCTTCCTTTACG
			GAGGAGGGCAGCAAACGAAAAGTTGCATAGATTTGATAGCCTA T
			CGAAAAGTGGAACGTAGAAGGCACCTAGAAGAGTCTTCCTTTACG
			GAGGAGGGCAGCAAACGGAACGGGTCTTCTTTCCATCCAAATAAA
			CTGGCTGATAATACACTCCCATTTATAGAAGAGTCTTCCTTTACG
			GAGGAGGGCAGCAAACGGAACATACACCGCAATCATTATGCC A
			GGAAGAGATATCAACACAGAGGAAGTAGAAGAGTCTTCCTTTACG
			GAGGAGGGCAGCAAACGGAAGAAAGGGCCGTGAATTACAAAAT A
			TTTTTGGTGTTCGTTTCATTGCATATAGAAGAGTCTTCCTTTACG
			GAGGAGGGCAGCAAACGGAAGATGGATGCTGTGCACAATATGAC A
			ATCAACTTATCATAATAAATTATAGAAGAGTCTTCCTTTACG
			GAGGAGGGCAGCAAACGGAATTTCCGAACGCCAATAGCTTAGC A
			AAAGAAGTAAACAAATCACAAATCATAGAAGAGTCTTCCTTTACG
			GAGGAGGGCAGCAAACGGAAGTACAGCAACTAAGAGGTCCGACA C
			GGTATGTAGTTACAAATGGCATCACTAGAAGAGTCTTCCTTTACG
			GAGGAGGGCAGCAAACGGAATGTTTGAAGCTTTTTACTATTCCC
			TAATGATAAAATGAGAAGATTTGAATAGAAGAGTCTTCCTTTACG
			GAGGAGGGCAGCAAACGGAATTTGTGCCTAAAACCATTAACGCA A
			GCTATACACTAAGCAATTTCCAATAGAAGAGTCTTCCTTTACG
			GAGGAGGGCAGCAAACGGAAGCGTGTAATAGATATTGGCGGGT C
			CTAACGTCCTAGTGCCTGCTGCCATAGAAGAGTCTTCCTTTACG
Mg DR1	MGAL_10B080807	B1	GAGGAGGGCAGCAAACGGAATAGTCTTTTGTGTTGAGCGCGTTT

			CAAAGCAGTTACCTTGTCTTTTCCTAGAAAGAGTCTTCCTTTACG
			GAGGAGGGCAGCAAACGGAAGAATAGGAATTGTTAGGACTACGAT
			ACGGTTCATCGTATACTCGGGTTTAGAAGAGTCTTCCTTTACG
			GAGGAGGGCAGCAAACGGAACACAAGACTTTGGAAATAAAATTC
			G
			CGTAACCGTTTCTATGTTCTATGGATAGAAGAGTCTTCCTTTACG
			GAGGAGGGCAGCAAACGGAAGATACTGTAAATAATAGGATTTAA
			G
			AAATGCGTCTCGGAATTCCTGATTGTAGAAGAGTCTTCCTTTACG
			GAGGAGGGCAGCAAACGGAATTTTGAATAGAATTAAGGAACA
			C
			GAATTTACGTATCCAAGCCATGTTATAGAAGAGTCTTCCTTTACG
			GAGGAGGGCAGCAAACGGAATGAAAAAGGCAACCAACAGAAT
			AA
			TACAAAATGCAGCTATAAGGTTGATTAGAAGAGTCTTCCTTTACG
			GAGGAGGGCAGCAAACGGAATGCTGCTTTGTGATCTTGCTAGAA
			TACACCTACAATAATTCCTCAAGTCTAGAAGAGTCTTCCTTTACG
			GAGGAGGGCAGCAAACGGAATGTGTTTTCTTTATACTTTTAAAT
			TTTTGCCACCACCAAATGTGGTGTAGAAGAGTCTTCCTTTACG
			GAGGAGGGCAGCAAACGGAATAATAGCTAACATTACAATACAAG
			G
			GACGTGCGTAGCAATATAACTGTATTAGAAGAGTCTTCCTTTACG
			GAGGAGGGCAGCAAACGGAATGAATACACTGGATTTAATCCAT
			G
			ATAAAAGCTGATTGTGGACGAAACATAGAAGAGTCTTCCTTTACG
			GAGGAGGGCAGCAAACGGAACGATCCTCTGCGTTCCTTATGCCACT
			CACACATTTTCTCCAATGGTTTGCTAGAAGAGTCTTCCTTTACG
			GAGGAGGGCAGCAAACGGAATAAGACATAATCCAAACCGCACTTA
			T
			AATGTATCGGGATGAACGAGATCGCTAGAAGAGTCTTCCTTTACG
			GAGGAGGGCAGCAAACGGAATTTCTCGTATCGGAATGGATCTCTA
			GGCGGCAATTTTCTTCCAGTTCATCTAGAAGAGTCTTCCTTTACG
			GAGGAGGGCAGCAAACGGAACACAGATTTAGTATGGAGGCTGTA
			G
			TGTATGTATCTATCGAGACTTATGATAGAAGAGTCTTCCTTTACG
			GAGGAGGGCAGCAAACGGAACACAAAATGTAGCTCCGAATATCC
			A
			ACATGATATCGCCAGATATCCAAATTAGAAGAGTCTTCCTTTACG
			GAGGAGGGCAGCAAACGGAACGTCATCACCAGGATAGCTACTAG
			T
			ATCAAGAATGTCATTGATAACAGCATAGAAGAGTCTTCCTTTACG
			GAGGAGGGCAGCAAACGGAATAATTAAGATGCTTTAAACGT
			C
			TCTGCTATAGCTAACGATACCAGTATAGAAGAGTCTTCCTTTACG
			GAGGAGGGCAGCAAACGGAATTTCCGACTATCGCTAGGATAAT
			CCGTAATAACGCAACGCAGACTAATAGAAGAGTCTTCCTTTACG
			GAGGAGGGCAGCAAACGGAATTTTTCAGCCAGTTGGTAGCCGTT
			TAGAGATAATATGGTCCCAATAATATAGAAGAGTCTTCCTTTACG
			GAGGAGGGCAGCAAACGGAACATTTGTGCTATTTATAGTATCAA
			GTTGCCTCTTCGTTTGTATTGTTTCGTAGAAGAGTCTTCCTTTACG

			GAGGAGGGCAGCAAACGGAAGGTCCAATATAGAAAAATTTGTTA T
			TTGTATAATTCGGACTATCCGAAGATAGAAGAGTCTTCCTTTACG
Mg DR2	MGAL_10B006356	B1	GAGGAGGGCAGCAAACGAAAATTGAAGTAGATGAACAGTTATT A
			TAGACGGTCTGTACATGTCACTGTGTAGAAGAGTCTTCCTTTACG
			GAGGAGGGCAGCAAACGGAAGGGCAGCATGCAAATAAAATTTTG C
			GTTTTTCTGTATTCAAAGTGTGTTTAGAAGAGTCTTCCTTTACG
			GAGGAGGGCAGCAAACGAAAAGAATATATAACCGGATTCATTC C
			AAGCTCGACGAAAATCTTTCATCGATAGAAGAGTCTTCCTTTACG
			GAGGAGGGCAGCAAACGGAATGGAAAGACTATTTCTGGAGATGT T
			GTTAATATATCCTAACCGTAAATTAGAAGAGTCTTCCTTTACG
			GAGGAGGGCAGCAAACGAAAATATTAACACAAAAAATGGCATC C
			CACGCCGTATGACAAATCCAATATAGAAGAGTCTTCCTTTACG
			GAGGAGGGCAGCAAACGGAATAAAGTTTTGCCGCCTTTGTTC
			ATATAATGAAAACACCAACAATATTAGAAGAGTCTTCCTTTACG
			GAGGAGGGCAGCAAACGAAAAGCAAAGTGTGTAATTTTCGAGT A
			GGCAATTTTGTCAATTTTTTGCTTTAGAAGAGTCTTCCTTTACG
			GAGGAGGGCAGCAAACGAAAATAGACGCACGTGCTGATTCTGGT G
			TTTTTAGCCTGTCTCCAGGTGATTTAGAAGAGTCTTCCTTTACG
			GAGGAGGGCAGCAAACGAAAATTTTCGTAGGTATTAGAATATTC
			AGCTCTGATTTTCAGGATCGATGACTAGAAGAGTCTTCCTTTACG
			GAGGAGGGCAGCAAACGGAAGTGAATTCGTAAGTCATGACCTC T
			CGATGATTGTGAGTCATTCCGCCCTAGAAGAGTCTTCCTTTACG
			GAGGAGGGCAGCAAACGAAAATTTAGATCCAATTTTAAACTCC
			TTACCATGACTACCATTGATGTTATAGAAGAGTCTTCCTTTACG
			GAGGAGGGCAGCAAACGGAATCCAATAAACGAACATCATTACGA A
			TTTGTGAGCGGCTGCTAAATATATTAGAAGAGTCTTCCTTTACG
			GAGGAGGGCAGCAAACGAAAAATATTAATAGGCACTATCTTCT
			AGGACAGTAAATGAAAACAAACGAATAGAAGAGTCTTCCTTTACG
			GAGGAGGGCAGCAAACGGAATTTGGAGTTACGGCTTTCCACCACG
			AAGAAACACATACCGCTTGGCAGATTAGAAGAGTCTTCCTTTACG
			GAGGAGGGCAGCAAACGAAAAAGCCAAACAAATGCAATCAATA G
			TAGCAGGAAATGAAATTCCTGCAGATAGAAGAGTCTTCCTTTACG
			GAGGAGGGCAGCAAACGAAAATACGCTATTGGATCGGAAATTGC C
			TACTTTGCATGATGACATTTTTGTATAGAAGAGTCTTCCTTTACG
			GAGGAGGGCAGCAAACGGAATTTAATATAGATGCAGTACTTGCCA
			TACCTATCAAGGGAAATGATACACATAGAAGAGTCTTCCTTTACG
			GAGGAGGGCAGCAAACGAAAATTCAGATCCAAATAGCCATACTT G
			CGTCAAACGAATGCCACATATCACATAGAAGAGTCTTCCTTTACG
GAGGAGGGCAGCAAACGGAACATTACAATACCTCCCACCATAAG A			

			TGTCAGTTC AAGACTA A TACTAAATTAGAAGAGTCTTCCTTTACG
			GAGGAGGGCAGCAAACGGAATTAGTTATTGTCCTTAAATATAACT
			GCAACAGCTAGTGATACTATGAAATTAGAAGAGTCTTCCTTTACG
			GAGGAGGGCAGCAAACGGAATCCCAAGAATTGTTACTAGTGAAA A
			TATAGACCGAAACGATAACAAGCAATAGAAGAGTCTTCCTTTACG
			GAGGAGGGCAGCAAACGGAATTTTAGATCATATTGGGAATTTGTA
			GGAAAGAACGGCACCAATAGCAGGATAGAAGAGTCTTCCTTTACG
			GAGGAGGGCAGCAAACGAAAGAAGTGATGAATTGTAATATATA A
			TTTGATGAATTTAAAGAAACCTACTAGAAGAGTCTTCCTTTACG
			GAGGAGGGCAGCAAACGGAAGATTGAGTAAGAAATAATCGTCCA G
			TTGTAGCGGCGTCCGTTTTATCCGATAGAAGAGTCTTCCTTTACG
			GAGGAGGGCAGCAAACGGAATGGTATTTCTCGTTGGTCGTCGTT
			TTTTTCTCCTTTGGATTATTACATAGAAGAGTCTTCCTTTACG
			GAGGAGGGCAGCAAACGGAATTGTATCGGATAATTCATCATTAA
			TGATTGATGTTGCTATTAGTCATTATAGAAGAGTCTTCCTTTACG
			GAGGAGGGCAGCAAACGGAATAATCAGTATATTCCGTATTGTAAA
			GAGATTGGTAATGGTATTTGTATGTAGAAGAGTCTTCCTTTACG
			GAGGAGGGCAGCAAACGGAAGAATGCTTTCCTGAATTCTGGATTA
			TTTGCAACAATCGGTCAAAATCTTTTAGAAGAGTCTTCCTTTACG
			GAGGAGGGCAGCAAACGGAACTATTTATGTACCCTAACAGACA A
			ATTGTGTAGATCGCTGGATTAAGAATAGAAGAGTCTTCCTTTACG
			GAGGAGGGCAGCAAACGGAATATTGGATTTTCCATGAGGTTAGA
			CACTAAC AAGGATCATATTCTGCTGTAGAAGAGTCTTCCTTTACG
			GAGGAGGGCAGCAAACGGAAGTTGATTGTGAAAAATGGAACCCA G
			AAATTTGATGCATATGGCGTTTGTTTAGAAGAGTCTTCCTTTACG
			GAGGAGGGCAGCAAACGGAATGTCTTTGTAGCTTTCTTTTCTC
			AAGAGGAAAACACCTAAGACGATGGTAGAAGAGTCTTCCTTTACG
			GAGGAGGGCAGCAAACGGAATACTCGTTCGTCTATGAAAATACTT
			TTGATGATGATTTTTTCTTTCTTTT TAGAAGAGTCTTCCTTTACG
			GAGGAGGGCAGCAAACGGAAGCGTTTACTGGTTTCGTGTCATTG
			TACAGTACGTTTCTCCTTTCGCCTCTAGAAGAGTCTTCCTTTACG
			GAGGAGGGCAGCAAACGGAATCTCCGGTTTTCCACGCCGTTCCG
			GGAATTA ACTGACACTTGTGTTCAATAGAAGAGTCTTCCTTTACG
			GAGGAGGGCAGCAAACGGAATTTCCATTTGAGTGTCTACATTACA
			ACGGTGTAGATGAAAAC TTTGTCTCTAGAAGAGTCTTCCTTTACG
			GAGGAGGGCAGCAAACGGAATTCTACATGTCTTACAGCAACTGGG
			TCCATTTCCATTGCCGTCAATTTGTTAGAAGAGTCTTCCTTTACG
			GAGGAGGGCAGCAAACGGAATCCACATCGTCAGCACTATCCGGA C
			ATAATTA ACTCTGCCTCCTTCTCCTTAGAAGAGTCTTCCTTTACG
			GAGGAGGGCAGCAAACGGAAGTTCACTAGAGTCGGTATTTGTGGC
<i>Mg</i> DR3-like	MGAL_10B006731	B1	GAGGAGGGCAGCAAACGGAAGAATGCTTTCCTGAATTCTGGATTA
			TTTGCAACAATCGGTCAAAATCTTTTAGAAGAGTCTTCCTTTACG
			GAGGAGGGCAGCAAACGGAACTATTTATGTACCCTAACAGACA A
			ATTGTGTAGATCGCTGGATTAAGAATAGAAGAGTCTTCCTTTACG
			GAGGAGGGCAGCAAACGGAATATTGGATTTTCCATGAGGTTAGA
			CACTAAC AAGGATCATATTCTGCTGTAGAAGAGTCTTCCTTTACG
			GAGGAGGGCAGCAAACGGAAGTTGATTGTGAAAAATGGAACCCA G
			AAATTTGATGCATATGGCGTTTGTTTAGAAGAGTCTTCCTTTACG
			GAGGAGGGCAGCAAACGGAATGTCTTTGTAGCTTTCTTTTCTC
			AAGAGGAAAACACCTAAGACGATGGTAGAAGAGTCTTCCTTTACG
			GAGGAGGGCAGCAAACGGAATACTCGTTCGTCTATGAAAATACTT
			TTGATGATGATTTTTTCTTTCTTTT TAGAAGAGTCTTCCTTTACG
			GAGGAGGGCAGCAAACGGAAGCGTTTACTGGTTTCGTGTCATTG
			TACAGTACGTTTCTCCTTTCGCCTCTAGAAGAGTCTTCCTTTACG
			GAGGAGGGCAGCAAACGGAATCTCCGGTTTTCCACGCCGTTCCG
			GGAATTA ACTGACACTTGTGTTCAATAGAAGAGTCTTCCTTTACG
			GAGGAGGGCAGCAAACGGAATTTCCATTTGAGTGTCTACATTACA
			ACGGTGTAGATGAAAAC TTTGTCTCTAGAAGAGTCTTCCTTTACG
			GAGGAGGGCAGCAAACGGAATTCTACATGTCTTACAGCAACTGGG
			TCCATTTCCATTGCCGTCAATTTGTTAGAAGAGTCTTCCTTTACG
			GAGGAGGGCAGCAAACGGAATCCACATCGTCAGCACTATCCGGA C
			ATAATTA ACTCTGCCTCCTTCTCCTTAGAAGAGTCTTCCTTTACG
			GAGGAGGGCAGCAAACGGAAGTTCACTAGAGTCGGTATTTGTGGC

			TTTGACCACTATCGTCGTCGTTATATAGAAGAGTCTTCCTTTACG
			GAGGAGGGCAGCAAACGGAAAATTAATAACTGGTTTGGGGCTTTG
			ATTACTGACATTGTCATCACAGACATAGAAGAGTCTTCCTTTACG
			GAGGAGGGCAGCAAACGGAAATCCATGCTCTTAGCTAAACCTGTTT
			GTATTGTATGTGGATATTTTACCATTAGAAGAGTCTTCCTTTACG
			GAGGAGGGCAGCAAACGGAAATTGTAGCGGTATTTTCTATAACTTT
			TAGTAGGCTCCGTTTTTGTGGCATTTAGAAGAGTCTTCCTTTACG
			GAGGAGGGCAGCAAACGGAACTTTTTCTTCTGTGCTTTTGACGA
			AGTGGATGTCTTTGTGCGTTTTTGCTTAGAAGAGTCTTCCTTTACG
			GAGGAGGGCAGCAAACGGAAAAAACATCATTATAATGGAAGGT A
			CGTAAAACCTCCATATTCGCCAGTTAGAAGAGTCTTCCTTTACG
			GAGGAGGGCAGCAAACGGAAAGAAAATCAGAATTAATAAATGCAC A
			AAAATGATCCCATGGAAGAATAAATTAGAAGAGTCTTCCTTTACG
			GAGGAGGGCAGCAAACGGAAAAACCTAATGCTATAGGTGCCGGC T
			GCCTGGCTTCCGTTCTTCGGAATAGTAGAAGAGTCTTCCTTTACG
			GAGGAGGGCAGCAAACGGAAAAACGTCAAAATACACGTTTGAA T
			GCTACGGAAATAACCCAAGTCAATGTAGAAGAGTCTTCCTTTACG
			GAGGAGGGCAGCAAACGGAAATCACTGCTATAAATCTATCTACACT
			TATGTTTCGAGTATTTGATTGGTTGTAGAAGAGTCTTCCTTTACG
			GAGGAGGGCAGCAAACGGAAACATGCCATGACGTCAGACGCCAC C
			GGCCGTAAATTTAATATAGAAGCTTAGAAGAGTCTTCCTTTACG
			GAGGAGGGCAGCAAACGGAAACATGACTGCGCAACCTCTAAGTAA A
			GCATCACATAACGCATCACTGAGTATAGAAGAGTCTTCCTTTACG
			GAGGAGGGCAGCAAACGGAAATTATGTCCGCTACGGCAAGGGAAC A
			CTGGTGGCATTACTACTACGGCGACTAGAAGAGTCTTCCTTTACG
			GAGGAGGGCAGCAAACGGAAATCTTTCACGAACAACACTCATAAC G
			AAAATAATTCGTGGCTGTTTCAACTAGAAGAGTCTTCCTTTACG
			GAGGAGGGCAGCAAACGGAAAGGGAAAAACAATAATGCGAAAAG CC
			AGGACGTTTCCAAACACAGTTAAAATAGAAGAGTCTTCCTTTACG
			GAGGAGGGCAGCAAACGGAACTCTGTAGAATTAAGAAAATCAC C
			ATCTGTTGGCAGCAAGTACATCTGTTAGAAGAGTCTTCCTTTACG
			GAGGAGGGCAGCAAACGGAAATAACCCTGTCGTCACCTCCGCTGTG
			AGTGTTTAATGTTACCATATCTGTTTAGAAGAGTCTTCCTTTACG
			GAGGAGGGCAGCAAACGGAAAGACACCAGGTGTCGTTGTCATCA C
			TTTGATATCCATGACGTATCATTAAATAGAAGAGTCTTCCTTTACG
			GAGGAGGGCAGCAAACGGAAACGTAGTTCCAATATCAGCTGTGTT
			TGAACGGCCATAAGTCCGACATAGATAGAAGAGTCTTCCTTTACG
			GAGGAGGGCAGCAAACGGAAATTCATAATTTGATTGTCGTTTGGC
			CGTTGTGTCGGAATACCACGTTGTAGAAGAGTCTTCCTTTACG

Mg TPH	MGAL_10B020038	B2	CCTCGTAAATCCTCATCAAACGGTGTCTTCTGCTTCTCTTTCTGCC
			ATTCGATTTGATTTGTCTCGGAGTTAAATCATCCAGTAAACCGCC
			CCTCGTAAATCCTCATCAAATGTTGTAACCGTCTGAGTGCATCAC
			AATTCCTCTCTTCTCTATTCTAAAATCATCCAGTAAACCGCC
			CCTCGTAAATCCTCATCAAATAACAGCATTGGCAATACAACGAGT
			CTATGCACAAATCGCCACGTAATTCAAATCATCCAGTAAACCGCC
			CCTCGTAAATCCTCATCAAATGGGTTATATCGGACAGCAAATGGT
			GTTAAGTACGTCAACAGTTTGTGTGAAATCATCCAGTAAACCGCC
			CCTCGTAAATCCTCATCAAACCTGTCCTTTGCCTTTCAAAGCTTT
			TTAATAGTACAAGCATATTGCCTCAAATCATCCAGTAAACCGCC
			CCTCGTAAATCCTCATCAAATTATAAGACATTCCTGTTTAGATGT
			TATAAAAGTAAACATCTTGAAAAGTAAATCATCCAGTAAACCGCC
			CCTCGTAAATCCTCATCAAACCTGTCAGTTAATGCATGCTTAAGT
			AACTGGTTCAAATGGTATTTTCTTGAAATCATCCAGTAAACCGCC
			CCTCGTAAATCCTCATCAAATATACCCGCATAAGTCCGTCTTGTT
			CCAATAGAAGACAGAAGTCCAGCACAAATCATCCAGTAAACCGCC
			CCTCGTAAATCCTCATCAAAAAAGGTAGCTAATTTCTGTACTGC
			ATAATCCAAATTCAACAGTAAAGAAAAATCATCCAGTAAACCGCC
			CCTCGTAAATCCTCATCAAATAATTCTTGTGAGAAGTGTGCAAAG
			ATCACTGGCACCAAGTGATGCTAGCAAATCATCCAGTAAACCGCC
			CCTCGTAAATCCTCATCAAAAAGTAATTCGTGGCAACAATCAGGTT
			GGATCAGCTAATAGTGGCATGTGTCAAATCATCCAGTAAACCGCC
			CCTCGTAAATCCTCATCAAATTATATACTGTGTACAATGAAACAC
			GTGTATATAAGGGATCAGAACTATGAAATCATCCAGTAAACCGCC
			CCTCGTAAATCCTCATCAAATGATGTTAGGTAACCAGCAACTGGG
			GAAAGCCAAACCAGCAAGGAAATCAAATCATCCAGTAAACCGCC
			CCTCGTAAATCCTCATCAAAAATTCGACACATCCTCCAGTTGTG
			AGCTGAAATCCTGTTTTCTCTTTTAAAATCATCCAGTAAACCGCC
			CCTCGTAAATCCTCATCAAACCTGTTAGCTGAGGAATATTTCTTAA
			CATTATCTTTCCTATATCCACAAAAAATCATCCAGTAAACCGCC
			CCTCGTAAATCCTCATCAAACCTTCATCAGCTCCGTGAAAACAGTT
			TTCTCGACATGCGTGTGAAGGATACAAATCATCCAGTAAACCGCC
			CCTCGTAAATCCTCATCAAATCAATTCTAGGTATAGGTTCTCCAT
			CATGTTTAAATCTTCTTTCAGTATAAATCATCCAGTAAACCGCC
			CCTCGTAAATCCTCATCAAATTTTTCTCCTTAATCTATAAACCTT
			TGTACTTGAAAGCAATATCTGCAAAAAATCATCCAGTAAACCGCC
			CCTCGTAAATCCTCATCAAACCTCTGATCCGTACATCAATACTCTA
			TTTGAATCCCGGATGATCAGCATCAAATCATCCAGTAAACCGCC
			CCTCGTAAATCCTCATCAAACCTAGGAAACCACGGTATATTCTGTA
			GCAGACTTATCTAGGTCTGATACTTAAATCATCCAGTAAACCGCC

			CCTCGTAAATCCTCATCAAACGGTAGCCGGTGATGGCGGTATAGG
			CATCGTCTAAATAAGTAATACGTGAAAATCATCCAGTAAACCGCC
			CCTCGTAAATCCTCATCAAATTTCTTAAGTCGCTTGATTAATTCT
			ATCGTTGTATGATATACTGTTGACCAAATCATCCAGTAAACCGCC
			CCTCGTAAATCCTCATCAAAATATAAATATCATACATAGAATCAC
			AGTCGGATGTTATCCGCTCTATATAAATCATCCAGTAAACCGCC
			CCTCGTAAATCCTCATCAAACAACATTGATATGGTGTTCTTGAAA
			GCCTTGACCTCCTGGATTCTATACGAAATCATCCAGTAAACCGCC
			CCTCGTAAATCCTCATCAAATAAGCTTCTACTTCGTTTTGAAGA
			CACCTTCAGTCTTTTTACTGCTCTTAAATCATCCAGTAAACCGCC
			CCTCGTAAATCCTCATCAAATTTCTAATTCTTGTATTGTTTTGTG
			AAATGCAAATACTGCATCGATACCTAAATCATCCAGTAAACCGCC
			CCTCGTAAATCCTCATCAAATTTTAATAGTGGCTGCATAGCGCTT
			AAGGATCATAGCGTACTTCAAATTGAAATCATCCAGTAAACCGCC
			CCTCGTAAATCCTCATCAAAAACCACAAAATAAATTGGCTGGATA
			TTTCTGCATCATGTCATCAAAGATAAATCATCCAGTAAACCGCC
			CCTCGTAAATCCTCATCAAATTCTCTGGATCGAATGGATATTTTT
			TCATCTGTATACACTTGTACTGAAGAAATCATCCAGTAAACCGCC
			CCTCGTAAATCCTCATCAAACCCCGTAAGATGACAACGTCCCAGC
			GTGCATCAGACAAGGCGTGTCTGTAATAATCATCCAGTAAACCGCC
			CCTCGTAAATCCTCATCAAAACATAGACCAAATTCACCGTAAAC
			ATATGCTCTTAGACTACCCTGTTCCAAATCATCCAGTAAACCGCC
			CCTCGTAAATCCTCATCAAAGCATCTGAGGCTCCAAGAGATGTCA
			TACAGGGTGGCGAATTTTTCAATATAAATCATCCAGTAAACCGCC
			CCTCGTAAATCCTCATCAAATTTGGATTCGCTAACATTGGCACGTG
			CTATTTCTTGTGAAAACCTGCGCAAAAAATCATCCAGTAAACCGCC
			CCTCGTAAATCCTCATCAAAAGGAGAGTGATCTGGTTTTGACCCA
			AAGCAACTCGTGAATACAATCTGGTAAATCATCCAGTAAACCGCC
			CCTCGTAAATCCTCATCAAACGATATGCAAGACTAGCTAAAAAGT
			CGAACATACTGGGTACACTGGAAAAAATCATCCAGTAAACCGCC
			CCTCGTAAATCCTCATCAAAGTAACTGGAACCTGTTCTTCGTTT
			GTGCTGATAATAAACCGGAAACTGGAAATCATCCAGTAAACCGCC
			CCTCGTAAATCCTCATCAAAAATTTTATCTTCACTATAACCACAA
			GAAATTAGATACATCTTCTAACTGTAATCATCCAGTAAACCGCC
			CCTCGTAAATCCTCATCAAATGTTCTTTACAAGCATGCGTTGGAA
			TGTTCTAGTATTTTGAAGTTCTCAAAAATCATCCAGTAAACCGCC
			CCTCGTAAATCCTCATCAAACCCATGTGTCATTTTCTTCTGTGT
			GATCTTGAAGATGTTTGTACACGTGAAATCATCCAGTAAACCGCC
			CCTCGTAAATCCTCATCAAATCTGTAATCGAATGCTATGTCTGCG
			TTCTACTCTGGGAATAAGTTGACCAAATCATCCAGTAAACCGCC
Mg TH	MGAL_10B068234	B2	

			CCTCGTAAATCCTCATCAAATCTGTATATCCCGGGTGATCACTGT
			ATTTTACGTCGTTCTCTGTACTTTTAAATCATCCAGTAAACCGCC
			CCTCGTAAATCCTCATCAAAGTGTGCAGTTATCTAGTTCTGAAAT
			GTTCCGGTTCAAACCTCGTGACAAGAAATCATCCAGTAAACCGCC
			CCTCGTAAATCCTCATCAAAAACCTTCTTGATCCGATACAATTGCA
			TCTTGAAACCAAATAACTTTATTTAAATCATCCAGTAAACCGCC
			CCTCGTAAATCCTCATCAAAGAATTAACATGTGACGTGATTCTAT
			TCAGCTATAGACGTGACCATGCGTAAAATCATCCAGTAAACCGCC
			CCTCGTAAATCCTCATCAAAACAAATTGTGCTCCGGATTTCCTGGA
			GTGACCCAACACATTTTATCAAAATAAATCATCCAGTAAACCGCC
			CCTCGTAAATCCTCATCAAACCTTGTATGCCTCAAATATTCTTAAG
			CCGTGATTTCGATGTGATCTATTATCAAATCATCCAGTAAACCGCC
			CCTCGTAAATCCTCATCAAATGCTAATAATCAAAGCACGGCAT
			CTGGACAGACTTGAAATACCATCTAAATCATCCAGTAAACCGCC
			CCTCGTAAATCCTCATCAAAATTCACCATTCTGTACAAATACTTC
			GAGGTTCTGTTTCAATTGGAGATATAAATCATCCAGTAAACCGCC
			CCTCGTAAATCCTCATCAAAACTTAATGCCTTTCTCGTTTTTCA
			TTCTTCTCACTGATAGAGTTTCTAAAATCATCCAGTAAACCGCC
			CCTCGTAAATCCTCATCAAAGCATCTCAATCAGACTCTCCGCC
			TCTAAATTTGTCACAGTTTCGAATTAATCATCCAGTAAACCGCC
			CCTCGTAAATCCTCATCAAAATTTTCTGGAAGGCAAGCCTCCTTTT
			ATGATCCTCCATGCTCTTGGCTATAAAAATCATCCAGTAAACCGCC
			CCTCGTAAATCCTCATCAAACCTACTACTATCAGATAGATAC
			CTCTAATGAAGTTTTGTTTTGAATGAAATCATCCAGTAAACCGCC
			CCTCGTAAATCCTCATCAAAGCAAACCTAACATCATCTGATGTAG
			CTTGACAATTCTTGTATAACTTTCCAAATCATCCAGTAAACCGCC
			CCTCGTAAATCCTCATCAAAAATAAATATCTCTAAACTTTGAAGG
			TAGAAGCACAAACAGCAAATCGTAGAAATCATCCAGTAAACCGC C
			CCTCGTAAATCCTCATCAAACGCCTTCAGCAGCATTTTCATTTCTA
			TAAATGTATTCTTCCATCTTCATTGAAATCATCCAGTAAACCGCC
			CCTCGTAAATCCTCATCAAAGACCCATTTTAACCTCTCTATAA
			TTTTTGCCCTTAAATCTGAAGCAAGAAATCATCCAGTAAACCGCC
			CCTCGTAAATCCTCATCAAACCTTAAACTCATGAGCCAATCTTAC
			CAAAATTATGGTCCGTCTTCACCAGAAATCATCCAGTAAACCGCC
			CCTCGTAAATCCTCATCAAACCTGACCAAACAATCTCAAGACAAAC
			CTTTCTAATGTTTTCTGAAGCCCTAAATCATCCAGTAAACCGCC
			CCTCGTAAATCCTCATCAAAAATGGTATGTGCCAATGCCTGTAAT
			AGCTTTAAAGACCTAAATCTTCTCAAATCATCCAGTAAACCGCC
			CCTCGTAAATCCTCATCAAAAATATAGTGGATCTACATTAATGC
			GAATTTTCTTGGTGATCATGTTTAAATCATCCAGTAAACCGCC
Mg AADC	MGAL_10B028036	B2	CCTCGTAAATCCTCATCAAACCTACTACTATCAGATAGATAC
			CTCTAATGAAGTTTTGTTTTGAATGAAATCATCCAGTAAACCGCC
			CCTCGTAAATCCTCATCAAAGCAAACCTAACATCATCTGATGTAG
			CTTGACAATTCTTGTATAACTTTCCAAATCATCCAGTAAACCGCC
			CCTCGTAAATCCTCATCAAAAATAAATATCTCTAAACTTTGAAGG
			TAGAAGCACAAACAGCAAATCGTAGAAATCATCCAGTAAACCGC C
			CCTCGTAAATCCTCATCAAACGCCTTCAGCAGCATTTTCATTTCTA
			TAAATGTATTCTTCCATCTTCATTGAAATCATCCAGTAAACCGCC
			CCTCGTAAATCCTCATCAAAGACCCATTTTAACCTCTCTATAA
			TTTTTGCCCTTAAATCTGAAGCAAGAAATCATCCAGTAAACCGCC
			CCTCGTAAATCCTCATCAAACCTTAAACTCATGAGCCAATCTTAC
			CAAAATTATGGTCCGTCTTCACCAGAAATCATCCAGTAAACCGCC
			CCTCGTAAATCCTCATCAAACCTGACCAAACAATCTCAAGACAAAC
			CTTTCTAATGTTTTCTGAAGCCCTAAATCATCCAGTAAACCGCC
			CCTCGTAAATCCTCATCAAAAATGGTATGTGCCAATGCCTGTAAT
			AGCTTTAAAGACCTAAATCTTCTCAAATCATCCAGTAAACCGCC
			CCTCGTAAATCCTCATCAAAAATATAGTGGATCTACATTAATGC
			GAATTTTCTTGGTGATCATGTTTAAATCATCCAGTAAACCGCC

			CCTCGTAAATCCTCATCAAACATAGCTGAACAATCAAAGTTGACC
			ACTACTAACTGGCTGTCTTTTACCAAATCATCCAGTAAACCGCC
			CCTCGTAAATCCTCATCAAAGACATGGCATACTCTATACCGTTTA
			AACCATTTATGTGGGTTGAAGTTAAAAATCATCCAGTAAACCGCC
			CCTCGTAAATCCTCATCAAAAACCTCCCTGCATATGCAGCATCTAT
			TTGGCCTGAATTCTGGACAAATAAAAAATCATCCAGTAAACCGCC
			CCTCGTAAATCCTCATCAAAAAGGACCTACTTCTAAGATATTATCA
			CATCCAAATATCCTCTTCTTTACATAAAATCATCCAGTAAACCGCC
			CCTCGTAAATCCTCATCAAAGCACAAACAAAGAAAGGAACAAGC C
			GCACATGATGGTGTAGTTCCTAAAGAAATCATCCAGTAAACCGCC
			CCTCGTAAATCCTCATCAAATTAGGTTGCTGCCTCTCATTGCACC
			TCGATTTATCTTTTTCAATGGCTAGAAATCATCCAGTAAACCGCC
			CCTCGTAAATCCTCATCAAATACACAACCAATCAAACCAGCTCTT
			GTCGTCTGCTGGGATTTCTCTCATCAAATCATCCAGTAAACCGCC
			CCTCGTAAATCCTCATCAAATAAGCTATGAGTTTTGGCATAATTT
			ACAGATGAATGACTCTGATCAGAGCAAATCATCCAGTAAACCGCC
			CCTCGTAAATCCTCATCAAAAATAATTTCTGATCATCTTGGTTCT
			CCTGATCTTTGTAATCTCCAGTCTCAAATCATCCAGTAAACCGCC
			CCTCGTAAATCCTCATCAAAACTTGCTGTGCCCTGAATTACTCCC
			TGACAACAAAGCCACTAAGGTTGCTAAATCATCCAGTAAACCGCC
			CCTCGTAAATCCTCATCAAATCTTGTGGTAGATCTAACATCTTGC
			CCTTTCTCCTCCAGAACAGAAAGAGGAAAATCATCCAGTAAACCGCC
			CCTCGTAAATCCTCATCAAACTGTACAGGCAGGACTTGAGGCCCA
			GCCAATCCATCACAACCATCTCTAGAAATCATCCAGTAAACCGCC
			CCTCGTAAATCCTCATCAAATAATATGTCTGCTACAATAGCTGGG
			AAATCCAATACAACCAATAGCATCTAAATCATCCAGTAAACCGCC
			CCTCGTAAATCCTCATCAAAAATTGTGGAGAATGCCAATGGGTTAC
			GAGTTCAGTTGAAAAATAGGCATGAAATCATCCAGTAAACCGCC
			CCTCGTAAATCCTCATCAAAGAAAACATCGTCCATTTATCTGGT
			AGGCATGATAACTCTTTCTATATCTAAATCATCCAGTAAACCGCC
			CCTCGTAAATCCTCATCAAATTGATATATCCCGTTTCCACTTCAG
			TTTGGGGCATGGTCTGGTAATAACTAAATCATCCAGTAAACCGCC
			CCTCGTAAATCCTCATCAAAGATAGTCTGCTACATAATCTATCAT
			ATGGTCTACGATCACGAATATTCTCAAATCATCCAGTAAACCGCC
<i>Mg</i> MAO-A like	MGAL_10B047901	B2	CCTCGTAAATCCTCATCAAAAAGCTAATACTCCTGCAGATAACAATT
			ACGGAGATGTCTCTGATACAATACAAAATCATCCAGTAAACCGCC
			CCTCGTAAATCCTCATCAAAGGCACTGATGGAAGGTGTCTATTCA
			ACACTCCCTAACATTCCAAAAAATCAAATCATCCAGTAAACCGCC
			CCTCGTAAATCCTCATCAAACTCGCTTATTTTTCAGGTTCTGTCTG
			AGGACGATGGAAACGGACTTGATTTAAATCATCCAGTAAACCGCC

			CCTCGTAAATCCTCATCAAATTCAGTCAAAACCTCTCTGGCACTT
			AATTTCTGATGCAGATAATTTCCCAAATCATCCAGTAAACCGCC
			CCTCGTAAATCCTCATCAAATAACCAGACCATTCCGGTAGCGGTTT
			TCTCCAGCTTGTACAGCACCTTCCAAAATCATCCAGTAAACCGCC
			CCTCGTAAATCCTCATCAAAGTGTTCTAAGTTCACTGCCAAATTT
			TTCCAGCAAATACATTTTACCAACAAATCATCCAGTAAACCGCC
			CCTCGTAAATCCTCATCAAAGTAGCATCCACCAGACCATTGCTCT
			AAGAAATCCAGGTGGCATCATTGTTAAATCATCCAGTAAACCGCC
			CCTCGTAAATCCTCATCAAAGGATGTTTGCTTTATCTGATTTGA
			GGCCAATTTAATTCTTCATAATGTAAAATCATCCAGTAAACCGCC
			CCTCGTAAATCCTCATCAAAGTTTCCTTTTCATCTCGGATAAGAC
			CTTTTGCATAAAGTTCACCAATTCTAAATCATCCAGTAAACCGCC
			CCTCGTAAATCCTCATCAAAAAATCCCATCAGTGCTGGACATGAG
			TAATGTCTTGCTTTGTCTGCTAATAAATCATCCAGTAAACCGCC
			CCTCGTAAATCCTCATCAAACCTATAATAGCATCTTCATCATCAA
			TCAGGATTGACGTTATCCATGGTAAAAATCATCCAGTAAACCGCC
			CCTCGTAAATCCTCATCAAATCCAGAATGGTGAGTCATAATACAT
			CAGAGGATCCACAAAACCCGTCTTTAAATCATCCAGTAAACCGCC
			CCTCGTAAATCCTCATCAAATCGCTGAATCAACTGATTTCCGGTTT
			GGTTTTTATTACAGATCCCATGGGCAAATCATCCAGTAAACCGCC
			CCTCGTAAATCCTCATCAAATTTTGTAGTGGTACTGGAAC TGACA
			GGTAATGGAGGTTTCATATACTATTCAAATCATCCAGTAAACCGCC
			CCTCGTAAATCCTCATCAAACATGGAGATCTTTAATTGTGACATC
			TTACATATTTTGCCATATAAGTGTTAAATCATCCAGTAAACCGCC
			CCTCGTAAATCCTCATCAAAACAGCTGAGGATAACTTTTTCTTTT
			ACCATTCTGTTTTATATGACAAACAAAATCATCCAGTAAACCGCC
			CCTCGTAAATCCTCATCAAATGTTGAGAACCGCCTACAAATTTTC
			AATTTTTCTACAATCCGCTTGCTTAAAATCATCCAGTAAACCGCC
			CCTCGTAAATCCTCATCAAATTCGCATGGAACCTCCTGCACATTT
			CCTGCCCTCCATTAGTTGTTGAATAAAATCATCCAGTAAACCGCC
			CCTCGTAAATCCTCATCAAACCTATAAGGTTTCGGAGGTCACATTC
			ATACCAAAGCAACCATAATAAAGATAAAATCATCCAGTAAACCGCC
			CCTCGTAAATCCTCATCAAAGCTGCAGCTGTCCACACATTATTAT
			TGTACGAAGCATGTTGCAAAGCTTAAATCATCCAGTAAACCGCC
			CCTCGTAAATCCTCATCAAACCTCCTTTGCTTTCAGTGCATCCCA
			AAAATTCCTTGACTGTCAATTGAATCAAATCATCCAGTAAACCGCC
			CCTCGTAAATCCTCATCAAATTTGTCGATAAGTCGAAACAAATTG
			CGCCTCCATAGGTATCTCTTCGCCCAAATCATCCAGTAAACCGCC
			CCTCGTAAATCCTCATCAAATTTGGTGGAAATGTTCCAGTGAATC
			ATATCCATGTATGCCAGAAAACCTCAAATCATCCAGTAAACCGCC

			CCTCGTAAATCCTCATCAAACATCTTCGACTTCATTGTTAGGTA
			TTGATTTTCCCTTGTATAGAAAATAAATCATCCAGTAAACCGCC
			CCTCGTAAATCCTCATCAAATAAGATACGGTTTTGAGTTGGACCC
			GTCGATGCCAAATTCATCTGCTAATAAATCATCCAGTAAACCGCC
			CCTCGTAAATCCTCATCAAACCTTTGGGATTGTGTTCTGTAAATG
			TATGCACCACCTAGGTCGACATATTAATCATCCAGTAAACCGCC
			CCTCGTAAATCCTCATCAAAGAACAAGAACTTCGATTCCCTTTTC
			GACCGCAAACCTCTATCTCGTGCCTCAAATCATCCAGTAAACCGCC
			CCTCGTAAATCCTCATCAAATAATCCAGCTCCGACCACAATAACG
			TAATAGCTTCGCAGCAGACAAACCAAAATCATCCAGTAAACCGCC
			CCTCGTAAATCCTCATCAAACCTATCAGCATAATGTTGTGTTTCTA
			TCGGTTGGAAAATTATCATGATTAATAAATCATCCAGTAAACCGCC
			CCTCGTAAATCCTCATCAAACACCTGCCTTACCCTGGACATTATC
			AGAAGGCACTAAACTGCCCGTATGTAAATCATCCAGTAAACCGCC
			CCTCGTAAATCCTCATCAAAAAGTTTCTGTGCTTGATACTTCCAGA
			ATAGTACGATGTGTATACCTGCAAAAAATCATCCAGTAAACCGCC
			CCTCGTAAATCCTCATCAAACCACATTTTTTCATTTGACCCGTTT
			CGTCCTGAGGGTGGATGCTCAACTCAAATCATCCAGTAAACCGCC
			CCTCGTAAATCCTCATCAAAGCTGTTTCAATATCGTATGGTGTTT
			TTTTTATGTGATCCCCTAGACGTAAAATCATCCAGTAAACCGCC
			CCTCGTAAATCCTCATCAAATTACATTTTCGTTCAAAGGAGTATA
			CTACAGGAGCAATTTACCTGTTGGAAATCATCCAGTAAACCGCC
			CCTCGTAAATCCTCATCAAAGTCTATATTAAGTGAACCTTGTCCA
			GTCAGCGTTGACCTTGATAATGTGAAAATCATCCAGTAAACCGCC
			CCTCGTAAATCCTCATCAAATTAATGGGCGTGGCTTTAGTAGTAG
			AGGTAAAAATGAATGATTGGTTAAAATCATCCAGTAAACCGCC
			CCTCGTAAATCCTCATCAAACATTGGTCAGTTCGTATGTAACAGT
			CTGTATAATCTATGATAAATTCATTAATCATCCAGTAAACCGCC
			CCTCGTAAATCCTCATCAAACCATCGGGACTTGTGTACGACATC
			AGTTAGTTCCCCTGGATAATTCTCCAAATCATCCAGTAAACCGCC
			CCTCGTAAATCCTCATCAAACATACAACCTTATCAAACCTTTCA
			ACTTTGAATCTTTAACATCAGCTTAAATCATCCAGTAAACCGCC
			CCTCGTAAATCCTCATCAAATAATCGCAAGTTTATAGTCAGTTCC
			CTCCATGAAGATGGTTAGGACCATTAAATCATCCAGTAAACCGCC
			CCTCGTAAATCCTCATCAAATTTGCGACTCTACCACACAAGCA
			TAATGTAAACTTCCATCAGCGATTAATCATCCAGTAAACCGCC
			CCTCGTAAATCCTCATCAAACCTTTAATATCATCAAACCTTAGGT
			AAATATCTCTGAAGCGGACTCTCGTAAATCATCCAGTAAACCGCC
			CCTCGTAAATCCTCATCAAAGGACCAGGATGTCCGGTCACTATGGC
			TGTCCTGTACATCGCCTTTTCTGTCAAATCATCCAGTAAACCGCC

			CCTCGTAAATCCTCATCAAAGTTTTGATTCTTCAGTGTAACATT
			ATAACTGATTATTCTTATTGTAACAAAATCATCCAGTAAACCGCC
			CCTCGTAAATCCTCATCAAAAATTCACAAGTCATTTGTAAGGCA
			AGCTGATCAAGAGAGGGCCGACATCAAATCATCCAGTAAACCGCC
Mg DBH-like3	MGAL_10B074188	B2	CCTCGTAAATCCTCATCAAACGGAGCATACTTTGTTGGTTCGGGA
			ATGACCACTTGGACATTGTCTAGGAAAATCATCCAGTAAACCGCC
			CCTCGTAAATCCTCATCAAATTAGCGCTTTTGTC AAGTCCATAGC
			TGGAAATTGCCCTGTTAAAAATGGAAAATCATCCAGTAAACCGCC
			CCTCGTAAATCCTCATCAAATTTTCATTAAGTTATCACGAACAGA
			TATAATTGTACGTAGAATTGTCAACAAATCATCCAGTAAACCGCC
			CCTCGTAAATCCTCATCAAATTTTACAGCATGCCAAGGAACGCTG
			ATCTTTCCAGTCCCAAGTATTTAGTAAATCATCCAGTAAACCGCC
			CCTCGTAAATCCTCATCAAACAAAACGTAACATTCATTTTGGAT
			AGTTGGTCATAGTTGGGTTGACTGAAAATCATCCAGTAAACCGCC
			CCTCGTAAATCCTCATCAAAATGTGGTCGGTAAACCACCAACAGT
			AGAACAAGAAAGCCAAGCACATCTCAAATCATCCAGTAAACCGC C
			CCTCGTAAATCCTCATCAAAACAGTCCATTGCAAGGCTGTCGCCG
			TTTGGTTCTTGACGAGGAATCGTAGAAATCATCCAGTAAACCGCC
			CCTCGTAAATCCTCATCAAACAAAATCTTGGAATCAAAATCAT
			TTGATTTCTTCTTCTTGTTCATGGAAATCATCCAGTAAACCGCC
			CCTCGTAAATCCTCATCAAACCTCTATCCCCTCGAAAATGACGTGC
			TGTCGTCTTTTCGAGAATGGCTCAAGAAATCATCCAGTAAACCGCC
			CCTCGTAAATCCTCATCAAAAAGAAGAACACCAAAACACCTTTAAA
			CAACTTGGCACCCAGTAAATGGGCAAAATCATCCAGTAAACCGCC
			CCTCGTAAATCCTCATCAAATGCAGTCCCTCGTACAGTGACTTT
			TTTGTCTGATTACCAACAGCCATTTAAATCATCCAGTAAACCGCC
			CCTCGTAAATCCTCATCAAATAAACTGTAAGTTGTTAACCATTGC
			ATACGAATCCCTTTTCGTATGGGGGAAATCATCCAGTAAACCGCC
			CCTCGTAAATCCTCATCAAATCTTAATGTTGGCGTACTGTTATT
			AATTTCAAGCATTCTGCATCATACAAATCATCCAGTAAACCGCC
			CCTCGTAAATCCTCATCAAATTTAATGTTGGATTAGTAAATGTG
			AAACCTGAACTATCTACGATGCCTGAAATCATCCAGTAAACCGCC
			CCTCGTAAATCCTCATCAAAGTGCATTCAATGAAAACCCAGCGTT
			CCAGAAGTAGATATCGTGGATCTCAAATCATCCAGTAAACCGCC
			CCTCGTAAATCCTCATCAAATGCCATGCTAACATGACATCGTTG
			AGGAAAGTCATATCCAACGCCACCAAAATCATCCAGTAAACCGCC
			CCTCGTAAATCCTCATCAAATAACAGTTAAAGACAGATCCTTCAT
			TTTCAAATTTCTTTGGTTGACACAAATCATCCAGTAAACCGCC
			CCTCGTAAATCCTCATCAAACAACAAAGTGATGGACGACATCTTC
CATCTGTTGCAGTTGGACAACCTGTA AAAATCATCCAGTAAACCGCC			

			CCTCGTAAATCCTCATCAAATATCATATGGCGCTTGGAAGGTTTT
			ACCACGGGTGATTATTGGTTCAAACAAATCATCCAGTAAACCGCC
			CCTCGTAAATCCTCATCAAAGTAGTATCTGTATTGGCTGGAACAT
			GGCACTTTAAAAATTGTACATTGGTAAATCATCCAGTAAACCGCC
			CCTCGTAAATCCTCATCAAACCTGCATCAGGTGGTAATTGGTAGTC
			AATTGTTATGAAGTATATCGAATTGAAATCATCCAGTAAACCGCC
			CCTCGTAAATCCTCATCAAACCTTTTAGCTCCTCGTCTGTTTGCC
			TGCCCTGACCGCCGAGAGCAACATTAAATCATCCAGTAAACCGCC
			CCTCGTAAATCCTCATCAAAGGATCATCAGGTGGTACGAATATA
			TGCCATGGCAGTGTATCGAACGATGAAATCATCCAGTAAACCGCC
			CCTCGTAAATCCTCATCAAAGTCTTTGTGCATCACATGTATCTAA
			CCTTGATAGTATTATCTGTAATTTGAAATCATCCAGTAAACCGCC
			CCTCGTAAATCCTCATCAAAGTTATCTTCAAGTCCCTGTAGAAGC
			CCTAACAACTTTAATACTGTTCCAAAATCATCCAGTAAACCGCC
			CCTCGTAAATCCTCATCAAAGCATAGTGACCTTCAGTATGACAAT
			CAGTCTGGCTTACATCAATGGTAGAAATCATCCAGTAAACCGCC
			CCTCGTAAATCCTCATCAAACCCAGCCAACAACACTACATCAGATGG
			TAAAATGAGCCGTTCCGTTGCTGTCAAATCATCCAGTAAACCGCC
			CCTCGTAAATCCTCATCAAAGCCGACATATCCCTTAGTCTTAACG
			CATTTACCATTAGATGATAGACCAAAATCATCCAGTAAACCGCC
			CCTCGTAAATCCTCATCAAAGTTTTCCAAAATAACCAATAACTTC
			GTCTCAAACGTTATATGTGTTGCATAAAATCATCCAGTAAACCGCC
			CCTCGTAAATCCTCATCAAAAAATCTCAGTTGGCGTGGTTTGGA
			CACTGTCTAGTTGCCAGCTATTCCCAAATCATCCAGTAAACCGCC
			CCTCGTAAATCCTCATCAAATTTCCCTATGCTTGTACCGAACAAA
			CGACACATGTTGGGTAACGGCATTAAATCATCCAGTAAACCGCC
			CCTCGTAAATCCTCATCAAATGGTGTGTATTTAATTTCGAGGTTCT
			CTGGCTCCCGGGCACTGTCTAGGGAAATCATCCAGTAAACCGCC
			CCTCGTAAATCCTCATCAAAGGGCTATCTGGATGTGTGTACTAT
			ACACGGTAAACATTCTGTTGATAACAAATCATCCAGTAAACCGCC
			CCTCGTAAATCCTCATCAAATAATATCTTTGAATTTGTTCTTAAC
			ATTCATGGTACAAATTGGTCTTATTTAAATCATCCAGTAAACCGCC
			CCTCGTAAATCCTCATCAAACGTATCAACATTGTGGTAAGGGTTT
			TTGGTTCTGCCAGTTCCAACATACAAATCATCCAGTAAACCGCC
			CCTCGTAAATCCTCATCAAATGACAGTTGCTTATTTTCAGTTTTTG
			CCGATTTGATCATACAAAGGCATACAAATCATCCAGTAAACCGCC
			CCTCGTAAATCCTCATCAAACCTCCGCAGTTGACAATCCTCCCAA
			AGTAATAGATAAAGGCTAAACACATAAAATCATCCAGTAAACCGCC
			CCTCGTAAATCCTCATCAAATGGCAGTCAATGGTTAAACTATCG
			CGGTTTAGTTCTTCTGTTGAATCGAAATCATCCAGTAAACCGCC
<i>Mg</i> DBH-like4	MGAL_10B091849	B2	CCTCGTAAATCCTCATCAAATGGTGTGTATTTAATTTCGAGGTTCT
			CTGGCTCCCGGGCACTGTCTAGGGAAATCATCCAGTAAACCGCC
			CCTCGTAAATCCTCATCAAAGGGCTATCTGGATGTGTGTACTAT
			ACACGGTAAACATTCTGTTGATAACAAATCATCCAGTAAACCGCC
			CCTCGTAAATCCTCATCAAATAATATCTTTGAATTTGTTCTTAAC
			ATTCATGGTACAAATTGGTCTTATTTAAATCATCCAGTAAACCGCC
			CCTCGTAAATCCTCATCAAACGTATCAACATTGTGGTAAGGGTTT
			TTGGTTCTGCCAGTTCCAACATACAAATCATCCAGTAAACCGCC
			CCTCGTAAATCCTCATCAAATGACAGTTGCTTATTTTCAGTTTTTG
			CCGATTTGATCATACAAAGGCATACAAATCATCCAGTAAACCGCC
			CCTCGTAAATCCTCATCAAACCTCCGCAGTTGACAATCCTCCCAA
			AGTAATAGATAAAGGCTAAACACATAAAATCATCCAGTAAACCGCC
			CCTCGTAAATCCTCATCAAATGGCAGTCAATGGTTAAACTATCG
			CGGTTTAGTTCTTCTGTTGAATCGAAATCATCCAGTAAACCGCC

			CCTCGTAAATCCTCATCAAAATTCTATTATCTTGGTAGTCAAAGT
			TATTTAATTTCTCTCTCTTTGGAAAAATCATCCAGTAAACCGCC
			CCTCGTAAATCCTCATCAAAATTCTACGTCACCACGAATATGTCG
			AAGAAAGGTCTTGTGCCAAAGGTTCAAATCATCCAGTAAACCGCC
			CCTCGTAAATCCTCATCAAAATGAAGAAGTGTGCAAAAAGCTTTC
			AACAATACTTGTTCGAAGTAAATGGAAATCATCCAGTAAACCGCC
			CCTCGTAAATCCTCATCAAAATGTAACACTGTTGACTACATGAAT
			CTGTTTGTGTTTGTACCAAAGCTAAATCATCCAGTAAACCGCC
			CCTCGTAAATCCTCATCAAAAGAACAACTGAAGTTTATTAACTTT
			GTGATAGAAAAATCTTTCTCATATGGAAATCATCCAGTAAACCGCC
			CCTCGTAAATCCTCATCAAACTGACGTATTGTGTGCGTAGCTGTA
			ACCTGCTTGCAAAATTCAGCATCAAAATCATCCAGTAAACCGCC
			CCTCGTAAATCCTCATCAAAGACTTCATTGTTGGATTATTAAGT
			CTTAAACGAGAACTATCAACAATACAAATCATCCAGTAAACCGCC
			CCTCGTAAATCCTCATCAAAACAGGTGTCATGAAGGAGAATCCAGC
			TTTCATTACAAGGTACTGTGGGTCAAATCATCCAGTAAACCGCC
			CCTCGTAAATCCTCATCAAAAACAGCCCATGCAATCACCACATCA
			CGATGGAAAATCAAATGCTACACCAAATCATCCAGTAAACCGCC
			CCTCGTAAATCCTCATCAAAATAGCATTATACACCTTGCCAACGT
			CACTTGAGATTTCTAGGTCGATGTCAAATCATCCAGTAAACCGCC
			CCTCGTAAATCCTCATCAAAACAAAATATGATGAACGTAAGCTTC
			CATCTGTAGCGGTCGGACAGTTATAAAATCATCCAGTAAACCGCC
			CCTCGTAAATCCTCATCAAAGATCATATGATACTTCTGGGTTTG
			ACCGGGAGATATTACGGGTTATATAAAATCATCCAGTAAACCGCC
			CCTCGTAAATCCTCATCAAAGTCGTTTCCTTTGCTGGTACATGGA
			GGAACTTTAAAAACTTTACATTGATAAATCATCCAGTAAACCGCC
			CCTCGTAAATCCTCATCAAAACATCAGAGGGTGGAACATATTCATT
			TATTGTGAAGCATATCAAACGTTCAAATCATCCAGTAAACCGCC
			CCTCGTAAATCCTCATCAAATTTGGCCCTCGTCTTTCTGCACCA
			TTTTACAGATGATAGCAACATCAAAAAATCATCCAGTAAACCGCC
			CCTCGTAAATCCTCATCAAAATCATCAGGATGGTATGAGTAGATTA
			CAAGGTAGGGAACATAAACGAAGCAGAAATCATCCAGTAAACCGC C
			CCTCGTAAATCCTCATCAAACGTTATCATCATGTATCCAACCTT
			TGACAGTACTCTCCGTTATAAGATAAAATCATCCAGTAAACCGCC
			CCTCGTAAATCCTCATCAAAATCCTCTTTGCCAAGTAAACAAAAAC
			TGTAAATTTTAAAACTGTTCCAAAAAATCATCCAGTAAACCGCC
			CCTCGTAAATCCTCATCAAAATAGTGTCTTCTGTATGACAATCCT
			TCCTGACTAGCATCAATTATCGGTGAAATCATCCAGTAAACCGCC
			CCTCGTAAATCCTCATCAAAATCCGATGACAACATCTGAGGGAAA
			AGTGTGCTGTGCCATTGCTGTCAACAAATCATCCAGTAAACCGCC

			CCTCGTAAATCCTCATCAAAAACATATCCTTTAGTCTTTACGTT
			TTTACCATTAGACGAAAGTCCAAAGAAATCATCCAGTAAACCGCC
			CCTCGTAAATCCTCATCAAAATCCAAAACAACCAGTAGTTCCCTT
			TCGAAGGTTATGTGTGTTGCATTTCGAAATCATCCAGTAAACCGCC
			CCTCGTAAATCCTCATCAAAATCTCGGTAGGAGTTGGTTCTGTTGT
			CATCTAACTTCCAGACGTTACCAAAAAATCATCCAGTAAACCGCC
			CCTCGTAAATCCTCATCAAAATTTCCGATACATTTTGCAACTAAC
			TGCCGGAACATTATCCTCTGGATTAATAATCATCCAGTAAACCGCC
			CCTCGTAAATCCTCATCAAACTCTGAGGAGGATGGTATATTTCT
			AACTTGCCCATTTGTCTTTTTGGCAGAAATCATCCAGTAAACCGCC
			CCTCGTAAATCCTCATCAAAATTAAGAAATGACGGGTTTCTTGAT
			GGACGTAGTCTATCCACAGTCTTGAAAATCATCCAGTAAACCGCC
			CCTCGTAAATCCTCATCAAAATGTTATTCCTAAATAGAAGTCTAGC
			ATGATGACCTATATTTGTTTTTCAAATCATCCAGTAAACCGCC
			CCTCGTAAATCCTCATCAAAAAATTTCACTTGTCTGGTGGTTTC
			GCGGTCCTCCAGTTGTAACCCTGTAATCATCCAGTAAACCGCC
			CCTCGTAAATCCTCATCAAAATAGGGTCAGCTAAACAGCCATCCA
			TCTTTGATTTGGGGATGGTATCAAAAATCATCCAGTAAACCGCC
			CCTCGTAAATCCTCATCAAAAAATACACATCTCATCGGTGGTAGC
			GCATTCGGGGATAGTAGAAAATGAAAATCATCCAGTAAACCGCC
			CCTCGTAAATCCTCATCAAAATGTCGAGTCATATGTACATTGTGTA
			ACCGCCAGTGTCAAGTTGGTTCTGAAATCATCCAGTAAACCGCC
			CCTCGTAAATCCTCATCAAAATCTTTCTGAGTAGCCGATTGTT
			AGACTATACCCATTTTCAATGGAAAATCATCCAGTAAACCGCC
			CCTCGTAAATCCTCATCAAAACAAAAGGCTCGATTTCTTTCCGTT
			AATTGAAATCATAGGCTTGATCATCAATCATCCAGTAAACCGCC
			CCTCGTAAATCCTCATCAAAACAAAAGATGAGAATGTTGCCATGCA
			TAGATGTTTTGTTGTCATAGCATAGAAATCATCCAGTAAACCGCC
			CCTCGTAAATCCTCATCAAAATCTTTCAGTCCCTGTTCTAAACATT
			AAAACCTTGACTTGCTGGCCTGGCAAAATCATCCAGTAAACCGCC
			CCTCGTAAATCCTCATCAAAACCGTTTCATGCGGCGGAATCATATG
			CTTGACAGAAGCCTGTGTTTACGAAAATCATCCAGTAAACCGCC
			CCTCGTAAATCCTCATCAAAATAGTCCTGCATCGTACTTCTGAGG
			TGGACCAATTTGAACTCCAGTAGTAAAATCATCCAGTAAACCGCC
			CCTCGTAAATCCTCATCAAACTATCCACTAGATCACTACGCAGTT
			GGTGTAATGTAATGCGCATGCCTGAAATCATCCAGTAAACCGCC
			CCTCGTAAATCCTCATCAAAATGTAGCGTCGTTCTGGTTTACC
			GATTGTTATAATGTACTTCCATGATAAATCATCCAGTAAACCGCC
			CCTCGTAAATCCTCATCAAAAGAAGTCCTGCTCCTCATACTCCCAA
			AGGCATACCAACATTGTCGGGGAAAAATCATCCAGTAAACCGCC
<i>Mg</i> DBH-like5	MGAL_10B026354	B2	

			CCTCGTAAATCCTCATCAAATCTCTCCATTAAGATAACAGAAAT
			AAGAAGACACTGCCACATGGTGCCAAAATCATCCAGTAAACCGCC
			CCTCGTAAATCCTCATCAAAGGGGACATTTGTAGACTAGAATGTG
			CCTTGTTTATCCATTCTTTGCTAAGAAATCATCCAGTAAACCGCC
			CCTCGTAAATCCTCATCAAATGGGACTCAAACCTAATCATGTGA
			GACATATGGTTCATCCCACGCTGAAAATCATCCAGTAAACCGCC
			CCTCGTAAATCCTCATCAAAGCTTTACATCGGTAAGTGGTAACTT
			TTCTCCCTAGATTTGACAGGGTAAAAATCATCCAGTAAACCGCC
			CCTCGTAAATCCTCATCAAATATCTCTGGTGATAATGTTCCCGA
			GTGGGACGTGATAGTTGGTTTGTATAAATCATCCAGTAAACCGCC
			GTCCCTGCCTCTATATCTTTGGAATGATTGGGTACCTCTGTTGGG
			CAGCTGCACCGGGATAACAACATCATTCCACTCAACTTTAACCCG
			GTCCCTGCCTCTATATCTTTCTCCTGGAGTTACAAAGAACAAAT
			ACCATAGATCTTAGACGCTCTGCCGTTCCACTCAACTTTAACCCG
			GTCCCTGCCTCTATATCTTTACGATGAAACGATAAACCATCCTAA
			TTGCGTAACTGGTATACACAATAGTTCCACTCAACTTTAACCCG
			GTCCCTGCCTCTATATCTTTCCATACTGGGGTGGCATAGGCTGA
			GTAGGACCAGGTTGAAAATCATACTTCCACTCAACTTTAACCCG
			GTCCCTGCCTCTATATCTTTAACACGGACTGATGGTCGTCCAAC
			AAGGACATGATAAAAAAGTGAAATATTCCACTCAACTTTAACCCG
			GTCCCTGCCTCTATATCTTTCTAACATTGACTGAATGTCGTTACT
			TTCTCAAAATATCCCTGGTCTAAATTCCACTCAACTTTAACCCG
			GTCCCTGCCTCTATATCTTTGACAGCAACAGATTCAAGGAAAACA
			TCTTCAACACAATCATAAATCCACTTCCACTCAACTTTAACCCG
			GTCCCTGCCTCTATATCTTTACATCCAACAACCTGGACGACATATA
			AATATAATTGATATAGGAGCTCCAATTCCACTCAACTTTAACCCG
			GTCCCTGCCTCTATATCTTTCTAAAAAGCAATAACACATCAGACC
			CACCATATGTAATAGTAGGAAGTGATTCCACTCAACTTTAACCCG
			GTCCCTGCCTCTATATCTTTATGTGGCCACTCATCTAGTATGCCT
			AACGAACAATTTCTGTGTTTCGTTTCCACTCAACTTTAACCCG
			GTCCCTGCCTCTATATCTTTGTATCTAACCAGTGTAATAAGCA
			GTTATTGCTTCTAATCCTCCAAATGTTCCACTCAACTTTAACCCG
			GTCCCTGCCTCTATATCTTTATAACTCTAATGATGACAGAGCCTC
			AAAAGAATAAGATTGCCAGAAGGGTCCACTCAACTTTAACCCG
			GTCCCTGCCTCTATATCTTTATCTCTAGCCACGTTATCCACTGTT
			ATAAACAATAAATATCAATCCAACATTCCACTCAACTTTAACCCG
			GTCCCTGCCTCTATATCTTTACCGAAAATACAACAAACCCTGCCA
			CCAGACATATGTGACATATGACCAATTCCACTCAACTTTAACCCG
			GTCCCTGCCTCTATATCTTTTCAGTAATGCATCTCTGTAACAGTT
			AACTTGTATACAATTTATCGTACTTCCACTCAACTTTAACCCG
Mg SERT1-like	MGAL_10B037675	B3	

			GTCCCTGCCTCTATATCTTTTAAAAGGACACCAAAACCTGGACCT
			GTCTAACTGTTGTAACTTGATAGCTTCCACTCAACTTTAACCCG
			GTCCCTGCCTCTATATCTTTATCCATATTCTAGTTTCTAGGAGTT
			GAAAAGAAAATTTGTGCTGCCGCAGTTCCACTCAACTTTAACCCG
			GTCCCTGCCTCTATATCTTTTGCCTTTCATGACCCTGATAACAA
			TCCAATCTGGAGTAAGATAATACATTTCCACTCAACTTTAACCCG
			GTCCCTGCCTCTATATCTTTTGCATATGGCATTGTTGCTGTTATC
			ACCCCTACTAACAAGATTATCAGATTCCACTCAACTTTAACCCG
			GTCCCTGCCTCTATATCTTTTCCACATTGCAAAGTAAACTATAA
			ACTGCCTTCCGGAACTTTTGACTCTTCCACTCAACTTTAACCCG
			GTCCCTGCCTCTATATCTTTTCCAGTTTACACCTCTACATCTTC
			ATACTCAAACAGACATAAAGCTAATTCCACTCAACTTTAACCCG
			GTCCCTGCCTCTATATCTTTTGTATTTCAAAGAATTCTTCTGTT
			GGCATCGGCATAATTTAACCCGAGTTTCCACTCAACTTTAACCCG
			GTCCCTGCCTCTATATCTTTTGGTTACGTTTGCAATAGTCAGAT
			GTCTTTGTGTCGTCGACTATAGTGATTCCACTCAACTTTAACCCG
			GTCCCTGCCTCTATATCTTTCATTGTTTTCTCGTCCGTCATATAC
			ATGGATTCAATGTAACAGAATTATTTCCACTCAACTTTAACCCG
			GTCCCTGCCTCTATATCTTTTATTACAAGATTTCCATGGCACATCT
			ACATTTGTCTATGCTATTCCATGAATTCCACTCAACTTTAACCCG
			GTCCCTGCCTCTATATCTTTTGCCCATGCAATTATAGTGTGTAAT
			GCCATTGCTGAGAAAAAATAGAACATTCCACTCAACTTTAACCCG
			GTCCCTGCCTCTATATCTTTTGTCTAATCCAATTCCTTTAAAGC
			ACGAAACATAAGTTGCAATTACAATTCCACTCAACTTTAACCCG
			GTCCCTGCCTCTATATCTTTCCCGCATCTTTGGAAGTGCCTAAT
			ACATATTCTCTTCCAGACCGTCAAATTCCACTCAACTTTAACCCG
			GTCCCTGCCTCTATATCTTTCCAAAGATTAACATTATAACGTATG
			AGTTCCATATAGAACAGTGGCAATCTTCCACTCAACTTTAACCCG
			GTCCCTGCCTCTATATCTTTATATCGTTTCGCATACCAGTTTGTG
			ACCAATAACAGTCTGAGTTGTCAGTTTCCACTCAACTTTAACCCG
			GTCCCTGCCTCTATATCTTTTCCAGCGCCATTGTGTACGTGCCA
			CGCCCCGTTTGTTCGCAGTGTCCGTTTCCACTCAACTTTAACCCG
			GTCCCTGCCTCTATATCTTTTGGTTCTCCAGGAGCCCAATGTTG
			CTTCTAAACAATGTTCTGTGCCATCTTCCACTCAACTTTAACCCG
			GTCCCTGCCTCTATATCTTTTGTGAGCATGTATCATCTCTTGAAC
			CCTGAATTCAAATATCATTTGGATCTTCCACTCAACTTTAACCCG
			GTCCCTGCCTCTATATCTTTTGTGTCATAGATTCAATCTCATTC
			TGTTTGTATAGTTTCTCAATTGTCGTTCCACTCAACTTTAACCCG
			GTCCCTGCCTCTATATCTTTGTTTTCTCGAGTTATTATGACATGG
			CTATGCCTCCTTACATAATACATTTTCCACTCAACTTTAACCCG
<i>Mg</i> SERT2-like	MGAL_10B092215 a	B3	GTCCCTGCCTCTATATCTTTATATCGTTTCGCATACCAGTTTGTG
			ACCAATAACAGTCTGAGTTGTCAGTTTCCACTCAACTTTAACCCG
			GTCCCTGCCTCTATATCTTTTCCAGCGCCATTGTGTACGTGCCA
			CGCCCCGTTTGTTCGCAGTGTCCGTTTCCACTCAACTTTAACCCG
			GTCCCTGCCTCTATATCTTTTGGTTCTCCAGGAGCCCAATGTTG
			CTTCTAAACAATGTTCTGTGCCATCTTCCACTCAACTTTAACCCG
			GTCCCTGCCTCTATATCTTTTGTGAGCATGTATCATCTCTTGAAC
			CCTGAATTCAAATATCATTTGGATCTTCCACTCAACTTTAACCCG
			GTCCCTGCCTCTATATCTTTTGTGTCATAGATTCAATCTCATTC
			TGTTTGTATAGTTTCTCAATTGTCGTTCCACTCAACTTTAACCCG
			GTCCCTGCCTCTATATCTTTGTTTTCTCGAGTTATTATGACATGG
			CTATGCCTCCTTACATAATACATTTTCCACTCAACTTTAACCCG

			GTCCCTGCCTCTATATCTTTTCCATAGTCCATACAGTTTTCTCTG
			GTCAATCCACTGCATGTATATTCTTTCCACTCAACTTTAACCCG
			GTCCCTGCCTCTATATCTTTGGACTCCAGTTGAAATATCCAATGG
			ACCCCAAAGTAATGGTCTGGCTGTCTTCCACTCAACTTTAACCCG
			GTCCCTGCCTCTATATCTTTCTTCATTTGTAATATCCGTACCATC
			GACCTGTGGTATACCAAACCCACTTTTCCACTCAACTTTAACCCG
			GTCCCTGCCTCTATATCTTTTATAGATTTGATAAAATCTTGCTCG
			CCAGATTGTTACATGCATAGGTTCCCTTCCACTCAACTTTAACCCG
			GTCCCTGCCTCTATATCTTTCCGTATCTTTTGCATGTTTCTCTAG
			AAGTTTTCTATGATTGGAAGATGTTTTCCACTCAACTTTAACCCG
			GTCCCTGCCTCTATATCTTTCTAGGTAGCAATATTTGAACTCTC
			CAATAAGTGCATCACAGATTCATTTTCCACTCAACTTTAACCCG
			GTCCCTGCCTCTATATCTTTGCCTGTTGTTGTAGTAAGAGATTGA
			GTAATGCCAGTGATTCGGACATCGATTCCACTCAACTTTAACCCG
			GTCCCTGCCTCTATATCTTTGTGGTTGCCACTGGGTGTGTTGTC
			GTCTGAGTCTGGGTTGGAGTACTAGTTCCTCAACTTTAACCCG
			GTCCCTGCCTCTATATCTTTGGTGTGTTGTCTGGGTTGGAGTGCT
			TTGGAGTGCTAGTTGTTGTTGCCACTTCCACTCAACTTTAACCCG
			GTCCCTGCCTCTATATCTTTGTTGCAAAATGTGTCGTAGCGTTG
			TGTTGTTGCCGCTGGGTGTGTTGCTTCCACTCAACTTTAACCCG
			GTCCCTGCCTCTATATCTTTCCACAACATCTGGCTGTACTAGAAC
			AGAAAGTGATCATTGCATAACTCTGTTCCACTCAACTTTAACCCG
			GTCCCTGCCTCTATATCTTTTTGTAGAAAATAAATGATCACTTCC
			TTGTACAGGTCGACTTTTGAATACATTCCACTCAACTTTAACCCG
			GTCCCTGCCTCTATATCTTTGTCTGGTCCACATAACGTTATATCA
			CTGTATTTGTTCTAAATAACAATCTTCCACTCAACTTTAACCCG
			GTCCCTGCCTCTATATCTTTTCAGTCGTAACATAAAAATTCCTTCTA
			CACATATCTGGTGCTGCCTGTTGTTTTCCACTCAACTTTAACCCG
			GTCCCTGCCTCTATATCTTTTTCTGTTGCACAAATCTCCATTTTG
			GTAATCTTTCAGGAGATCCACAACCTTCCACTCAACTTTAACCCG
			GTCCCTGCCTCTATATCTTTACGTGTCTCCTAAAATGTCGATT
			TTTTCCAATGCCGATGGGAACAGCATTCCACTCAACTTTAACCCG
			GTCCCTGCCTCTATATCTTTGTAAATCTGCCCTGTGCATCTGAAC
			AAAAGTCTCAATCGCTGTTCAAAACTTCCACTCAACTTTAACCCG
			GTCCCTGCCTCTATATCTTTCTGTTATCTCTCTTTGAACGTAACA
			CTACACTATACCATGCTATCCCCTTCCACTCAACTTTAACCCG
			GTCCCTGCCTCTATATCTTTATTACAATCACGTGGTTGAACAAC
			CTCATGCTCCCCACAAGCGTTACATTCCACTCAACTTTAACCCG
			GTCCCTGCCTCTATATCTTTCCGGATAATGTTTGACATACAGAAG
			TTGCAGCTAAGACATAATGGTCTTTTCCACTCAACTTTAACCCG

			GTCCCTGCCTCTATATCTTTGATTGTCTTCGTAACTATTAATCA
			AAAAAAGAGGGTACAAGTGATAATTTCCACTCAACTTTAACCCG
			GTCCCTGCCTCTATATCTTTAATTTTCGCCAATCGAGATAAGGAA
			CACCCACATGACAAAATATGTAGTATTCCACTCAACTTTAACCCG
			GTCCCTGCCTCTATATCTTTGACGTTCCGGAGGCCGCATATGATGA
			AATTAGACCTTCCGGAGCACTTGTCTTCCACTCAACTTTAACCCG
			GTCCCTGCCTCTATATCTTTACTGAAGTTATTTTCCTGTAGCGC
			AGTCAAAAATACTTTATTTGTATAATTCCACTCAACTTTAACCCG
			GTCCCTGCCTCTATATCTTTTCTTGTTCAATGTGAGATGGTATTG
			GTATTGTCATATAAATGTCTTGATTTTCCACTCAACTTTAACCCG
			GTCCCTGCCTCTATATCTTTGCTTGAATGTCCCAGGTGTGACAAT
			ATGGACGAATCATTCTGAGAATTTTTTCCACTCAACTTTAACCCG
			GTCCCTGCCTCTATATCTTTGATTAATGAAATGGAAGATATAGTC
			AAGATATATAATGTAGATGGGTATATTCCACTCAACTTTAACCCG
			GTCCCTGCCTCTATATCTTTACGTATCCATTTAGTTCTATGCCGT
			CCTATAGCTAATGACCATTGTGGGTTTCCACTCAACTTTAACCCG
			GTCCCTGCCTCTATATCTTTCAATGAGGCAAATTGGGCATATAAA
			AGTAATATATTGATAAAAATGAATAATTCCACTCAACTTTAACCCG
			GTCCCTGCCTCTATATCTTTCTGAAATCCTAACATAGTTTGATA
			CCAGCATATTTCCAAAATATACCATTCCACTCAACTTTAACCCG
			GTCCCTGCCTCTATATCTTTTCAGTTAACAGCTATTGCTTACAGA
			TCTGAAAAGTGTGTACACCATAAATTCCACTCAACTTTAACCCG
			GTCCCTGCCTCTATATCTTTTCATGTCTGTCTAACAACTAACAAAT
			AAATACAAATAAGTGGTATTGGAGCTTCCACTCAACTTTAACCCG
			GTCCCTGCCTCTATATCTTTTGAACCCAGGAAGCAATATATTATA
			TTGTCCACCATTGTGGTAGACGGTTTCCACTCAACTTTAACCCG
			GTCCCTGCCTCTATATCTTTTTGACTACTTTGAATGAATCCATAA
			CCGAGAACAAGCCATTCCCGTCGTCTTCCACTCAACTTTAACCCG
			GTCCCTGCCTCTATATCTTTACGTAAGTCCATGCCTAGTGTGAT
			CCGTAATCACTGCCTCAAGTCCACCTTCCACTCAACTTTAACCCG
			GTCCCTGCCTCTATATCTTTTACTGAACCATCCAACGTCGCTAGT
			CATAACAAAGAATAAGATAGACCAATTCCACTCAACTTTAACCCG
			GTCCCTGCCTCTATATCTTTGGACCTTCCATAGCTACTTTATCTA
			TCAGGGTATACCATAAACTAGGCTTCCACTCAACTTTAACCCG
			GTCCCTGCCTCTATATCTTTCTAATACGGAAAATACCACAAAACC
			CCTTTGTGTGATATGAGCCATGTATTCCACTCAACTTTAACCCG
			GTCCCTGCCTCTATATCTTTAGCCGTTGCAAGAGCATCTACATAA
			TAAAATGCTGGTAAAACAATTGATGTTCCACTCAACTTTAACCCG
			GTCCCTGCCTCTATATCTTTAATGCCAATAAGGTGCCGAAACCTG
			TTGTTGTGAAATTTGTTATAACTTGTTCACTCAACTTTAACCCG

			GTCCCTGCCTCTATATCTTTCATCTAACCATACTTCCACTTTAAG
			CCAACGAGAAGAATATCTGTGATGCTTCCACTCAACTTTAACCCG
			GTCCCTGCCTCTATATCTTTAATTATGCCATCTTTGGCACCAGGT
			CTTGTCCTACTGTGGTCTGAGGTAGTTCCACTCAACTTTAACCCG
			GTCCCTGCCTCTATATCTTTAATACAACGTAAGGAACGGTAGCAG
			GTACATCCCCTTACCAACAAGATGATTCCACTCAACTTTAACCCG
			GTCCCTGCCTCTATATCTTTTCCCCTTCCACAAGGAAAAATAAAC
			CCCACACTGCCTTTCTGAGGATTTTCCACTCAACTTTAACCCG
			GTCCCTGCCTCTATATCTTTCATTTGCCATTTAGGCGAACCAACT
			AACAAAGACTGCTATCAAACACAGCTTCCACTCAACTTTAACCCG
			GTCCCTGCCTCTATATCTTTAAAACCTAAATAAGTAAAAATTCTG
			TCAATACCATAAGCTTTTGGTCCTTCCACTCAACTTTAACCCG
			GTCCCTGCCTCTATATCTTTGACTAACATTGTATCCGTCACAAC
			CTGCTAACATTGAGTTGTTGGTCACTTCCACTCAACTTTAACCCG
			GTCCCTGCCTCTATATCTTTGTTGCAATGAGACCAGGGAAGTTCC
			TACGCAGTCAGCAGTGTCCACGTGTCCACTCAACTTTAACCCG
			GTCCCTGCCTCTATATCTTTGCCATGCGATCACTGTGTTATAAT
			CGGAACGAAGCAAACAAGTAATATATCCACTCAACTTTAACCCG
			GTCCCTGCCTCTATATCTTTTCCATAACCGAGACTGTAAACAT
			TTCCGACGAATGTGGCAACGAAACATTCCACTCAACTTTAACCCG
			GTCCCTGCCTCTATATCTTTACCACAGCGTTGATATTGTCCTAAC
			ACAAAGTCTGTTCCATATAGAAATTTCCACTCAACTTTAACCCG
			GTCCCTGCCTCTATATCTTTAAGAAAAAAGCATAAAAAAGTATG
			AACTCCATGTAAAACAAGGGTAATCTTCCACTCAACTTTAACCCG
			GTCCCTGCCTCTATATCTTTTCATCATGTCGATGTTACGAGAAGC
			TCAAAAAGGCACCGAATACAAACATTTCCACTCAACTTTAACCCG
Mg DAT	MGAL_10B004526	B3	GTCCCTGCCTCTATATCTTTGCCATTCACTTCTGACGTCATTGTAT
			TACACCTTCTCCTCAACGTCTGCCTTCCACTCAACTTTAACCCG
			GTCCCTGCCTCTATATCTTTGTTGGTTAAGTAAATAACGTATTC
			GCTTTGATATAATTGTCTCTGTCTTTTCCACTCAACTTTAACCCG
			GTCCCTGCCTCTATATCTTTATCCTATAAGGGCAAACAATGGAAT
			CTACTGGTGACCCGCTTGCTTGACATTCCACTCAACTTTAACCCG
			GTCCCTGCCTCTATATCTTTACCAATGATATTTGCTCCATCGGGA
			TATGACGGAGGAACCAGCCACAACTTCCACTCAACTTTAACCCG
			GTCCCTGCCTCTATATCTTTAATGATATTACACCATACAACATGA
			ACATAATCCGCATATGTGATTGGTTTTCCACTCAACTTTAACCCG
			GTCCCTGCCTCTATATCTTTTCCAACAGATTCTCCAGTAAGGTCC
			CTAGGAGGAAAACCTGGTGCAACCCTTCCACTCAACTTTAACCCG
			GTCCCTGCCTCTATATCTTTACCAGAAAATCGGCCAACTCCATAG
			TCCATGTCCAATCATGGTTTCAATGTTCCACTCAACTTTAACCCG

			GTCCCTGCCTCTATATCTTTACTGCAAACAATATAGAATATCCGG
			CAAGAAACAATCATAGTTTCAAAGATTCCACTCAACTTTAACCCG
			GTCCCTGCCTCTATATCTTTGGACTCCACCCTCTGTACAAAACGC
			CAAAATTATCCATTAAGTTCACAACCTCCACTCAACTTTAACCCG
			GTCCCTGCCTCTATATCTTTACAGAAGACGAACAACCTCTCTGTGT
			GCCAACTATAAAGTAAAGAGCAAACCTCCACTCAACTTTAACCCG
			GTCCCTGCCTCTATATCTTTGCTGTAATGATTGCTTCTGAACCTC
			CGCAATATAGGAAATTCATCCGATATCCACTCAACTTTAACCCG
			GTCCCTGCCTCTATATCTTTGCATCAAGAAAAATATGACGGCCCA
			AGGAACTATCAAGCCCAAGAGTGAGTTCCTCAACTTTAACCCG
			GTCCCTGCCTCTATATCTTTTCCGGGTAGACTATAAATACTAGT
			TGGTGCACCGGTAATGTTGCAATATCCACTCAACTTTAACCCG
			GTCCCTGCCTCTATATCTTTTGGACGCCTGCTTTTCAGCCATGT
			GGACCTTCTGGGCAACACTAGAGATTCCACTCAACTTTAACCCG
			GTCCCTGCCTCTATATCTTTAGAAAAAACTAGTCAAACAATTAAT
			CTAATATCATGAAGATGACAAAGCCTTCCACTCAACTTTAACCCG
			GTCCCTGCCTCTATATCTTTATTATTATGAAGTTCATTATAACTG
			ACTTGTGATCAAAGCATCTCTATAATCCACTCAACTTTAACCCG
			GTCCCTGCCTCTATATCTTTCCAATGAGAAAAACACTTGTGTTG
			AATGCAAGTAAACACCAAATCCTGTTCCACTCAACTTTAACCCG
			GTCCCTGCCTCTATATCTTTGTTTTGTGGTATTAGGGGTGAGGTA
			CATCTACCCATACTTGTGATTCTGTTCCACTCAACTTTAACCCG
			GTCCCTGCCTCTATATCTTTTGTCAATCTTATCATCAAAATA
			ATAAATCCCTGTCCAGGCGCCATCTTCCACTCAACTTTAACCCG
			GTCCCTGCCTCTATATCTTTAACCATACAACCTTCCCAGATGTGT
			AATACCACATACGGAAACAAAGCTGTTCCACTCAACTTTAACCCG
			GTCCCTGCCTCTATATCTTTAACTGCTACACTTGAGCAAGAAGAA
			GGATATGCGATCGGCTAACATTCCCTTCCACTCAACTTTAACCCG
			GTCCCTGCCTCTATATCTTTAAAATAGTATAATTCTCTCCAAATG
			ATTCTTGGACGGCTCTGGCTATAATCCACTCAACTTTAACCCG
			GTCCCTGCCTCTATATCTTTAGAAACCAGTAAAGAGTGGAATAGT
			ATATTATGGTAGATACAAACATAACTTCCACTCAACTTTAACCCG
			GTCCCTGCCTCTATATCTTTCAACGGATTTGTAATCAACTGTACA
			TCCTATTCTGTTTCGTTAAAGGTCCTTCCACTCAACTTTAACCCG
			GTCCCTGCCTCTATATCTTTTGGACGTTCTCGTTTGCTAGTTCCG
			GCCTTCGATGCAAACATTAAGCCGATTCCACTCAACTTTAACCCG
			GTCCCTGCCTCTATATCTTTCATAACTTGTACATTTATTGGTGT
			TTCGAATTGTTGGAAGTGCATAGTTTCCACTCAACTTTAACCCG
			GTCCCTGCCTCTATATCTTTAGCTGTGTAGGCATTGTAATTTTTT
			TGTTATATTTTACATATATACTCTTCCACTCAACTTTAACCCG
Mg VMAT	MGAL_10B041819	B3	GTCCCTGCCTCTATATCTTTAACTGCTACACTTGAGCAAGAAGAA
			GGATATGCGATCGGCTAACATTCCCTTCCACTCAACTTTAACCCG
			GTCCCTGCCTCTATATCTTTAAAATAGTATAATTCTCTCCAAATG
			ATTCTTGGACGGCTCTGGCTATAATCCACTCAACTTTAACCCG
			GTCCCTGCCTCTATATCTTTAGAAACCAGTAAAGAGTGGAATAGT
			ATATTATGGTAGATACAAACATAACTTCCACTCAACTTTAACCCG
			GTCCCTGCCTCTATATCTTTCAACGGATTTGTAATCAACTGTACA
			TCCTATTCTGTTTCGTTAAAGGTCCTTCCACTCAACTTTAACCCG
			GTCCCTGCCTCTATATCTTTTGGACGTTCTCGTTTGCTAGTTCCG
			GCCTTCGATGCAAACATTAAGCCGATTCCACTCAACTTTAACCCG
			GTCCCTGCCTCTATATCTTTCATAACTTGTACATTTATTGGTGT
			TTCGAATTGTTGGAAGTGCATAGTTTCCACTCAACTTTAACCCG
			GTCCCTGCCTCTATATCTTTAGCTGTGTAGGCATTGTAATTTTTT
			TGTTATATTTTACATATATACTCTTCCACTCAACTTTAACCCG

			GTCCCTGCCTCTATATCTTTTTTGAACACATTTCAGTAATATTTT
			ACAGTTTGAAACATATTTAAAGATTTTCCACTCAACTTAAACCCG
			GTCCCTGCCTCTATATCTTTCATATGGATAATCTAATTTACGTAG
			TGTAATATGTAGTCACATTCTGAACTTCCACTCAACTTAAACCCG
			GTCCCTGCCTCTATATCTTTTAGAAGCATATTATCTAAGAAAAGA
			ATTTGGCACAATTGGTACTACAGTTTTCCACTCAACTTAAACCCG
			GTCCCTGCCTCTATATCTTTCGTGACTGACGACATCTTGTTAGGC
			ATGAATACTATAACTAAAATAATTTTCCACTCAACTTAAACCCG

Appendix Table 1. Table of HCR probes to localise monoaminergic genes. In the first column, name of gene is reported, the gene ID is reported in the second column. Column three and four report, respectively, the amplifier used and the probes of the genes.

<i>Mg</i> annotation	Sequence ID	Amplifier	Probe sequence
7B2	MGAL_10B074274	B2	CCTCGTAAATCCTCATCAaaACCAACAATTGATAGACTTTGTAAT
			CAAAACGTAATATATTTTATTTAAaaATCATCCAGTAAACCGCC
			CCTCGTAAATCCTCATCAaaCGTGAACATAATGTTATAAAATCAC
			GAACCGTTAAATACCCTCAATAAAAaaATCATCCAGTAAACCGCC
			CCTCGTAAATCCTCATCAaaAGAGTTCATCAATAATTGTGTGGC
			GGAATTTGGAATCGTTGAACGCCAaaATCATCCAGTAAACCGCC
			CCTCGTAAATCCTCATCAaaAGTTGTTTCTTATTTATGGCAAGAA
			AAGCAGATAAATTGCAGGAAAATAAaaATCATCCAGTAAACCGCC
			CCTCGTAAATCCTCATCAaaACCTACAGTGTAAACACATCTATTG
			TCTGTCTGTTGCTGTTACAAGGCAaaATCATCCAGTAAACCGCC
			CCTCGTAAATCCTCATCAaaAAATGATTCCATACATAACAATGAA
			ATTTTCCGTATTCGAGACAGCAAAAaaATCATCCAGTAAACCGCC
			CCTCGTAAATCCTCATCAaaCATCGTCCGACCTGGAGAACCCCAT
			GGAGACAGTCTGCATTA AAAACAaaATCATCCAGTAAACCGCC
			CCTCGTAAATCCTCATCAaaGTATAACTTTTAATTTACTAAATTT
			AAAATTTGTGGTTTGTCTATATCTaaATCATCCAGTAAACCGCC
			CCTCGTAAATCCTCATCAaaGAAAAGAAAGATCCTTTTTGCAAC
			TGAGTAACTTCAAAACAAAGACACAaaATCATCCAGTAAACCGCC
			CCTCGTAAATCCTCATCAaaATTTTTACCAATACACTTTTCTGTA
			AAAGAAAGAAAAAATAGTACTCAaaATCATCCAGTAAACCGCC
			CCTCGTAAATCCTCATCAaaAATAGCAACAACCATTTTTTATCCG
			TTTACGGACATTTCCGAAGAGGACTaaATCATCCAGTAAACCGCC
			CCTCGTAAATCCTCATCAaaTATGAATAATGCTTTAAATTGTTAT
			CAAGTCTGGTGCTAAACCTTTCATaaATCATCCAGTAAACCGCC
			CCTCGTAAATCCTCATCAaaTAAAATACATTTTTAAAAAGAAATA
			CATCTCTAGAATTTTGAAATTATCGaaATCATCCAGTAAACCGCC
			CCTCGTAAATCCTCATCAaaACTAAACCCATTGGTTTTACGCGCG
			ACAATAAGCAACATAACTTTTGCAaaATCATCCAGTAAACCGCC
			CCTCGTAAATCCTCATCAaaGCCTTTTTTGGCAGCAACCTCTCTG
			AACTCAATGTTTGTTCATTAGAGGAaaATCATCCAGTAAACCGCC
			CCTCGTAAATCCTCATCAaaATTTTCTCAAGTTTAGATTGAAGTA
			GGTCCGCTAAAATAAGGGTTGTTCTaaATCATCCAGTAAACCGCC
			CCTCGTAAATCCTCATCAaaATCTCATGTGGTTGCCACCTTTCTT
			CCATTATGCGTTCATTGTCCCTTCTaaATCATCCAGTAAACCGCC
			CCTCGTAAATCCTCATCAaaATCTGAGTTTGAGTTGTGTTCCATC
			GCGTTTCTCCAAATTCATGCTATCCaaATCATCCAGTAAACCGCC
			CCTCGTAAATCCTCATCAaaTCCTGGTCAATTTACGCCGGACATG
			TCTGGATAGTTTCTGTTTGTAAaaATCATCCAGTAAACCGCC
			CCTCGTAAATCCTCATCAaaCTTGTGTTTTAACAGACGGCGATT
			ACATGTGTTCTGCATCGCATGGACAaaATCATCCAGTAAACCGCC
			CCTCGTAAATCCTCATCAaaGCAGTTATCATCAGCTGTATATCCA
			GTCAAGGGAATTCTCAAACCTTTTCCaaATCATCCAGTAAACCGCC
			CCTCGTAAATCCTCATCAaaGCTGGAAGAACTTTATCAGTTTTTA

			GGGCAAGGATTTGGTGGGTTACAGTaaATCATCCAGTAAACCGCC
			CCTCGTAAATCCTCATCAaaTTCCACCAGACATGGACTGGTATCC
			GTTTAGGATTTTCTTTCCACCTCCaaATCATCCAGTAAACCGCC
			CCTCGTAAATCCTCATCAaaTGGGTCCCTAATTGATGCTCTGCTG
			AAGGCTAGGCAACTGTTGTATTAATaaATCATCCAGTAAACCGCC
			CCTCGTAAATCCTCATCAaaCAATCATCAGCATACTCCGTCCAA
			AGATTAGGGTCATCCATGTTTAAGGaaATCATCCAGTAAACCGCC
			CCTCGTAAATCCTCATCAaaCACCTGATTGAGTTGTTGAAGTTG
			GCTCGTCGCATAGTAACCATATCGaaATCATCCAGTAAACCGCC
			CCTCGTAAATCCTCATCAaaGTCAGAATAGCTGGCTCCTTGTGTG
			GAGCTGAGAAAGGTCGTTTCAGAAGaaATCATCCAGTAAACCGCC
			CCTCGTAAATCCTCATCAaaATGGGCAGCATGTTTAAGCCCTTT
			TATACTGTCATTGACAGGGCAAAAAaaATCATCCAGTAAACCGCC
			CCTCGTAAATCCTCATCAaaAATGTCCAGGCTGTTTTGTTTTGT
			GATAAAGCTCTTGATTTCGAAGTATaaATCATCCAGTAAACCGCC
			CCTCGTAAATCCTCATCAaaTTGCTTTGCTTCCGTCACTTCTCCA
			GGCGCTGGCTTTCAGAAAGGAATTaaATCATCCAGTAAACCGCC
			CCTCGTAAATCCTCATCAaaTTCCATATACGTCAGAGCGGAAAC
			AAGAATCGATATGGTGACAGAAATCaaATCATCCAGTAAACCGCC
7B2	MGAL_10B074274	B1	GAGGAGGGCAGCAAACGGaaACCAACAATTGATAGACTTTGTAAT
			CAAAACGTAAATATATTTTATTTAAaGAAGAGTCTTCCTTTACG
			GAGGAGGGCAGCAAACGGaaCGTGAACATAATGTTATAAAATCAC
			GAACCGTTAAATACCCTCAATAAAAaGAAGAGTCTTCCTTTACG
			GAGGAGGGCAGCAAACGGaaAGAGTTCATCAATAATTGTGTTGGC
			GGAATTTGGAATCGTTGAACGCCAtaGAAGAGTCTTCCTTTACG
			GAGGAGGGCAGCAAACGGaaAGTTGTTTCTTATTATGGCAAGAA
			AAGCAGATAAATTGCAGGAAAATAaGAAGAGTCTTCCTTTACG
			GAGGAGGGCAGCAAACGGaaACCTACAGTGTAAACACATCTATTCCG
			TCTGTCTGTTGTCTGTTACAAGGCAaGAAGAGTCTTCCTTTACG
			GAGGAGGGCAGCAAACGGaaAAATGATTCCATACATAACAATGAA
			ATTTTCCGTATTCGAGACAGCAAAAaGAAGAGTCTTCCTTTACG
			GAGGAGGGCAGCAAACGGaaCATCGTCCGACCTGGAGAACCCCAT
			GGAGACAGTCTGCATTA AAAACAAAaGAAGAGTCTTCCTTTACG
			GAGGAGGGCAGCAAACGGaaGTATAACTTTTAATTTACTAAATTT
			AAAATTTGTGGTTTGTCTATATCTaGAAGAGTCTTCCTTTACG
			GAGGAGGGCAGCAAACGGaaGAAAAGAAAGATCCTTTTTGCAAC
			TGAGTAACTTCAAAACAAAGACACAtaGAAGAGTCTTCCTTTACG
			GAGGAGGGCAGCAAACGGaaAATACACTTTTCTGTAACATTTACG
			AAAAAATAGTACTCAACAATTTTTaGAAGAGTCTTCCTTTACG
			GAGGAGGGCAGCAAACGGaaAACCATTTTTATCCGGACCAAGTC
			ATTTCCGAAGAGGACTACAATAGCAtaGAAGAGTCTTCCTTTACG
			GAGGAGGGCAGCAAACGGaaTGCTTTAAATTGTTATTGTCATCTC

			GTGCTAAACCTTTCATAGTATGAATtaGAAGAGTCTTCCTTTACG
			GAGGAGGGCAGCAAACGGaaTTTTTAAAAAGAAATACGAACAATA
			AATTTTGAAATTATCGTCTAAAATaTaGAAGAGTCTTCCTTTACG
			GAGGAGGGCAGCAAACGGaaATTGGTTTTACGCGGAACAACCTCA
			AACATAACTTTTGCAAACCTAAACtaGAAGAGTCTTCCTTTACG
			GAGGAGGGCAGCAAACGGaaGGCAGCAACCTCTCTGTGTGGTCCG
			TTTGTTTCATTAGAGGATCGCCTTTtaGAAGAGTCTTCCTTTACG
			GAGGAGGGCAGCAAACGGaaAGTTTAGATTGAAGTATTCCATTA
			AAATAAGGGTTGTTCTTCATTTTCTtaGAAGAGTCTTCCTTTACG
			GAGGAGGGCAGCAAACGGaaGGTTGCCACCTTTCTCTCGCGTTT
			GTTCATTGTCCCTTCTATATCTCATtaGAAGAGTCTTCCTTTACG
			GAGGAGGGCAGCAAACGGaaTGAGTTGTGTTCATCCATTCTGGA
			CAAATTCATGCTATCCAAATCTGAGtaGAAGAGTCTTCCTTTACG
			GAGGAGGGCAGCAAACGGaaATTCAGCCGGACATGAAAACATGT
			TTTCCTGTTTGCTTAATTCCTGGTtaGAAGAGTCTTCCTTTACG
			GAGGAGGGCAGCAAACGGaaTTAACAGACGGCGATTATTGTCAAG
			CTGCATCGCATGGACAGTCTTGTTGtaGAAGAGTCTTCCTTTACG
			GAGGAGGGCAGCAAACGGaaATCAGCTGTATATCCAACAGGGCAA
			ATTCTCAAACCTTTCCACGCAGTTaTaGAAGAGTCTTCCTTTACG
			GAGGAGGGCAGCAAACGGaaACTTTATCAGTTTTTACTTGTTTAG
			TTTGGTGGGTTACAGTAAGCTGGAAaTaGAAGAGTCTTCCTTTACG
			GAGGAGGGCAGCAAACGGaaACATGGACTGGTATCCCCAAAGGCT
			TTCTTTTCCACCTCTGTTCACCTaGAAGAGTCTTCCTTTACG
			GAGGAGGGCAGCAAACGGaaAATTGATGCTCTGCTGAATAGATTA
			CAACTGTTGTATTAATTCTGGGTCCtaGAAGAGTCTTCCTTTACG
			GAGGAGGGCAGCAAACGGaaGGCATACTCCGTCCAACCTAGCTCGT
			TCATCCATGTTTAAAGACCAATCATtaGAAGAGTCTTCCTTTACG
			GAGGAGGGCAGCAAACGGaaCAGGTTGTTGAAGTTGATAGAGCTG
			CATAGTAACCATATCGTCCACCTGAtaGAAGAGTCTTCCTTTACG
			GAGGAGGGCAGCAAACGGaaGCTGGCTCCTTGTGTGGTATATACT
			AAGGTCGTTCAGAAGAAGGTCAGAAaTaGAAGAGTCTTCCTTTACG
			GAGGAGGGCAGCAAACGGaaATGTTTAAAGCCCTTTGTAGATAAA
			ATTGACAGGGCAAAAATAATGGGCAtaGAAGAGTCTTCCTTTACG
			GAGGAGGGCAGCAAACGGaaGCTGTTTTGTTTTTGAATGGCGCT
			CTTGATTTTCAAGTATCTAATGTCtaGAAGAGTCTTCCTTTACG
			GAGGAGGGCAGCAAACGGaaTTCCGTCCTTCTCCAAGAAAGAAT
			TTTCAGAAAGGGAATTGATTGCTTTtaGAAGAGTCTTCCTTTACG
7B2	MGAL_10B074274	B3	GTCCCTGCCTCTATATCTttACCAACAATTGATAGACTTTGTAAT
			CAAAACGTAATATATTTTTATTTAAttCCAACCTCAACTTTAACCCG
			GTCCCTGCCTCTATATCTttCGTGAACATAATGTTATAAAAATCAC

			GAACCGTTAAATACCCTCAATAAAAAttCCACTCAACTTTAACCCG
			GTCCCTGCCTCTATATCTttAGAGTTCATCAATAATTGTGTGGC
			GGAATTTGGAATCGTTGAACGCCAAttCCACTCAACTTTAACCCG
			GTCCCTGCCTCTATATCTttAGTTGTTTCTTATTTATGGCAAGAA
			AAGCAGATAAATTGCAGGAAAATAAttCCACTCAACTTTAACCCG
			GTCCCTGCCTCTATATCTttACCTACAGTGTAACACATCTATTCCG
			TCTGTCTGTTGCTGTTACAAGGCAAttCCACTCAACTTTAACCCG
			GTCCCTGCCTCTATATCTttAAATGATTCCATACATAACAATGAA
			ATTTTCCGTATTTCGAGACAGCAAAAAttCCACTCAACTTTAACCCG
			GTCCCTGCCTCTATATCTttCATCGTCCGACCTGGAGAACCCCAT
			GGAGACAGTCTGCATTA AAAACA AAAAttCCACTCAACTTTAACCCG
			GTCCCTGCCTCTATATCTttGTATAACTTTTAATTTACTAAATTT
			AAAATTTGTGGTTTGTCTTATATCTttCCACTCAACTTTAACCCG
			GTCCCTGCCTCTATATCTttGAAAAAGAAAGATCCTTTTGGCAAC
			TGAGTAACTTCAAAACAAAGACACAAttCCACTCAACTTTAACCCG
			GTCCCTGCCTCTATATCTttATTTTTACCAATACACTTTTCTGTA
			AAAGAAAGAAAAAATAGTACTCAAAttCCACTCAACTTTAACCCG
			GTCCCTGCCTCTATATCTttAATAGCAACAACCATTTTTATCCG
			TTTACGGACATTTCCGAAGAGGACTttCCACTCAACTTTAACCCG
			GTCCCTGCCTCTATATCTttTATGAATAATGCTTTAAATTGTAT
			CAAGTCTGGTGCTAAACCTTTCATttCCACTCAACTTTAACCCG
			GTCCCTGCCTCTATATCTttTAAAATACATTTTTAAAAAGAAATA
			CATCTCTAGAATTTTGAAATTATCGttCCACTCAACTTTAACCCG
			GTCCCTGCCTCTATATCTttACTAAACCCATTGGTTTTACGCGCG
			ACAATAAGCAACATAACTTTTGCAAttCCACTCAACTTTAACCCG
			GTCCCTGCCTCTATATCTttGCCTTTTTTGGCAGCAACCTCTCTG
			AACTCAATGTTTGTTCATTAGAGGAAttCCACTCAACTTTAACCCG
			GTCCCTGCCTCTATATCTttATTTTCTCAAGTTTAGATTGAAGTA
			GGTCCGCTAAAATAAGGGTTGTCTttCCACTCAACTTTAACCCG
			GTCCCTGCCTCTATATCTttATCTCATGTGGTTGCCACCTTCTT
			CCATTATGCGTTCATTGTCCCTTCTttCCACTCAACTTTAACCCG
			GTCCCTGCCTCTATATCTttATCTGAGTTTGAGTTGTGTCCATC
			GCGTTTCTCAAATTCATGCTATCCttCCACTCAACTTTAACCCG
			GTCCCTGCCTCTATATCTttTCCTGGTCAATTTAGCCGGACATG
			TCTGGATAGTTTCTGTTTGTAAAttCCACTCAACTTTAACCCG
			GTCCCTGCCTCTATATCTttCTTGTTGTTTAAACAGACGGCGATT
			ACATGTGTTCTGCATCGCATGGACAAttCCACTCAACTTTAACCCG
			GTCCCTGCCTCTATATCTttGCAGTTATCATCAGCTGTATATCCA
			GTCAAGGGAATTCTCAAACCTTTTCCttCCACTCAACTTTAACCCG
			GTCCCTGCCTCTATATCTttGCTGGAAGAACTTTATCAGTTTTTA

			GGGCAAGGATTTGGTGGGTACAGTtCCACTCAACTTTAACCCG
			GTCCCTGCCTCTATATCTtTTCCACCAGACATGGACTGGTATCC
			GTTTAGGATTTTCTTTTCCACCTCCtCCACTCAACTTTAACCCG
			GTCCCTGCCTCTATATCTtTGGGTCCCTAATTGATGCTCTGCTG
			AAGGCTAGGCAACTGTTGTATTAATtCCACTCAACTTTAACCCG
			GTCCCTGCCTCTATATCTtCAATCATCAGGCATACTCCGTCCAA
			AGATTAGGGTCATCCATGTTTAAGGtCCACTCAACTTTAACCCG
			GTCCCTGCCTCTATATCTtCACCTGATTAGGTTGTTGAAGTTG
			GCTCGTCGCATAGTAACCATATCGtCCACTCAACTTTAACCCG
			GTCCCTGCCTCTATATCTtGTCAGAATAGCTGGCTCCTTGTGTG
			GAGCTGAGAAAGGTCGTTTCAGAAAGtCCACTCAACTTTAACCCG
			GTCCCTGCCTCTATATCTtATGGGCAGCATGTTTAAGCCCCTTT
			TATACTGTCATTGACAGGGCAAAAAtCCACTCAACTTTAACCCG
			GTCCCTGCCTCTATATCTtAATGTCCAGGCTGTTTTGTTTTGT
			GATAAAGCTCTTGATTTTGAAGTATtCCACTCAACTTTAACCCG
			GTCCCTGCCTCTATATCTtTTGCTTTGCTTCCGTCACCTTCTCCA
			GGCGCTGGCTTTCAGAAAGGAATTtCCACTCAACTTTAACCCG
			GTCCCTGCCTCTATATCTtTTCCATATACGTCAGAGCGGAAAAC
			AAGAATCGATATGGTGACAGAAATtCCACTCAACTTTAACCCG
			GAGGAGGGCAGCAAACGGaaATTGTGTATTGTGTCAAGGGTAAC
			CGTGGCTCTGTACTTATACATCTCTtaGAAGAGTCTTCCTTTACG
			GAGGAGGGCAGCAAACGGaaTGTTGACTGCTCTATCCCTATTTTG
			TTTTTAGTGATCAAGATTATAACACtaGAAGAGTCTTCCTTTACG
			GAGGAGGGCAGCAAACGGaaACCCAGCTATAAAACCAGGTTAAT
			AATTTGATGCGACTGTCATGCAAGTtaGAAGAGTCTTCCTTTACG
			GAGGAGGGCAGCAAACGGaaCGCGCTGCTGGCGTACTAAATTATA
			CACTGATGAGTCTAGTTGTAGACGAtaGAAGAGTCTTCCTTTACG
			GAGGAGGGCAGCAAACGGaaGAATTTTCTATGAGTCAGTCAGTA
			GCCATTTCAATTAGGGACTTACCACTtaGAAGAGTCTTCCTTTACG
			GAGGAGGGCAGCAAACGGaaTAAGAATTGTTATAGATATATATTT
			CCACAATACAGTATTTCTTTTGTGTtaGAAGAGTCTTCCTTTACG
			GAGGAGGGCAGCAAACGGaaTGATGACAACATATAGTATGACATA
			AAAAACGGTTTTGAGCAAACATTAAtaGAAGAGTCTTCCTTTACG
			GAGGAGGGCAGCAAACGGaaATACTGACAGGTAATATAGCTATAT
			TAACATTGATTTATCACACAAGTGCtaGAAGAGTCTTCCTTTACG
			GAGGAGGGCAGCAAACGGaaAAAATATATTTTAGCTTTAATGGTA
			TCTGATGCTCAATTGTTTCTTATCTtaGAAGAGTCTTCCTTTACG
			GAGGAGGGCAGCAAACGGaaCATAACAAAATTGCTCATCAACAAA
			AAAAATTAACAATGATAGACACATAtaGAAGAGTCTTCCTTTACG
			GAGGAGGGCAGCAAACGGaaCATTTGTAATCTTTTGATTGAATG
			TTTTTCATAAATAACGTGCAAGATTtaGAAGAGTCTTCCTTTACG
			GAGGAGGGCAGCAAACGGaaATACTGTTGTTCTTAATGGCTAAAT
Tektin	MGAL_10B026084	B1	

			CCAAGACATTTTTCTCTGTCGATGAtaGAAGAGTCTTCCTTTACG
			GAGGAGGGCAGCAAACGGaaTTCTGTAAATCTCTTGTACTTCTGAT
			AAGTTTCATCTGGAGAGATTCTACTtaGAAGAGTCTTCCTTTACG
			GAGGAGGGCAGCAAACGGaaTGGGTTGTTCCTTATCCTGGATGGC
			TTCCAGACGAGAATGAGCCACCTGtaGAAGAGTCTTCCTTTACG
			GAGGAGGGCAGCAAACGGaaTCAGTTGATTCCTGGCATCTCTTGG
			AGATGTGTCTGGAGTCTGTTTCTAGtaGAAGAGTCTTCCTTTACG
			GAGGAGGGCAGCAAACGGaaACGGGAGGCAGCTCTCTCACTCTGT
			CACACTTCTATCTCGTTTCTCATtaGAAGAGTCTTCCTTTACG
			GAGGAGGGCAGCAAACGGaaATGACAATCCCCTGGAGTTGTTCCT
			GGTCTACTCTTGCATTCCATTGTGtaGAAGAGTCTTCCTTTACG
			GAGGAGGGCAGCAAACGGaaAGACCAAGTTGTACGTTGGCCCGTT
			TCTAACTCGTGTGTGCAGCACGGTtaGAAGAGTCTTCCTTTACG
			GAGGAGGGCAGCAAACGGaaTTTTGATGATATCTACTTCCCGAAT
			CTGTATTTCTCATCTTGTCTTGACAtaGAAGAGTCTTCCTTTACG
			GAGGAGGGCAGCAAACGGaaGTCAATTCCTTGACGTTTTTCTCTG
			TTCTTTCTCTGGGTTATCATGTACAtaGAAGAGTCTTCCTTTACG
			GAGGAGGGCAGCAAACGGaaGGATTTTCTGTCTCCTGTAGAGCTT
			TACAGACTCTTGAGAAATGTGAAtaGAAGAGTCTTCCTTTACG
			GAGGAGGGCAGCAAACGGaaCTCCAATTTCTGTCATCATGTTATC
			CCAAAATTCTCTTGGCTTCATTCAGtaGAAGAGTCTTCCTTTACG
			GAGGAGGGCAGCAAACGGaaTGAAATATCACCGATTCCGCTCTCCA
			TTCATGATTAACCTCCGTTTTCCAGtaGAAGAGTCTTCCTTTACG
			GAGGAGGGCAGCAAACGGaaTTTGTTTTGTCTCCGTTTCTCTGC
			CGTTTACCAACGTCGCTTTGTGTTCtaGAAGAGTCTTCCTTTACG
			GAGGAGGGCAGCAAACGGaaCAGCAGCACTTCTTGTTTTATCCGA
			GACGAACTGTATCAAATCGTAGACGtaGAAGAGTCTTCCTTTACG
			GAGGAGGGCAGCAAACGGaaCCAATCGTTAGGAGAAAATCGTGTA
			TAAATAATTACTTTGATTTGAATTAtaGAAGAGTCTTCCTTTACG
			GAGGAGGGCAGCAAACGGaaGAAGGAACTTTAACATTGTCCAATT
			ATAGCGTTTCTAGCCGAGCAAACAtaGAAGAGTCTTCCTTTACG
			GAGGAGGGCAGCAAACGGaaCTGGCATACTTCTGACTAAAGCTGA
			AAAGTTGATTCTTAGCAGAGAAAGGtaGAAGAGTCTTCCTTTACG
			GAGGAGGGCAGCAAACGGaaTGTACTTGGCCTCCAAGGAAGTGTG
			AGGATTTACACGTGCGGTTTGGTAGtaGAAGAGTCTTCCTTTACG
			GAGGAGGGCAGCAAACGGaaGGATAAGTGTCAATGGCCTTATATG
			AAAGATCTCCTTAGAGGTGAAGGGtaGAAGAGTCTTCCTTTACG
			GAGGAGGGCAGCAAACGGaaATGTTTGTGTATTGCTACCACCGAG
			CTTGCATTGTACTTATACTAGGCAAtaGAAGAGTCTTCCTTTACG
			GAGGAGGGCAGCAAACGGaaTGTGTGACCCAAGTATTCATCTTG
			TGGACCGTTCATATAGGTGGCAGTCTaGAAGAGTCTTCCTTTACG
			GAGGAGGGCAGCAAACGGaaGTGAATGTAATGGTATAAAGTGACA
			GGTCTAAATGTAGGTACGGCTTCACtaGAAGAGTCTTCCTTTACG

Appendix Table 2. Table of HCR probes of tissues genes. Table structure is the same of Appendix Table 1.

Mg annotation	Sequence ID	Amplifier	Probe
Mg nrf-1	MGAL_10B039405	B1	GAGGAGGGCAGCAAACGGaaTCATTCATTTTTTGTGGCAGATTT
			CATTCATTCATTCTTTATTTATTCtaGAAGAGTCTTCCTTTACG
			GAGGAGGGCAGCAAACGGaaAATAAAACATAAACCAATTAAGTTT
			TTTTTTCTTACCTCCAAAACCGATGtaGAAGAGTCTTCCTTTACG
			GAGGAGGGCAGCAAACGGaaTACGTATGTAAGTAAGGTACCACTT
			TCTTTGTTTCTTCAGTTGATTTAGAtaGAAGAGTCTTCCTTTACG
			GAGGAGGGCAGCAAACGGaaGCATTGATAATGGCCATGAAGGTTT
			GCGAAGAATGTATCTACTGATACTTtaGAAGAGTCTTCCTTTACG
			GAGGAGGGCAGCAAACGGaaCAATATTACCTGCTAAATTCATGCC
			TCTTTATCAGTGCTCCAAAAAGTGTtaGAAGAGTCTTCCTTTACG
			GAGGAGGGCAGCAAACGGaaACTCATACTGATAAACCGTATACCG
			TGCGAATGTGTGCTCTAGAATAACctGAAGAGTCTTCCTTTACG
			GAGGAGGGCAGCAAACGGaaTTTGTACTCAATATTTTGGCTCCAT
			ACAGCAGTTAGCGTGCCAGAACCTTtaGAAGAGTCTTCCTTTACG
			GAGGAGGGCAGCAAACGGaaTTCCAAGAAATCCTGGTTTGATGG
			TGTAAACAGAAAATGACAGCAGTAAtaGAAGAGTCTTCCTTTACG
			GAGGAGGGCAGCAAACGGaaCTTTTCCGGCTCTTTAAATTGATAT
			TGTGGACGGATCTTCAGCTGACATTtaGAAGAGTCTTCCTTTACG
			GAGGAGGGCAGCAAACGGaaCATGCCCATACCAGCTGAATCATA
			TTTTTCGCCCTCATATCCGTTATTtaGAAGAGTCTTCCTTTACG
			GAGGAGGGCAGCAAACGGaaACTGTTTTTCTTTGGTTTTGACATG
			CGTAGCATGAGCATCGGATAGATCCtaGAAGAGTCTTCCTTTACG
			GAGGAGGGCAGCAAACGGaaATGATCGCAAGTCCAACAAGTATAC
			TGAATAACACATCGTACGTGGTAGtaGAAGAGTCTTCCTTTACG
			GAGGAGGGCAGCAAACGGaaAATCAATAGGTTGGTCTTGTGTTCTT
			TTACGATGAAGGCTATTCTTGCTTtaGAAGAGTCTTCCTTTACG
			GAGGAGGGCAGCAAACGGaaATTTGACATCCTAGGTAACACGGAA
			TTCTCCGCCAGTTGCAAATACTGTGtaGAAGAGTCTTCCTTTACG
			GAGGAGGGCAGCAAACGGaaCAAGTATTCGGCACACATAGCCGA
			AACAGATTTTTTATATCTAAAATGGtaGAAGAGTCTTCCTTTACG
			GAGGAGGGCAGCAAACGGaaAAGGATTGGTAAGAGAAGTAACATA
			GGATTTCCATTCTTTTGCTCTCGTtaGAAGAGTCTTCCTTTACG
			GAGGAGGGCAGCAAACGGaaTTCCTCAGCTGATATACCAATGCAT
			TTTGGAAGACAGTATTCTCCGTTGtaGAAGAGTCTTCCTTTACG
			GAGGAGGGCAGCAAACGGaaCCGCTCAGTAAACCTGCTGGAGGCT
			TCATAATCACCAAGCCACGCAATTTtaGAAGAGTCTTCCTTTACG
			GAGGAGGGCAGCAAACGGaaATTGTTTTCTCCAAATAATCCTGC
			CCAAAGCATCTAACATTTGCATAGtaGAAGAGTCTTCCTTTACG
			GAGGAGGGCAGCAAACGGaaTGCATTCACTTTAGGTAAGGGTGGG
			AACACTTTGAGTATGGTTCAAGCAaGAAGAGTCTTCCTTTACG
			GAGGAGGGCAGCAAACGGaaGCCGTCATTTACGGGTAGAAGTGT
			GTAAGTGGCTGTTACTGGAGAATTAGtaGAAGAGTCTTCCTTTACG
			GAGGAGGGCAGCAAACGGaaCAGTTGGTGTTCCTTTGCAAGTGT
			TTGGCATTGCCTTTGTGGTTACGGAtaGAAGAGTCTTCCTTTACG
GAGGAGGGCAGCAAACGGaaCGTTGTAGGCAAAGAATTAATGTAT			

			ATCACCTTGTTCATGAGTTGCATAAaGAAGAGTCTTCCTTTACG
			GAGGAGGGCAGCAAACGGaaAAATCATGAATATTAGTGGTATTTCT
			TTCTGGTTTAAAGTCGAAGTGACATaGAAGAGTCTTCCTTTACG
			GAGGAGGGCAGCAAACGGaaCTGAAAACCTGTCCAACCTCATCTGA
			TTAAAACACTAGTACTATCAGATAGaGAAGAGTCTTCCTTTACG
			GAGGAGGGCAGCAAACGGaaTACATTCAGTGCTTTATTCATTGCA
			TGTCTGAAGATTGTCTAATATGGTCaGAAGAGTCTTCCTTTACG
			GAGGAGGGCAGCAAACGGaaTTATGCTGTGAATATCCTTTCAATA
			ATATCTTGAAATAAAACCGTCTGGTtaGAAGAGTCTTCCTTTACG
			GAGGAGGGCAGCAAACGGaaAATTATCATCTAAAGCCACTGAACA
			GGAAAACGTTTTGTATTATGTCATGtaGAAGAGTCTTCCTTTACG
			GAGGAGGGCAGCAAACGGaaATACATCTTTGCCATGGTGTAAAC
			GAATAGAAGTAAAAGGAAACAGTAcGAAGAGTCTTCCTTTACG
			GAGGAGGGCAGCAAACGGaaAGTCAACTCCAAGATAATATACCTT
			TCGATGGCATCAACTGGGACTGTTtaGAAGAGTCTTCCTTTACG
			GAGGAGGGCAGCAAACGGaaGAAAAACACGTCCCATATTTTCACT
			ACCCGAGACTTTCGCAATATATTGAtaGAAGAGTCTTCCTTTACG
			GAGGAGGGCAGCAAACGGaaAAAATGCTTAGATACAATCCCTGAT
			TTACCCAAATGTGGAAACTCCAAGTtaGAAGAGTCTTCCTTTACG
			GAGGAGGGCAGCAAACGGaaATAACAATTGTGCCTGCAATCTTCG
			ATTGATGTTGCAAGCAAAAAGATGCTaGAAGAGTCTTCCTTTACG
			GAGGAGGGCAGCAAACGGaaTGATTATATAAAAACCTGCATATCATT
			AGTAAAGAGGTACGATTATGATTGGtaGAAGAGTCTTCCTTTACG
			GAGGAGGGCAGCAAACGGaaTTCACTAACTGGTTTGAAGTTATTT
			TAAATACCAGGTCCAGGAAAAACAcGAAGAGTCTTCCTTTACG
			GAGGAGGGCAGCAAACGGaaTTACAGTAGTTTTTCTCGAAGCCAT
			TATAATAGATTCCACCACCAGTGTtaGAAGAGTCTTCCTTTACG
			GAGGAGGGCAGCAAACGGaaAAGGAAATACTGCTATGTAATCCC
			TGGGCCAGAAAGTCCGTTTCCAATtaGAAGAGTCTTCCTTTACG
			GAGGAGGGCAGCAAACGGaaCCAAAAACGATGAAAATAAAATAGA
			AATCAACATGTAGGGAGGGGTCAATtaGAAGAGTCTTCCTTTACG
			GAGGAGGGCAGCAAACGGaaATCTGTTTCAGAGTTAAATAGGTTA
			CAGTTAATCTTTCCTTTGCTTTTCTtaGAAGAGTCTTCCTTTACG
			GAGGAGGGCAGCAAACGGaaCTACAGCAACCGGGGCATTCATGAC
			GAAGACCACTGAGAGCAAAGAACGTtaGAAGAGTCTTCCTTTACG
			GAGGAGGGCAGCAAACGGaaTGGAAATATCGTGGCAATATTTTCT
			CATAAATGAGAGCCTCTTTATATAcGaGAAGAGTCTTCCTTTACG
			GAGGAGGGCAGCAAACGGaaGTATGACCCAGTATTATCCAGGTCA
			CTCCCTGCATAAATCCAAATACAaGaGAAGAGTCTTCCTTTACG
			GAGGAGGGCAGCAAACGGaaTTAATGTCCAGCTGATTGGTGTGT
			TAATGAATCGGATACCATTGATAGcGaGAAGAGTCTTCCTTTACG
			GAGGAGGGCAGCAAACGGaaGGAAAAGGATAAGAGTAATTGTCCA
			TAGAATCTTGGAAACCATTCTGTATtaGAAGAGTCTTCCTTTACG
			GAGGAGGGCAGCAAACGGaaTCCTCCTTGTACTTTGTTCTCTTG
			ATCCCGTGCTCAATGGTTGATTTTTtaGAAGAGTCTTCCTTTACG
			GAGGAGGGCAGCAAACGGaaTGGAGTAGGTTTCCCCCTTATTGC
Mg nrf-2	MGAL_10B006948	B1	GAGGAGGGCAGCAAACGGaaAAAATGCTTAGATACAATCCCTGAT
			TTACCCAAATGTGGAAACTCCAAGTtaGAAGAGTCTTCCTTTACG
			GAGGAGGGCAGCAAACGGaaATAACAATTGTGCCTGCAATCTTCG
			ATTGATGTTGCAAGCAAAAAGATGCTaGAAGAGTCTTCCTTTACG
			GAGGAGGGCAGCAAACGGaaTGATTATATAAAAACCTGCATATCATT
			AGTAAAGAGGTACGATTATGATTGGtaGAAGAGTCTTCCTTTACG
			GAGGAGGGCAGCAAACGGaaTTCACTAACTGGTTTGAAGTTATTT
			TAAATACCAGGTCCAGGAAAAACAcGAAGAGTCTTCCTTTACG
			GAGGAGGGCAGCAAACGGaaTTACAGTAGTTTTTCTCGAAGCCAT
			TATAATAGATTCCACCACCAGTGTtaGAAGAGTCTTCCTTTACG
			GAGGAGGGCAGCAAACGGaaAAGGAAATACTGCTATGTAATCCC
			TGGGCCAGAAAGTCCGTTTCCAATtaGAAGAGTCTTCCTTTACG
			GAGGAGGGCAGCAAACGGaaCCAAAAACGATGAAAATAAAATAGA
			AATCAACATGTAGGGAGGGGTCAATtaGAAGAGTCTTCCTTTACG
			GAGGAGGGCAGCAAACGGaaATCTGTTTCAGAGTTAAATAGGTTA
			CAGTTAATCTTTCCTTTGCTTTTCTtaGAAGAGTCTTCCTTTACG
			GAGGAGGGCAGCAAACGGaaCTACAGCAACCGGGGCATTCATGAC
			GAAGACCACTGAGAGCAAAGAACGTtaGAAGAGTCTTCCTTTACG
			GAGGAGGGCAGCAAACGGaaTGGAAATATCGTGGCAATATTTTCT
			CATAAATGAGAGCCTCTTTATATAcGaGAAGAGTCTTCCTTTACG
			GAGGAGGGCAGCAAACGGaaGTATGACCCAGTATTATCCAGGTCA
			CTCCCTGCATAAATCCAAATACAaGaGAAGAGTCTTCCTTTACG
			GAGGAGGGCAGCAAACGGaaTTAATGTCCAGCTGATTGGTGTGT
			TAATGAATCGGATACCATTGATAGcGaGAAGAGTCTTCCTTTACG
			GAGGAGGGCAGCAAACGGaaGGAAAAGGATAAGAGTAATTGTCCA
			TAGAATCTTGGAAACCATTCTGTATtaGAAGAGTCTTCCTTTACG
			GAGGAGGGCAGCAAACGGaaTCCTCCTTGTACTTTGTTCTCTTG
			ATCCCGTGCTCAATGGTTGATTTTTtaGAAGAGTCTTCCTTTACG
			GAGGAGGGCAGCAAACGGaaTGGAGTAGGTTTCCCCCTTATTGC

			TACGCACTACTGGAGTATCTGCGTTaGAAGAGTCTTCCTTTACG
			GAGGAGGGCAGCAAACGGaaATTAACCGTATATTTACTTGTCTTG
			TGTCTCTGTGATTCATTAGTTGAAaGAAGAGTCTTCCTTTACG
			GAGGAGGGCAGCAAACGGaaTCAAAGATTGTTGCTATTGACATTA
			CGTTTGAAAATTTGTCTTGTGATTAaGAAGAGTCTTCCTTTACG
			GAGGAGGGCAGCAAACGGaaGGGCTATAGCTCTGGTATCAAGTTT
			CAACAAAGACAACACAAACTGAAATaGAAGAGTCTTCCTTTACG
			GAGGAGGGCAGCAAACGGaaAGCATAAATTCGGTTGTTGGTCAAT
			ACCTGGTTCCTGGCACGTTAAATCAaGAAGAGTCTTCCTTTACG
			GAGGAGGGCAGCAAACGGaaTCTTCTCTTTTCGTACAAGTATCAG
			GGGGCGACTGCACTTAACAATACAaGAAGAGTCTTCCTTTACG
			GAGGAGGGCAGCAAACGGaaCATCCGCTTTTGTACCAGGGTTTGG
			TACACAATCCAATTTTAATTGAAACaGAAGAGTCTTCCTTTACG
			GAGGAGGGCAGCAAACGGaaGTATTTTCTTTGAACGTTTCGGCT
			TCCTGTTATCCAAAATGAACCCAGaGAAGAGTCTTCCTTTACG
			GAGGAGGGCAGCAAACGGaaTCCCAGGTTAAAATAAAATTCAACA
			ATACGAAGACATTCTTCATAATCTCaGAAGAGTCTTCCTTTACG
			GAGGAGGGCAGCAAACGGaaTCATTCGTAAGCCCAATCTTTTGA
			CTGATGGAGGCTTCCGTTAGCATCaGAAGAGTCTTCCTTTACG
			GAGGAGGGCAGCAAACGGaaATCATTTAAACATCTTGAAGAATTG
			TTCCACTCCAGGAACAATGCTTTGgaGAAGAGTCTTCCTTTACG
			GAGGAGGGCAGCAAACGGaaTTGCTGTTGTCTATAACATGTGCAT
			TTAATGCATCGTTCGTCTCAATaGAAGAGTCTTCCTTTACG
			GAGGAGGGCAGCAAACGGaaCATCAAACCTTCGATAACACATCATT
			TCGTAATAAATGATAAGACGTCTTtaGAAGAGTCTTCCTTTACG
			GAGGAGGGCAGCAAACGGaaCACATTCTCGACTTTATTACTGCT
			TTGTGCGTTTGTGTATAAATTCcaGAAGAGTCTTCCTTTACG
			GAGGAGGGCAGCAAACGGaaTCATCGTAATTGTCCGTTATAGCGT
			AAAGCAGACCCGACATTGTTCAACaGAAGAGTCTTCCTTTACG
			GAGGAGGGCAGCAAACGGaaTTATTTACTGAACCGGAGAGCCAC
			TAAAAGGTACAGTCTCGTTGTTATTaGAAGAGTCTTCCTTTACG
			GAGGAGGGCAGCAAACGGaaTGCTGTGTCGTTCTTTCAGAACAG
			TTAACTATATCTGCTAAACTTAGTtaGAAGAGTCTTCCTTTACG
Mg nrf-6	MGAL_10B065682	B1	GAGGAGGGCAGCAAACGGaaAATAAGGTACTTTCATATTCATATT
			TTGACACAAATTCATATGCATTTTAtaGAAGAGTCTTCCTTTACG
			GAGGAGGGCAGCAAACGGaaGCCACAAATGCAACTCCATAAGCCA
			ATCATTGGTGATTCAAATACCAGTgaGAAGAGTCTTCCTTTACG
			GAGGAGGGCAGCAAACGGaaACAAGTGGGTGTATCAGGTAGGCA
			TTTTCTGTGATTTGTAGTAAAAGTACaGAAGAGTCTTCCTTTACG
			GAGGAGGGCAGCAAACGGaaATATGACCCAACAGACAGCAGCACC
			AACCTCCATTTCCAGTAGCATGCaGAAGAGTCTTCCTTTACG
			GAGGAGGGCAGCAAACGGaaAGTACAGCTAAAGCCGACGCAGCAA
			CCATTTATGTCGTCATATATACCATaGAAGAGTCTTCCTTTACG
			GAGGAGGGCAGCAAACGGaaAACCAGGTATGGACCAATTCGACAG
			GTAAAGAATATAGCCTGTGTACATTaGAAGAGTCTTCCTTTACG
			GAGGAGGGCAGCAAACGGaaTTGCTGCGGCTGTTCTTAACCATAT

			GGTCCTTATGTAAGTATATCCtaGAAGAGTCTTCCTTTACG
			GAGGAGGGCAGCAAACGGaaTTTGCCAAATACCATGACGACAA
			GGACTTATAACATAAACTGCATATtaGAAGAGTCTTCCTTTACG
			GAGGAGGGCAGCAAACGGaaATTTGTTATCCACATGGGTCCGCTT
			ATCTTTACAGTAATTCTTTTCGAAGtaGAAGAGTCTTCCTTTACG
			GAGGAGGGCAGCAAACGGaaATCATAATTAACATATATGGAGGAG
			AGATATTTTGAGATACATATCTGCAtaGAAGAGTCTTCCTTTACG
			GAGGAGGGCAGCAAACGGaaTAAACCAATTCAGTTGCGCTTTTGT
			ACCTCCAAAACCGATGAAAATAAAAtaGAAGAGTCTTCCTTTACG
			GAGGAGGGCAGCAAACGGaaAAGTAAGGTACCCTTAAAGCGAAG
			CTTCAGTTGATTTAGAACTACGTATtaGAAGAGTCTTCCTTTACG
			GAGGAGGGCAGCAAACGGaaATAGCCATGAAGGTTTTTCTCTTTA
			GTATCTACTGATACTTCAGCATTGtaGAAGAGTCTTCCTTTACG
			GAGGAGGGCAGCAAACGGaaCTACTGACAACAAGCCAAACGCGTA
			GTTCTCCATAAAGCGTACCAATATTtaGAAGAGTCTTCCTTTACG
			GAGGAGGGCAGCAAACGGaaTATAAACCGTATACCGTTGACAGCA
			GTGTCCTAGAATAACCCAGCTCATGtaGAAGAGTCTTCCTTTACG
			GAGGAGGGCAGCAAACGGaaAATATCTTAGCTCCATTTGTGTAAA
			AGCGTGCCAGAACCTTGGTTGTACTaGAAGAGTCTTCCTTTACG
			GAGGAGGGCAGCAAACGGaaATCCAGAGTTGAACAGATTTTTTAT
			AAAATGACAGCAGTAACCTTCCAAGtaGAAGAGTCTTCCTTTACG
			GAGGAGGGCAGCAAACGGaaTATCCCGACCATAATTTCCATTCCT
			TGAAATAGAGCAAGTATTCGGCACAtaGAAGAGTCTTCCTTTACG
			GAGGAGGGCAGCAAACGGaaGCAACATAAACTTGGCAAGACAGT
			GCTTTCGTTAGTGGATTGAAATAGtaGAAGAGTCTTCCTTTACG
			GAGGAGGGCAGCAAACGGaaCAATACATTCGTCATAATCACCAAG
			CTCCGTGGAATTCCTCGGCTTCTATtaGAAGAGTCTTCCTTTACG
			GAGGAGGGCAGCAAACGGaaAGGAGGCTTTCCAGAGCATCCAAC
			CGCAAATTTCCGCGAAGTAAACCTtaGAAGAGTCTTCCTTTACG
			GAGGAGGGCAGCAAACGGaaAGTCCCGCAAGAATACTTTGGGTAT
			TGCATAGCCCATTTGTTTTCTCCAAtaGAAGAGTCTTCCTTTACG
			GAGGAGGGCAGCAAACGGaaAGGGTGAATTGTATTGGCTGTAAC
			TCAAGCAGAGTGCATTCCTTTAGGtaGAAGAGTCTTCCTTTACG
			GAGGAGGGCAGCAAACGGaaTAGAACTGTTGTTGGTATTGATTTT
			AGACTTAGAAGCAGTAACCTGTTACGtaGAAGAGTCTTCCTTTACG
			GAGGAGGGCAGCAAACGGaaGCAAGTGTGGTATCACCTGTTTCAG
			GTAACGGGAACAGTTGGTGTCTTtaGAAGAGTCTTCCTTTACG
			GAGGAGGGCAGCAAACGGaaTGATATCTGTGTTCTGGTTTAAAGT
			TTGCATAAGCCGTTGTAGGCAAAGAtaGAAGAGTCTTCCTTTACG
			GAGGAGGGCAGCAAACGGaaGGTATTTCCAATTATAACTATCC
			AGTGACATCAAAAACATTAGCATActGAAGAGTCTTCCTTTACG
			GAGGAGGGCAGCAAACGGaaGAAAATGTCTGAAGATTGTCTAATA
			AGTTCTGATAATTTGTCCAACCTCATtaGAAGAGTCTTCCTTTACG
			GAGGAGGGCAGCAAACGGaaCATTTATATCTTGAAGTAAAACCGT
			TCCGTACATTCATGCTTTATTCATtaGAAGAGTCTTCCTTTACG
			GAGGAGGGCAGCAAACGGaaTGTTTGATAACTGTTTGTATTATG

			GTTAACATGCTGTGAATATCCTTTCTaGAAGAGTCTTCCTTTACG
			GAGGAGGGCAGCAAACGGaaCATCTGAGTAGTAGTAATAGGAAAC
			TGATAATTATCTTCTAAAGCAACTGtaGAAGAGTCTTCCTTTACG
Mg nrf-9	MGAL_10B035396	B1	GAGGAGGGCAGCAAACGGaaTGAAGCCAAAACCTTCGTCCAAATGC
			TGAAGAATCTCGAGGGATGTCCTTCTaGAAGAGTCTTCCTTTACG
			GAGGAGGGCAGCAAACGGaaATGTAAACATTTCTAAGAAATTTCT
			TTGTGAGAAGCGGAGAATGGCTGTTaGAAGAGTCTTCCTTTACG
			GAGGAGGGCAGCAAACGGaaTCAATGTCGGATGACGAATTTATAT
			TTTATATCGGCATTGCTTGAAAGATaGAAGAGTCTTCCTTTACG
			GAGGAGGGCAGCAAACGGaaCCAACAGACGGCAGCACCCCACT
			ATTTCCAGTAGCACATGCAAATATGtaGAAGAGTCTTCCTTTACG
			GAGGAGGGCAGCAAACGGaaCAGCTAAAGCCGACGCAGCAAACAC
			TTACGTCGTCATATATACCATAAAGtaGAAGAGTCTTCCTTTACG
			GAGGAGGGCAGCAAACGGaaAGGTATGGCCCAATTCGACAGTATG
			AGAATATAGCCTGTGTACATTCCAAtaGAAGAGTCTTCCTTTACG
			GAGGAGGGCAGCAAACGGaaTATGGCTGTCCCTACCATAAATATG
			CTTCTGCACTGAAATAACTGCTGTTaGAAGAGTCTTCCTTTACG
			GAGGAGGGCAGCAAACGGaaCCAAGTACCAAGCATGGGCAAAAACA
			TTATAACATAAAAACCTGCATATCATTaGAAGAGTCTTCCTTTACG
			GAGGAGGGCAGCAAACGGaaTTTGCCACATGGGTCCGCTTCCCA
			TTACAGTGCTGATTGTTGAAGCCATaGAAGAGTCTTCCTTTACG
			GAGGAGGGCAGCAAACGGaaCTCAGCATTGATAATGGCCATGAAG
			CAAAGCGAAGAATGTATCTACTGATaGAAGAGTCTTCCTTTACG
			GAGGAGGGCAGCAAACGGaaCCCAACTCATACTGATAAACCGTAT
			CAAATGCGTATGTGTGTCCTAGAATaGAAGAGTCTTCCTTTACG
			GAGGAGGGCAGCAAACGGaaAACTTTCCAAGAAATCTGGTTTGT
			TTTGTGTAACAGAAAATGACAGCAtaGAAGAGTCTTCCTTTACG
			GAGGAGGGCAGCAAACGGaaTTGACTTTTCCGGCTTTTAAATTG
			GCGTTGTGGACGGATCTTCAGCTGAtaGAAGAGTCTTCCTTTACG
			GAGGAGGGCAGCAAACGGaaCATGCCCATACCAGCTGAATCATA
			TTTTTCGCCCTCATATCCGTTATTaGAAGAGTCTTCCTTTACG
			GAGGAGGGCAGCAAACGGaaACTGTTTTCTTTGGTTTTGACATG
			CGTAGCATGAGCATCGGATAGATCCtaGAAGAGTCTTCCTTTACG
			GAGGAGGGCAGCAAACGGaaATGATCGCAAGTCCAACAAGTATAC
			TGAATAAACACATCGTACGTGGTAGtaGAAGAGTCTTCCTTTACG
			GAGGAGGGCAGCAAACGGaaAATCAATAGGTTGGTCTTGTTCCTT
			TTACGATGAAGGCTATTCTTGCTTTaGAAGAGTCTTCCTTTACG
			GAGGAGGGCAGCAAACGGaaATTTGACATCTAGGTAACACGGAA
			TTCTCCGCCAGTTGCAAATACTGTGtaGAAGAGTCTTCCTTTACG
			GAGGAGGGCAGCAAACGGaaCAAGTATTCGGCACACATAGCCCGA
			AACAGATTTTTTATATCTAAAATGGtaGAAGAGTCTTCCTTTACG
			GAGGAGGGCAGCAAACGGaaAAGGATTGGTAAGAGAAGTAACATA
			GGATTTCCATTCCTTTTGTCTCGTtaGAAGAGTCTTCCTTTACG
GAGGAGGGCAGCAAACGGaaTTCCTTAGCTGCTATTCCAATGCAT			
TTTGCAAGACAGTATTCTCCGTTGtaGAAGAGTCTTCCTTTACG			
GAGGAGGGCAGCAAACGGaaCCGCTAAGTAAACCTGCAGGAGGCT			

			TCATAATCACCAAGCCACGCAATTTaGAAGAGTCTTCCTTTACG
			GAGGAGGGCAGCAAACGGaaATTGTTTTCTTCCAAATAATCCTGC
			CCAAAGCATCTAACATTTGCATAGctaGAAGAGTCTTCCTTTACG
			GAGGAGGGCAGCAAACGGaaTGCATTCACTTTAGGTAAGGGTGGG
			AATACTTTGAGTATGGTTCAAGCAGtaGAAGAGTCTTCCTTTACG
			GAGGAGGGCAGCAAACGGaaGCCGTCCTGTTACGGGTAGAACTG
			GTACTGGCTGTAAGTGGAGAATAAGtaGAAGAGTCTTCCTTTACG
			GAGGAGGGCAGCAAACGGaaCAGTTGGTTTTTCCTTTGCAATTGT
			TTGGCATTGACTTTGTGGTTACGAGtaGAAGAGTCTTCCTTTACG
			GAGGAGGGCAGCAAACGGaaCGTTGTAGGCAAAGATTTAATGTAT
			ATCACCTTGTTTCATGAGTTGCAAAAtaGAAGAGTCTTCCTTTACG
			GAGGAGGGCAGCAAACGGaaAAATCATAGATATTAGTGGTATTTCT
			TTCTGGTTTGAAGTCGATGTGACATtaGAAGAGTCTTCCTTTACG
			GAGGAGGGCAGCAAACGGaaCTGAGAAGTGTCCAAGTCACTGA
			TTAAAACACTAGTACTATCAGATAGtaGAAGAGTCTTCCTTTACG
			GAGGAGGGCAGCAAACGGaaTACATTCAGTGCTTTATTCAATTGCA
			TGTCTGAAGATTGTCTAATATGTTTtaGAAGAGTCTTCCTTTACG
			GAGGAGGGCAGCAAACGGaaACATGCTGTGAATATCCTTTCAATA
			ATATCTTGAGTAAAGCCGCTGGTtaGAAGAGTCTTCCTTTACG

Appendix Table 3. Table of HCR probes of nrf genes. Table structure is the same of Appendix Table 1.

References

- Achim, K., Eling, N., Vergara, H.M., Bertucci, P.Y., Musser, J., Vopalensky, P., Brunet, T., Collier, P., Benes, V., Marioni, J.C., Arendt, D., 2018. Whole-Body Single-Cell Sequencing Reveals Transcriptional Domains in the Annelid Larval Body. *Mol. Biol. Evol.* 35, 1047–1062. <https://doi.org/10.1093/molbev/msx336>
- Adamo, S., 2008. Norepinephrine and octopamine: linking stress and immune function across phyla. *Invertebr. Surviv. J.*
- Aladaileh, S., Mohammad, M.G., Ferrari, B., Nair, S.V., Raftos, D.A., 2008. In vitro effects of noradrenaline on Sydney rock oyster (*Saccostrea glomerata*) hemocytes. *Comp. Biochem. Physiol. A. Mol. Integr. Physiol.* 151, 691–697. <https://doi.org/10.1016/j.cbpa.2008.08.028>
- Alavi, S.M.H., Nagasawa, K., Takahashi, K.G., Osada, M., 2017. Structure-Function of Serotonin in Bivalve Molluscs, in: Shad, K.F. (Ed.), *Serotonin - A Chemical Messenger Between All Types of Living Cells*. InTech. <https://doi.org/10.5772/intechopen.69165>
- Albert, P.R., Lemonde, S., 2004. 5-HT1A receptors, gene repression, and depression: guilt by association. *Neurosci. Rev. J. Bringing Neurobiol. Neurol. Psychiatry* 10, 575–593. <https://doi.org/10.1177/1073858404267382>
- Alex, K.D., Pehek, E.A., 2007. Pharmacologic mechanisms of serotonergic regulation of dopamine neurotransmission. *Pharmacol. Ther.* 113, 296. <https://doi.org/10.1016/j.pharmthera.2006.08.004>
- Altieri, S.C., Garcia-Garcia, A.L., Leonardo, E.D., Andrews, A.M., 2012. Rethinking 5-HT1A Receptors: Emerging Modes of Inhibitory Feedback of Relevance to Emotion-Related Behavior. *ACS Chem. Neurosci.* 4, 72–83. <https://doi.org/10.1021/cn3002174>
- Álvarez-Muñoz, D., Llorca, M., Blasco, J., Barceló, D., 2016. Chapter 1 - Contaminants in the Marine Environment, in: Blasco, Julián, Chapman, P.M., Campana, O., Hampel, M. (Eds.), *Marine Ecotoxicology*. Academic Press, pp. 1–34. <https://doi.org/10.1016/B978-0-12-803371-5.00001-1>
- Amador, M.H.B., McDonald, M.D., 2018. Molecular and functional characterization of the Gulf toadfish serotonin transporter (SERT; SLC6A4). *J. Exp. Biol.* jeb.170928. <https://doi.org/10.1242/jeb.170928>
- Aman, T.K., Shen, R.-Y., Haj-Dahmane, S., 2007. D2-Like Dopamine Receptors Depolarize Dorsal Raphe Serotonin Neurons through the Activation of Nonselective Cationic Conductance. *J. Pharmacol. Exp. Ther.* 320, 376–385. <https://doi.org/10.1124/jpet.106.111690>
- Amini, H., Rezabakhsh, A., Heidarzadeh, M., Hassanpour, M., Hashemzadeh, S., Ghaderi, S., Sokullu, E., Rahbarghazi, R., Reiter, R.J., 2021. An Examination of the Putative Role of Melatonin in Exosome Biogenesis. *Front. Cell Dev. Biol.* 9. <https://doi.org/10.3389/fcell.2021.686551>
- Anctil, M., 2009. Chemical transmission in the sea anemone *Nematostella vectensis*: A genomic perspective. *Comp. Biochem. Physiol. Part D Genomics Proteomics* 4, 268–289. <https://doi.org/10.1016/j.cbd.2009.07.001>
- Andersen, J., Olsen, L., Hansen, K.B., Taboureau, O., Jørgensen, F.S., Jørgensen, A.M., Bang-Andersen, B., Egebjerg, J., Strømgaard, K., Kristensen, A.S., 2010. Mutational Mapping and Modeling of the Binding Site for (S)-Citalopram in the Human Serotonin Transporter. *J. Biol. Chem.* 285, 2051–2063. <https://doi.org/10.1074/jbc.M109.072587>
- Andersen, J., Stuhr-Hansen, N., Zachariassen, L.G., Koldsø, H., Schiøtt, B., Strømgaard, K., Kristensen, A.S., 2014. Molecular Basis for Selective Serotonin Reuptake Inhibition by

- the Antidepressant Agent Fluoxetine (Prozac). *Mol. Pharmacol.* 85, 703–714. <https://doi.org/10.1124/mol.113.091249>
- Andersen, J., Taboureau, O., Hansen, K.B., Olsen, L., Egebjerg, J., Strømgaard, K., Kristensen, A.S., 2009. Location of the Antidepressant Binding Site in the Serotonin Transporter*. *J. Biol. Chem.* 284, 10276–10284. <https://doi.org/10.1074/jbc.M806907200>
- Ankley, G.T., Bennett, R.S., Erickson, R.J., Hoff, D.J., Hornung, M.W., Johnson, R.D., Mount, D.R., Nichols, J.W., Russom, C.L., Schmieder, P.K., Serrano, J.A., Tietge, J.E., Villeneuve, D.L., 2010. Adverse outcome pathways: A conceptual framework to support ecotoxicology research and risk assessment. *Environ. Toxicol. Chem.* 29, 730–741. <https://doi.org/10.1002/etc.34>
- Ankley, G.T., Brooks, B.W., Huggett, D.B., Sumpter, A.J.P., 2007. Repeating History: Pharmaceuticals in the Environment. *Environ. Sci. Technol.* 41, 8211–8217. <https://doi.org/10.1021/es072658j>
- Anne, C., Gasnier, B., 2014. Chapter Three - Vesicular Neurotransmitter Transporters: Mechanistic Aspects, in: Bevensee, M.O. (Ed.), *Current Topics in Membranes, Exchangers*. Academic Press, pp. 149–174. <https://doi.org/10.1016/B978-0-12-800223-0.00003-7>
- Apaydin, O., Altaikyzy, A., Filosa, A., Sawamiphak, S., 2023. Alpha-1 adrenergic signaling drives cardiac regeneration via extracellular matrix remodeling transcriptional program in zebrafish macrophages. *Dev. Cell* 58, 2460-2476.e7. <https://doi.org/10.1016/j.devcel.2023.09.011>
- AquaMaps, 2019. Computer generated distribution maps for *Mytilus galloprovincialis* (Mediterranean mussel), with modelled year 2050 native range map based on IPCC RCP8.5 emissions scenario [WWW Document]. URL <https://www.aquamaps.org>
- ASTM, 2004. International standard guide for conducting static acute toxicity tests starting with embryos of four species of salt water bivalve mollusks (No. E724- 04).
- Azpeitia, K., Ortiz-Zarragoitia, M., Revilla, M., Mendiola, D., 2017. Variability of the reproductive cycle in estuarine and coastal populations of the mussel *Mytilus galloprovincialis* Lmk. from the SE Bay of Biscay (Basque Country). *Int. Aquat. Res.* 9, 329–350. <https://doi.org/10.1007/s40071-017-0180-3>
- Balbi, T., Camisassi, G., Montagna, M., Fabbri, R., Franzellitti, S., Carbone, C., Dawson, K., Canesi, L., 2017a. Impact of cationic polystyrene nanoparticles (PS-NH₂) on early embryo development of *Mytilus galloprovincialis*: Effects on shell formation. *Chemosphere* 186, 1–9. <https://doi.org/10.1016/j.chemosphere.2017.07.120>
- Balbi, T., Fabbri, R., Montagna, M., Camisassi, G., Canesi, L., 2017b. Seasonal variability of different biomarkers in mussels (*Mytilus galloprovincialis*) farmed at different sites of the Gulf of La Spezia, Ligurian sea, Italy. *Mar. Pollut. Bull.* 116, 348–356. <https://doi.org/10.1016/j.marpolbul.2017.01.035>
- Balbi, T., Franzellitti, S., Fabbri, R., Montagna, M., Fabbri, E., Canesi, L., 2016. Impact of bisphenol A (BPA) on early embryo development in the marine mussel *Mytilus galloprovincialis*: Effects on gene transcription. *Environ. Pollut.* 218, 996–1004. <https://doi.org/10.1016/j.envpol.2016.08.050>
- Balbi, T., Miglioli, A., Montagna, M., Piazza, D., Risso, B., Dumollard, R., Canesi, L., 2023a. The biocide triclosan as a potential developmental disruptor in *Mytilus* early larvae. *Environ. Sci. Pollut. Res.* 30, 106342–106354. <https://doi.org/10.1007/s11356-023-29854-2>
- Balbi, T., Montagna, M., Fabbri, R., Carbone, C., Franzellitti, S., Fabbri, E., Canesi, L., 2018. Diclofenac affects early embryo development in the marine bivalve *Mytilus galloprovincialis*. *Sci. Total Environ.* 642, 601–609. <https://doi.org/10.1016/j.scitotenv.2018.06.125>

- Balbi, T., Trenti, F., Guella, G., Miglioli, A., Sepčić, K., Ciacci, C., Canesi, L., 2023b. Changes in phospholipid profiles in early larval stages of the marine mussel *Mytilus galloprovincialis* indicate a role of ceramides in bivalve development. *Int. J. Biochem. Mol. Biol.* 14, 87–100.
- Bard, S.M., 2000. Multixenobiotic resistance as a cellular defense mechanism in aquatic organisms. *Aquat. Toxicol.* 48, 357–389. [https://doi.org/10.1016/S0166-445X\(00\)00088-6](https://doi.org/10.1016/S0166-445X(00)00088-6)
- Baronio, D., Chen, Y.-C., Panula, P., 2022. Abnormal brain development of monoamine oxidase mutant zebrafish and impaired social interaction of heterozygous fish. *Dis. Model. Mech.* 15, dmm049133. <https://doi.org/10.1242/dmm.049133>
- Barrington, E.J.W., 2024. Hormone. *Encycl. Br.*
- Bauknecht, P., Jékely, G., 2017. Ancient coexistence of norepinephrine, tyramine, and octopamine signaling in bilaterians. *BMC Biol.* 15, 6. <https://doi.org/10.1186/s12915-016-0341-7>
- Bergman, Å., Heindel, J., Jobling, S., Kidd, K., Zoeller, R.T., 2012. State-of-the-science of endocrine disrupting chemicals, 2012. *Toxicol. Lett.* 211, S3. <https://doi.org/10.1016/j.toxlet.2012.03.020>
- Bertram, M.G., Gore, A.C., Tyler, C.R., Brodin, T., 2022. Endocrine-disrupting chemicals. *Curr. Biol.* 32, R727–R730. <https://doi.org/10.1016/j.cub.2022.05.063>
- Bhatia, A., Lenchner, J.R., Saadabadi, A., 2024. Biochemistry, Dopamine Receptors, in: *StatPearls*. StatPearls Publishing, Treasure Island (FL).
- Blenau, W., Baumann, A., 2001. Molecular and pharmacological properties of insect biogenic amine receptors: Lessons from *Drosophila melanogaster* and *Apis mellifera*. *Arch. Insect Biochem. Physiol.* 48, 13–38. <https://doi.org/10.1002/arch.1055>
- Blenau, W., Bremer, A.-S., Schwietz, Y., Friedrich, D., Ragionieri, L., Predel, R., Balfanz, S., Baumann, A., 2022. PaOct β 2R: Identification and Functional Characterization of an Octopamine Receptor Activating Adenylyl Cyclase Activity in the American Cockroach *Periplaneta americana*. *Int. J. Mol. Sci.* 23, 1677. <https://doi.org/10.3390/ijms23031677>
- Bogomolov, A.I., Voronezhskaya, E.E., 2022. An Increase in the Level of Intracellular Serotonin in Blastomeres Leads to the Disruption in the Spiral Cleavage Pattern in the Mollusc *Lymnaea stagnalis*. *Russ. J. Dev. Biol.* 53, 115–120. <https://doi.org/10.1134/S1062360422020035>
- Boos, J.R., Shubbar, A., Geldenhuys, W.J., 2021. Dual monoamine oxidase B and acetylcholine esterase inhibitors for treating movement and cognition deficits in a *C. elegans* model of Parkinson's disease. *Med. Chem. Res.* 30, 1166–1174. <https://doi.org/10.1007/s00044-021-02720-x>
- Boulais, M., Demoy-Schneider, M., Alavi, S.M.H., Cosson, J., 2019. Spermatozoa motility in bivalves: Signaling, flagellar beating behavior, and energetics. *Theriogenology* 136, 15–27. <https://doi.org/10.1016/j.theriogenology.2019.06.025>
- Boulton, A.A., Wu, P.H., 1973. Biosynthesis of Cerebral Phenolic Amines. II. In Vivo Regional Formation of p-Tyramine and Octopamine from Tyrosine and Dopamine. *Can. J. Biochem.* 51, 428–435. <https://doi.org/10.1139/o73-050>
- Boulton, A.A., Wu, P.H., 1972. Biosynthesis of Cerebral Phenolic Amines. I. In Vivo Formation of p-Tyramine, Octopamine, and Synephrine. *Can. J. Biochem.* 50, 261–267. <https://doi.org/10.1139/o72-037>
- Boutet, I., Tanguy, A., Moraga, D., 2004. Molecular identification and expression of two non-P450 enzymes, monoamine oxidase A and flavin-containing monooxygenase 2, involved in phase I of xenobiotic biotransformation in the Pacific oyster, *Crassostrea*

- gigas*. *Biochim. Biophys. Acta BBA - Gene Struct. Expr.* 1679, 29–36. <https://doi.org/10.1016/j.bbaexp.2004.04.001>
- Brady, S.T., Siegel, G.J., Albers, R.W., Price, D.L., 2012. *Basic Neurochemistry*, Eighth Edition. ed. Elsevier. <https://doi.org/10.1016/C2009-0-00066-X>
- Braley, R.D., 1985. Serotonin-induced spawning in giant clams (Bivalvia: Tridacnidae). *Aquaculture* 47, 321–325. [https://doi.org/10.1016/0044-8486\(85\)90217-0](https://doi.org/10.1016/0044-8486(85)90217-0)
- Brooks, B.W., Foran, C.M., Richards, S.M., Weston, J., Turner, P.K., Stanley, J.K., Solomon, K.R., Slattery, M., La Point, T.W., 2003. Aquatic ecotoxicology of fluoxetine. *Toxicol. Lett.* 142, 169–183. [https://doi.org/10.1016/S0378-4274\(03\)00066-3](https://doi.org/10.1016/S0378-4274(03)00066-3)
- Brown, J.W., Schaub, B.M., Klusas, B.L., Tran, A.X., Duman, A.J., Haney, S.J., Boris, A.C., Flanagan, M.P., Delgado, N., Torres, G., Rolón-Martínez, S., Vaasjo, L.O., Miller, M.W., Gillette, R., 2018. A role for dopamine in the peripheral sensory processing of a gastropod mollusc. *PLOS ONE* 13, e0208891. <https://doi.org/10.1371/journal.pone.0208891>
- Burke, R.D., Angerer, L.M., Elphick, M.R., Humphrey, G.W., Yaguchi, S., Kiyama, T., Liang, S., Mu, X., Agca, C., Klein, W.H., Brandhorst, B.P., Rowe, M., Wilson, K., Churcher, A.M., Taylor, J.S., Chen, N., Murray, G., Wang, D., Mellott, D., Olinski, R., Hallböök, F., Thorndyke, M.C., 2006. A genomic view of the sea urchin nervous system. *Dev. Biol., Sea Urchin Genome: Implications and Insights* 300, 434–460. <https://doi.org/10.1016/j.ydbio.2006.08.007>
- Burman, C., Evans, P.D., 2010. Amphioxus expresses both vertebrate-type and invertebrate-type dopamine D1 receptors. *Invert. Neurosci.* 10, 93–105. <https://doi.org/10.1007/s10158-010-0111-0>
- Burman, C., Maqueira, B., Coadwell, J., Evans, P.D., 2007. Eleven new putative aminergic G-protein coupled receptors from Amphioxus (*Branchiostoma floridae*): identification, sequence analysis and phylogenetic relationship. *Invert. Neurosci.* 7, 87–98. <https://doi.org/10.1007/s10158-006-0041-z>
- Buznikov, G.A., 1984. The action of neurotransmitters and related substances on early embryogenesis. *Pharmacol. Ther.* 25, 23–59. [https://doi.org/10.1016/0163-7258\(84\)90023-8](https://doi.org/10.1016/0163-7258(84)90023-8)
- Buznikov, G.A., Lambert, W.H., Lauder, J.M., 2001. Serotonin and serotonin-like substances as regulators of early embryogenesis and morphogenesis. *Cell Tissue Res.* 305, 177–186. <https://doi.org/10.1007/s004410100408>
- Buznikov, G.A., Shmukler, Y.B., Lauder, J.M., 1996. From oocyte to neuron: do neurotransmitters function in the same way throughout development? *Cell. Mol. Neurobiol.* 16, 537–559. <https://doi.org/10.1007/BF02152056>
- Buznikov, G.A., Shmukler, Yu.B., Lauder, J.M., 1999. Changes in the physiological roles of neurotransmitters during individual development. *Neurosci. Behav. Physiol.* 29, 11–21. <https://doi.org/10.1007/BF02461353>
- Bylund, D.B., 2003. Norepinephrine, in: Aminoff, M.J., Daroff, R.B. (Eds.), *Encyclopedia of the Neurological Sciences*. Academic Press, New York, pp. 638–640. <https://doi.org/10.1016/B0-12-226870-9/01397-6>
- Byrne, J.H., 2019. *The Oxford Handbook of Invertebrate Neurobiology*. Oxford University Press.
- Camicia, F., Herz, M., Prada, L.C., Kamenetzky, L., Simonetta, S.H., Cucher, M.A., Bianchi, J.I., Fernández, C., Brehm, K., Rosenzvit, M.C., 2013. The nervous and pre-nervous roles of serotonin in *Echinococcus* spp. *Int. J. Parasitol.* 43, 647–659. <https://doi.org/10.1016/j.ijpara.2013.03.006>
- Camicia, F., Vaca, H.R., Guarnaschelli, I., Koziol, U., Mortensen, O.V., Fontana, A.C.K., 2022. Molecular characterization of the serotonergic transporter from the cestode

- Echinococcus granulosus*: pharmacology and potential role in the nervous system. *Parasitol. Res.* 121, 1329–1343. <https://doi.org/10.1007/s00436-022-07466-y>
- Candiani, S., Moronti, L., Ramoino, P., Schubert, M., Pestarino, M., 2012. A neurochemical map of the developing amphioxus nervous system. *BMC Neurosci.* 13, 59. <https://doi.org/10.1186/1471-2202-13-59>
- Candy, J., Collet, C., 2005. Two tyrosine hydroxylase genes in teleosts. *Biochim. Biophys. Acta BBA - Gene Struct. Expr.* 1727, 35–44. <https://doi.org/10.1016/j.bbaexp.2004.11.005>
- Canesi, L., Fabbri, E., 2015. Environmental Effects of BPA: Focus on Aquatic Species. *Dose-Response* 13, 1559325815598304. <https://doi.org/10.1177/1559325815598304>
- Canesi, L., Miglioli, A., Balbi, T., Fabbri, E., 2022. Physiological Roles of Serotonin in Bivalves: Possible Interference by Environmental Chemicals Resulting in Neuroendocrine Disruption. *Front. Endocrinol.* 13. <https://doi.org/10.3389/fendo.2022.792589>
- Cao, J., Shi, F., Liu, X., Huang, G., Zhou, M., 2010. Phylogenetic analysis and evolution of aromatic amino acid hydroxylase. *FEBS Lett.* 584, 4775–4782. <https://doi.org/10.1016/j.febslet.2010.11.005>
- Cao, L.-Y., Xu, Y.-H., He, S., Ren, X.-M., Yang, Y., Luo, S., Xie, X.-D., Luo, L., 2020. Antimicrobial Triclocarban Exhibits Higher Agonistic Activity on Estrogen-Related Receptor γ than Triclosan at Human Exposure Levels: A Novel Estrogenic Disruption Mechanism. *Environ. Sci. Technol. Lett.* 7, 434–439. <https://doi.org/10.1021/acs.estlett.0c00338>
- Capolupo, M., Díaz-Garduño, B., Martín-Díaz, M.L., 2018. The impact of propranolol, 17 α -ethinylestradiol, and gemfibrozil on early life stages of marine organisms: effects and risk assessment. *Environ. Sci. Pollut. Res.* 25, 32196–32209. <https://doi.org/10.1007/s11356-018-3185-6>
- Carlsson, A., Waldeck, B., 1964. β -Hydroxylation of Tyramine in Vivo. *Acta Pharmacol. Toxicol. (Copenh.)* 20, 371–374. <https://doi.org/10.1111/j.1600-0773.1964.tb01759.x>
- Carrillo-Baltodano, A.M., Donnellan, R.D., Williams, E.A., Jékely, G., Martín-Durán, J.M., 2024. The development of the adult nervous system in the annelid *Owenia fusiformis*. *Neural Develop.* 19, 3. <https://doi.org/10.1186/s13064-024-00180-8>
- Carroll, M.A., Catapane, E.J., 2007. The nervous system control of lateral ciliary activity of the gill of the bivalve mollusc, *Crassostrea virginica*. *Comp. Biochem. Physiol. A. Mol. Integr. Physiol.* 148, 445–450. <https://doi.org/10.1016/j.cbpa.2007.06.003>
- Carson, M.J., Thomas, E.A., Danielson, P.E., Sutcliffe, J.G., 1996. The 5-HT_{5A} serotonin receptor is expressed predominantly by astrocytes in which it inhibits cAMP accumulation: A mechanism for neuronal suppression of reactive astrocytes. *Glia* 17, 317–326. [https://doi.org/10.1002/\(SICI\)1098-1136\(199608\)17:4<317::AID-GLIA6>3.0.CO;2-W](https://doi.org/10.1002/(SICI)1098-1136(199608)17:4<317::AID-GLIA6>3.0.CO;2-W)
- Caveney, S., Cladman, W., Verellen, L., Donly, C., 2006. Ancestry of neuronal monoamine transporters in the Metazoa. *J. Exp. Biol.* 209, 4858–4868. <https://doi.org/10.1242/jeb.02607>
- Chen, M., Yang, H., Xu, B., Wang, F., Liu, B., 2008. Catecholaminergic responses to environmental stress in the hemolymph of zhihong scallop *Chlamys farreri*. *J. Exp. Zool. Part Ecol. Genet. Physiol.* 309A, 289–296. <https://doi.org/10.1002/jez.458>
- Chen, Y., Wang, J., Xu, P., Xiang, J., Xu, D., Cheng, P., Wang, X., Wu, L., Zhang, N., Chen, Z., 2022. Antidepressants as emerging contaminants: Occurrence in wastewater treatment plants and surface waters in Hangzhou, China. *Front. Public Health* 10, 963257. <https://doi.org/10.3389/fpubh.2022.963257>
- Cheng, W., Ka, Y.-W., Chang, C.-C., 2016. Dopamine beta-hydroxylase participate in the immunoendocrine responses of hypothermal stressed white shrimp, *Litopenaeus*

- vannamei. Fish Shellfish Immunol. 59, 166–178. <https://doi.org/10.1016/j.fsi.2016.10.036>
- Chopra, S., Kumar, D., 2018. Pharmaceuticals and Personal Care Products (PPCPs) as Emerging Environmental Pollutants: Toxicity and Risk Assessment, in: Gahlawat, S.K., Duhan, J.S., Salar, R.K., Siwach, P., Kumar, S., Kaur, P. (Eds.), *Advances in Animal Biotechnology and Its Applications*. Springer, Singapore, pp. 337–353. https://doi.org/10.1007/978-981-10-4702-2_19
- Choy, R.K.M., Kemner, J.M., Thomas, J.H., 2006. Fluoxetine-Resistance Genes in *Caenorhabditis elegans* Function in the Intestine and May Act in Drug Transport. *Genetics* 172, 885–892. <https://doi.org/10.1534/genetics.103.024869>
- Choy, R.K.M., Thomas, J.H., 1999. Fluoxetine-Resistant Mutants in *C. elegans* Define a Novel Family of Transmembrane Proteins. *Mol. Cell* 4, 143–152. [https://doi.org/10.1016/S1097-2765\(00\)80362-7](https://doi.org/10.1016/S1097-2765(00)80362-7)
- Chu, A., Wadhwa, R., 2024. Selective Serotonin Reuptake Inhibitors, in: *StatPearls*. StatPearls Publishing, Treasure Island (FL).
- Cikos, S., Fabian, D., Makarevich, A.V., Chrenek, P., Koppel, J., 2011. Biogenic monoamines in preimplantation development. *Hum. Reprod.* 26, 2296–2305. <https://doi.org/10.1093/humrep/der233>
- Coleman, J.A., Green, E.M., Gouaux, E., 2016. X-ray structures and mechanism of the human serotonin transporter. *Nature* 532, 334–339. <https://doi.org/10.1038/nature17629>
- Coon, S.L., Bonar, D.B., 1987. Pharmacological evidence that alpha1.-adrenoceptors mediate metamorphosis of the pacific oyster, *Crassostrea gigas*. *Neuroscience* 23, 1169–1174. [https://doi.org/10.1016/0306-4522\(87\)90190-4](https://doi.org/10.1016/0306-4522(87)90190-4)
- Coon, S.L., Bonar, D.B., Weiner, R.M., 1986. Chemical production of cultchless oyster spat using epinephrine and norepinephrine. *Aquaculture* 58, 255–262. [https://doi.org/10.1016/0044-8486\(86\)90090-6](https://doi.org/10.1016/0044-8486(86)90090-6)
- Corrochano-Fraile, A., Davie, A., Carboni, S., Bekaert, M., 2022. Evidence of multiple genome duplication events in *Mytilus* evolution. *BMC Genomics* 23, 340. <https://doi.org/10.1186/s12864-022-08575-9>
- Cortez, F.S., Souza, L. da S., Guimarães, L.L., Pusceddu, F.H., Maranhão, L.A., Fontes, M.K., Moreno, B.B., Nobre, C.R., Abessa, D.M. de S., Cesar, A., Pereira, C.D.S., 2019. Marine contamination and cytogenotoxic effects of fluoxetine in the tropical brown mussel *Perna perna*. *Mar. Pollut. Bull.* 141, 366–372. <https://doi.org/10.1016/j.marpolbul.2019.02.065>
- Croll, R.P., Dickinson, A.J.G., 2004. Form and function of the larval nervous system in molluscs. *Invertebr. Reprod. Dev.* 46, 173–187. <https://doi.org/10.1080/07924259.2004.9652620>
- Croll, R.P., Jackson, D.L., Voronezhskaya, E.E., 1997. Catecholamine-Containing Cells in Larval and Postlarval Bivalve Molluscs. *Biol. Bull.* 193, 116–124. <https://doi.org/10.2307/1542757>
- Cunha, D.L., De Araujo, F.G., Marques, M., 2017. Psychoactive drugs: occurrence in aquatic environment, analytical methods, and ecotoxicity—a review. *Environ. Sci. Pollut. Res.* 24, 24076–24091. <https://doi.org/10.1007/s11356-017-0170-4>
- Dag, U., Nwabudike, I., Kang, D., Gomes, M.A., Kim, J., Atanas, A.A., Bueno, E., Estrem, C., Pugliese, S., Wang, Z., Towilson, E., Flavell, S.W., 2023. Dissecting the functional organization of the *C. elegans* serotonergic system at whole-brain scale. *Cell* 186, 2574–2592.e20. <https://doi.org/10.1016/j.cell.2023.04.023>
- D’Aniello, E., Paganos, P., Anishchenko, E., D’Aniello, S., Arnone, M.I., 2020. Comparative Neurobiology of Biogenic Amines in Animal Models in Deuterostomes. *Front. Ecol. Evol.* 8, 587036. <https://doi.org/10.3389/fevo.2020.587036>

- de Sa Alves, F.R., Barreiro, E.J., Manssour Fraga, C.A., 2009. From Nature to Drug Discovery: The Indole Scaffold as a 'Privileged Structure.' *Mini Rev. Med. Chem.* 9, 782–793. <https://doi.org/10.2174/138955709788452649>
- Deguchi, R., Osanai, K., 1995. Serotonin-Induced Meiosis Reinitiation from the First Prophase and from the First Metaphase in Oocytes of the Marine Bivalve *Hiatella flaccida*: Respective Changes in Intracellular Ca²⁺ and pH. *Dev. Biol.* 171, 483–496. <https://doi.org/10.1006/dbio.1995.1298>
- Dehal, P., Satou, Y., Campbell, R.K., Chapman, J., Degnan, B., De Tomaso, A., Davidson, B., Di Gregorio, A., Gelpke, M., Goodstein, D.M., Harafuji, N., Hastings, K.E.M., Ho, I., Hotta, K., Huang, W., Kawashima, T., Lemaire, P., Martinez, D., Meinertzhagen, I.A., Nacula, S., Nonaka, M., Putnam, N., Rash, S., Saiga, H., Satake, M., Terry, A., Yamada, L., Wang, H.-G., Awazu, S., Azumi, K., Boore, J., Branno, M., Chin-bow, S., DeSantis, R., Doyle, S., Francino, P., Keys, D.N., Haga, S., Hayashi, H., Hino, K., Imai, K.S., Inaba, K., Kano, S., Kobayashi, K., Kobayashi, M., Lee, B.-I., Makabe, K.W., Manohar, C., Matassi, G., Medina, M., Mochizuki, Y., Mount, S., Morishita, T., Miura, S., Nakayama, A., Nishizaka, S., Nomoto, H., Ohta, F., Oishi, K., Rigoutsos, I., Sano, M., Sasaki, A., Sasakura, Y., Shoguchi, E., Shin-i, T., Spagnuolo, A., Stainier, D., Suzuki, M.M., Tassy, O., Takatori, N., Tokuoka, M., Yagi, K., Yoshizaki, F., Wada, S., Zhang, C., Hyatt, P.D., Larimer, F., Detter, C., Doggett, N., Glavina, T., Hawkins, T., Richardson, P., Lucas, S., Kohara, Y., Levine, M., Satoh, N., Rokhsar, D.S., 2002. The Draft Genome of *Ciona intestinalis*: Insights into Chordate and Vertebrate Origins. *Science* 298, 2157–2167. <https://doi.org/10.1126/science.1080049>
- Denker, E., Ebbesson, L.O.E., Hazlerigg, D.G., Macqueen, D.J., 2019. Phylogenetic Reclassification of Vertebrate Melatonin Receptors To Include Mel1d. *G3 GenesGenomesGenetics* 9, 3225–3238. <https://doi.org/10.1534/g3.119.400170>
- Di Poi, C., Evariste, L., Séguin, A., Mottier, A., Pedelucq, J., Lebel, J.-M., Serpentine, A., Budzinski, H., Costil, K., 2016. Sub-chronic exposure to fluoxetine in juvenile oysters (*Crassostrea gigas*): uptake and biological effects. *Environ. Sci. Pollut. Res.* 23, 5002–5018. <https://doi.org/10.1007/s11356-014-3702-1>
- Di Poi, C., Evariste, L., Serpentine, A., Halm-Lemeille, M.P., Lebel, J.M., Costil, K., 2014. Toxicity of five antidepressant drugs on embryo–larval development and metamorphosis success in the Pacific oyster, *Crassostrea gigas*. *Environ. Sci. Pollut. Res.* 21, 13302–13314. <https://doi.org/10.1007/s11356-013-2211-y>
- Diamanti-Kandarakis, E., Bourguignon, J.-P., Giudice, L.C., Hauser, R., Prins, G.S., Soto, A.M., Zoeller, R.T., Gore, A.C., 2009. Endocrine-Disrupting Chemicals: An Endocrine Society Scientific Statement. *Endocr. Rev.* 30, 293–342. <https://doi.org/10.1210/er.2009-0002>
- Diaz Soria, C.L., Attenborough, T., Lu, Z., Fontenla, S., Graham, J., Hall, C., Thompson, S., Andrews, T.G.R., Rawlinson, K.A., Berriman, M., Rinaldi, G., 2024. Single-cell transcriptomics of the human parasite *Schistosoma mansoni* first intra-molluscan stage reveals tentative tegumental and stem-cell regulators. *Sci. Rep.* 14, 5974. <https://doi.org/10.1038/s41598-024-55790-3>
- Dickinson, A.J.G., Nason, J., Croll, R.P., 1999. Histochemical localization of FMRFamide, serotonin and catecholamines in embryonic *Crepidula fornicata* (Gastropoda, Prosobranchia). *Zoomorphology* 119, 49–62. <https://doi.org/10.1007/s004350050080>
- Dong, W., Liu, Z., Qiu, L., Wang, W., Song, X., Wang, X., Li, Y., Xin, L., Wang, L., Song, L., 2017. The modulation role of serotonin in Pacific oyster *Crassostrea gigas* in response to air exposure. *Fish Shellfish Immunol.* 62, 341–348. <https://doi.org/10.1016/j.fsi.2017.01.043>

- Donly, B.C., Caveney, S., 2005. A transporter for phenolamine uptake in the arthropod CNS. *Arch. Insect Biochem. Physiol.* 59, 172–183. <https://doi.org/10.1002/arch.20063>
- Duarte, I.A., Reis-Santos, P., Fick, J., Cabral, H.N., Duarte, B., Fonseca, V.F., 2023. Neuroactive pharmaceuticals in estuaries: Occurrence and tissue-specific bioaccumulation in multiple fish species. *Environ. Pollut.* 316, 120531. <https://doi.org/10.1016/j.envpol.2022.120531>
- Duerr, J.S., Frisby, D.L., Gaskin, J., Duke, A., Asermely, K., Huddleston, D., Eiden, L.E., Rand, J.B., 1999. The cat-1 Gene of *Caenorhabditis elegans* Encodes a Vesicular Monoamine Transporter Required for Specific Monoamine-Dependent Behaviors. *J. Neurosci.* 19, 72–84. <https://doi.org/10.1523/JNEUROSCI.19-01-00072.1999>
- Dwyer, D.S., Aamodt, E., Cohen, B., Buttner, E.A., 2014. Drug elucidation: invertebrate genetics sheds new light on the molecular targets of CNS drugs. *Front. Pharmacol.* 5. <https://doi.org/10.3389/fphar.2014.00177>
- Dyachuk, V., Wanninger, A., Voronezhskaya, E.E., 2012. Innervation of Bivalve Larval Catch Muscles by Serotonergic and FMRFamideergic Neurons. *Acta Biol. Hung.* 63, 221–229. <https://doi.org/10.1556/ABiol.63.2012.Suppl.2.30>
- Eibak, L.E.E., Gjelstad, A., Rasmussen, K.E., Pedersen-Bjergaard, S., 2010. Kinetic electro membrane extraction under stagnant conditions—Fast isolation of drugs from untreated human plasma. *J. Chromatogr. A* 1217, 5050–5056. <https://doi.org/10.1016/j.chroma.2010.06.018>
- Elphick, M.R., Mirabeau, O., Larhammar, D., 2018. Evolution of neuropeptide signalling systems. *J. Exp. Biol.* 221, jeb151092. <https://doi.org/10.1242/jeb.151092>
- Erspamer, V., Boretti, G., 1951. Identification and characterization, by paper chromatography, of enteramine, octopamine, tyramine, histamine and allied substances in extracts of posterior salivary glands of octopoda and in other tissue extracts of vertebrates and invertebrates. *Arch. Int. Pharmacodyn. Ther.* 88, 296–332.
- Escoubas, J.-M., Gourbal, B., Duval, D., Green, T.J., Charrière, G.M., Destoumieux-Garzón, D., Montagnani, C., 2016. Immunity in Molluscs, in: Ratcliffe, M.J.H. (Ed.), *Encyclopedia of Immunobiology*. Academic Press, Oxford, pp. 417–436. <https://doi.org/10.1016/B978-0-12-374279-7.12004-1>
- Esteban, S., Lladó, J., Sastre-Coll, A., García-Sevilla, J.A., 1999. Activation and desensitization by cyclic antidepressant drugs of α_2 -autoreceptors, α_2 -heteroreceptors and 5-HT_{1A}-autoreceptors regulating monoamine synthesis in the rat brain in vivo. *Naunyn. Schmiedeberg's Arch. Pharmacol.* 360, 135–143. <https://doi.org/10.1007/s002109900045>
- Estévez-Calvar, N., Canesi, L., Montagna, M., Faimali, M., Piazza, V., Garaventa, F., 2017. Adverse effects of the SSRI antidepressant sertraline on early life stages of marine invertebrates. *Mar. Environ. Res., Blue Growth and Marine Environmental Safety* 128, 88–97. <https://doi.org/10.1016/j.marenvres.2016.05.021>
- European Commission, 2022. Commission Implementing Decision (EU) 2022/1307 of 22 July 2022 establishing a watch list of substances for Union-wide monitoring in the field of water policy pursuant to Directive 2008/105/EC of the European Parliament and of the Council (notified under document C(2022) 5098), OJ L.
- Evans, P.D., Maqueira, B., 2005. Insect octopamine receptors: a new classification scheme based on studies of cloned *Drosophila* G-protein coupled receptors. *Invert. Neurosci.* 5, 111–118. <https://doi.org/10.1007/s10158-005-0001-z>
- Fabbri, E., Balbi, T., Canesi, L., 2024. Neuroendocrine functions of monoamines in invertebrates: Focus on bivalve molluscs. *Mol. Cell. Endocrinol.* 588, 112215. <https://doi.org/10.1016/j.mce.2024.112215>

- Fabbri, E., Franzellitti, S., 2016. Human pharmaceuticals in the marine environment: Focus on exposure and biological effects in animal species. *Environ. Toxicol. Chem.* 35, 799–812. <https://doi.org/10.1002/etc.3131>
- Fabbri, E., Valbonesi, P., Moon, T.W., 2023. Chapter 2 - Pharmaceuticals in the marine environment: occurrence, fate, and biological effects, in: León, V.M., Bellas, J. (Eds.), *Contaminants of Emerging Concern in the Marine Environment*. Elsevier, pp. 11–71. <https://doi.org/10.1016/B978-0-323-90297-7.00008-1>
- Fabbri, R., Montagna, M., Balbi, T., Raffo, E., Palumbo, F., Canesi, L., 2014. Adaptation of the bivalve embryotoxicity assay for the high throughput screening of emerging contaminants in *Mytilus galloprovincialis*. *Mar. Environ. Res.* 99, 1–8. <https://doi.org/10.1016/j.marenvres.2014.05.007>
- FAO, 2022. *The State of World Fisheries and Aquaculture 2022. Towards Blue Transformation*.
- Farooqui, T., 2012. Review of octopamine in insect nervous systems. *Open Access Insect Physiol.* 4, 1–17. <https://doi.org/10.2147/OAIP.S20911>
- Farooqui, T., 2007. Octopamine-Mediated Neuromodulation of Insect Senses. *Neurochem. Res.* 32, 1511–1529. <https://doi.org/10.1007/s11064-007-9344-7>
- Farzam, K., Kidron, A., Lakhkar, A.D., 2024. Adrenergic Drugs, in: *StatPearls*. StatPearls Publishing, Treasure Island (FL).
- FDA, 2018. Selective Serotonin Reuptake Inhibitors (SSRIs) Information [WWW Document]. *Sel. Serotonin Reuptake Inhib. SSRIs Inf.* URL <https://www.fda.gov/drugs/information-drug-class/selective-serotonin-reuptake-inhibitors-ssris-information> (accessed 8.15.24).
- Feng, W., Deng, Y., Yang, F., Miao, Q., Ngien, S.K., 2023. Systematic Review of Contaminants of Emerging Concern (CECs): Distribution, Risks, and Implications for Water Quality and Health. *Water* 15, 3922. <https://doi.org/10.3390/w15223922>
- Fent, K., Weston, A.A., Caminada, D., 2006. Ecotoxicology of human pharmaceuticals. *Aquat. Toxicol.* 76, 122–159. <https://doi.org/10.1016/j.aquatox.2005.09.009>
- Finberg, J.P.M., Rabey, J.M., 2016. Inhibitors of MAO-A and MAO-B in Psychiatry and Neurology. *Front. Pharmacol.* 7. <https://doi.org/10.3389/fphar.2016.00340>
- Finetti, L., Roeder, T., Calò, G., Bernacchia, G., 2021. The Insect Type 1 Tyramine Receptors: From Structure to Behavior. *Insects* 12, 315. <https://doi.org/10.3390/insects12040315>
- Fong, P.P., Ford, A.T., 2014. The biological effects of antidepressants on the molluscs and crustaceans: A review. *Aquat. Toxicol.* 151, 4–13. <https://doi.org/10.1016/j.aquatox.2013.12.003>
- Fong, P.P., Wade, S., Rostafin, M., 1996. Characterization of serotonin receptor mediating parturition in fingernail clams *Sphaerium* (Musculium) spp. from eastern North America. *J. Exp. Zool.* 275, 326–330. [https://doi.org/10.1002/\(SICI\)1097-010X\(19960701\)275:4<326::AID-JEZ11>3.0.CO;2-8](https://doi.org/10.1002/(SICI)1097-010X(19960701)275:4<326::AID-JEZ11>3.0.CO;2-8)
- Francis, W.R., Eitel, M., Vargas, S., Adamski, M., Haddock, S.H.D., Krebs, S., Blum, H., Erpenbeck, D., Wörheide, G., 2017. The genome of the contractile demosponge *Tethya wilhelma* and the evolution of metazoan neural signalling pathways. <https://doi.org/10.1101/120998>
- Franzellitti, S., Balbi, T., Montagna, M., Fabbri, R., Valbonesi, P., Fabbri, E., Canesi, L., 2019. Phenotypical and molecular changes induced by carbamazepine and propranolol on larval stages of *Mytilus galloprovincialis*. *Chemosphere* 234, 962–970. <https://doi.org/10.1016/j.chemosphere.2019.06.045>
- Franzellitti, S., Buratti, S., Du, B., Haddad, S.P., Chambliss, C.K., Brooks, B.W., Fabbri, E., 2015. A multibiomarker approach to explore interactive effects of propranolol and fluoxetine in marine mussels. *Environ. Pollut.* 205, 60–69. <https://doi.org/10.1016/j.envpol.2015.05.020>

- Franzellitti, S., Buratti, S., Valbonesi, P., Fabbri, E., 2013. The mode of action (MOA) approach reveals interactive effects of environmental pharmaceuticals on *Mytilus galloprovincialis*. *Aquat. Toxicol.* 140–141, 249–256. <https://doi.org/10.1016/j.aquatox.2013.06.005>
- Fraser, M., Fortier, M., Foucher, D., Roumier, P.-H., Brousseau, P., Fournier, M., Surette, C., Vaillancourt, C., 2018. Exposure to low environmental concentrations of manganese, lead, and cadmium alters the serotonin system of blue mussels. *Environ. Toxicol. Chem.* 37, 192–200. <https://doi.org/10.1002/etc.3942>
- Frazer, A., Hensler, J.G., 1999. Serotonin Receptors, in: *Basic Neurochemistry: Molecular, Cellular and Medical Aspects*. 6th Edition. Lippincott-Raven.
- Frese, A.N., Mariossi, A., Levine, M.S., Wühr, M., 2024. Quantitative proteome dynamics across embryogenesis in a model chordate. *iScience* 27, 109355. <https://doi.org/10.1016/j.isci.2024.109355>
- Gainey, L.F., Walton, J.C., Greenberg, M.J., 2003. Branchial Musculature of a Venerid Clam: Pharmacology, Distribution, and Innervation. *Biol. Bull.* 204, 81–95. <https://doi.org/10.2307/1543498>
- Gallo, V.P., Accordi, F., Chimenti, C., Civinini, A., Crivellato, E., 2016. Catecholaminergic System of Invertebrates: Comparative and Evolutionary Aspects in Comparison With the Octopaminergic System, in: *International Review of Cell and Molecular Biology*. Elsevier, pp. 363–394. <https://doi.org/10.1016/bs.ircmb.2015.12.006>
- Gaw, S., Thomas, K.V., Hutchinson, T.H., 2014. Sources, impacts and trends of pharmaceuticals in the marine and coastal environment. *Philos. Trans. R. Soc. B Biol. Sci.* 369, 20130572. <https://doi.org/10.1098/rstb.2013.0572>
- Gerdol, M., Moreira, R., Cruz, F., Gómez-Garrido, J., Vlasova, A., Rosani, U., Venier, P., Naranjo-Ortiz, M.A., Murgarella, M., Greco, S., Balseiro, P., Corvelo, A., Frias, L., Gut, M., Gabaldón, T., Pallavicini, A., Canchaya, C., Novoa, B., Alioto, T.S., Posada, D., Figueras, A., 2020. Massive gene presence-absence variation shapes an open pan-genome in the Mediterranean mussel. *Genome Biol.* 21, 275. <https://doi.org/10.1186/s13059-020-02180-3>
- Gibbons, M.C., Castagna, M., 1984. Serotonin as an inducer of spawning in six bivalve species. *Aquaculture* 40, 189–191. [https://doi.org/10.1016/0044-8486\(84\)90356-9](https://doi.org/10.1016/0044-8486(84)90356-9)
- Gnegy, M.E., 2012. Chapter 14 - Catecholamines, in: Brady, S.T., Siegel, G.J., Albers, R.W., Price, D.L. (Eds.), *Basic Neurochemistry (Eighth Edition)*. Academic Press, New York, pp. 283–299. <https://doi.org/10.1016/B978-0-12-374947-5.00014-6>
- Gonzalez-Rey, M., Bebianno, M.J., 2013. Does selective serotonin reuptake inhibitor (SSRI) fluoxetine affects mussel *Mytilus galloprovincialis*? *Environ. Pollut.* 173, 200–209. <https://doi.org/10.1016/j.envpol.2012.10.018>
- Gore, A.C., 2010. Neuroendocrine targets of endocrine disruptors. *Hormones* 9, 16–27. <https://doi.org/10.14310/horm.2002.1249>
- Gosling, E., 2015. *Marine Bivalve Molluscs*. ohn Wiley & Sons, Ltd.
- Gouly, M., Botton-Amiot, G., Rosato, E., Sprecher, S.G., Feuda, R., 2023. The monoaminergic system is a bilaterian innovation. *Nat. Commun.* 14, 3284. <https://doi.org/10.1038/s41467-023-39030-2>
- Gunnarsson, L., Jauhiainen, A., Kristiansson, E., Nerman, O., Larsson, D.G.J., 2008. Evolutionary Conservation of Human Drug Targets in Organisms used for Environmental Risk Assessments. *Environ. Sci. Technol.* 42, 5807–5813. <https://doi.org/10.1021/es8005173>
- Gust, M., Buronfosse, T., Giamberini, L., Ramil, M., Mons, R., Garric, J., 2009. Effects of fluoxetine on the reproduction of two prosobranch mollusks: *Potamopyrgus*

- antipodarum and *Valvata piscinalis*. *Environ. Pollut.* 157, 423–429. <https://doi.org/10.1016/j.envpol.2008.09.040>
- Hadfield, M., Meleshkevitch, E., Boudko, D., 2000. The apical sensory organ of a gastropod veliger is a receptor for settlement cues. *Biol. Bull.* 198, 67–76. <https://doi.org/10.2307/1542804>
- Hartenstein, V., 2019. Development of the Nervous System of Invertebrates, in: Byrne, J.H. (Ed.), *The Oxford Handbook of Invertebrate Neurobiology*. Oxford University Press, p. 0. <https://doi.org/10.1093/oxfordhb/9780190456757.013.3>
- Hartenstein, V., 2016. The Central Nervous System of Invertebrates, in: *The Wiley Handbook of Evolutionary Neuroscience*. John Wiley & Sons, Ltd, pp. 173–235. <https://doi.org/10.1002/9781118316757.ch8>
- Hartenstein, V., 2006. The neuroendocrine system of invertebrates: a developmental and evolutionary perspective. *J. Endocrinol.* 190, 555–570. <https://doi.org/10.1677/joe.1.06964>
- Hasan, A., Yeom, H.-S., Ryu, J., Bode, H.B., Kim, Y., 2019. Phenylethylamides derived from bacterial secondary metabolites specifically inhibit an insect serotonin receptor. *Sci. Rep.* 9, 20358. <https://doi.org/10.1038/s41598-019-56892-z>
- Hill, S.J., 1991. Histamine receptors and interactions between second messenger transduction systems. *Agents Actions. Suppl.* 33, 145–159. https://doi.org/10.1007/978-3-0348-7309-3_11
- Hirai, S., Kishimoto, T., Kadam, A.L., Kanatani, H., Koide, S.S., 1988. Induction of spawning and oocyte maturation by 5-hydroxytryptamine in the surf clam. *J. Exp. Zool.* 245, 318–321. <https://doi.org/10.1002/jez.1402450312>
- Honkoop, P.J.C., Luttkhuizen, P.C., Piersma, T., 1999. Experimentally extending the spawning season of a marine bivalve using temperature change and fluoxetine as synergistic triggers. *Mar. Ecol. Prog. Ser.* 180, 297–300. <https://doi.org/10.3354/meps180297>
- Hoyer, D., 2019a. Chapter Four - Serotonin receptors nomenclature, in: Tricklebank, M.D., Daly, E. (Eds.), *The Serotonin System*. Academic Press, pp. 63–93. <https://doi.org/10.1016/B978-0-12-813323-1.00004-9>
- Hoyer, D., 2019b. Serotonin receptors nomenclature, in: *The Serotonin System*. Elsevier, pp. 63–93. <https://doi.org/10.1016/B978-0-12-813323-1.00004-9>
- Hutchinson, T.H., Lyons, B.P., Thain, J.E., Law, R.J., 2013. Evaluating legacy contaminants and emerging chemicals in marine environments using adverse outcome pathways and biological effects-directed analysis. *Mar. Pollut. Bull., The Global State of the Ocean; Interactions Between Stresses, Impacts and Some Potential Solutions*. Synthesis papers from the International Programme on the State of the Ocean 2011 and 2012 Workshops 74, 517–525. <https://doi.org/10.1016/j.marpolbul.2013.06.012>
- Invernizzi, R., Carli, M., Di Clemente, A., Samanin, R., 1991. Administration of 8-hydroxy-2-(Di-n-propylamino)tetralin in raphe nuclei dorsalis and medianus reduces serotonin synthesis in the rat brain: differences in potency and regional sensitivity. *J. Neurochem.* 56, 243–247. <https://doi.org/10.1111/j.1471-4159.1991.tb02587.x>
- Ivashkin, E.G., Khabarova, M.Yu., Voronezhskaya, E.E., 2012. Serotonin Transport and Synthesis Systems During Early Development of Invertebrates: Functional Analysis on a Bivalve Model. *Acta Biol. Hung.* 63, 217–220. <https://doi.org/10.1556/ABiol.63.2012.Suppl.2.29>
- Iyer, L.M., Aravind, L., Coon, S.L., Klein, D.C., Koonin, E.V., 2004. Evolution of cell–cell signaling in animals: did late horizontal gene transfer from bacteria have a role? *Trends Genet.* 20, 292–299. <https://doi.org/10.1016/j.tig.2004.05.007>
- Janah, H., Aghzar, A., Presa, P., Ouagajjou, Y., 2024. Influence of Pediveliger Larvae Stocking Density on Settlement Efficiency and Seed Production in Captivity of *Mytilus*

- galloprovincialis in Amsa Bay, Tetouan. *Animals* 14, 239. <https://doi.org/10.3390/ani14020239>
- Jékely, G., 2021. The chemical brain hypothesis for the origin of nervous systems. *Philos. Trans. R. Soc. B Biol. Sci.* 376, 20190761. <https://doi.org/10.1098/rstb.2019.0761>
- Jia, Y., Yang, B., Dong, W., Liu, Z., Lv, Z., Jia, Z., Qiu, L., Wang, L., Song, L., 2018. A serotonin receptor (Cg5-HTR-1) mediating immune response in oyster *Crassostrea gigas*. *Dev. Comp. Immunol.* 82, 83–93. <https://doi.org/10.1016/j.dci.2017.12.029>
- Jockers, R., Maurice, P., Boutin, J.A., Delagrangé, P., 2008. Melatonin receptors, heterodimerization, signal transduction and binding sites: what's new? *Br. J. Pharmacol.* 154, 1182–1195. <https://doi.org/10.1038/bjp.2008.184>
- Joyce, A., Vogeler, S., 2018. Molluscan bivalve settlement and metamorphosis: Neuroendocrine inducers and morphogenetic responses. *Aquaculture* 487, 64–82. <https://doi.org/10.1016/j.aquaculture.2018.01.002>
- Kapoor, R., Peyear, T.A., Koeppe, R.E., Andersen, O.S., 2019. Antidepressants are modifiers of lipid bilayer properties. *J. Gen. Physiol.* 151, 342–356. <https://doi.org/10.1085/jgp.201812263>
- Kapsenberg, L., Bitter, M.C., Miglioli, A., Aparicio-Estalella, C., Pelejero, C., Gattuso, J.-P., Dumollard, R., 2022. Molecular basis of ocean acidification sensitivity and adaptation in *Mytilus galloprovincialis*. *iScience* 25, 104677. <https://doi.org/10.1016/j.isci.2022.104677>
- Kapsenberg, L., Miglioli, A., Bitter, M.C., Tambutté, E., Dumollard, R., Gattuso, J.-P., 2018. Ocean pH fluctuations affect mussel larvae at key developmental transitions. *Proc. R. Soc. B Biol. Sci.* 285, 20182381. <https://doi.org/10.1098/rspb.2018.2381>
- Karki, S., Saadaoui, M., Dunsing, V., Kerridge, S., Da Silva, E., Philippe, J.-M., Maurange, C., Lecuit, T., 2023. Serotonin signaling regulates actomyosin contractility during morphogenesis in evolutionarily divergent lineages. *Nat. Commun.* 14, 5547. <https://doi.org/10.1038/s41467-023-41178-w>
- Kempf, S.C., Page, L.R., Pires, A., 1997. Development of serotonin-like immunoreactivity in the embryos and larvae of nudibranch mollusks with emphasis on the structure and possible function of the apical sensory organ. *J. Comp. Neurol.* 386, 507–528. [https://doi.org/10.1002/\(SICI\)1096-9861\(19970929\)386:3<507::AID-CNE12>3.0.CO;2-7](https://doi.org/10.1002/(SICI)1096-9861(19970929)386:3<507::AID-CNE12>3.0.CO;2-7)
- Kezmarsky, N., Xu, H., Graham, D., White, R., 2005. Identification and characterization of a -tyrosine decarboxylase in. *Biochim. Biophys. Acta BBA - Gen. Subj.* 1722, 175–182. <https://doi.org/10.1016/j.bbagen.2004.12.003>
- Khotimchenko, Yu.S., 1991. Biogenic monoamines in oocytes of echinoderms and bivalve molluscs. A formation of intracellular regulatory systems in oogenesis. *Comp. Biochem. Physiol. Part C Comp. Pharmacol.* 100, 671–675. [https://doi.org/10.1016/0742-8413\(91\)90059-3](https://doi.org/10.1016/0742-8413(91)90059-3)
- Kirchner, M.K., Althammer, F., Donaldson, K.J., Cox, D.N., Stern, J.E., 2023. Changes in neuropeptide large dense core vesicle trafficking dynamics contribute to adaptive responses to a systemic homeostatic challenge. *iScience* 26, 108243. <https://doi.org/10.1016/j.isci.2023.108243>
- Kleine, B., Rossmannith, W.G., 2016. Hormones Derived by Amino Acid Conversion, in: Kleine, B., Rossmannith, W.G. (Eds.), *Hormones and the Endocrine System: Textbook of Endocrinology*. Springer International Publishing, Cham, pp. 237–245. https://doi.org/10.1007/978-3-319-15060-4_7
- Kniazkina, M., Dyachuk, V., 2022. Neurogenesis of the scallop *Azumapekten farreri*: from the first larval sensory neurons to the definitive nervous system of juveniles. *Front. Zool.* 19, 22. <https://doi.org/10.1186/s12983-022-00468-7>

- Kniprath, E., 1981. Ontogeny of the Molluscan Shell Field: a Review. *Zool. Scr.* 10, 61–79. <https://doi.org/10.1111/j.1463-6409.1981.tb00485.x>
- Kniprath, E., 1980. Larval development of the shell and the shell gland in *Mytilus* (Bivalvia). *Wilhelm Roux Arch. Dev. Biol.* 188, 201–204. <https://doi.org/10.1007/BF00849049>
- Kocot, K.M., Aguilera, F., McDougall, C., Jackson, D.J., Degnan, B.M., 2016. Sea shell diversity and rapidly evolving secretomes: insights into the evolution of biomineralization. *Front. Zool.* 13, 23. <https://doi.org/10.1186/s12983-016-0155-z>
- Koelch, M., Pfalzer, A.-K., Kliegl, K., Rothenhöfer, S., Ludolph, A.G., Fegert, J.M., Burger, R., Mehler-Wex, C., Stingl, J., Taurines, R., Egberts, K., Gerlach, M., 2011. Therapeutic Drug Monitoring of Children and Adolescents Treated with Fluoxetine. *Pharmacopsychiatry* 45, 72–76. <https://doi.org/10.1055/s-0031-1291294>
- Kotsyuba, E., Dyachuk, V., 2023. Role of the Neuroendocrine System of Marine Bivalves in Their Response to Hypoxia. *Int. J. Mol. Sci.* 24, 1202. <https://doi.org/10.3390/ijms24021202>
- Kotsyuba, E., Kalachev, A., Kameneva, P., Dyachuk, V., 2020. Distribution of Molecules Related to Neurotransmission in the Nervous System of the Mussel *Crenomytilus grayanus*. *Front. Neuroanat.* 14, 35. <https://doi.org/10.3389/fnana.2020.00035>
- Kriegstein, A.R., 1977. Development of the nervous system of *Aplysia californica*. *Proc. Natl. Acad. Sci.* 74, 375–378. <https://doi.org/10.1073/pnas.74.1.375>
- Kristan, U., Kanduč, T., Osterc, A., Šlejkovec, Z., Ramšak, A., Stibilj, V., 2014. Assessment of pollution level using *Mytilus galloprovincialis* as a bioindicator species: The case of the Gulf of Trieste. *Mar. Pollut. Bull.* 89, 455–463. <https://doi.org/10.1016/j.marpolbul.2014.09.046>
- Kuchel, R.P., Raftos, D.A., 2011. *In vitro* effects of noradrenaline on Akoya pearl oyster (*Pinctada imbricata*) haemocytes. *Fish Shellfish Immunol.* 31, 365–372. <https://doi.org/10.1016/j.fsi.2011.05.025>
- Kullyev, A., Dempsey, C.M., Miller, S., Kuan, C.-J., Hapiak, V.M., Komuniecki, R.W., Griffin, C.T., Sze, J.Y., 2010. A Genetic Survey of Fluoxetine Action on Synaptic Transmission in *Caenorhabditis elegans*. *Genetics* 186, 929–941. <https://doi.org/10.1534/genetics.110.118877>
- Kumar, P., Lee, Jin-Hyung, Lee, Jintae, 2021. Diverse roles of microbial indole compounds in eukaryotic systems. *Biol. Rev. Camb. Philos. Soc.* 96, 2522–2545. <https://doi.org/10.1111/brv.12765>
- Kuo, H.-W., Cheng, W., 2021. Cloning and characterization of tyrosine decarboxylase (TDC) from *Litopenaeus vannamei*, and its roles in biogenic amines synthesis, immune regulation, and resistance to *Vibrio alginolyticus* by RNA interference. *Dev. Comp. Immunol.* 123, 104167. <https://doi.org/10.1016/j.dci.2021.104167>
- Kutchko, K.M., Siltberg-Liberles, J., 2013. Metazoan innovation: from aromatic amino acids to extracellular signaling. *Amino Acids* 45, 359–367. <https://doi.org/10.1007/s00726-013-1509-x>
- Lacaze, E., Pédelucq, J., Fortier, M., Brousseau, P., Auffret, M., Budzinski, H., Fournier, M., 2015. Genotoxic and immunotoxic potential effects of selected psychotropic drugs and antibiotics on blue mussel (*Mytilus edulis*) hemocytes. *Environ. Pollut.* 202, 177–186. <https://doi.org/10.1016/j.envpol.2015.03.025>
- Lacoste, A., Malham, S.K., Cueff, A., Jalabert, F., Gélébart, F., Poulet, S.A., 2001. Evidence for a form of adrenergic response to stress in the mollusc *Crassostrea gigas*. *J. Exp. Biol.* 204, 1247–1255. <https://doi.org/10.1242/jeb.204.7.1247>
- Lai, Y., 2013. 1 - Membrane transporters and the diseases corresponding to functional defects, in: Lai, Y. (Ed.), *Transporters in Drug Discovery and Development*, Woodhead

- Publishing Series in Biomedicine. Woodhead Publishing, pp. 1–146. <https://doi.org/10.1533/9781908818287.1>
- Larsen, M.B., Fontana, A.C.K., Magalhães, L.G., Rodrigues, V., Mortensen, O.V., 2011. A catecholamine transporter from the human parasite *Schistosoma mansoni* with low affinity for psychostimulants. *Mol. Biochem. Parasitol.* 177, 35–41. <https://doi.org/10.1016/j.molbiopara.2011.01.006>
- Lauder, J.M., 1993. Neurotransmitters as growth regulatory signals: role of receptors and second messengers. *Trends Neurosci.* 16, 233–240. [https://doi.org/10.1016/0166-2236\(93\)90162-F](https://doi.org/10.1016/0166-2236(93)90162-F)
- Lawal, H.O., Krantz, D.E., 2013. SLC18: Vesicular neurotransmitter transporters for monoamines and acetylcholine. *Mol. Aspects Med.* 34, 360–372. <https://doi.org/10.1016/j.mam.2012.07.005>
- Le Crom, S., Kapsimali, M., Barôme, P.-O., Vernier, P., 2003. Dopamine receptors for every species: Gene duplications and functional diversification in Craniates, in: Meyer, A., Van De Peer, Y. (Eds.), *Genome Evolution*. Springer Netherlands, Dordrecht, pp. 161–176. https://doi.org/10.1007/978-94-010-0263-9_16
- Lee, C.M., Lin, J.T., Tsai, T.S., 1993. Effects of neuroactive agents on the isolated heart activities of marine bivalve *Meretrix lusoria*. *Chin. J. Physiol.* 36, 165–170.
- Levin, M., Buznikov, G.A., Lauder, J.M., 2006. Of Minds and Embryos: Left-Right Asymmetry and the Serotonergic Controls of Pre-Neural Morphogenesis. *Dev. Neurosci.* 28, 171–185. <https://doi.org/10.1159/000091915>
- Li, Y., Lv, Y., Bian, C., You, X., Deng, L., Shi, Q., 2018. A Comparative Genomic Survey Provides Novel Insights into Molecular Evolution of l-Aromatic Amino Acid Decarboxylase in Vertebrates. *Molecules* 23, 917. <https://doi.org/10.3390/molecules23040917>
- Libersat, F., Pflueger, H.-J., 2004. Monoamines and the Orchestration of Behavior. *BioScience* 54, 17. [https://doi.org/10.1641/0006-3568\(2004\)054\[0017:MATOOB\]2.0.CO;2](https://doi.org/10.1641/0006-3568(2004)054[0017:MATOOB]2.0.CO;2)
- Lin, H.-Y., Kuo, H.-W., Song, Y.-L., Cheng, W., 2020. Cloning and characterization of DOPA decarboxylase in *Litopenaeus vannamei* and its roles in catecholamine biosynthesis, immunocompetence, and antibacterial defense by dsRNA-mediated gene silencing. *Dev. Comp. Immunol.* 108, 103668. <https://doi.org/10.1016/j.dci.2020.103668>
- Lin, M.-F., Leise, E.M., 1996. Gangliogenesis in the prosobranch gastropod *Ilyanassa obsoleta*. *J. Comp. Neurol.* 374, 180–193. [https://doi.org/10.1002/\(SICI\)1096-9861\(19961014\)374:2<180::AID-CNE2>3.0.CO;2-Z](https://doi.org/10.1002/(SICI)1096-9861(19961014)374:2<180::AID-CNE2>3.0.CO;2-Z)
- Liu, Z., Li, M., Yi, Q., Wang, L., Song, L., 2018. The Neuroendocrine-Immune Regulation in Response to Environmental Stress in Marine Bivalves. *Front. Physiol.* 9, 1456. <https://doi.org/10.3389/fphys.2018.01456>
- Liu, Z., Zhou, Z., Zhang, Y., Wang, L., Song, X., Wang, W., Zheng, Y., Zong, Y., Lv, Z., Song, L., 2020. Ocean acidification inhibits initial shell formation of oyster larvae by suppressing the biosynthesis of serotonin and dopamine. *Sci. Total Environ.* 735, 139469. <https://doi.org/10.1016/j.scitotenv.2020.139469>
- Madikizela, L.M., Ncube, S., Tutu, H., Richards, H., Newman, B., Ndungu, K., Chimuka, L., 2020. Pharmaceuticals and their metabolites in the marine environment: Sources, analytical methods and occurrence. *Trends Environ. Anal. Chem.* 28, e00104. <https://doi.org/10.1016/j.teac.2020.e00104>
- Magni, S., Parolini, M., Della Torre, C., de Oliveira, L.F., Catani, M., Guzzinati, R., Cavazzini, A., Binelli, A., 2017. Multi-biomarker investigation to assess toxicity induced by two antidepressants on *Dreissena polymorpha*. *Sci. Total Environ.* 578, 452–459. <https://doi.org/10.1016/j.scitotenv.2016.10.208>

- Malagoli, D., Ottaviani, E., 2017. Cross-talk among immune and neuroendocrine systems in molluscs and other invertebrate models. *Horm. Behav.* 88, 41–44. <https://doi.org/10.1016/j.yhbeh.2016.10.015>
- Marquina-Solis, J., Vandewyer, E., Hawk, J., Colón-Ramos, D.A., Beets, I., Bargmann, C.I., 2022. Peptidergic signaling controls the dynamics of sickness behavior in *Caenorhabditis elegans*. <https://doi.org/10.1101/2022.04.16.488560>
- Martin, C.A., Krantz, D.E., 2014. *Drosophila melanogaster* as a genetic model system to study neurotransmitter transporters. *Neurochem. Int.* 73, 71–88. <https://doi.org/10.1016/j.neuint.2014.03.015>
- Martín-Durán, J.M., Hejnal, A., 2021. A developmental perspective on the evolution of the nervous system. *Dev. Biol.* 475, 181–192. <https://doi.org/10.1016/j.ydbio.2019.10.003>
- Matsuo, R., Tanaka, M., Fukata, R., Kobayashi, S., Aonuma, H., Matsuo, Y., 2016. Octopaminergic system in the central nervous system of the terrestrial slug *Limax*. *J. Comp. Neurol.* 524, 3849–3864. <https://doi.org/10.1002/cne.24039>
- Maugars, G., Nourizadeh-Lillabadi, R., Weltzien, F.-A., 2020. New Insights Into the Evolutionary History of Melatonin Receptors in Vertebrates, With Particular Focus on Teleosts. *Front. Endocrinol.* 11. <https://doi.org/10.3389/fendo.2020.538196>
- Mbikay, M., Seidah, N.G., Chrétien, M., 2001. Neuroendocrine secretory protein 7B2: structure, expression and functions. *Biochem. J.* 357, 329–342.
- Meinertzhagen, I.A., 2019. Morphology of Invertebrate Neurons and Synapses, in: Byrne, J.H. (Ed.), *The Oxford Handbook of Invertebrate Neurobiology*. Oxford University Press, p. 0. <https://doi.org/10.1093/oxfordhb/9780190456757.013.9>
- Mell, L.D., Carpenter, D.O., 1980. Fluorometric determination of octopamine in tissue homogenates by high-performance liquid chromatography. *Neurochem. Res.* 5, 1089–1096. <https://doi.org/10.1007/BF00966166>
- Mezzelani, M., Gorbi, S., Regoli, F., 2018. Pharmaceuticals in the aquatic environments: Evidence of emerged threat and future challenges for marine organisms. *Mar. Environ. Res.* 140, 41–60. <https://doi.org/10.1016/j.marenvres.2018.05.001>
- Miglioli, A., Balbi, T., Besnardeau, L., Dumollard, R., Canesi, L., 2021a. Bisphenol A interferes with first shell formation and development of the serotonergic system in early larval stages of *Mytilus galloprovincialis*. *Sci. Total Environ.* 758, 144003. <https://doi.org/10.1016/j.scitotenv.2020.144003>
- Miglioli, A., Balbi, T., Montagna, M., Dumollard, R., Canesi, L., 2021b. Tetrabromobisphenol A acts a neurodevelopmental disruptor in early larval stages of *Mytilus galloprovincialis*. *Sci. Total Environ.* 793, 148596. <https://doi.org/10.1016/j.scitotenv.2021.148596>
- Miglioli, A., Dumollard, R., Balbi, T., Besnardeau, L., Canesi, L., 2019. Characterization of the main steps in first shell formation in *Mytilus galloprovincialis*: possible role of tyrosinase. *Proc. R. Soc. B Biol. Sci.* 286, 20192043. <https://doi.org/10.1098/rspb.2019.2043>
- Miglioli, A., Tredez, M., Boosten, M., Sant, C., Carvalho, J.E., Dru, P., Canesi, L., Schubert, M., Dumollard, R., 2024. The Mediterranean mussel *Mytilus galloprovincialis*: a novel model for developmental studies in mollusks. *Development* 151, dev202256. <https://doi.org/10.1242/dev.202256>
- Miguel-Tomé, S., Llinás, R.R., 2021. Broadening the definition of a nervous system to better understand the evolution of plants and animals. *Plant Signal. Behav.* 16, 1927562. <https://doi.org/10.1080/15592324.2021.1927562>
- Mishra, P., Gong, Z., Kelly, B.C., 2017. Assessing biological effects of fluoxetine in developing zebrafish embryos using gas chromatography-mass spectrometry based metabolomics. *Chemosphere* 188, 157–167. <https://doi.org/10.1016/j.chemosphere.2017.08.149>

- Mole, R.A., Brooks, B.W., 2019. Global scanning of selective serotonin reuptake inhibitors: occurrence, wastewater treatment and hazards in aquatic systems. *Environ. Pollut.* 250, 1019–1031. <https://doi.org/10.1016/j.envpol.2019.04.118>
- Monjo, F., Romero, R., 2015. Embryonic development of the nervous system in the planarian *Schmidtea polychroa*. *Dev. Biol.* 397, 305–319. <https://doi.org/10.1016/j.ydbio.2014.10.021>
- Monti, J.M., Jantos, H., 2008. The roles of dopamine and serotonin, and of their receptors, in regulating sleep and waking, in: Di Giovanni, G., Di Matteo, V., Esposito, E. (Eds.), *Progress in Brain Research, Serotonin–Dopamine Interaction: Experimental Evidence and Therapeutic Relevance*. Elsevier, pp. 625–646. [https://doi.org/10.1016/S0079-6123\(08\)00929-1](https://doi.org/10.1016/S0079-6123(08)00929-1)
- Moret, C., Briley, M., 1992. Effect of antidepressant drugs on monoamine synthesis in brain *in vivo*. *Neuropharmacology* 31, 679–684. [https://doi.org/10.1016/0028-3908\(92\)90146-G](https://doi.org/10.1016/0028-3908(92)90146-G)
- Moroz, L.L., Romanova, D.Y., Kohn, A.B., n.d. Neural versus alternative integrative systems: molecular insights into origins of neurotransmitters. *Philos. Trans. R. Soc. B Biol. Sci.* 376, 20190762. <https://doi.org/10.1098/rstb.2019.0762>
- Mulinari, S., 2015. Divergence and convergence of commercial and scientific priorities in drug development: The case of Zeldin, the first SSRI antidepressant. *Soc. Sci. Med.* 138, 217–224. <https://doi.org/10.1016/j.socscimed.2015.06.020>
- Mustard, J.A., Beggs, K.T., Mercer, A.R., 2005. Molecular biology of the invertebrate dopamine receptors. *Arch. Insect Biochem. Physiol.* 59, 103–117. <https://doi.org/10.1002/arch.20065>
- Nezlin, L.P., Voronezhskaya, E.E., 2017. Early peripheral sensory neurons in the development of trochozoan animals. *Russ. J. Dev. Biol.* 48, 130–143. <https://doi.org/10.1134/S1062360417020060>
- Nichols, D.E., Nichols, C.D., 2008. Serotonin Receptors. *Chem. Rev.* 108, 1614–1641. <https://doi.org/10.1021/cr078224o>
- Nickel, M., 2010. Evolutionary emergence of synaptic nervous systems: what can we learn from the non-synaptic, nerveless Porifera? *Invertebr. Biol.* 129, 1–16. <https://doi.org/10.1111/j.1744-7410.2010.00193.x>
- Nieder, A., 2021. The Evolutionary History of Brains for Numbers. *Trends Cogn. Sci.* 25, 608–621. <https://doi.org/10.1016/j.tics.2021.03.012>
- Nielsen, C., 2005. Larval and adult brains1. *Evol. Dev.* 7, 483–489. <https://doi.org/10.1111/j.1525-142X.2005.05051.x>
- Nieuwenhuys, R., Donkelaar, H.J. ten, Nicholson, C., Smeets, W.J.A.J., Wicht, H., Meek, J., Dubbeldam, J.L., Dongen, P.A.M. van, Voogd, J., 2014. *The Central Nervous System of Vertebrates*, Softcover reprint of the original 1st ed. 1998 edition. ed. Springer.
- Nikishchenko, V., Kolotukhina, N., Dyachuk, V., 2023. Comparative Neuroanatomy of Pediveliger Larvae of Various Bivalves from the Sea of Japan. *Biology* 12, 1341. <https://doi.org/10.3390/biology12101341>
- Nikishchenko, V.E., Dyachuk, V.A., 2024. Comparison of neurogenesis in bivalves with different types of development. *Sci. Rep.* 14, 19495. <https://doi.org/10.1038/s41598-024-67622-5>
- Nishimura, K., Kitamura, Y., Inoue, T., Umesono, Y., Yoshimoto, K., Taniguchi, T., Agata, K., 2008. Characterization of tyramine β -hydroxylase in planarian *Dugesia japonica*: Cloning and expression. *Neurochem. Int.* 53, 184–192. <https://doi.org/10.1016/j.neuint.2008.09.006>

- Noguera-Oviedo, K., Aga, D.S., 2016. Lessons learned from more than two decades of research on emerging contaminants in the environment. *J. Hazard. Mater.* 316, 242–251. <https://doi.org/10.1016/j.jhazmat.2016.04.058>
- Nussey, S., Whitehead, S., 2001. Principles of endocrinology, in: *Endocrinology: An Integrated Approach*. BIOS Scientific Publishers.
- OECD, 2020. Adverse Outcome Pathways, Molecular Screening and Toxicogenomics: Report on OECD Workshop. OECD, Paris, France.
- Opazo, J.C., Zavala, K., Miranda-Rottmann, S., Araya, R., 2018. Evolution of dopamine receptors: phylogenetic evidence suggests a later origin of the DRD2l and DRD4rs dopamine receptor gene lineages. *PeerJ* 6, e4593. <https://doi.org/10.7717/peerj.4593>
- Ortega, A., Olivares-Bañuelos, T.N., 2020. Neurons and Glia Cells in Marine Invertebrates: An Update. *Front. Neurosci.* 14. <https://doi.org/10.3389/fnins.2020.00121>
- Oyarzún, P.A., Toro, J.E., Nuñez, J.J., Ruiz-Tagle, G., Gardner, J.P.A., 2024. The Mediterranean Mussel *Mytilus galloprovincialis* (Mollusca: Bivalvia) in Chile: Distribution and Genetic Structure of a Recently Introduced Invasive Marine Species. *Animals* 14, 823. <https://doi.org/10.3390/ani14060823>
- Paciotti, G.F., Higgins, W.J., 1985. Potentiation of the 5-hydroxytryptamine-induced increases in myocardial contractility in *Mercenaria mercenaria* ventricle by forskolin. *Comp. Biochem. Physiol. Part C Comp. Pharmacol.* 80, 325–329. [https://doi.org/10.1016/0742-8413\(85\)90064-7](https://doi.org/10.1016/0742-8413(85)90064-7)
- Paganos, P., Voronov, D., Musser, J.M., Arendt, D., Arnone, M.I., 2021. Single-cell RNA sequencing of the *Strongylocentrotus purpuratus* larva reveals the blueprint of major cell types and nervous system of a non-chordate deuterostome [WWW Document]. *eLife*. <https://doi.org/10.7554/eLife.70416>
- Panula, P., Chen, Y.-C., Baronio, D., Lewis, S., Sundvik, M., 2022. The Histamine System in Zebrafish Brain: Organization, Receptors, and Behavioral Roles. *Curr. Top. Behav. Neurosci.* 59, 291–302. https://doi.org/10.1007/7854_2021_259
- Parsons, M.E., Ganellin, C.R., 2006. Histamine and its receptors. *Br. J. Pharmacol.* 147, S127–S135. <https://doi.org/10.1038/sj.bjp.0706440>
- Pavlicek, A., Schwaha, T., Wanninger, A., 2018. Towards a ground pattern reconstruction of bivalve nervous systems: neurogenesis in the zebra mussel *Dreissena polymorpha*. *Org. Divers. Evol.* 18, 101–114. <https://doi.org/10.1007/s13127-017-0356-0>
- Pennati, R., Blumer, G., Mercurio, S., Scari, G., 2024. Serotonin system in tunicates: insight from morphological and molecular approaches. *Front. Ecol. Evol.* 12. <https://doi.org/10.3389/fevo.2024.1378927>
- Pennati, R., Candiani, S., Biggiogero, M., Zega, G., Gropelli, S., Oliveri, D., Parodi, M., De Bernardi, F., Pestarino, M., 2007. Developmental expression of tryptophan hydroxylase gene in *Ciona intestinalis*. *Dev. Genes Evol.* 217, 307–313. <https://doi.org/10.1007/s00427-007-0138-3>
- Peters, J.R., Granek, E.F., 2016. Long-term exposure to fluoxetine reduces growth and reproductive potential in the dominant rocky intertidal mussel, *Mytilus californianus*. *Sci. Total Environ.* 545–546, 621–628. <https://doi.org/10.1016/j.scitotenv.2015.12.118>
- Piovani, L., Leite, D.J., Yañez Guerra, L.A., Simpson, F., Musser, J.M., Salvador-Martínez, I., Marlétaz, F., Jékely, G., Telford, M.J., 2023. Single-cell atlases of two lophotrochozoan larvae highlight their complex evolutionary histories. *Sci. Adv.* 9, eadg6034. <https://doi.org/10.1126/sciadv.adg6034>
- Pironti, C., Ricciardi, M., Proto, A., Bianco, P.M., Montano, L., Motta, O., 2021. Endocrine-Disrupting Compounds: An Overview on Their Occurrence in the Aquatic Environment and Human Exposure. *Water* 13, 1347. <https://doi.org/10.3390/w13101347>
- Poli, A., Fabbri, E., 2018. *Fisiologia degli Animali Marini, II Edizione*. ed. EDISES.

- Porter, J.C., 1973. Neuroendocrine Systems: the Need for Precise Identification and Rigorous Description of their Operations*, in: Zimmermann, E., Gispen, W.H., Marks, B.H., De Wied, D. (Eds.), *Progress in Brain Research, Drug Effects on Neuroendocrine Regulation*. Elsevier, pp. 1–6. [https://doi.org/10.1016/S0079-6123\(08\)64062-5](https://doi.org/10.1016/S0079-6123(08)64062-5)
- Pörzgen, P., Park, S.K., Hirsh, J., Sonders, M.S., Amara, S.G., 2001. The Antidepressant-Sensitive Dopamine Transporter in *Drosophila melanogaster*: A Primordial Carrier for Catecholamines. *Mol. Pharmacol.* 59, 83–95. <https://doi.org/10.1124/mol.59.1.83>
- Pryce, K., Samuel, D., Lagares, E., Myrthil, M., Bess, F., Harris, A., Welsh, C., Carroll, M.A., Catapane, E.J., 2015. Presence of Octopamine and an Octopamine Receptor in *Crassostrea virginica*. *In Vivo* 37, 16–24.
- Pryor, A., Hart, S., Berry, M.D., 2016. Synthesis and Neurochemistry of Trace Amines*, in: Farooqui, T., Farooqui, A.A. (Eds.), *Trace Amines and Neurological Disorders*. Academic Press, San Diego, pp. 27–43. <https://doi.org/10.1016/B978-0-12-803603-7.00003-3>
- Przeslawski, R., Byrne, M., Mellin, C., 2015. A review and meta-analysis of the effects of multiple abiotic stressors on marine embryos and larvae. *Glob. Change Biol.* 21, 2122–2140. <https://doi.org/10.1111/gcb.12833>
- Purves, D., Augustine, G.J., Fitzpatrick, D., Katz, L.C., LaMantia, A.-S., McNamara, J.O., Williams, S.M., 2001. *Packaging Neurotransmitters*, in: *Neuroscience*. 2nd Edition. Sinauer Associates.
- Quintero-Villegas, A., Valdés-Ferrer, S.I., 2022. Central nervous system effects of 5-HT₇ receptors: a potential target for neurodegenerative diseases. *Mol. Med.* 28, 70. <https://doi.org/10.1186/s10020-022-00497-2>
- Rafiq, A., Capolupo, M., Addesse, G., Valbonesi, P., Fabbri, E., 2023. Antidepressants and their metabolites primarily affect lysosomal functions in the marine mussel, *Mytilus galloprovincialis*. *Sci. Total Environ.* 903, 166078. <https://doi.org/10.1016/j.scitotenv.2023.166078>
- Ram, J.L., Crawford, G.W., Walker, J.U., Mojares, J.J., Patel, N., Fong, P.P., Kyojuka, K., 1993. Spawning in the zebra mussel (*Dreissena polymorpha*): Activation by internal or external application of serotonin. *J. Exp. Zool.* 265, 587–598. <https://doi.org/10.1002/jez.1402650515>
- Ram, J.L., Moore, D., Putschakayala, S., Paredes, A.A., Ma, D., Croll, R.P., 1999. Serotonergic responses of the siphons and adjacent mantle tissue of the zebra mussel, *Dreissena polymorpha*. *Comp. Biochem. Physiol. C Pharmacol. Toxicol. Endocrinol.* 124, 211–220. [https://doi.org/10.1016/S0742-8413\(99\)00068-7](https://doi.org/10.1016/S0742-8413(99)00068-7)
- Ramirez, M.D., Bui, T.N., Katz, P.S., 2024. Cellular-resolution gene expression mapping reveals organization in the head ganglia of the gastropod, *Berghia stephanieae*. *J. Comp. Neurol.* 532, e25628. <https://doi.org/10.1002/cne.25628>
- Ravhe, I.S., Krishnan, A., Manoj, N., 2021. Evolutionary history of histamine receptors: Early vertebrate origin and expansion of the H₃-H₄ subtypes. *Mol. Phylogenet. Evol.* 154, 106989. <https://doi.org/10.1016/j.ympev.2020.106989>
- Ribeiro, P., Patocka, N., 2013. Neurotransmitter transporters in schistosomes: Structure, function and prospects for drug discovery. *Parasitol. Int.* 62, 629–638. <https://doi.org/10.1016/j.parint.2013.06.003>
- Richter, S., Loesel, R., Purschke, G., Schmidt-Rhaesa, A., Scholtz, G., Stach, T., Vogt, L., Wanninger, A., Brenneis, G., Döring, C., Faller, S., Fritsch, M., Grobe, P., Heuer, C.M., Kaul, S., Møller, O.S., Müller, C.H., Rieger, V., Rothe, B.H., Stegner, M.E., Harzsch, S., 2010. Invertebrate neurophylogeny: suggested terms and definitions for a neuroanatomical glossary. *Front. Zool.* 7, 29. <https://doi.org/10.1186/1742-9994-7-29>

- Robert, A., Schultz, I.R., Hucher, N., Monsinjon, T., Knigge, T., 2017. Toxicokinetics, disposition and metabolism of fluoxetine in crabs. *Chemosphere* 186, 958–967. <https://doi.org/10.1016/j.chemosphere.2017.08.018>
- Roelofs, J., Van Haastert, P.J., 2001. Genes lost during evolution. *Nature* 411, 1013–1014. <https://doi.org/10.1038/35082627>
- Rosenfeld, C.S., Denslow, N.D., Orlando, E.F., Gutierrez-Villagomez, J.M., Trudeau, V.L., 2017. Neuroendocrine Disruption of Organizational and Activational Hormone Programming in Poikilothermic Vertebrates. *J. Toxicol. Environ. Health B Crit. Rev.* 20, 276–304. <https://doi.org/10.1080/10937404.2017.1370083>
- Rosikon, K.D., Bone, M.C., Lawal, H.O., 2023. Regulation and modulation of biogenic amine neurotransmission in *Drosophila* and *Caenorhabditis elegans*. *Front. Physiol.* 14. <https://doi.org/10.3389/fphys.2023.970405>
- Ross, P.M., Parker, L., Byrne, M., 2016. Transgenerational responses of molluscs and echinoderms to changing ocean conditions. *ICES J. Mar. Sci.* 73, 537–549. <https://doi.org/10.1093/icesjms/fsv254>
- Rouabhi, Y.L., Grosjean, P., Boutiba, Z., Rouane Hacene, O., Richir, J., 2019. Reproductive cycle and follicle cleaning process of *Mytilus galloprovincialis* (Mollusca: Bivalvia) from a polluted coastal site in Algeria. *Invertebr. Reprod. Dev.* 63, 255–267. <https://doi.org/10.1080/07924259.2019.1631221>
- Roveri, V., Guimarães, L.L., Toma, W., Correia, A.T., 2020. Occurrence and ecological risk assessment of pharmaceuticals and cocaine in a beach area of Guarujá, São Paulo State, Brazil, under the influence of urban surface runoff. *Environ. Sci. Pollut. Res.* 27, 45063–45075. <https://doi.org/10.1007/s11356-020-10316-y>
- Ruuskanen, J.O., Peitsaro, N., Kaslin, J.V.M., Panula, P., Scheinin, M., 2005. Expression and function of alpha-adrenoceptors in zebrafish: drug effects, mRNA and receptor distributions. *J. Neurochem.* 94, 1559–1569. <https://doi.org/10.1111/j.1471-4159.2005.03305.x>
- Sadamoto, H., Takahashi, H., Okada, T., Kenmoku, H., Toyota, M., Asakawa, Y., 2012. De Novo Sequencing and Transcriptome Analysis of the Central Nervous System of Mollusc *Lymnaea stagnalis* by Deep RNA Sequencing. *PLOS ONE* 7, e42546. <https://doi.org/10.1371/journal.pone.0042546>
- Sáenz-de-Miera, L.E., Ayala, F.J., 2004. Complex evolution of orthologous and paralogous decarboxylase genes. *J. Evol. Biol.* 17, 55–66. <https://doi.org/10.1046/j.1420-9101.2003.00652.x>
- Saier, M.H., 2000. A Functional-Phylogenetic Classification System for Transmembrane Solute Transporters. *Microbiol. Mol. Biol. Rev.* 64, 354–411.
- Salatiello, F., Gerdol, M., Pallavicini, A., Locascio, A., Sirakov, M., 2022. Comparative analysis of novel and common reference genes in adult tissues of the mussel *Mytilus galloprovincialis*. *BMC Genomics* 23, 349. <https://doi.org/10.1186/s12864-022-08553-1>
- Salvi, D., Tavladoraki, P., 2020. The tree of life of polyamine oxidases. *Sci. Rep.* 10, 17858. <https://doi.org/10.1038/s41598-020-74708-3>
- Sánchez-Lazo, C., Martínez-Pita, I., 2012. Induction of settlement in larvae of the mussel *Mytilus galloprovincialis* using neuroactive compounds. *Aquaculture* 344–349, 210–215. <https://doi.org/10.1016/j.aquaculture.2012.03.021>
- Sauvé, S., Desrosiers, M., 2014. A review of what is an emerging contaminant. *Chem. Cent. J.* 8, 15. <https://doi.org/10.1186/1752-153X-8-15>
- Scammell, T.E., Jackson, A.C., Franks, N.P., Wisden, W., Dauvilliers, Y., 2019. Histamine: neural circuits and new medications. *Sleep* 42. <https://doi.org/10.1093/sleep/zsy183>

- Schug, T.T., Janesick, A., Blumberg, B., Heindel, J.J., 2011. Endocrine disrupting chemicals and disease susceptibility. *J. Steroid Biochem. Mol. Biol., Special Issue on Steroid Metabolism in Marine Organisms* 127, 204–215. <https://doi.org/10.1016/j.jsbmb.2011.08.007>
- Schwartz, J., Réalis-Doyelle, E., Le Franc, L., Favrel, P., 2021. A Novel Dop2/Invertebrate-Type Dopamine Signaling System Potentially Mediates Stress, Female Reproduction, and Early Development in the Pacific Oyster (*Crassostrea gigas*). *Mar. Biotechnol.* 23, 683–694. <https://doi.org/10.1007/s10126-021-10052-5>
- Schwartz, T.B., Norris, D.O., 2024. Endocrine system. *Encycl. Br.*
- Seralini, G.-E., Jungers, G., 2021. Endocrine disruptors also function as nervous disruptors and can be renamed endocrine and nervous disruptors (ENDs). *Toxicol. Rep.* 8, 1538–1557. <https://doi.org/10.1016/j.toxrep.2021.07.014>
- Sghendo, L., Mifsud, J., 2012. Understanding the molecular pharmacology of the serotonergic system: using fluoxetine as a model. *J. Pharm. Pharmacol.* 64, 317–325. <https://doi.org/10.1111/j.2042-7158.2011.01384.x>
- Siltberg-Liberles, J., Steen, I.H., Svebak, R.M., Martinez, A., 2008. The phylogeny of the aromatic amino acid hydroxylases revisited by characterizing phenylalanine hydroxylase from *Dictyostelium discoideum*. *Gene* 427, 86–92. <https://doi.org/10.1016/j.gene.2008.09.005>
- Sloley, B., 2004. Metabolism of Monoamines in Invertebrates: The Relative Importance of Monoamine Oxidase in Different Phyla. *NeuroToxicology* 25, 175–183. [https://doi.org/10.1016/S0161-813X\(03\)00096-2](https://doi.org/10.1016/S0161-813X(03)00096-2)
- Sloley, B.D., Juorio, A.V., 1995. Monoamine Neurotransmitters in Invertebrates and Vertebrates: An Examination of the Diverse Enzymatic Pathways Utilized to Synthesize and Inactivate Biogenic Amines, in: Bradley, R.J., Harris, R.A. (Eds.), *International Review of Neurobiology*. Academic Press, pp. 253–303. [https://doi.org/10.1016/S0074-7742\(08\)60528-0](https://doi.org/10.1016/S0074-7742(08)60528-0)
- Sohel, A.J., Shutter, M.C., Patel, P., Molla, M., 2024. Fluoxetine, in: *StatPearls*. StatPearls Publishing, Treasure Island (FL).
- Sourbron, J., Schneider, H., Kecskés, A., Liu, Y., Buening, E.M., Lagae, L., Smolders, I., de Witte, P., 2016. Serotonergic Modulation as Effective Treatment for Dravet Syndrome in a Zebrafish Mutant Model. *ACS Chem. Neurosci.* 7, 588–598. <https://doi.org/10.1021/acschemneuro.5b00342>
- Souza, J.F. de, Mello, A. de A., Portal, T.M., Nunes-da-Fonseca, R., Monteiro de Barros, C., 2021. Novel insights about the ascidian dopamine system: Pharmacology and phylogenetics of catecholaminergic receptors on the *Phallusia nigra* immune cells. *Fish Shellfish Immunol.* 109, 41–50. <https://doi.org/10.1016/j.fsi.2020.11.022>
- Squires, L.N., Rubakhin, S.S., Wadhams, A.A., Talbot, K.N., Nakano, H., Moroz, L.L., Sweedler, J.V., 2010. Serotonin and its metabolism in basal deuterostomes: insights from *Strongylocentrotus purpuratus* and *Xenoturbella bocki*. *J. Exp. Biol.* 213, 2647–2654. <https://doi.org/10.1242/jeb.042374>
- Stárka, L., Dušková, M., 2020. What Is a Hormone? *Physiol. Res.* 69, S183–S185. <https://doi.org/10.33549/physiolres.934509>
- Stiefel, C., Stintzing, F., 2023. Endocrine-active and endocrine-disrupting compounds in food – occurrence, formation and relevance. *NFS J.* 31, 57–92. <https://doi.org/10.1016/j.nfs.2023.03.004>
- Suo, S., Ishiura, S., Van Tol, H.H.M., 2004. Dopamine receptors in *C. elegans*. *Eur. J. Pharmacol.* 500, 159–166. <https://doi.org/10.1016/j.ejphar.2004.07.021>
- Swallow, J.G., Bubak, A.N., Grace, J.L., Guest Editors, 2016. Editorial The role of monoamines in modulating behavior. *Curr. Zool.* 62, 253–255. <https://doi.org/10.1093/cz/zow046>

- Tessmar-Raible, K., 2007. The evolution of neurosecretory centers in bilaterian forebrains: Insights from protostomes. *Semin. Cell Dev. Biol.* 18, 492–501. <https://doi.org/10.1016/j.semcdb.2007.04.007>
- Tierney, A.J., 2020. Feeding, hunger, satiety and serotonin in invertebrates. *Proc. R. Soc. B Biol. Sci.* 287, 20201386. <https://doi.org/10.1098/rspb.2020.1386>
- Tierney, A.J., 2018. Invertebrate serotonin receptors: a molecular perspective on classification and pharmacology. *J. Exp. Biol.* 221, jeb184838. <https://doi.org/10.1242/jeb.184838>
- Tomberlin, J.K., Crippen, T.L., Wu, G., Griffin, A.S., Wood, T.K., Kilner, R.M., 2017. Indole: An evolutionarily conserved influencer of behavior across kingdoms. *BioEssays* 39, 1600203. <https://doi.org/10.1002/bies.201600203>
- Unen, J. van, Rashidfarrokhi, A., Hoogendoorn, E., Postma, M., Gadella, T.W.J., Goedhart, J., 2016. Quantitative Single-Cell Analysis of Signaling Pathways Activated Immediately Downstream of Histamine Receptor Subtypes. *Mol. Pharmacol.* 90, 162–176. <https://doi.org/10.1124/mol.116.104505>
- Vandenberg, L.N., Blackiston, D.J., Rea, A.C., Dore, T.M., Levin, M., 2014. Left-right patterning in *Xenopus* conjoined twin embryos requires serotonin signaling and gap junctions. *Int. J. Dev. Biol.* 58, 799–809. <https://doi.org/10.1387/ijdb.140215ml>
- Vandenberg, L.N., Lemire, J.M., Levin, M., 2013. Serotonin has early, cilia-independent roles in *Xenopus* left-right patterning. *Dis. Model. Mech.* 6, 261–268. <https://doi.org/10.1242/dmm.010256>
- Vasskog, T., Berger, U., Samuelsen, P.-J., Kallenborn, R., Jensen, E., 2006. Selective serotonin reuptake inhibitors in sewage influents and effluents from Tromsø, Norway. *J. Chromatogr. A* 1115, 187–195. <https://doi.org/10.1016/j.chroma.2006.02.091>
- Vendelboe, T.V., Harris, P., Zhao, Y., Walter, T.S., Harlos, K., El Omari, K., Christensen, H.E.M., 2016. The crystal structure of human dopamine β -hydroxylase at 2.9 Å resolution. *Sci. Adv.* 2, e1500980. <https://doi.org/10.1126/sciadv.1500980>
- Verlinden, H., 2018. Dopamine signalling in locusts and other insects. *Insect Biochem. Mol. Biol.* 97, 40–52. <https://doi.org/10.1016/j.ibmb.2018.04.005>
- Vogeler, S., Bean, T.P., Lyons, B.P., Galloway, T.S., 2016. Dynamics of nuclear receptor gene expression during Pacific oyster development. *BMC Dev. Biol.* 16, 1–13. <https://doi.org/10.1186/s12861-016-0129-6>
- Voronezhskaya, E.E., Nezlin, L.P., Odintsova, N.A., Plummer, J.T., Croll, R.P., 2008. Neuronal development in larval mussel *Mytilus trossulus* (Mollusca: Bivalvia). *Zoomorphology* 127, 97–110. <https://doi.org/10.1007/s00435-007-0055-z>
- Wang, C., Jiang, Y., Ma, J., Wu, H., Wacker, D., Katritch, V., Han, G.W., Liu, W., Huang, X.-P., Vardy, E., McCorvy, J.D., Gao, X., Zhou, X.E., Melcher, K., Zhang, C., Bai, F., Yang, H., Yang, L., Jiang, H., Roth, B.L., Cherezov, V., Stevens, R.C., Xu, H.E., 2013. Structural Basis for Molecular Recognition at Serotonin Receptors. *Science* 340, 610–614. <https://doi.org/10.1126/science.1232807>
- Wang, Q., Lu, Q., Guo, Q., Teng, M., Gong, Q., Li, X., Du, Y., Liu, Z., Tao, Y., 2022. Structural basis of the ligand binding and signaling mechanism of melatonin receptors. *Nat. Commun.* 13, 454. <https://doi.org/10.1038/s41467-022-28111-3>
- Wanninger, A., Wollesen, T., 2015. Mollusca, in: Wanninger, A. (Ed.), *Evolutionary Developmental Biology of Invertebrates 2*. Springer Vienna, Vienna, pp. 103–153. https://doi.org/10.1007/978-3-7091-1871-9_7
- Watanabe, T., Sadamoto, H., Aonuma, H., 2011. Identification and expression analysis of the genes involved in serotonin biosynthesis and transduction in the field cricket *Gryllus bimaculatus*: 5-HT-related genes in the cricket. *Insect Mol. Biol.* 20, 619–635. <https://doi.org/10.1111/j.1365-2583.2011.01093.x>

- Watts, J.L., Browse, J., 2006. Dietary manipulation implicates lipid signaling in the regulation of germ cell maintenance in *C. elegans*. *Dev. Biol.* 292, 381–392. <https://doi.org/10.1016/j.ydbio.2006.01.013>
- Waxham, M.N., 2014. Chapter 10 - Neurotransmitter Receptors, in: Byrne, J.H., Heidelberger, R., Waxham, M.N. (Eds.), *From Molecules to Networks* (Third Edition). Academic Press, Boston, pp. 285–321. <https://doi.org/10.1016/B978-0-12-397179-1.00010-5>
- Wilson, R.J., Ahmed, T.H., Rahman, M.M., Cartwright, B.M., Jones, T.C., 2020. Identification and activity of monoamine oxidase in the orb-weaving spider *Larinioides cornutus*. *Gen. Comp. Endocrinol.* 299, 113580. <https://doi.org/10.1016/j.ygcen.2020.113580>
- Witt-Enderby, P.A., Bennett, J., Jarzynka, M.J., Firestine, S., Melan, M.A., 2003. Melatonin receptors and their regulation: biochemical and structural mechanisms. *Life Sci.* 72, 2183–2198. [https://doi.org/10.1016/S0024-3205\(03\)00098-5](https://doi.org/10.1016/S0024-3205(03)00098-5)
- WoRMS Editorial Board, 2024. World Register of Marine Species. <https://doi.org/10.14284/170>
- Wuttke, W., Jarry, H., Seidlova-Wuttke, D., 2010. Definition, classification and mechanism of action of endocrine disrupting chemicals. *Hormones* 9, 9–15. <https://doi.org/10.1007/BF03401276>
- Xin, X., Mains, R.E., Eipper, B.A., 2004. Monooxygenase X, a Member of the Copper-dependent Monooxygenase Family Localized to the Endoplasmic Reticulum. *J. Biol. Chem.* 279, 48159–48167. <https://doi.org/10.1074/jbc.M407486200>
- Xu, J., Li, Y., Lv, Y., Bian, C., You, X., Endoh, D., Teraoka, H., Shi, Q., 2019. Molecular Evolution of Tryptophan Hydroxylases in Vertebrates: A Comparative Genomic Survey. *Genes* 10, 203. <https://doi.org/10.3390/genes10030203>
- Xu, L., Jiang, H.-B., Chen, X.-F., Xiong, Y., Lu, X.-P., Pei, Y.-X., Smagghe, G., Wang, J.-J., 2018. How Tyramine β -Hydroxylase Controls the Production of Octopamine, Modulating the Mobility of Beetles. *Int. J. Mol. Sci.* 19, 846. <https://doi.org/10.3390/ijms19030846>
- Xu, Q., Song, Y., Liu, R., Chen, Y., Zhang, Y., Li, Y., Zhao, W., Chang, G., Chen, G., 2016. The dopamine β -hydroxylase gene in Chinese goose (*Anas cygnoides*): cloning, characterization, and expression during the reproductive cycle. *BMC Genet.* 17, 48. <https://doi.org/10.1186/s12863-016-0355-8>
- Yamamoto, K., Ruuskanen, J.O., Wullimann, M.F., Vernier, P., 2010. Two tyrosine hydroxylase genes in vertebrates: New dopaminergic territories revealed in the zebrafish brain. *Mol. Cell. Neurosci.* 43, 394–402. <https://doi.org/10.1016/j.mcn.2010.01.006>
- Yamamoto, K., Vernier, P., 2011. The Evolution of Dopamine Systems in Chordates. *Front. Neuroanat.* 5. <https://doi.org/10.3389/fnana.2011.00021>
- Yang, B., Ni, J., Zeng, Z., Shi, B., You, W., Ke, C., 2013. Cloning and characterization of the dopamine like receptor in the oyster *Crassostrea angulata*: Expression during the ovarian cycle. *Comp. Biochem. Physiol. B Biochem. Mol. Biol.* 164, 168–175. <https://doi.org/10.1016/j.cbpb.2012.12.006>
- Yang, B., Qin, J., Shi, B., Han, G., Chen, J., Huang, H., Ke, C., 2012. Molecular characterization and functional analysis of adrenergic like receptor during larval metamorphosis in *Crassostrea angulata*. *Aquaculture* 366–367, 54–61. <https://doi.org/10.1016/j.aquaculture.2012.08.040>
- Yilmaz, B., Terekeci, H., Sandal, S., Kelestimur, F., 2020. Endocrine disrupting chemicals: exposure, effects on human health, mechanism of action, models for testing and strategies for prevention. *Rev. Endocr. Metab. Disord.* 21, 127–147. <https://doi.org/10.1007/s11154-019-09521-z>

- You, Q., Li, Q., Lv, L., Lin, Z., Dong, Y., Yao, H., 2023. Genome-Wide Identification of 5-HT Receptor Gene Family in Razor Clam *Sinonovacula constricta* and Their Circadian Rhythm Expression Analysis. *Animals* 13, 3208. <https://doi.org/10.3390/ani13203208>
- Young, T., Alfaro, A.C., Sánchez-Lazo, C., Robertson, J., 2015. Putative involvement of adrenergic receptors in regulation of mussel (*Perna canaliculus*) larval settlement. *Mar. Biol. Res.* 11, 655–665. <https://doi.org/10.1080/17451000.2014.979833>
- Yurchenko, O.V., Dyachuk, V.A., 2022. Characterization of Neurodevelopment in Larvae of the Protobranch *Acila insignis* (Gould, 1861) in Order to Reconstruct the Last Common Ancestor of Bivalves. *Malacologia* 64. <https://doi.org/10.4002/040.064.0207>
- Yurchenko, O.V., Savelieva, A.V., Kolotuchina, N.K., Voronezhskaya, E.E., Dyachuk, V.A., 2019. Peripheral sensory neurons govern development of the nervous system in bivalve larvae. *EvoDevo* 10, 22. <https://doi.org/10.1186/s13227-019-0133-6>
- Yurchenko, O.V., Skiteva, O.I., Voronezhskaya, E.E., Dyachuk, V.A., 2018. Nervous system development in the Pacific oyster, *Crassostrea gigas* (Mollusca: Bivalvia). *Front. Zool.* 15, 10. <https://doi.org/10.1186/s12983-018-0259-8>
- Zhang, Y., Wang, H., Kage-Nakadai, E., Mitani, S., Wang, X., 2012. C. elegans Secreted Lipid-Binding Protein NRF-5 Mediates PS Appearance on Phagocytes for Cell Corpse Engulfment. *Curr. Biol.* 22, 1276–1284. <https://doi.org/10.1016/j.cub.2012.06.004>
- Zhou, Z., Zhen, J., Karpowich, N.K., Law, C.J., Reith, M.E.A., Wang, D.-N., 2009. Antidepressant specificity of serotonin transporter suggested by three LeuT-SSRI structures. *Nat. Struct. Mol. Biol.* 16, 652–657. <https://doi.org/10.1038/nsmb.1602>
- Zhu, M.-Y., Juorio, A.V., 1995. Aromatic l-amino acid decarboxylase: Biological characterization and functional role. *Gen. Pharmacol. Vasc. Syst.* 26, 681–696. [https://doi.org/10.1016/0306-3623\(94\)00223-A](https://doi.org/10.1016/0306-3623(94)00223-A)
- Zoeller, R.T., Brown, T.R., Doan, L.L., Gore, A.C., Skakkebaek, N.E., Soto, A.M., Woodruff, T.J., Vom Saal, F.S., 2012. Endocrine-Disrupting Chemicals and Public Health Protection: A Statement of Principles from The Endocrine Society. *Endocrinology* 153, 4097–4110. <https://doi.org/10.1210/en.2012-1422>